UNIVERSIDADE FEDERAL DO CEARÁ
CENTRO DE CIÊNCIAS AGRÁRIAS
DEPARTAMENTO DE ENGENHARIA AGRÍCOLA
PROGRAMA DE PÓS-GRADUAÇÃO EM ENGENHARIA AGRÍCOLA

HANS HEINRICH VOGT

ELECTRIC TRACTOR SYSTEM PROPELLED BY SOLAR ENERGY FOR SMALL-SCALE FAMILY FARMING IN SEMIARID REGIONS OF THE NORTHEAST OF BRAZIL

FORTALEZA
2018

HANS HEINRICH VOGT

ELECTRIC TRACTOR SYSTEM PROPELLED BY SOLAR ENERGY FOR SMALL-SCALE FAMILY FARMING IN SEMIARID REGIONS OF THE NORTHEAST OF BRAZIL

Doctoral Thesis submitted to the Postgraduate Program in Agricultural Engineering of the Center Agricultural Sciences of the Federal University of Ceará, as a partial requirement to obtain the Doctorate Degree in Agricultural Engineering. Concentration Area: Agricultural Systems.

Supervisor: Prof. Dr. Daniel Albiero.
Co-supervisor: Prof. Dr. Benedikt Schmülling.

FORTALEZA

2018

Dados Internacionais de Catalogação na Publicação
Universidade Federal do Ceará
Biblioteca Universitária
Gerada automaticamente pelo módulo Catalog, mediante os dados fornecidos pelo(a) autor(a)

V872e Vogt, Hans Heinrich.
Electric tractor system propelled by solar energy for small-scale farming in semiarid regions of the northeast of Brazil / Hans Heinrich Vogt. – 2018.
233 f. : il. color.

Tese (doutorado) – Universidade Federal do Ceará, , Fortaleza, 2018.
Orientação: Prof. Dr. Daniel Albiero .
Coorientação: Prof. Dr. Benedikt Schmülling .

1. Semiarid family farming. 2. Electric tractor. 3. Sustainable energy. I. Título.
CDD

HANS HEINRICH VOGT

ELECTRIC TRACTOR SYSTEM PROPELLED BY SOLAR ENERGY
FOR SMALL-SCALE FAMILY FARMING IN SEMIARID REGIONS
OF THE NORTHEAST OF BRAZIL

Doctoral Thesis submitted to the Postgraduate Program in Agricultural Engineering of the Center Agricultural Sciences of the Federal University of Ceará, as a partial requirement to obtain the Doctorate Degree in Agricultural Engineering. Concentration Area: Agricultural Systems.

Approved on: April 3, 2018.

EXAMINERS COMMITEE

Prof. Dr. Daniel Albiero (Supervisor)
Federal University of Ceará (UFC)

Prof. Dr. Fernando Luiz Marcelo Antunes (Internal Examiner)
Federal University of Ceará (UFC)

Prof. Dr. Sérgio Daher (Internal Examiner)
Federal University of Ceará (UFC)

Prof. Dr. Benedikt Schmülling (External Examiner)
Bergische Universität Wuppertal

Prof. Dr. Roberto Ney Ciarlini Teixeira (External Examiner)
University of Fortaleza (Unifor)

Dedicated to my late father, Heinrich Vogt.

ACKNOWLEDGEMENTS

Special thanks to my doctoral advisor, Professor Dr. Daniel Albiero.

Thanks also to all my friends and colleagues who contributed to the development of the system: Professor Dr. Sergio Daher, Professor Dr. Benedikt Schmuelling, Heribert Luegmair, Rodnei Regis, and Bonfim Rodrigues Campos.

For the revision and formatting of this text, thanks to my consistent friend, Amanda Vieira.

Last, but not least, thanks as well to the 77-year-old prototype builder, Sr. Monteiro, and his assistant mechanic, Sr. Alípio.

ABSTRACT

In Brazil, family farming is a significant factor in food production. This applies particularly to the Northeast semiarid regions. However, the majority of semiarid family farms lack appropriate motorized agricultural machinery that provides efficient farming. The hypothesis is that farming equipments developed for those specific climatic and farming conditions will increase productivity of semi-arid family farming. In order to make appropriate farming equipment available for this purpose, the project researched the feasibility of a small-size electric farming tractor, propelled by locally available renewable energy, and capable to pull implements tailored for semiarid family farming. Thus, since onboard availability of sufficient energy is a crucial factor for an electrical vehicle, this project investigated as well alternative systems of power supply, in order to enable the continuous operation of the tractor over longer time periods. The evaluated system included a prototype tractor, besides a scheme for local generation, storage and transmission of electric energy. The obtained result was that, in the semi-arid areas of Brazilian Northeast region, with its reliable and low-cost energy source (photovoltaic), the concept of an electric tractor already represents nowadays an economic and technical feasible solution.

Keywords: Semiarid family farming. Electric tractor. Sustainable energy.

RESUMO

No Brasil, a agricultura familiar é um fator significativo na produção de alimentos. Isto se aplica particularmente às regiões semiáridas do Nordeste. No entanto, a maioria das fazendas familiares do semiárido não possui maquinário agrícola motorizado apropriado que permita praticar a agricultura de modo eficiente. A hipótese é de que equipamentos agrícolas desenvolvidos para estas condições climáticas e agrícolas específicas aumentará a produtividade da agricultura familiar do semiárido. A fim de disponibilizar equipamentos agrícolas adequados para este propósito, o projeto pesquisou a viabilidade de um trator agrícola elétrico de pequeno porte, impulsionado por energia renovável localmente disponível, e capaz de puxar implementos sob medida para a agricultura familiar semiárida. Destarte, uma vez que a disponibilidade a bordo de energia suficiente é fator crucial para um veículo elétrico, este projeto investigou também sistemas alternativos de fonte de alimentação, a fim de permitir o funcionamento contínuo do trator por períodos de tempo mais longos. O sistema avaliado incluiu um protótipo de trator, além de um esquema para geração local, armazenamento e transmissão de energia elétrica. O resultado obtido foi que, nas áreas semiáridas do Nordeste brasileiro, com sua fonte de energia confiável e de baixo custo (fotovoltaica), o conceito de trator elétrico já representa, nos dias atuais, uma solução econômica e tecnicamente viável.

Palavras-chave: Agricultura familiar semiárida. Trator elétrico. Energia sustentável.

LIST OF FIGURES

LIST OF TABLES

LIST OF ABBREVIATIONS AND SYMBOLS

a	Highest group ordinal number
A	Area of mass flow [m^2]
A	Cross-section [mm^2]
AC	Alternating current
ANOVA	Analysis of Variance
APL	Average Power Level
ASABE	American Society of Agricultural and Biological Engineers
ASAE	Autoridade de Segurança Alimentar e Econômica (from Portugal)
BIC	Battery investment cost per KWh storage capacity
BRL	Brazilian Real (currency)
C1	Capacitor
CAD	Computer Aided Design
CC	Cycle costs
D	Detection
DC	Direct-current
DDP	Deep discharge protection
DD	Depth of discharge
DENA	Department of Agricultural Engineering of the Federal University of Ceará
Df	Degrees of freedom
DFMEA	Failure Mode and Effect Analysis applied to Design
D_h	Drawbar height
DNOCS	National Department for Works Against Droughts (Brazilian Institution)
DOD	Depth of discharge
DPY	Depreciation period in years
DSM	Demand Side Management
D_t	Detection of failure
DY	Depreciation per year

e	Efficiency
E	Energy [W]
Ed	Drawbar efficiency (%)
e_h	Horizontal offset
ESD	Extreme standardized deviate method
E_{ht}	Energy average hourly tractor requirements [kWh]
e_v	Vertical offset
EV	Electro-voltaic
f	Frequency [Hz]
F	Force [N]
FC	Fuel costs
Fd	Drawbar pull [kN]
F_i	Instant measured force
Fm	Mean traction force [kN]
FMEA	Failure Mode and Effect Analysis
FOPS	Falling Object Protective Structures
Fr	Transmission Ratio
FUNCEME	Ceará Institute for Meteorology and Water Resources
FWD	Dynamic front weight
FWS	Front static weight
g	Acceleration of gravity [9.8 m/s^2]
GEMASA	Energy and Machines for Semi-Arid Agriculture
GOPP	Goal oriented project planning
GT	Gross traction (theoretical pull)
GTR	Gross Traction Ratio
h	Height [m]
HC	Hourly costs
HC_{fix}	Hourly fixed costs
HD	Hourly depreciation

HFC	Hourly fuel cost
HFC_{on}	Hourly fuel consumption
H0	Null Hypothesis
HRE	Hourly required energy for the electric tractor operation [kWh]
I	Current [A]
Icell	Solar Cell current [A]
I_D	Diode current [A]
IEC	International Electrotechnical Commission
IIC	Initial investment costs
INPI	Instituto Nacional da Propriedade Industrial (National Institute of Industrial Property, Brazilian institution)
Iph	Photocurrent [A]
ITCZ	Intertropical Convergence Zone
K	Specific conductivity [Sm/mm^2]
l	Length [m]
L	Litre
LFA	Logical Framework Approach
m	Mass [kg]
M	Torque [N.m]
MR	Motion resistance force
MRf	Front motion resistance
MRR	Motion Resistance Ratio
Mt	Weight on drive wheels [kN]
N	Number of total observations in the experiment, or in each individual group
N_0	Number of pulses without traction load
N_1	Number of pulses with traction load
NC	Number of cycles during useful battery life
NAE	National Academy of Engineering
NPV	Net present value
NASA	National Aeronautics and Space Administration

NTR	Net traction Ratio
NT	Net traction (actual pull)
NTm	Mean net traction force
NREL	National Renewable Energy Laboratory
O	Occurrence
Oc	Occurrence of failure
OECD	Organization for Economic Co-operation and Development
Ov	Overheads
p	Pressure [N/m^2]
P	Power [W]
Papl	Tractor average power level [kW]
P_{av}	Tractor average power level [kW]
Pd	Drawbar power [kW]
PFMEA	Failure Mode and Effect Analysis applied to Process
Pm	Motor power [kW]
PV_{pa}	PV panel area [m^2]
Pnom	Tractor nominal power [kW]
PSEM	Personal sound exposure meter
PTO	Power takeoff
PV	Photovoltaic, Photovoltaic device
PWM	Pulse Width Modulation/Modulator
ρ	Fluid density [kg/m^3]
ρ	Specific resistance [$\Omega mm^2/m$]
ρ	Air density [kg/m^3]
Q	Coulomb [C]
R	Resistance [Ω]
RAMseS	Renewable Energy Agricultural Multipurpose System for Farmers
RMS	Root Mean Square
ROPS	Roll-over Protective Structures

RPN	Risk potential number
rr	Rolling radius
rt	Torque radius
RV	Residual value
RWD	Rear dynamic weight
RWS	Rear static weight
s	Runway section length [m]
S	Severity score values
S1, S2	Switches of the inverter
SD	Standard deviation
slr	Static loaded radius
SSB	Sum of Squares Between groups
SST	Total Sum of Squares
SSW	Sum of Squares Within Groups
Sv	Severity of failure
t	Time [s]; Test run time on the test track section [s]
T	Axle torque
TE	Tractive efficiency
ThC	Tractor hourly cost
THOC	Tractor hourly operation cost
TRR	Travel reduction ratio
TBSC	Tractor battery storage capacity [kWh]
T1	Upper temperature
T2	Lower temperature
U	Electrical tension or voltage [V]
UFC	Federal University of Ceará
UHY	Utilization hours' yearly
UN	United Nations
USAID	U.S. Agency for International Development

V, v	Velocity [m/s]
Va	Forward velocity
V_{actual}	Actual velocity
$V_{theoretical}$, Vt	Theoretical velocity
Vm	Mean velocity [$km.h^{-1}$]
W	Weight, static; Weight transfer
Wb	Wheelbase
Wd	Vertical dynamic reaction force
Wd	Weight, dynamic
x	Individual observation
$\bar{x}$	Mean value.
Ψ	Tractive Coefficient
η_{total}	efficiency total [%]
ω	Angular velocity [s^{-1}]; Rotational speed

SUMMARY

1 INTRODUCTION

Semiarid family farming is characterized by complex and harsh climatic challenges in form of regular droughts, irregular precipitation and archaic planting methods demanding hard physical work while being exposed to the hot equatorial sun.

Owing to these low-yield conditions in conjunction with small farm sizes, the semiarid family society is generally poor or even extremely poor and thus challenged by migration of the young people to the urban centers in search for better living conditions.

In contrast, family farming is crucial for the society as it is the chief food producer, especially in the northeast of Brazil with family farming representing 89% of the number of all farms.

One of the problems of semiarid family farming is that available modern farming equipment is generally designed for big scale farming in temperate climates and thus mostly not suitable and accessible for farming families in semiarid zones.

The hypothesis is: "*An electric micro tractor propelled by locally available renewable energy, designed to operate implements specifically designed for small scale semiarid family farming is technically and economically feasible and viable in terms of performance, operational costs and noise emission when compared to a common combustion engine powered micro tractor*".

The project therefore aims to investigate and qualify an appropriate motorization concept for small-scale farming in form of a small size farm tractor, propelled by clean energy from renewable sources together with an energy supply system that includes local energy generation, transformation, storage and transmission.

1.1 General objective

Confirmation or falsification of the technical and economic feasibility of an electric micro tractor that shall be propelled by locally available renewable energy and which is designed to operate implements specifically designed for small scale semiarid family farming.

1.2 Specific objectives

As the specific objectives of the present work, it can be cited:

1. Define operating data for an electric micro tractor capable to pull implements as used for small scale semiarid family farming;
2. Design, build and debug a prototype electric micro tractor on the base of the defined operation and system data;
3. Record operating data of the prototype electric micro tractor in experimental test runs on the UFC-DENA[1] test field;
4. Define a renewable energy conversion system based on the operating data of the electric micro tractor by utilizing locally renewable energy resources as available on semiarid family farms for generating electric energy;
5. Define an energy storage and transmission system for electric energy that shall ensure extended tractor operation (endurance) linking the energy conversion system with the tractor in operation;
6. Record inter alia operating and cost data for two cases: (*a*) Electric tractor running on electrical energy from the external power system: energy consumption, tractive performance and tractive peak power, battery charge and discharge characteristic, operating costs, noise emission; and (*b*) Compare available micro tractor(s) in with combustion engine powered tractor: tractive power and tractive peak power, operating costs, noise emission; and
7. Carry out a final comparative evaluation with the aim to confirm or falsify the hypothesis on the base of test data obtained during the various experimental test runs.

[1] UFC – DENA: Universidade Federal do Ceará - Departamento de Engenharia Agrícola (Fortaleza, Ceará, Brazil)

2 BIBLIOGRAFIC REVIEW Semi-Arid Agriculture

The semiarid climate phenomena in the northeast of Brazil occur because the position of the intertropical convergence zone varies over the year. It moves back and forth across the equator (Figure 1) following largely the sun's zenith. It_usually brings heavy rainfall to northeastern Brazil from February to May and a dry arid season usually lasting from August to December.

Figure 1 – Mean pass of Intertropical Convergence Zone, July *vs*. January

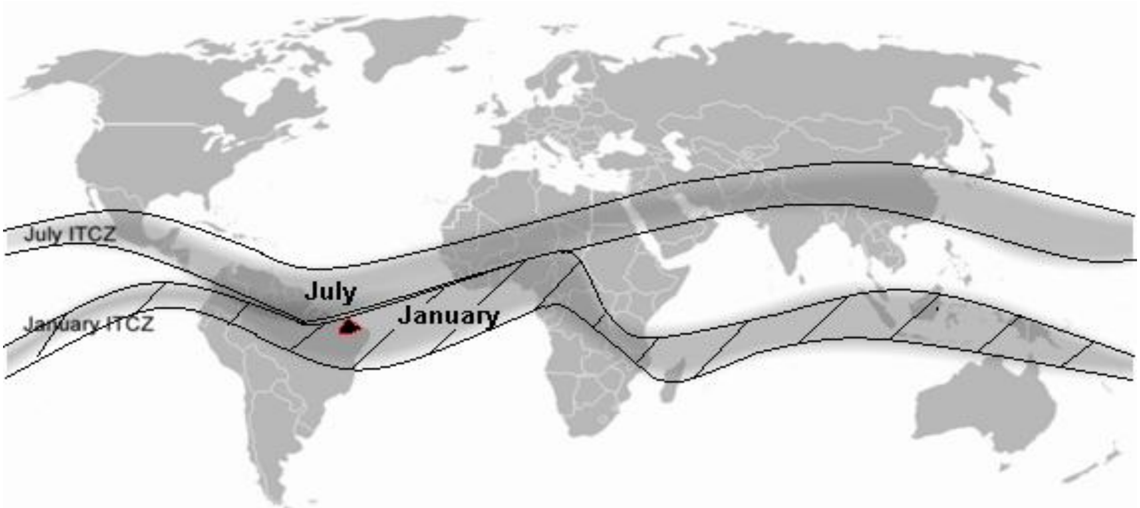

Source: HALLDIN (2016).

Like FUNCEME (2015), the Brazilian agency for weather forecast, points out:

> *"The Intertropical Convergence Zone - ITCZ is the most important weather system in determining how plentiful or poor the rains will be in the northern sector of the Northeast of Brazil", and "(...) the TSM-Sea surface temperature is a determining factor in determining its position and intensity."*

These climatic phenomena and a number of other challenges characterize farming in semi-arid regions in the northeast of Brazil. The most severe ones are the droughts that hit the land in an almost regular 10-year sequence. Like Santos (2012) points it out "The drought in the Northeast is an old problem that has always caused and still causes numerous disorders for the population, especially those with lower purchasing power."

It is estimated that the droughts in the Northeast region caused 3 million casualties between 1825 and 1983 (VILLA, 2001). The last decades have seen a huge effort to overcome this challenge through the construction of innumerous water reservoirs of all sizes and types by the government agency DNOCS and their interconnection by water transfer channels throughout the whole State of Ceará (MELLO, 2011).

Nowadays nobody has to perish because of the droughts but family farming in the Brazilian semi-arid region is still characterized by underprivileged humble life, hard physical work and a low income (Figure 2). The difficulties are dominated by the social situation of farming families in the semiarid region of northeastern Brazil, where the majority of the families are poor, or even extremely poor, lack the necessary education and the means for efficient farming (IBGE, 2006).

Very often family farms are without access to simple common farming and processing equipment. Apart from that many lack access to modern farming methods and in some communities, the main transport device for persons and goods is still the animal (horse, mule or donkey). Access to settlements is, in many cases, provided by narrow paths tailored for people, animals or motorcycles, following the natural topography of the land.

Of the 5175 million of registered agricultural establishments in Brazil in 2006, 84% are classified as family farms, according to the legal definition and a huge part of these farms in Brazil is cultivated only by family members (IBGE, 2006).

Figure 2 – Current situation of majority of semiarid family farms

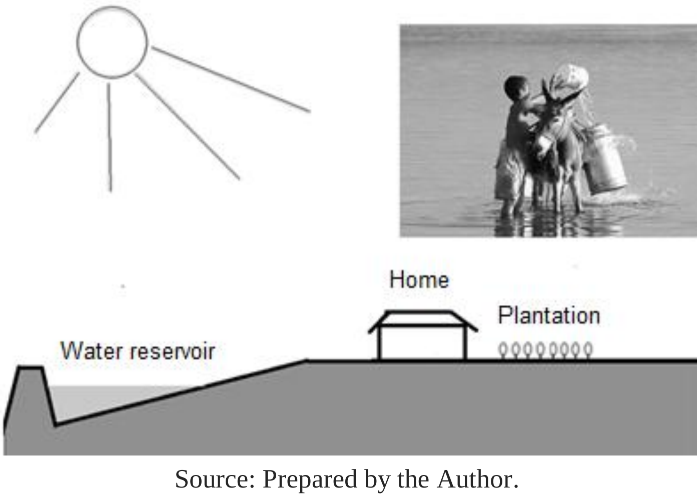

Source: Prepared by the Author.

The share of family farming varies considerably among the five Brazilian regions. At least 69% of establishments are classified as family farms in the Midwest and up to 89% in the Northeast. The latter region accounts for 50% of all family farms in the Brazil.

About 20% of family farms own less than 1 ha of land and 33% between 1 and 5 ha. A further 33% are in possession of land between 5 and 50 ha in the Northeast of Brazil (IBGE, 2006).

The imbalance in quality of life between urban societies and rural farming communities causes migration of young people to urban centers (CEARÀ 2011). Therefore, there is a lack of manpower and an increase in the average age of the workforce. This has a negative impact on soil preparation, cultivation, harvesting and transport, as workers - who are able to bear the hard conditions of physical work in a hot- semi-arid climate - are becoming increasingly rare.

The agricultural Census (IBGE, 2006) states that one of the issues which negatively affects the rural society is that the farming population is rather old. 39% of family farmers were over 55 years old in 2006. Helfan (2012) points out that low agricultural productivity is related to insufficient levels of physical human capital and access to mechanization.

On the other hand, family farms are a significant factor in securing food supply for the Brazilian society. The increasing demand for food over the coming decades, from both - new and traditional sources, will put growing pressure on agricultural resources. Agricultural production must as well adapt to the unpredictable consequences of climate change (EMBRAPA, 2001) since it is foreseeable that climate change will lead to increasing pressure on the supply side of agriculture from rising frequency of droughts and floods.

Strong competition for water will also come from industry, households and the preservation of natural habitats for maintaining biodiversity. For the production increases to happen, farmers must increase production efficiencies per hectare and per unit of inputs such as fertilizer and water. (BAWDEN et.al 2014)

An important aspect of the development potential of the semiarid farms in Northeastern Brazil is the availability of competitive renewable energy, partly via grid. The government program “Luz para Todos” has brought electricity access to 15.6 million rural families by 2015 (BRASIL, 2015) and electrical energy from the Brazilian grid is with over 80% coming from renewable hydropower.

But even without grid connection, the intense equatorial sun (marked with a reliable solar insulation exceeding 5 kWh/m^2 per day over the whole year) could be an effective and economical energy source in the semiarid region (SUDENE, 2015). This even more since the photovoltaic solar energy conversion is predictably becoming economically viable especially for semiarid regions with their intense and consistent solar irradiation.

Like the AGORA (2015) Energiewende in Germany, a study by *Fraunhofer-Institute* for Solar Energy Systems (ISE) in Germany, points out: "Solar power will soon be the cheapest form of electricity in many regions of the world."

For the semiarid agriculture the only possible solution to overcome the low productivity is the adoption of contemporary agricultural methods. Productivity could be increased by introducing motorization and mechanization. Exploitation of solar radiation as a free energy source and the use of state of the art PV-technology to convert it into electrical energy could propel the equipment. This in turn could offset the shortage of labor, relieve the farmer's tough daily life, improve incomes and make rural living more attractive for the younger generation.

However, this scheme necessitates equipment to harness and distribute the available renewable energy for the use in prime movers (tractors and machines) as well as by other consumers in food processing and households (Figure 3).

Most important in order to substitute the physical work of the farmer is a tractor which meets the local agricultural requirements and is designed to operate on renewable energy.

Figure 3 – Scheme of a sustainable motorized semiarid family farm with tractor

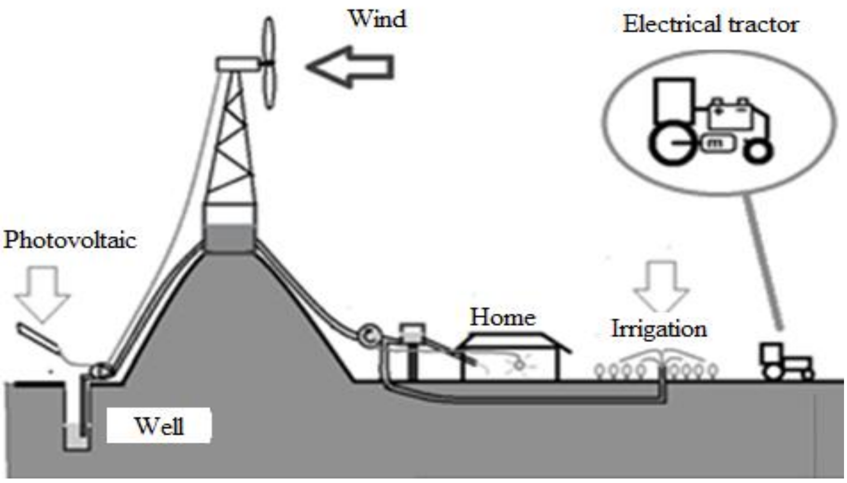

Source: Prepared by the Author

2.2 Energy sources

Energy has been throughout human history up to the present day a prerequisite for any kind of human civilization. Energy activates all the processes in the universe, from micro to macro scale, and is one of the indispensable foundations for life on earth (SUN AND WINDENERGY, 2010).

The main source of energy on earth is solar radiation (GREEPEACE, 2008). By means of photosynthetic processes, plants convert light energy into chemical energy, transforming thus atmospheric carbon dioxide into oxygen and organic compounds of carbon. For animals and humans, this is the only primary food source.

In the formation of the earth's crust, large amounts of organic carbon were retained in underground places in the form of coal, oil and gas. This process was purifying the Earth's atmosphere over time, due to the carbon dioxide removal and release of oxygen (HINDRICH and KLEINBACH 2004).

The most ordinary forms of energy used by humanity are light (sunlight) which when transformed by photosynthesis into food powers muscle work of Man and animals in order to perform the daily functions of the individual.

In prehistoric times, humanity began to use organic carbon in the form of wood or straw to feed a fire for the purpose of cooking, lighting, space heating or metal processing (MANN, 1986).

With the development of transport at sea and over inland waterways, humanity learned to use wind power to power their crafts (on river Nile, 5000 BC). Until the invention of the steam engine and the combustion engine, energy resources were used in a non-exhaustive perspective: “Nature was always producing more resources than what was consumed.”

The use of fossil organic carbon excessively increased with the advent of industrialization and urbanization. The basis of this development was the large scale conversion of fossil energy into mechanical energy by means of steam engines for electricity generation and by combustion engines for powering vehicles. In addition, large reserves of coal, oil and gas had been discovered and were exploited. Thus, energy in its various forms as heat, electricity or mechanical power became accessible for large parts of the society, worldwide (HINDRICH and KLEINBACH 2004).

Since conversion of heat energy into mechanical energy has been started with the invention of the steam engine in 1781 by *James Watt*, the rate of growth of energy is used as an indicator of the economic development of a society (SPORN, 1957).

Starting at the advent of industrialization, the use of fossil energy in all sectors of society has grown and continues to grow excessively. Today, almost half of the daily energy consumption in the world is related to burning of mineral oil. In contrast, muscle work represents nowadays less than 1% (MANN, 1986).

According to a definition of the United Nations (UN), sustainable development is a set of processes and attitudes that meets present needs without compromising the ability of future generations to meet their own needs (UN, 1987).

However, currently the most serious consequences of an excessive use of fossil energy are the exhaustion of these resources in the time span of a few generations. Besides this, a significant increase of CO_2 in the atmosphere takes place. In consequence, processes and attitudes of modern society meet present needs but compromise the ability of future generations to meet their needs. The existence of humanity may be threatened because of this negative development (GREENPEACE, 2007).

To avoid a global disaster, it is required that humanity reduces significantly the use of fossil fuels. To this end, renewable energy sources offer a sustainable alternative to meet the energy demand in the future.

Technically and economically, the use of renewable energy is feasible in the case of transforming hydraulic energy, biomass, wind and solar radiation (via photovoltaic) into electricity.

The use of hydropower and biomass in the form of alcohol has a long and successful history in Brazil, which currently produces more than 80% of its electricity from water resources and is an acknowledged world leader in this technology field and in the production of ethanol as an automotive fuel (BRAZIL, 2014).

The availability of primary energy sources and the technical means to convert them into mechanical energy freed industrial societies almost entirely of the dependency on their own muscles and that of draft animals for transport and farm work (LILJEDAHL, 1989).

Currently, the available and technically usable energy resources comprise:

1. Solar energy, direct (heating, illumination, radiation);
2. Solar energy, indirect:
   a) Fossil fuel:
      - Liquid and gaseous fuels derived from crude oil;
      - Natural Gas;
      - Coal;
      - Peat; and
      - Oil shale and tar sand.

   b) Photosynthesis (Biomass like wood, corncobs, biogas etc.);
   c) Wind;
   d) Tides; and
   e) Hydropower
3. Nuclear energy; and
4. Geothermal energy.

To make use of primary energy sources, conversion devices are required. Exceptions are human and animal power, which rely on biological processes.

The most common techniques in energy conversion are (LILJEDAHL, 1989):

1. Human and animal muscle work;
2. Reciprocating engines:
   - Diesel;
   - Petrol, including gas engines;
   - Rotary (Wankel);
   - Steam; and
   - Sterling.
3. Turbines:
   - Gas turbine;
   - Steam turbine;
   - Water turbine/water wheels; and
   - Wind turbine.
4. Fuel cell;
5. Photovoltaic effect;
6. Electric motor and generator;
7. Electrochemical battery; and
8. Miscellaneous (such as sails, thermoelectric effect etc.).

2.3 Renewable energy resources in semiarid zones of Brazilian Northeast region

The "*Balanço Energético do Ceará BEECE-2006*" (CEARÁ, 2006), the latest survey covering energy consumption and energy availability characteristics in the State of Ceará, which is located in the semiarid region of the Northeast of Brazil, shows that apart from the offshore wells supplying petrol and natural gas, the region is rich on renewable energy sources in form of firewood, wind and solar energy.

The Wind Energy ATLAS of Brazil (LEITE, 2001), for the northeast of Brazil illustrates that the coastal region and several mountain ranges offer wind speeds of 7 to 9 m/s in a height of 50 m above ground level. The inland semiarid regions in contrast offer only modest wind speeds of 4 to 5.5 m/s at a height of 50 m above ground level (Figure 4)

Figure 4 – Wind Energy ATLAS of Northeastern Brazil

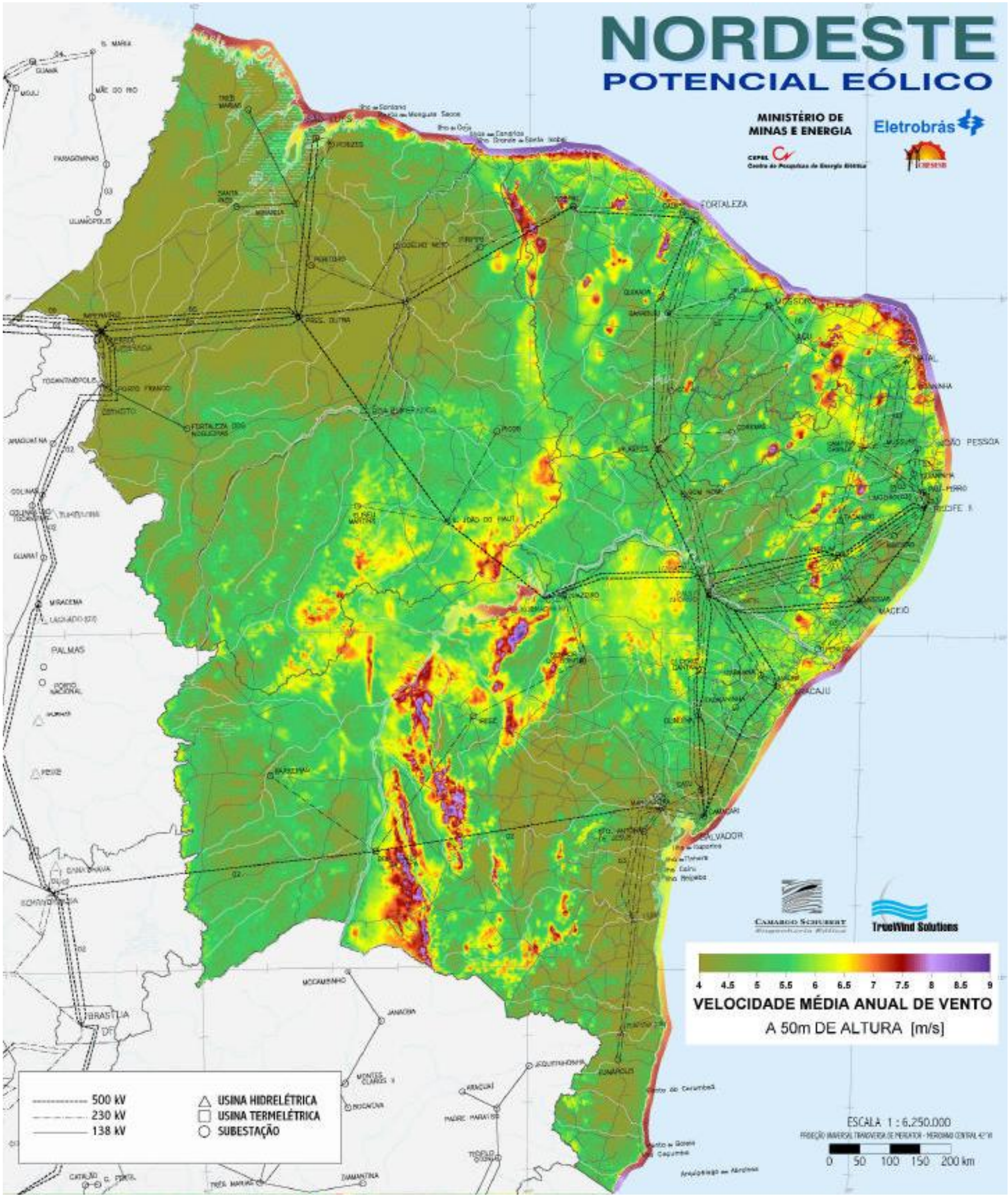

Source: Leite (2001).

Especially the semi-arid region offers intense solar energy. The SUDENE (2015) radiation chart (Figure 5) for the semiarid region of the northeast of Brazil shows up to 6 kWh/m^2 solar energy daily.

Considering an efficiency of 18% for solar panels, the solar radiation in the semiarid zones can provide 0.9 to 1.08 kWh/m^2 of electrical energy for a semiarid farmer.

Figure 5 – Radiation levels in the semi-arid region of Northeastern Brazil (kWh/m^2)

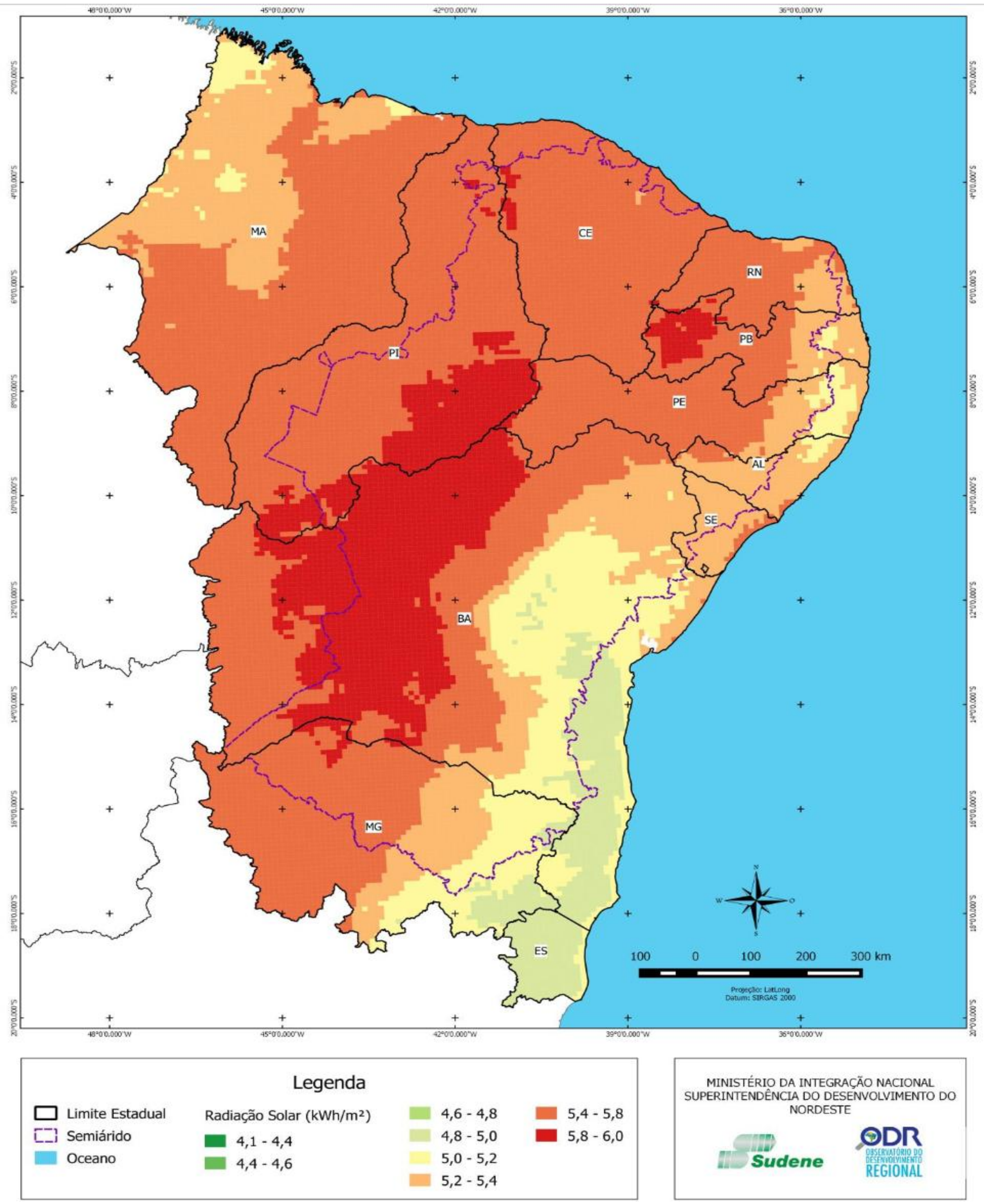

Source: SUDENE (2015).

2.4 Solar energy

Almost all of the available energy on earth, including fossil fuels, had and has its origin in the nuclear fusion process in the sun. At temperatures of approximately 15 - 20 million Kelvin hydrogen atoms fuse inside the sun to helium. In this process the mass difference between four hydrogens and one helium atom is converted entirely into energy and emitted into space as radiation on the Sun's outer surface, the photosphere. The sun surface has an effective blackbody temperature of approx. 6000 Kelvin (GERTHSEN, 1993).

The solar radiation reaching the outside of the earth atmosphere is known as the extra-terrestrial radiation and is expressed as solar constant in W/m^2. Since the orbit of the earth is not perfectly circular, it fluctuates slightly during a year between 1300 W/m^2 and 1390 W/m^2 (UNIVERSITÄT KASSEL, 2003). The maximum energy intensity in the radiation's spectral distribution is situated in the area of visible light between wavelengths of 380 nm up to 780 nm (Figure 6).

Figure 6 – Spectral distribution of solar radiation

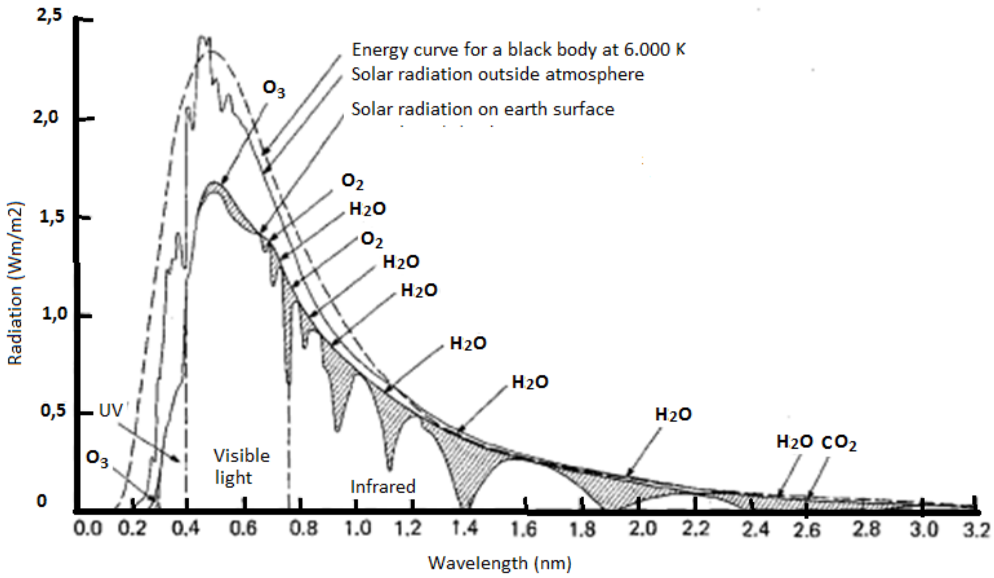

Source: PHYSICS STACK EXCHANGE (2016).

While penetrating into the earth atmosphere, the radiation is partly reflected by clouds or objects back into space or absorbed by the air masses (Figure 6). As a result, the maximum radiation reaching the Earth's surface does not exceed 1000 W/m^2. This applies only when the sky is cloudless blue, the air clean and the sun is at its highest position at noon.

Figure 7 – Radiation intensity in the Equator and Polar regions during Southern summer

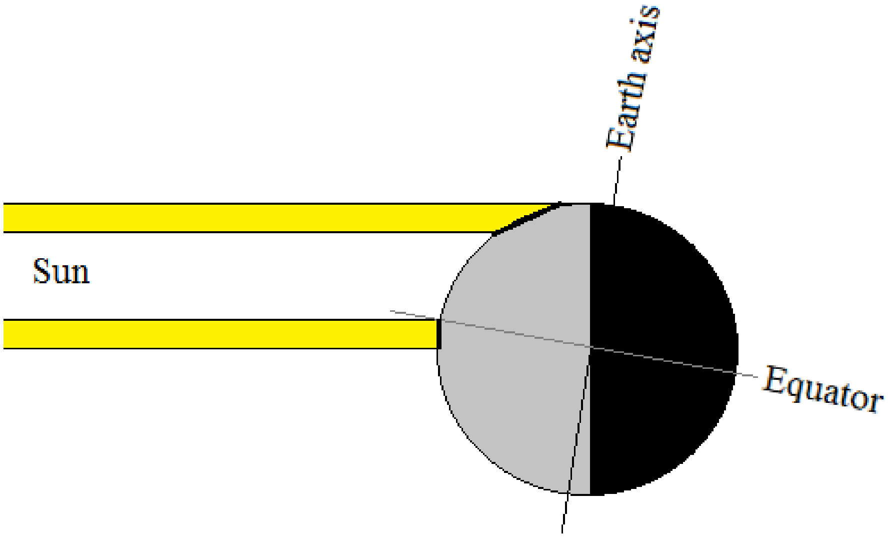

Source: Prepared by the Author.

Geographical position on earth as distance from the equator results in a different intensity of solar radiation (Figure 7). This is due to the changes of the Sun's position and the length of daylight caused by the tilt of the Earth's axis relative to the orbital plane.

Figure 8 displays the amount of solar radiation throughout the year at two different locations on earth, Fortaleza Brazil and Kassel Germany.

Figure 8 – Annual distribution of solar radiation at Fortaleza Brazil and Kassel Germany

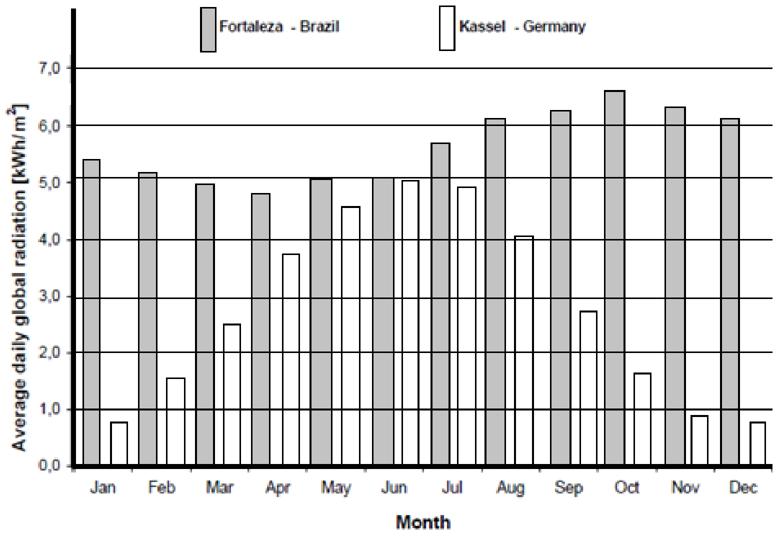

Source: Universität Kassel (2003).

The average annually available solar energy depends on the location and the dominating weather conditions. It varies between 1000 kWh/m^2 per year in Kassel Germany and double of that with 2000 kWh/m2 in Fortaleza Brazil. A peak is found in the Sahara with up to 2500 kWh/m^2 per year (Table 1).

Table 1 – Solar radiation energy per m^2 on horizontal surfaces at different locations

Location	kWh/^{2} per year
Kassel	1000
Thailand	1700 – 1800
Brazil	2000
Sahara	2200 – 2500

Source: Universität Kassel (2003).

The radiation energy on reaching the earth's surface is converted mainly into heat. A smaller fraction is consumed by plants' photosynthesis for cracking up CO_2 of the air and converting it into oxygen and biomass in form of carbohydrates, e.g. $C_6H_{12}O_6$. Fossil forms of energy like petrol, natural gas and coal are prehistoric biomasses that where compacted and sealed deep beneath the earth surface for millions of years.

Heat for its part causes evaporation of water and drives the global and regional wind systems which transport the moisture with the floating air masses (the wind) to distant places where it is occasionally dumped as precipitation (rain), thus, providing water that is required for all living beings all over the earth. In a similar manner, the surface waters of the ocean are heated causing sea-currents around the world coming from equatorial regions and heating northerly and southerly regions like northern Europe with the Gulfstream.

Biomass was always the sole physical energy source for animals and humans. Cooking with firewood is a prehistoric technique used by humans until today. The more advanced use of other forms of energy started most probably with the sailboats some estimated 5000 years ago, followed later on by windmills in Babylonia and China and finally with wind- and water mills in Europe using wind and rivers as energy source. In parallel, biomass has been used widely to provide energy for domesticated working animals, especially horses in order to substitute human muscle work for thousands of years (MANN, 1986).

This picture altered dramatically with the industrialisation based on the invention of the steam engine, which used biomass or forms of fossil energy as fuel. Mass production and mass transport became possible in the last century with the discovery of huge fossil fuel reserves, mainly coal, petrol and gas and the development of combustion engines that convert liquid and gaseous fuels into mechanical work (LILJEDAHL, 1989).

Today, humanity has run into serious problems with this development. Pollution and the increase of CO_2 in the atmosphere are causing climate change and are a serious threat to human existence. The *sustainable development*, defined by the United Nations (UNO. 1987) is not achievable by continuing today's practice to burn gigantic amounts of fossil fuels. Developed societies are conscious of that peril and science and industry are developing alternative ways to power machines with renewable energies at a global scale (HINDRICH, KLEINBACH, 2004).

The wide use of renewable energy started with electrification more than a century ago by using the gravitational potential energy of water in rivers to generate electricity. Dams were built to impound water as a type of potential energy storage which can be converted in electricity in a controlled manner (MANN, 1986).

Nowadays, all possible types of transformation of renewable energy into usable energy forms are investigated. However, so far only wind turbines conquered a bigger market share in electricity generation (ACKERMANN, 2005).

A very promising technology is the direct conversion of solar radiation into electrical energy by photovoltaic systems. The perspective is that this technology will be the most economic method of electricity generation in the very near future (Agora 2015).

2.5 Photovoltaic

In a photovoltaic device (abbreviated PV) a direct transformation of solar radiation energy into electrical energy occurs. The radiation energy interacts directly with the electrons of the atoms constituting the solar cell's crystals. Alexandre Edmond Becquerel discovered this photovoltaic effect in 1839.

Initially, solar cells were used as energy source in satellites to power the electrical systems. Applications in daily live first became common in watches, calculators and other small electronic devices in the 70^{th} of the last century. Today, the use of large PV generators is spreading as a key energy source in isolated areas with no grid connection and as decentralized electrical generation device for domestic purposes that feed locally generated surplus energy into the grid.

A solar cell of the most widely used type comprises two silicon layers, one doped with boron (B), a trivalent element and one doped with phosphorous (P), a pentavalent atom, as shown in Figure 9 (BERGELT, 2012).

Figure 9 – Doping of silicon: (*a*) with the pentavalent atom (Phosphor) and (*b*) with the trivalent atom (Boron)

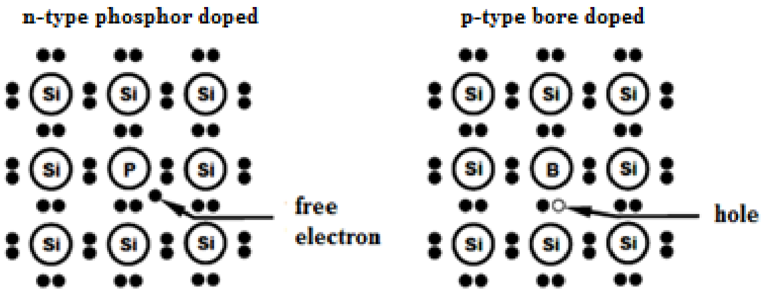

Source: Bergelt (2012).

An electric potential is created because there is an electron excess on the phosphorous layer (n – positive type of material) with many free electrons and a lack of electrons on the boron layer (p – negative type of material) with many holes (Figure 10). At the interface between these two layers the charge potential differences lead to the phenomena that electrons from the n-region diffuse into the p- region and holes from the p-region diffuse into the n-region.

Figure 10 – Charge carrier distribution at p-n junctions and currents through the junction

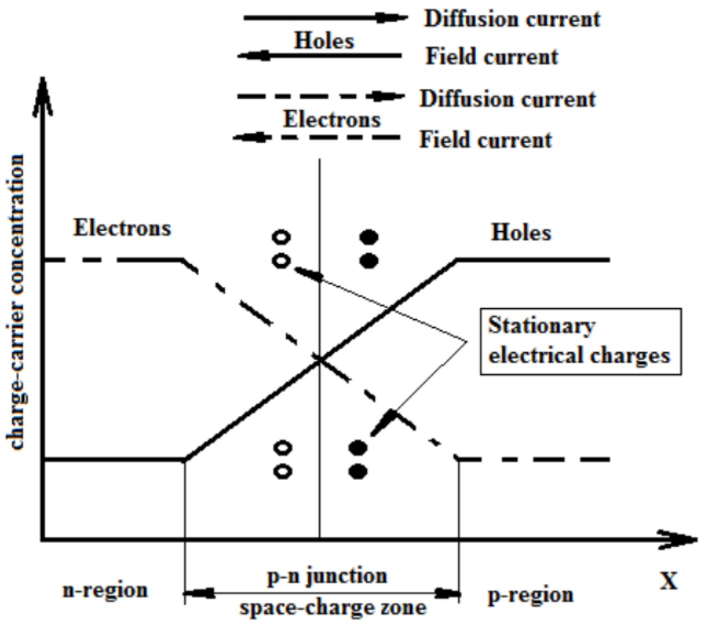

Source: Universität Kassel (2003).

The electrostatic fields extending over the boundary surface represent a potential difference, the diffusion voltage. When light falls on the solar cell, the photons excite the electrons. This is named the photoelectric absorption. When the photons energy is completely captivated by a bound electron, it becomes a free-electron.

Figure 11 – Operating principle of solar cells (schematic)

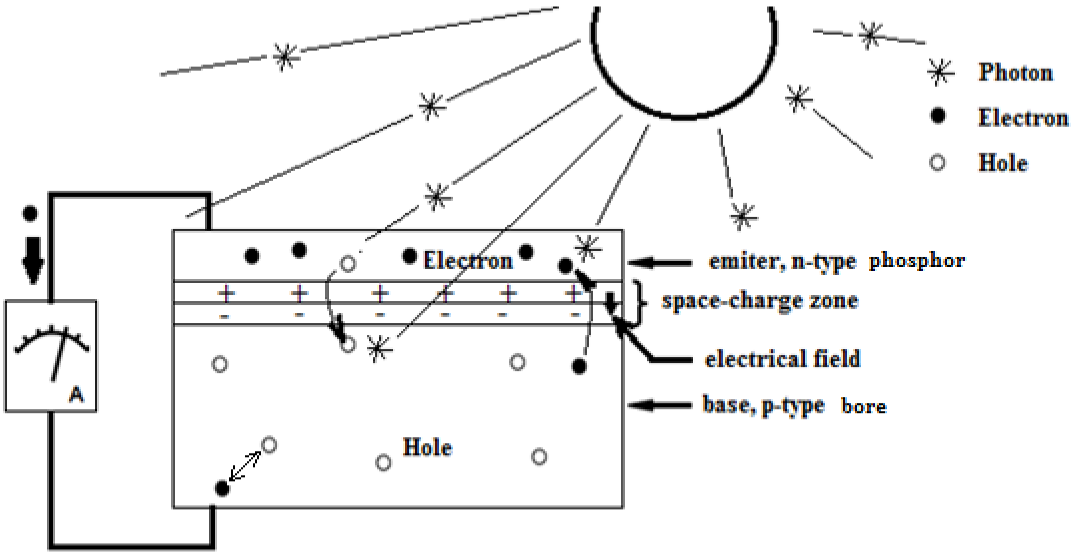

Source: Universität Kassel (2003).

A photon with sufficient energy penetrates the emitter, the n-type layer of the solar cell and is absorbed in the base, the p-type layer (Figure 11). An electron-hole pair develops due to the absorption. The free electron diffuses in the p-base until it arrives at the boundary of the space-charge zone. Subsequently, the electric field in the space-charge zone accelerates the electron and transports it to the emitter side (GREENPRO, 2003).

As the concentration of electrons at the n-emitter side growths, the number of holes at the p-base side growths correspondingly. Consequently, an electrical voltage builds up. If n-emitter and p-base are now connected via an electric load, electrons flow. This current flow continues as long as the sun’s radiation continues to excite the electrons of the solar cell. Hence, solar radiation energy is directly converted into electrical energy (UNIVERSITÄT KASSEL, 2003).

An equivalent circuit (Figure 12) with ideal electrical components serves as a model of a solar cell. The current depends on the radiation intensity and the wavelength spectrum (Equation 1).

$$I_{cell} = I_{ph} - I_D \tag{1}$$

where:

I_{cell} = Solar Cell current [A];
I_{ph} = Photocurrent [A]; and
I_D = Diode current [A].

Figure 12 – Equivalent circuit diagram of a solar cell connected to a load

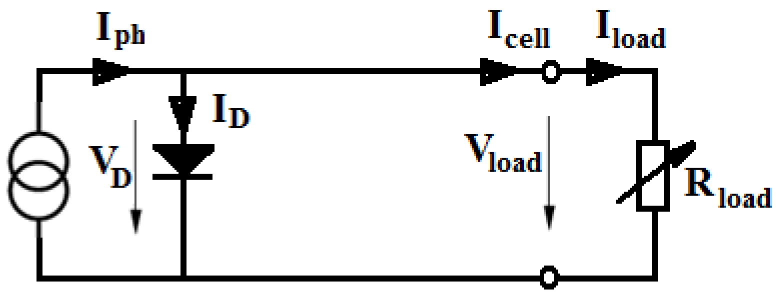

Source: Universität Kassel (2003)

Today's commercial grade solar panels have an efficiency of up to 18% and a lifetime expectancy of 20 to 30 years.

2.6 Wind energy

Wind is a mass of air in movement. It represents a form of kinetic energy (Equation 2).

$$E = m\frac{v^2}{2} \tag{2}$$

where:

E = energy [W];
m = mass [kg]; and
v = velocity [m/s].

The wind turbine is a device that extracts a major fraction of this kinetic energy aerodynamically and converts it via a mechanically driven generator into electric energy (GASCH, 2007).

Daniel Bernoulli (1700-1782) together with Leonhard Euler (1707-1783) discovered the laws of aerodynamics according to which the sum of the different forms of energy of a fluid in motion has to be constant (Equation 3).

$$v^2 + gh + {}^{p}/_{\rho} = constant \qquad (3)$$

where:

v = velocity [m/s];
g = acceleration of gravity [9.8 m/s^2];
h = height [m];
p = pressure [N/m^2]; and
ρ = density of the fluid [kg/m^3].

Figure 13 – Bernoulli's scheme of dynamic flow in a tube

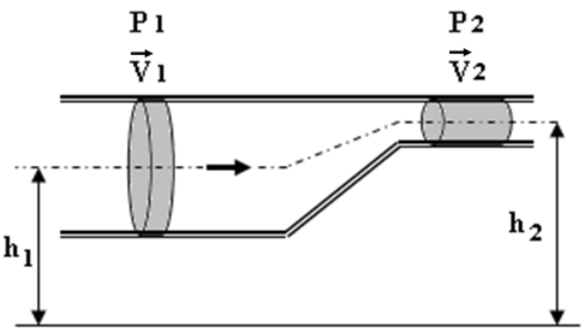

Source: Prepared by the Author

Consequently, in a flow of air forced to accelerate, the pressure drops to maintain the energy balance (Figure 13).

This is the effect that wings of a bird, a plane and the rotor blade of a wind turbine use to generate physical forces. At a wind turbine, these forces are used to drive the rotor disc. Via a mechanical link, i.e. gearbox, the rotational speed is increased to drive an electric generator. Large size wind turbines may also use direct-driven generators (CARVALHO, 2003).

The aerodynamics of the flow path of a wind turbine resemble a change in volume, speed and pressure. The air mass starts to decelerate in relation to the wind speed already upstream of the rotor plane and continues to do so after passing it. The pressure consequently increases upstream of the rotor plane with a sharp drop when passing it (which is actually the force that moves the blade) and equalizes to the surrounding air pressure after passing the plane of the rotor (BURTON, 2003).

Downstream of the rotor plane, the cross sectional area of the air mass flow increases further, and the air mass continues to decelerate (Figure 14) for a certain distance, up to a point where turbulence mixes the air passing through the turbine with the surrounding air mass.

Figure 14 – Air flow tube near the blades of a wind turbine

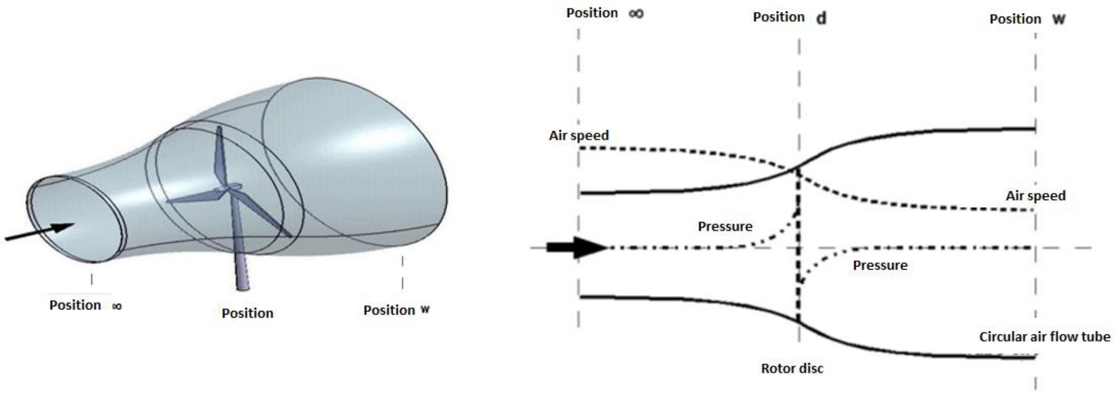

Source: Prepared by the Author

In Physics, it is expressed as the mass is constant in (Equation 4):

$$\rho A_{\infty} v_{\infty} = \rho A_d v_d = \rho A_w v_w \quad (4)$$

where:

ρ = density of air [kg/m^3];
A = area of mass flow [m^2]; and
v = velocity [m/s].

The whole unit of rotor, mechanical power transmission and generator has to be placed at an elevated position (Figure 15) since wind speed increases with the height above ground and the flow moves more laminar. This is especially important since the speed enters with the cube in the energy equation and turbulent flow minimizes efficiency.

Figure 15 – Wind turbine at an elevated position

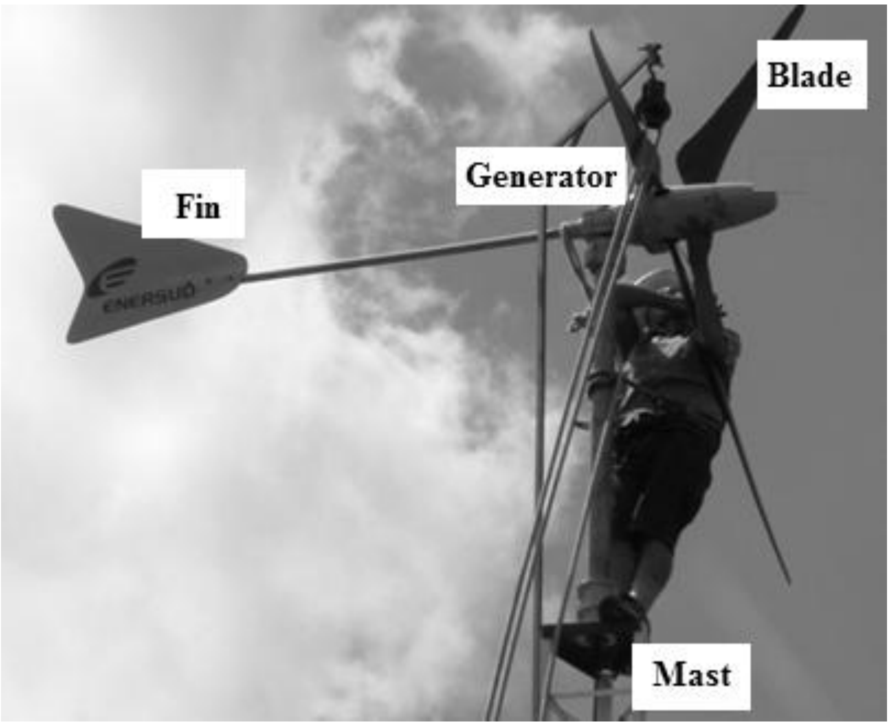

Source: Prepared by the Author

2.7 Local renewable electric energy systems

2.7.1 *Electric Fundamentals*

By powering a device, a motor or engine (prime mover) performs in terms of physics mechanical work. To enable the motor to perform this mechanical work, energy is to be made available. This can be in the form of chemical energy or as investigated in this document electrical energy.

Electrical energy is generally made available to electrical consumers by connecting them via a transmission system to a power generation plant, i.e. the power generated is consumed at the same moment. This is the preferred concept since storage of electrical energy requires cost intensive technical devices.

On the other hand, this approach restricts the use of electric energy for freely moving vehicles. However, all this changes with the development of batteries exhibiting a substantially higher power density.

All electrical phenomena are caused by electrical charges. An electrical charge is a basic physical property and is expressed in Coulomb [C] which represents a current of 1 Ampere that passes through an electrical conductor in 1 second.

$$[Q] = \text{Coulomb} = C = As$$

All electrical charges are composed of elementary charges [e]:

$$e \approx 1602 * 10^{-19} \text{ C}$$

An electrical current is a flow of electrical charges [Q] that pass a cross section of the conductor (Equation 5) during a defined time interval [t]. The strength of the electric current is named amperage [I]:

$$I = \frac{\Delta Q}{\Delta t} \tag{5}$$

where:

I = Current [A];
Q = Coulomb [C]; and
t = time [s].

The flow of charges occurs usually through an electrical conductor. An electrically conductive material is characterized by free moving electrons. When an electrical tension is applied to a conductor these negative charges move in form of a current from the negative side to the positive side of the conductor. However, technically the flow direction of the current is considered from positive to negative as if positive charges would be freely moving from the positive side to the negative side.

Generally, electrical conductors exhibit resistance when current is flowing through them. The resistance depends on the type of material of the conductor, its temperature and its geometrical properties. Only superconductors at extreme low temperatures near 0-degree Kelvin can conduct electricity or transport electrons from one atom to another with no resistance.

This ohmic resistance of a conductor is calculated as (Equation 6):

$$R(conductor) = \rho(conductor) * \frac{l}{A} = \frac{l}{K_{(conductor)} * A} \tag{6}$$

where:

R = resistance [Ω];
ρ = specific resistance [$\Omega mm^2/m$];
K = specific conductivity [Sm/mm^2];
A = cross-section [mm^2]; and
l = length of the conductor [m].

Metals have free moving electrons and silver, copper, gold and aluminum have the highest specific conductivity, but for economic reasons only copper and aluminum are commonly used for electrical conductors. Hence, when a current flows a part of the transitory energy is converted into heat.

The heat represents the loss of power and is calculated as given below by Equation 7:

$$P_{loss} = I^2 * R \tag{7}$$

where:

P_{loss} = Power loss [W];
I = Current [A]; and
R = Resistance [Ω].

For determining the current the following formula applies (Equation 8):

$$I = P/U \tag{8}$$

where:

I = Current [A];
P = Total power [W]; and
U = Electrical tension or voltage [V].

According to the above given formulas, the power loss depends on the conductivity but even more on the voltage because a higher voltage reduces the amperage of the current (with power constant) which enters with the square in the power loss calculation.

The use of renewable energy in rural areas is increasing, but since wind and sun are an inconstant source, the combination of a low-cost renewable technology with common technology via a grid connection provides a solution. Those hybrid power systems incorporate different components as generation, storage, power conditioning and system control (ACKERMANN, 2005).

The classic hybrid system includes both a direct-current (DC) bus with a battery bank and an alternating-current (AC) bus and a backup engine generator (if grid connection is not available). Small isolated systems use batteries to store surplus energy and the battery bank acts as power dampener, smoothing out fluctuations in the power flow.

Figure 16 illustrates a DC-bus power system providing AC power via a power converter. The backup generator can also be operated with biogas (if biogas is available and the engine is adapted to burn it). The bidirectional inverter offers the possibility to connect the system to the grid (if available) for backup power supply or alternatively to store surplus energy (ACKERMANN, 2005). In this case, the system can be operated without a battery bank.

Figure 16 – System with connection to public grid

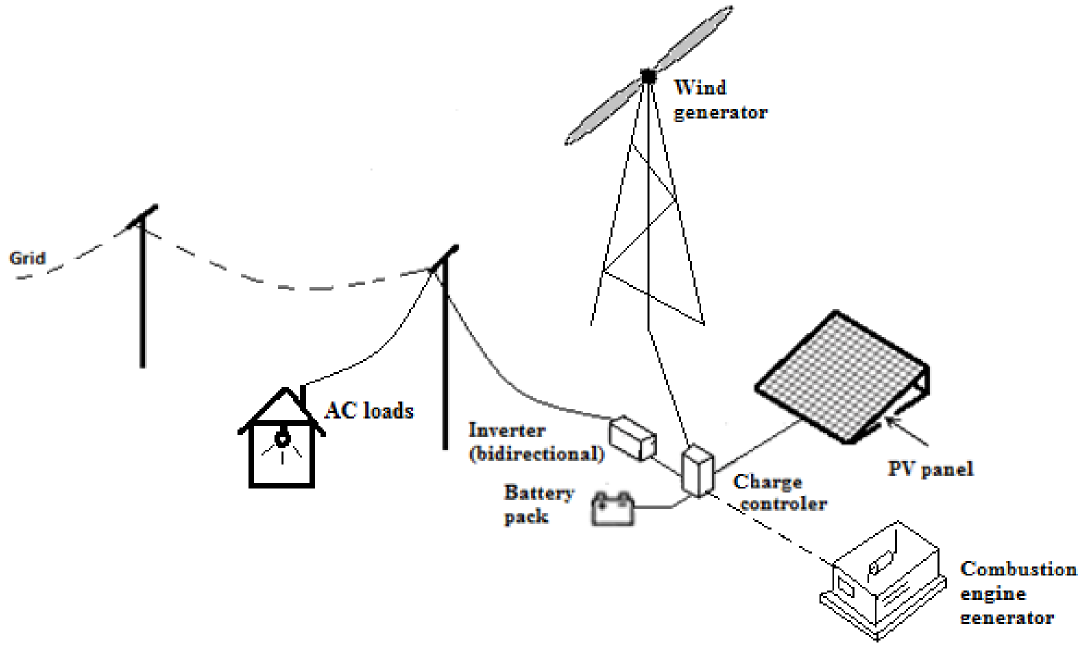

Source: Prepared by the Author

2.7.2 *Transmission and conversion/inversion*

Renewable energy systems with a small wind or PV generator but without battery storage are connected directly to the consumer. This applies for instance for minor loads such as ventilators or small water pumps (Figure 17 a).

Systems with a converter are applied if the voltage of the generation system has to align with the voltage of the consumer. A DC/DC boost converter transforms the generator's DC voltage to the DC voltage of the consumer (Figure 17 b).

Figure 17 – Configuration of (*a*) direct coupled system and (*b*) system with DC-DC boost converter

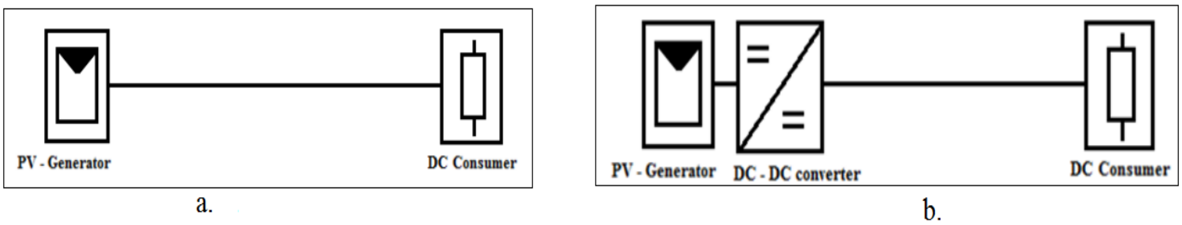

Source: Universität Kassel, 2003

An AC system uses converters, which transform DC power into AC power. This kind of system is commonly used for electrical loads and electrical motors consuming more than 2 kW (Figure 18).

Figure 18 – Configuration of a system with DC-AC converter

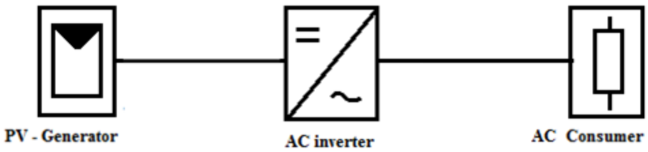

Source: Universität Kassel, 2003

If available, the system is linked to the public grid by means of suitable (bidirectional) frequency inverters (Figure19). In this case, the energy storage capacity of the battery can be sized much smaller or it is not necessary at all. This is because the grid assumes the function of a storage device and a power dampener, smoothing out fluctuations in the power flow.

Figure 19 – Configuration of a system connected to the grid

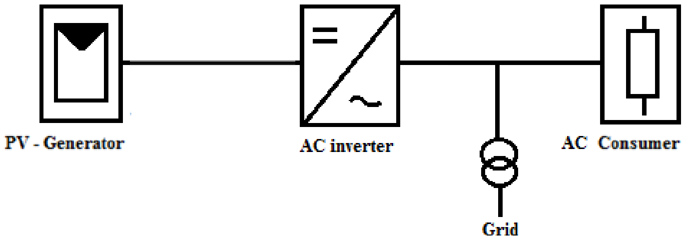

Source: Universität Kassel, 2003

Systems with battery storage (Figure 20) generally have to use a charge regulator to protect the batteries from overcharge and deep discharge (DDP). This is to ensure the longest possible battery life.

Figure 20 – Configuration of a DC-coupled system with battery backup

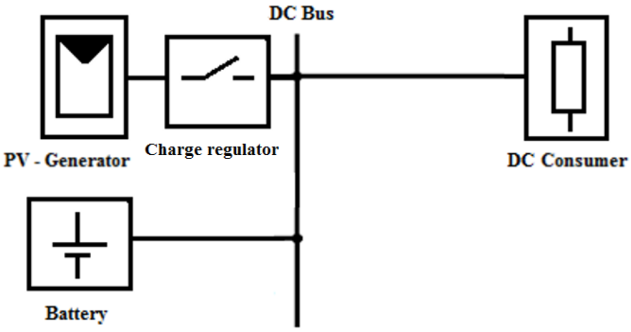

Source: Universität Kassel, 2003

For systems with battery storage and higher power needs (in conventional households with AC consumers or in the case of industrial electrical devices), an AC-DC-inverter has to be included (Figure 21).

Figure 21 – Configuration of a system with an AC consumer

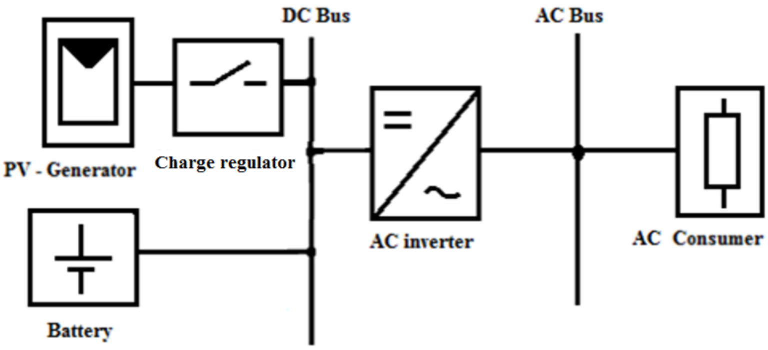

Source: Universität Kassel, 2003

This type of system normally combines a back-up generator (Figure 22) to safeguard power supply when the batteries are discharged and sun and wind are temporarily not available as energy sources.

Figure 22 – Configuration of a hybrid system with backup generator

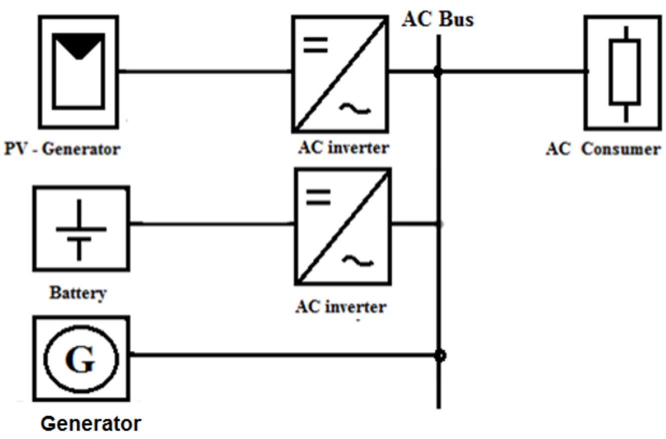

Source: Universität Kassel, 2003

2.7.3 *Storage systems*

A central issue with electrical energy is that it is hard to store it at a high power density (like chemical energy in the form of petrol).

The most common mobile energy sources used by electric vehicles are usually chemical batteries, whereas capacitors are usually intermediate energy storage devices building up brake energy to release it for propulsion when indicated.

A capacitor is an electrical component that stores electrical energy in an electric field. Two electrical conductors of a circuit in sufficient close proximity are separated with a dielectric insulation material. When the two conductors experience a potential difference, an electric field develops causing a positive charge on one side and a negative charge on the other side. If a varying voltage is applied a current is caused to flow through the connected circuit.

The electrochemical battery in contrast is a device that converts chemical energy directly to electrical energy and vice versa. Batteries are a viable source of energy if they sustain a high number of charging cycles, feature a high specific energy (per unit mass) and energy density (per unit volume) and are safe to operate.

Batteries rely on chemical processes to store electric energy during the charging cycle or supply electric energy during the discharge cycle. Basically, an electrochemical battery consists of three primary elements: two electrons (positive and negative), immersed in the electrolyte (Figure 23).

Figure 23 – A typical electrochemical battery

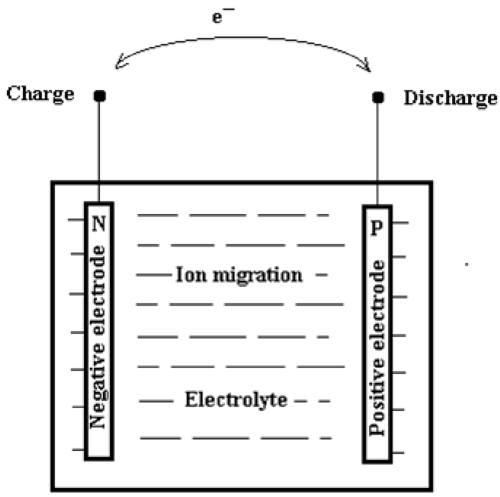

Source: Mehrdad (2010).

Batteries are specified by their coulometric capacity in Ampere-Hours, i.e., as ampere-hours provided when discharging the battery from fully charged until it is down to its cut-off voltage (Figure 24).

Figure 24 – Cut-off voltage of a typical battery

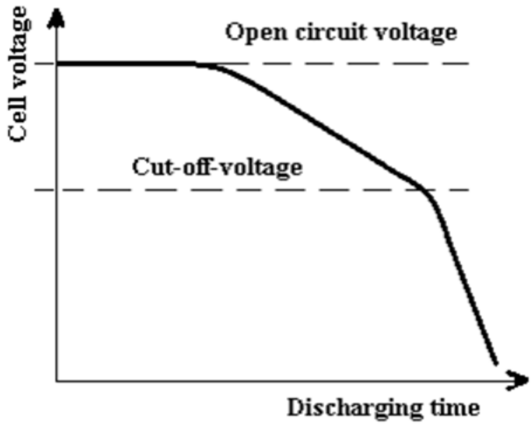

Source: Mehrdad (2010).

An important characteristic in terms of battery capacity is the number of ampere-hours vs different discharge current rates. With a higher discharge rate, the capacity generally decreases significantly (Figure 25).

Figure 25 – Discharge characteristic of a lead-acid battery

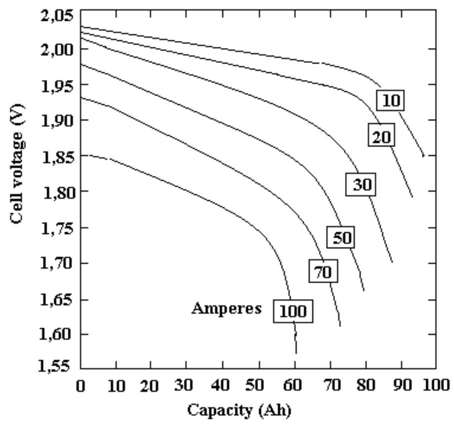

Source: Mehrdad (2010).

A common example of an electrochemical reaction in batteries used in vehicles is the lead-acid battery (Figure 26). It uses an aqueous solution of sulfuric acid ($2H^{+} + SO_4^{-2}$) as electrolyte. The electrodes are of porous lead (Pb) in case of the anode (-, negative) and porous lead oxide (PbO_2) in case of the cathode (+, positive).

Figure 26 – Electrochemical process of a lead acid battery cell:
(*a*) discharging and (*b*) charging

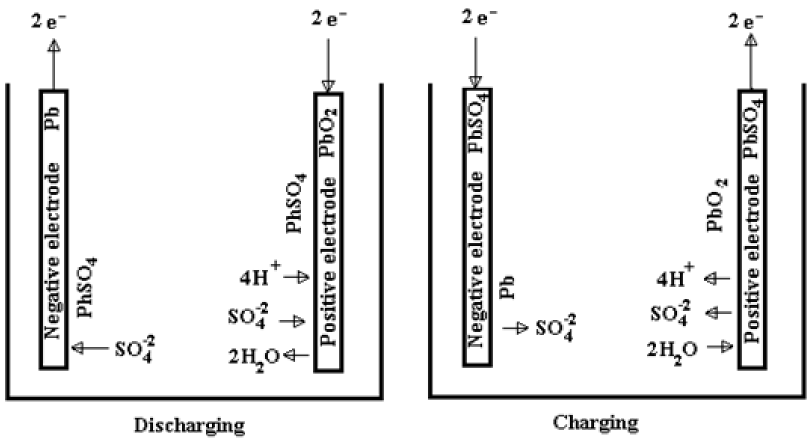

Source: Mehrdad (2010).

The chemical reaction on the anode during the discharge phase is: $Pb + SO^{-2}{}_4 \rightarrow PbSO_4 + 2e^{-}$. This reaction releases electrons which generate a negative charge on the electrode. By the flow of electrons through an external circuit to the positive cathode electric energy is generated to power a load (for example in form of an electric motor).

At the positive electrode, PbO_2 is converted to $PbSO_4$ and water is produced. Charging reverses the chemical reaction on the anode and cathode.

Cycle life of batteries

Battery cycle life is the capability of the battery to endure a specific number of charge/discharge cycles. The depth of discharge (DOD) is a critical figure in battery life. The typical lead-acid battery in an automobile has a limited cycling capability of less than 100 nominal cycles of deep discharges.

However, as the lifetime of a battery depends not only on the cycles but as well on the depth of discharge (expressed as a percentual of the rated deep discharge capacity), a battery with a nominal 100 cycles of deep discharges is able to endure 500 cycles of 20% discharge depths (Figure 27 and 28). This can roughly be expressed by:

*Nominal cycles of battery life = actual cycles * (depth of discharge [%] / 100)*

Battery capacity is normally expressed in Ah (Ampere-hours), but energetic content is more precisely defined in Wh (Watt-hours). These values are related with the battery voltage through the equation:

$$I\ (A) * U\ (V) * t\ (h) = E\ (Wh)$$

Figure 27 – Cycle life as a function of depth of discharge for different types of batteries

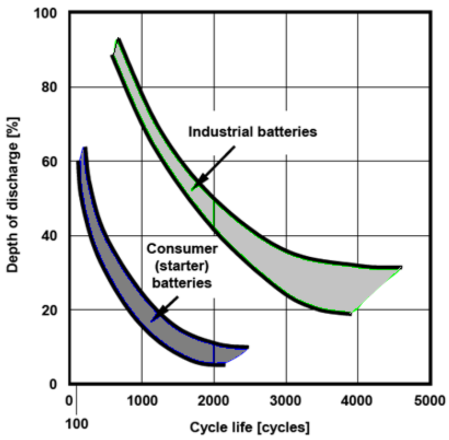

Source: Universität Kassel (2003).

Figure 28 – Cycle life *versus* depth of discharge DOD of Ni/Cd cells

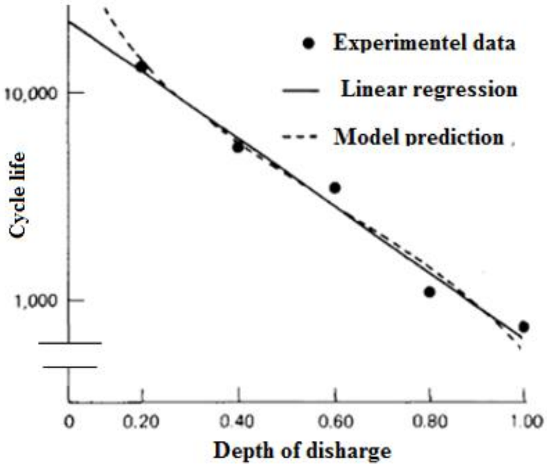

Source: NASA (1987).

Apart from the number of load cycles, capacity is also affected by temperature with about 1% capacity loss per degree below about 20°C. On the other hand extremely high temperatures decrease capacity too, accelerate aging, and self-discharge (Figure 29).

Figure 29 – Cycle life as a function of depth of discharge DOD and temperature of Ni/Cd cells

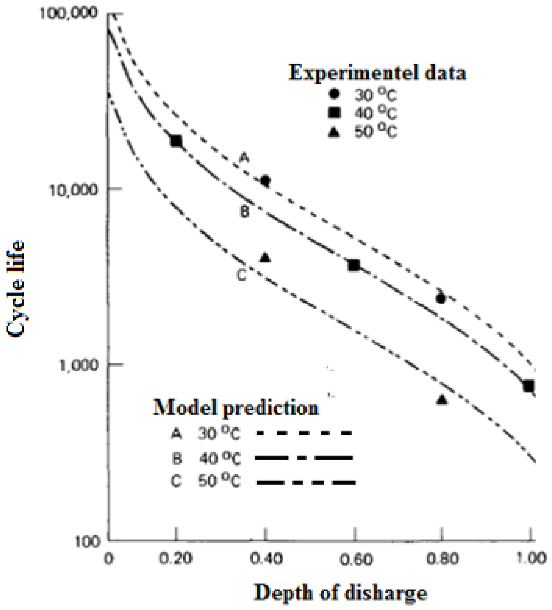

Source: NASA (1987).

Electric energy storage by means of batteries is a significant cost factor in isolated power systems and therefore optimization is required by taking into account the overall efficiency and lifetime (see Table 2). Furthermore, aspects like self-discharge, maintenance requirements, reliability, mechanical integrity and safe operation have to be considered.

Table 2 – Costs, energy and efficiency comparison of different battery types

Type	Cycle live for 80% DOD	Investment cost (€/kWh)	Specific kWh cost (€/kWh$_\Sigma$)	Self-discharge [%/month]	Temp-range [°C]
Pb	1500 ... 3500	85 ... 350	0.17 ... 0.30	>80	-15° to +50°
NiCd	1500 ... 3500	650 ... 1500	0.30 ... 1.00	71	-40° to +45°
NiFe	3000	1000	0.33	40	-0° to +40°

Source: Universität Kassel (2003).

The type of battery widely used since a century is the lead-acid battery. But actually the battery favored for mobile use is the Li-ion battery because of its superior performance with respect to energy density and its load and discharge characteristic. Compared to lead-acid, the Li-ion battery has a higher energy density (Figure 30), a better charge and discharge characteristic and is expected to become the most economical alternative for mobile use in the near future.

Figure 30 – Energy density comparison of batteries

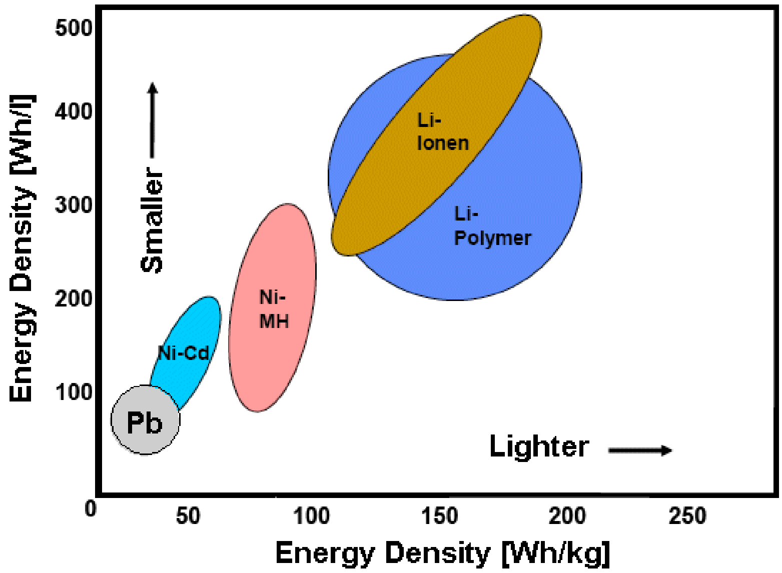

Source: Föll *et al*. (2009).

2.7.4 *Motors*

Electric motors exhibit a different torque, speed and power characteristic as compared to combustion engines. The design of an electric vehicle has to consider these specific properties which result in a different configuration and layout of the drive train. Especially the torque and speed characteristic of an inverter controlled squirrel cage induction motor exposes a significant difference to a combustion engine as shown in the graphic below (Figure 31).

Figure 31 – Typical torque characteristic of combustion engine *vs*. electric motor

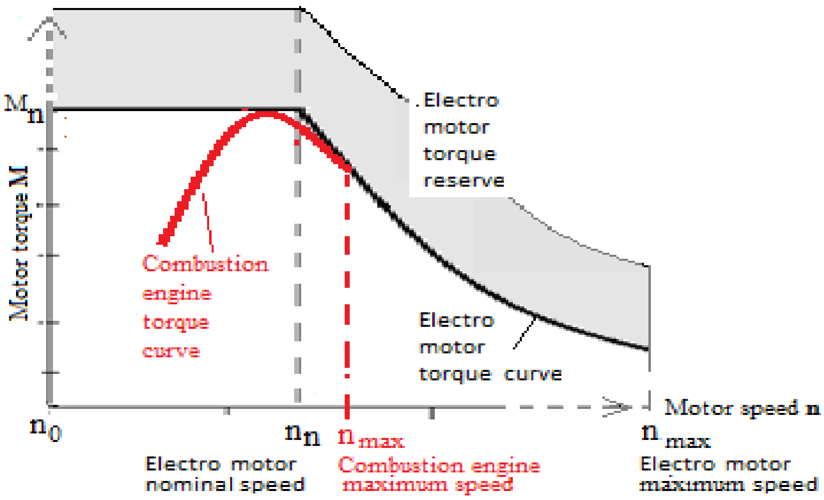

Source: Prepared by the Author.

Whereas the torque curve of the combustion engine reaches a peak next to the maximum speed n_{max}, the electric motor delivers its nominal torque M_n from standstill n_o to nominal speed n_n.

To Mehrdad (2010), the "variable-speed electric motor drives usually exhibit the characteristic that in the low-speed region (up to nominal speed), the motor has a constant torque. In the high-speed region (over nominal speed), the motor has constant power".

Apart from the torque characteristic these motors allow to drive and brake forward and in reverse (Figure 32).

Figure 32 – Forward and reverse torque characteristic of an electric motor

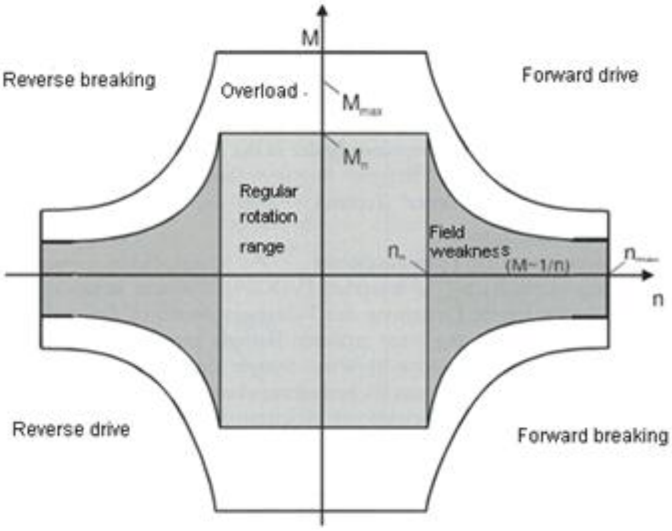

Source: Strategien zur Elektrifizierung des Antriebsstranges (p.92).

Another characteristic of the electric motor that has a significant influence on the tractor's pull characteristic is its torque reserve. For a limited time, it is able to generate several times the nominal torque (see Figure 31 – "Electric motor torque reserve").

A common configuration to power an electric vehicle is a squirrel cage induction motor controlled by a frequency inverter which draws the required energy from the onboard battery (Figure 33).

Figure 33 – Electrical vehicle onboard electric architecture

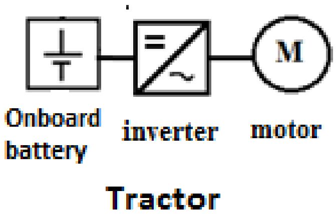

Source: Prepared by the Author.

The inverter allows to control the torque and rotational speed infinitely variable and smooth from zero to maximum (torque and speed). These specific characteristics offer diverse options for the design of the drive train and the overall mechanical layout of an electric vehicle as investigated in paragraph 4.5.2.

2.7.5 *Inverters and converters*

Inverters are electrical current power-conditioning elements. They invert the direct current of an electric energy source in an alternating frequency (AC). Some renewable energy system components like photovoltaic systems (PV) and batteries operate with direct current (DC) but the majority of electrical consumer equipment is running on alternating current (AC). A device (inverter) is required to link the two systems.

Apart from that, inverters align voltage and frequency of decentrally generated electrical energy with the public grid, and therefore allow its injection into it. Finally, yet importantly, inverters make it possible to control the speed and torque of AC electric induction motors. Those motors, when connected to the public grid without an inverter, synchronize with the grid frequency and can rotate only at the fixed, not variable speed of the grid voltage frequency.

The symbol used to describe an inverter is shown in Figure 34. The input is a direct current while the output is an alternating current.

Figure 34 – Symbols to describe: (*a*) inverter and (*b*) converter

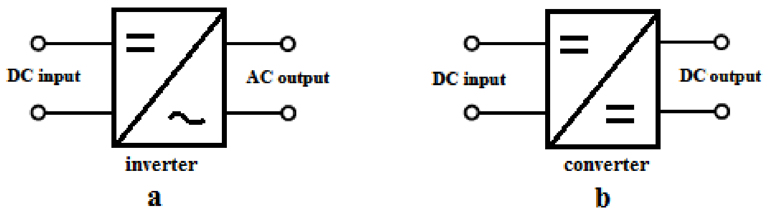

Source: Universität Kassel, 2003

Inverter principles

A simple inverter is a square-wave inverter (Figure 35). The DC current is converted into a square-wave by alternatively closing and opening of the S1 and S2 switches. The use of this type is restricted to loads that can operate with square-wave currents, for example incandescent light, bulbs etc.

Figure 35 – Scheme of a square-wave inverter

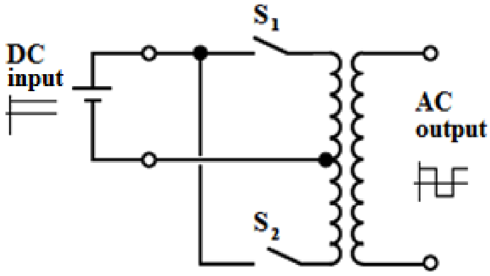

Source: Universität Kassel, 2003

The majority of electrical consumers and the public grids operate on the basis of sine-wave type voltage, known as alternating current (AC). Consequently, sine-wave inverters (Figure 36) are required. With this type of electrical system, the voltage and the matching current at the output is no longer constant and correspondingly, the current at the input will fluctuate. To mitigate this effect, a storage capacitor C1 has to be provided.

Figure 36 – Scheme of a sine-wave inverter

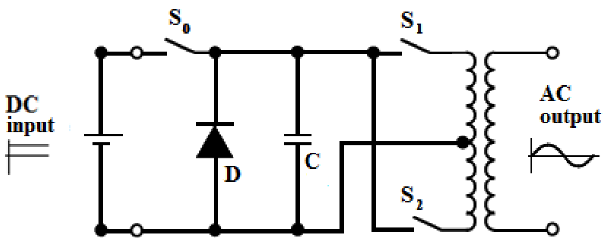

Source: Universität Kassel, 2003

The voltage transformation between the DC source V2 at the output of a converter can be given as in Equation 9:

$$V2 = V1\,\frac{ton}{T} \tag{9}$$

where:

t_{on} = the time when the switch is in ON position; and
T = the time of one switching period.

For applications in combination with public grids and to control AC electric motors, a three-phase inverter is to be used (Figure 37).

Figure 37 – Scheme of a three-phase inverter for control of speed or torque of synchronous AC electric motors controlled by pulse width modulation PWW

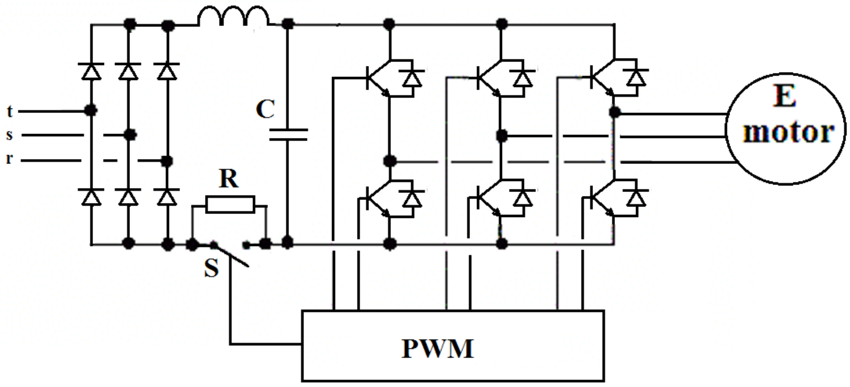

Source: Universität Kassel, 2003

This type of inverter is normally suitable for a power range above 2 kW and is commonly used to control speed and torque of synchronous AC electric motors.

DC to DC Boost – Buck Converter

Agarwal (2015) explains that a DC-DC converter is a power electronics device and converts a DC input voltage into a DC output voltage, whereby the output voltage of the DC converter is different from the input voltage. It serves to match the voltage required to operate the loads. DC to DC converter circuits include a switch (Figure 38), an inductor, a diode and a capacitor.

Figure 38 – Configurations of a boost converter: Position “a” switch S “on”, and position “b” switch S “off”

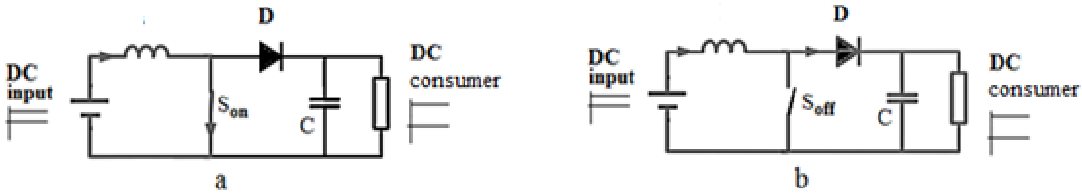

Source: Universität Kassel, 2003

DC to DC converters operate in two modes: Continuous Conduction Mode and Discontinuous Conduction Mode. A pulse width modulator (PWM) usually controls the converter circuit switch.

When this switch is in ON position, then energy will ramp up in the inductor. When the switch is in OFF position for some period, then the inductor's charge will be released until the next switching cycle occurs (Figure 39). The capacitor buffers the charge and discharge cycles.

Figure 39 – Current ramp up in charge and discharge phase

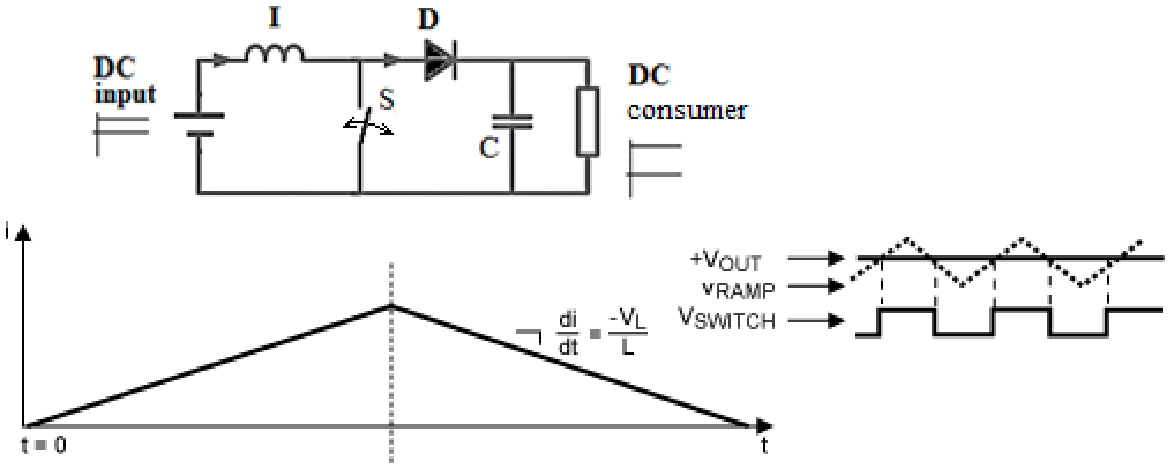

Source: Universität Kassel, 2003

Sequence starts with the charging phase and the switch closed. In this configuration, current ramps up through the inductor. In the next step, the discharge phase, the switch opens and current flows to the load through the rectifying diode.

2.7.6 *Energy management*

The objective of the energy management is to maximize autonomy and efficiency while minimizing the necessary storage and generation capacity and simultaneously ensuring a high degree of energy availability.

That includes the electrical architecture as well as the fluctuating demand and supply characteristic of the power supply system (Figure 40). The strategy is to minimize the necessary storage and generation capacity by simultaneously ensuring a high degree of energy availability, which means the implementation of a hardware/software system that allows the application of the so called Demand Side Management (DSM) techniques.

Figure 40 – Graph showing fluctuating demand and supply characteristics

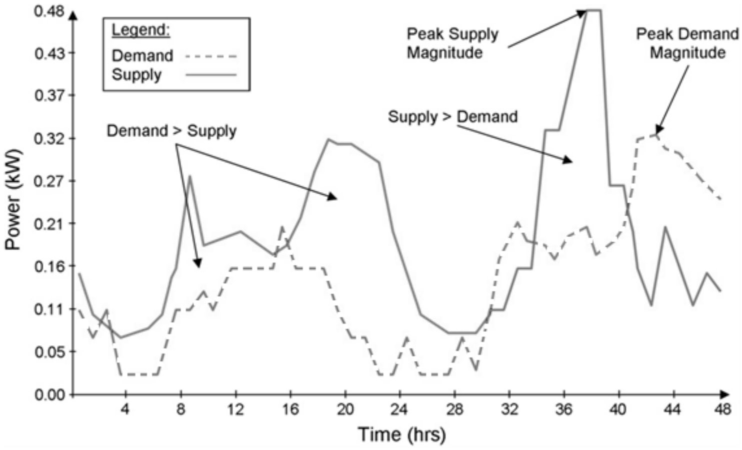

Source: CALLUM, R. BRADLEY (2012).

This concept works mainly with peak clipping, conservation, load building, valley filling, load shifting and flexible load shape. This needs data acquisition like expected and actual energy generation, predicted and actual consumption, consumer priorities, as well as emergency supply requirements (Figure 41).

Figure 41 – The various DSM techniques and their impact on demand profiles

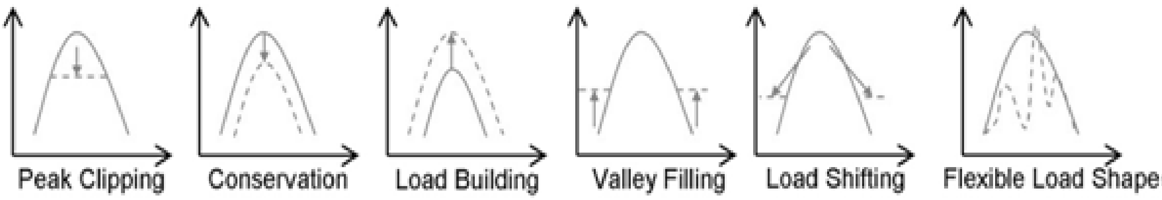

Source: CALLUM, R. BRADLEY (2012).

2.8 Agricultural tractor

To Liljedahl (1989), the tractor has been the central element of motorization and mechanization in agriculture. It changed the farmers live from hard physical work to a more controlling farm work and it improved the quality of field operations. Since human beings are limited to less than 0.1 kW continues workforce output, they must control the power instead of being the power source itself.

The Lanz Bulldog shown schematically below was one of the earlier tractors with internal combustion engine (Figure 42).

Figure 42 – Lanz Bulldog 1922, 12 HP at 420 rpm

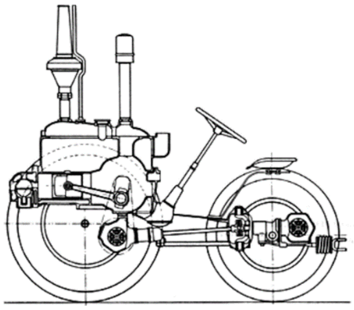

Source: Auerhammer (2013).

During World War II the tractor evolved to be the central mechanical element in western agriculture. This enabled the society to accommodate the increased demand for food and the reduction of the rural workforce. Productivity of the farmer's work had to improve to keep pace with this situation (Figure 39). At this stage, the tractor had already progressed from a substitute of draft animals to an agricultural device of multiple applications such as traction, power take off and mounted implements (LILJEDAHL, 1989).

Figure 43 – Number of draft animals and tractors in the US 1910-1960

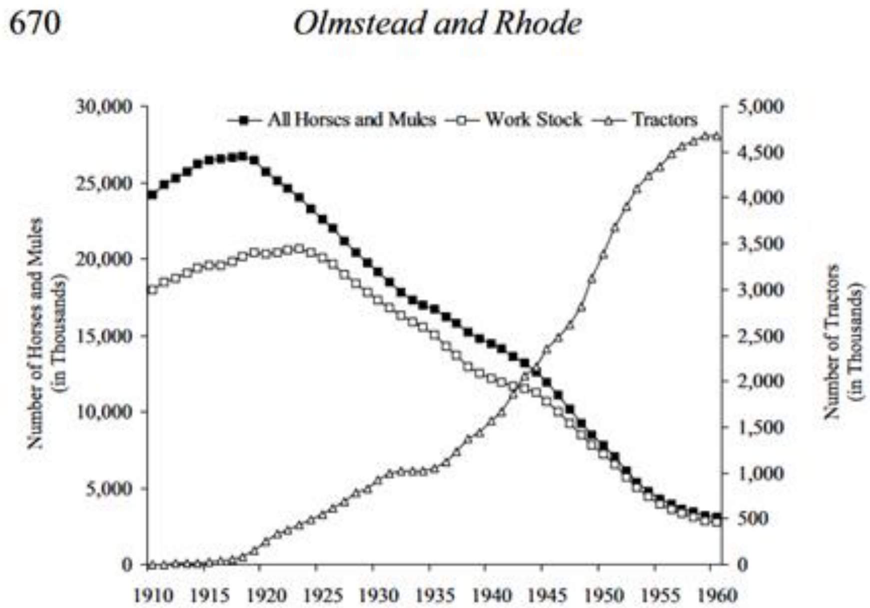

Source: Brodell and Jennings (1962).

In the US, the rapid increase in the number of agricultural tractors was balanced by a sharp decrease in the number of draft animals. Furthermore, the arising market for tractors demanded a regulation for testing. The Nebraska Tractor Test Law of 1919 specified that each tractor sold in the State of Nebraska should be tested and the result be published. These tests were the base of standards for tractors and have improved since then, eliminating types that did not meet design and performance requirements (LILJEDAHL, 1989).

The first tractors were powered by steam engines. The steam plowing engine by J.W. Fawakes in 1858 is known as the first drawing 8 plows at 4.8 km/h. Only after the Otto patent for internal combustion engines expired 1886, it became the new power source for tractors from 1889 on (LILJEDAHL, 1989).

In Brazil, Ford started tractor assembly, under the brand name Fordson, in 1917 (BARICELO and BACCHA, 2013). The tractor increased the effectiveness of the farmer's effort to produce food and allowed the use of land in climatic areas that require intensive and demanding farming (MARQUEZ, 1990).

For the NAE (National Academy of Engineering), the agricultural mechanization is the seventh most important innovation in the twentieth century, more important than the computer or the outer space technology (RUSSINI, 2009).

For a limited period, in the beginning of the 20^{th} century, electric tractors were developed in parallel with combustion engine tractors (Figures 44 and 45). Examples from England, Germany and Russia, and several patents (see Annex) of that time document these efforts.

Figure 44 – Electric tractors

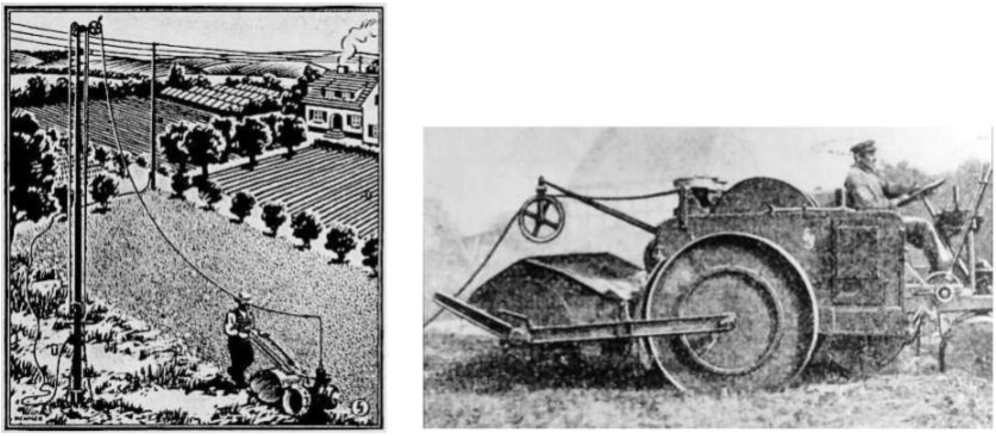

Source: Tallin (2015).

Figure 45 – An electric tractor working alongside a horse team in Canterbury (England) in the 1930s

Source: Tallin (2015).

Among the main advantages of the use of *electric tractors*:

- Zero carbon emissions if renewable energy is used;
- Low noise level; and
- Low operating and maintenance cost, due to the mechanical simplicity and high efficiency of electrical motors (FEDRIZZI, 2007).

Actually, there are isolated efforts to investigate the use of electric tractors, like the project "Renewable Energy Agricultural Multipurpose System for Farmers" (RAMseS, 2006), as shown in Figure 46, a general report on the environmental and agricultural impact of the installed integrated systems on rural communities and stakeholders.

Figure 46 – RAMseS electric tractor, in field tests in Europe and Lebanon, (a) mowering, (b) spraying, (C) seeding) and (d) plowing

(a) Mowering (b) Spraying (c) Seeding (d) Plowing

Source: RAMseS (2006).

Or Kulan, an experimental electric tractor, shown in Figure 47:

Figure 47 – Kulan electric tractor

Source: Kulan (2015).

Currently, commercially available electric tractors are limited to specific applications in vineyards (Figure 48). Big tractor manufacturers like John Deere and Fendt are developing actually their prototypes of heavy electric tractors (Figure 48). John Deere the SESAM equipped with two 150 kW motors and Fendt the e 100Vario with a 50 kW motor (Agri World).

Figure 48 – Examples of a vineyard electric tractor, and two heavy prototype electric tractors: Fendt e 100Vario (left) and John Deere SESAM (right)

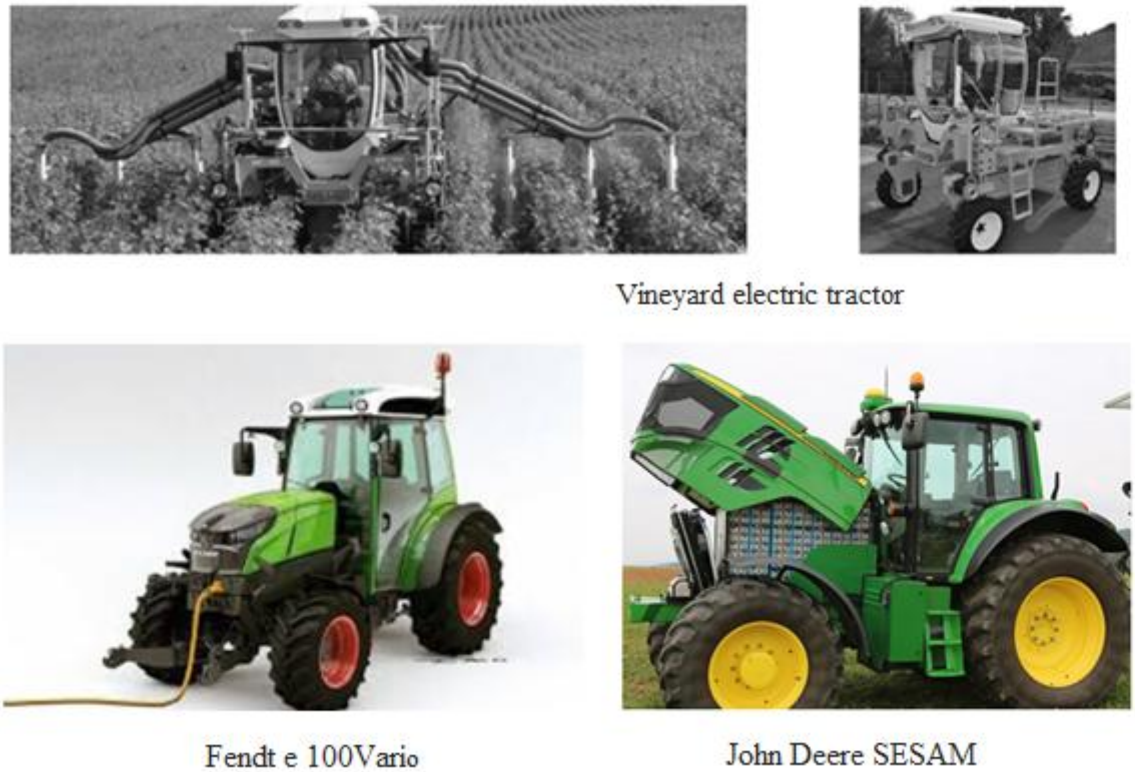

Sources: Kremer (2015) and Agri World (2018).

The standard tractor for small and medium size farms is designed mainly for traction. It is powered by a diesel engine with a rear two-wheel drive. The center of gravity is about one-third of the wheelbase in front of the rear axle. Nowadays, a wide variety of tractor types exist, differentiated in categories of power rating, steering concepts, arrangement of frames, traction methods, application etc.

They are used to propel and operate a variety of implements which in turn affect the design of the tractors. Crop clearance, wheelbase, width, power, weight distribution, safety and operator controls and comfort have to be considered. Implements are generally attached at a three-point hitch at the back or front, trailed, semi mounted or fully mounted (MACIMILLAN, 2002). Power is transmitted to the implement by a power take off shaft, by tapping the tractor's hydraulic system or by the implement's wheels (LILJEDAHL, 1989).

As energy source, today's farming depends almost entirely on crude oil based derivatives. Internal combustion engines transform the chemical energy of the fuel in the necessary mechanical power. The second law of thermodynamics affirms that the efficiency of conversion of heat into work is limited by the upper and the lower temperature in the thermodynamic process and is usually called the Carnot cycle efficiency (Equation 10):

$$e = \frac{T1 - T2}{T1} \qquad (10)$$

where:

T1 = upper temperature;
T2 = lower temperature; and
e = efficiency.

In practice, this limits the useful energy to about one-third of the lower heating value of the fuel. Conventional combustion engines have hundreds of parts, a moderate efficiency and components of reciprocating units stop and go thousand times per minute but, they are the most common energy conversion devices in today's society for mobile applications (LILJEDAHL, 1989).

To allow the driver to carry out all necessary agricultural tasks with efficiency, precision, safety, and a minimum fatigue, human factors play a central role in tractor design. The driver has to be protected from extremes in noise, temperatures, humidity, wind, thermal radiation, dust and chemicals exposure and work in a minimum of comfort to stand the long working hours especially in harvest seasons (LILJEDAHL, 1989).

Noise, as it is slowly causing hearing loss over a long period of years is treacherous because it happens imperceptibly, slowly and painlessly. Nowadays, it is a significant factor to be considered since manufacturers and operators have come to the conclusion that working with tractors over years can damage the hearing ability (Table 4). Hearing loss is a widespread and the most common occupational disease (RENIUS, 1985).

In 1971, the average noise level at the driver's ear position for all tractors without cabin tested at the Nebraska Tractor Test laboratory at 75% pull was 95.2 dB(A). Tractors with cabin had an average of 91.4 dB(A). This lowered to 94.0 dB(A) for tractors without cabins and 79.6 dB(A) for tractors with cabins in 1984 (LILJEDAHL, 1989).

The Walsh-Healy Act in its Table 9.2 defines the official recommendation in the United States to the present suitable levels for noise exposure time per day (see Table 3):

Table 3 – Occupational Safety and Health Act Noise Criteria

Duration per day [hours]	Sound level [dB(A)]
8	85
4	95
1	105
0.5	110

Source: US Department of Labor.

Noise as for its physical properties is a vibration of the air particles in form of a pressure change and a single tone is a sinusoid vibration (Figure 49) at a specific frequency (Equation 11).

$$f = \frac{1}{\mathrm{T}} \tag{11}$$

where:

f = frequency [Hz]; and
T = time [s].

Figure 49 – A sinusoidal vibration with its peak and RMS value

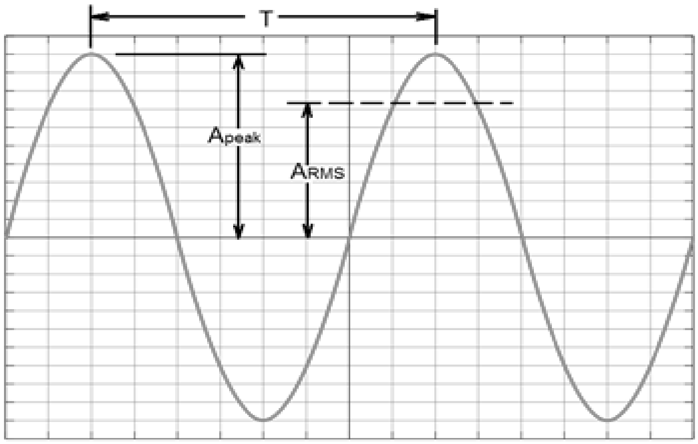

Source: Source: Prepared by the Author

To express the energy content of a tone the Root Mean Square [RMS] is used and is written as (Equation 12):

$$\boldsymbol{A_{RMS}} = = \frac{1}{\sqrt{2}}\boldsymbol{Apeak} \tag{12}$$

where:

A_{RMS} = Energy content [J]; and
A_{peak} = Peak Energy [J].

Table 4 – Typical pressure levels in logarithmic units of dB

dB	Source (with distance)
150	Jet Engine at 30m
120	Rock concert: threshold of pain
110	Accelerating motorcycle at 5m
100	Pneumatic hammer at 2m or inside a disco
90	Loud factory, heavy truck at 1m
80	Vacuum cleaner at 1m, curb side of busy street
70	Busy traffic at 5m
60	Office or restaurant inside
40	Residential area at night
30	Theatre, no talking
10	Human breathing at 3m
0	Threshold of hearing (human with good ears)

Source: Environmental Pollution (2016)[2].

[2] Note: Sound pressure doubles with every 6 dB, but sound power doubles already with every 3 dB.

2.8.1 *Traction Mechanics*

Typical functions of the tractor are inter alia: Provide power in the form drawbar pull (Figure 50), drive and control a range of implements in different ways, function as a transport system in both on-road and off-road conditions (MACMILIAN, 2002).

Figure 50 – Typical power mechanics of traction on a tractor

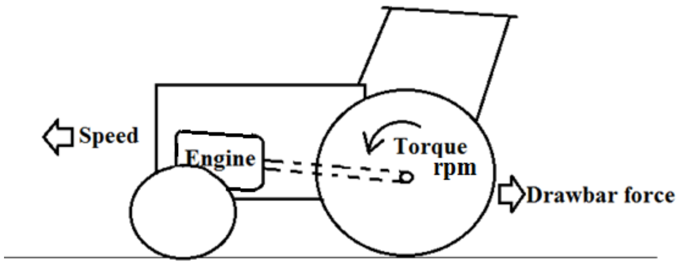

Source: Prepared by the Author.

To meet these requirements, the tractor needs a power source, power train and power outlets, which could be the drawbar, the PTO and/or the hydraulics (Figure 51).

Figure 51 – Schematic power mechanics of traction on a tractor

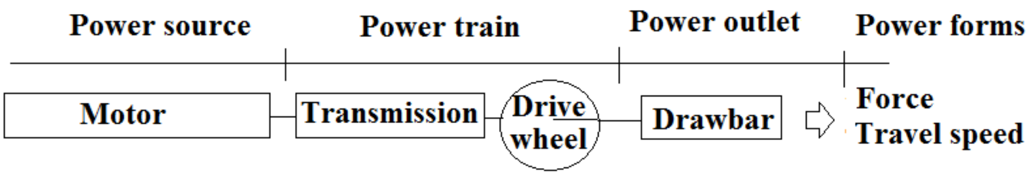

Source: Prepared by the Author.

2.8.2 *Driving and steering systems (BAWDEN, 2010)*

Vehicle design starts usually with a listing of functional requirements considering aspects like:

- ✓ Intended application;
- ✓ Environmental impact;
- ✓ Vehicle operation;
- ✓ Ergonomics;
- ✓ Vehicle dimensions and weight;
- ✓ Payload capacity;
- ✓ Production and manufacturing logistics and costs;
- ✓ Safety; and

✓ Cleaning and maintenance.

Depending on the tractor application envelope, different driving and steering system are applied. The Try-cycle configuration was developed in the US for use in crop rows during the early development stage of the tractor. The present day standard tractor featuring rear wheel drive is presumably the most commonly used tractor type worldwide.

The articulated-frame steering in connection with four-wheel drive tractors is used for special applications e.g. forest work. The skid-steer tractor with four-wheel drive is widely used for landscaping. Crawler tractors are used for landscaping and agricultural work on soft soil. Big farms with thousands of hectares of planted farmland use four-wheel-drive tractors with equal-sized wheels or a four track system and an engine power rating exceeding 500 Hp.

Figure 52 – Driving and steering systems of different tractor types

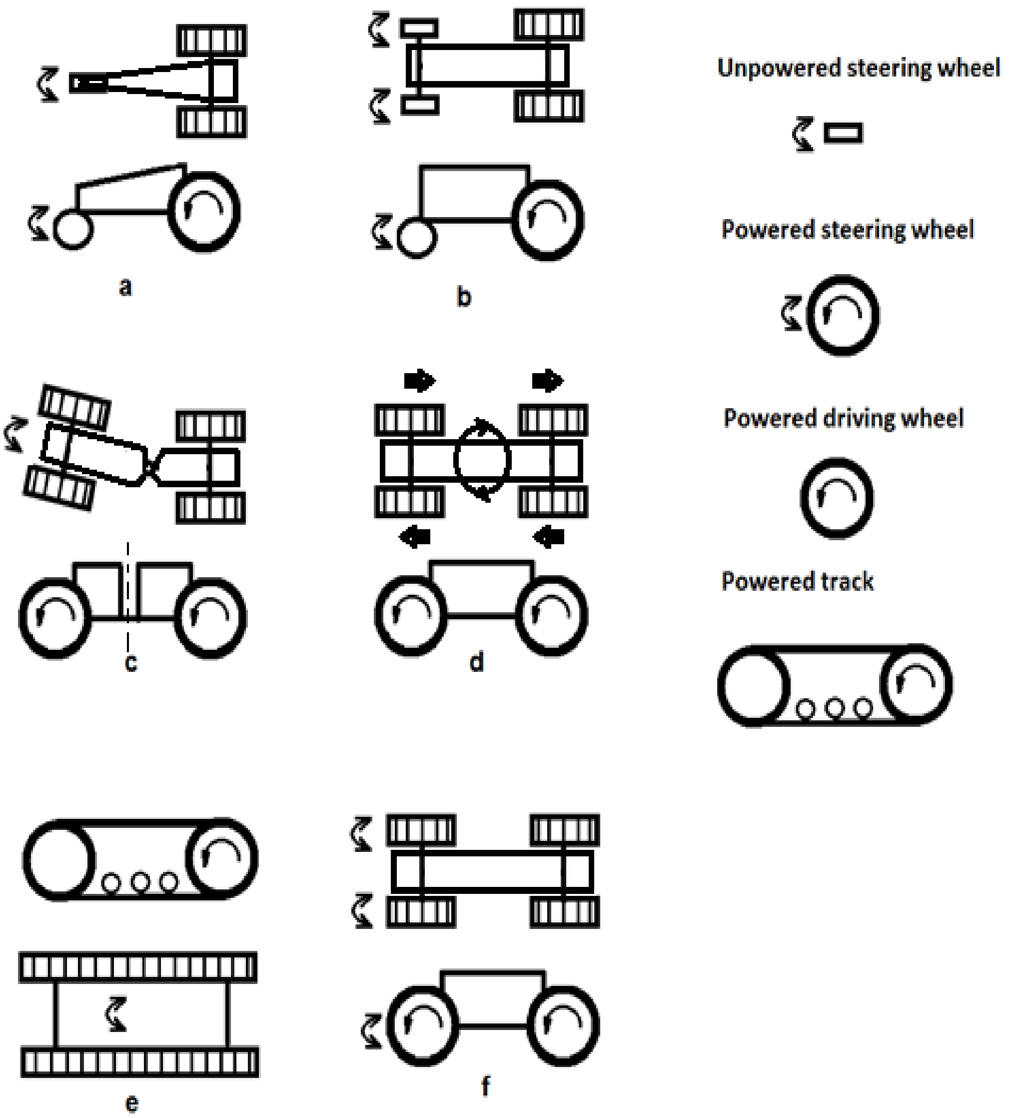

Source: Prepared by the Author.

Figure 52 (above) shows various basic driving and steering system configurations, as described below:

a. Try-cycle tractor with single or dual front wheel (obsolete design);
b. Standard tractor with two or four wheel drive;
c. Articulated-frame steering with four-wheel drive;
d. Skid-steer tractor with four-wheel drive;
e. Crawler tractor; and
f. Four-wheel-drive tractor with equal-sized wheels.

2.8.3 *Steering system of conventional tractors*

Steering gears with a rotational movement as input are used for steering the wheels on rigid front axles as shown in Figure 53 (CROLA, 2009).

The steering has to assist the driver in controlling the direction of the tractor with a minimum amount of force necessary at the steering wheel. The steering gearbox converts the rotary movement of the steering wheel into a translatory movement and limits the steering forces due to the gear ratio. The drop arm is connected to the steering arm of the stub axle via the drag link. Each stub axle has a steering arm which is connected via a track rod with ball-joints at each end. The track rod connects the stub axles and transfers steering forces from one side of the tractor to the other.

Figure 53 – Steering mechanism of a rigid front axle

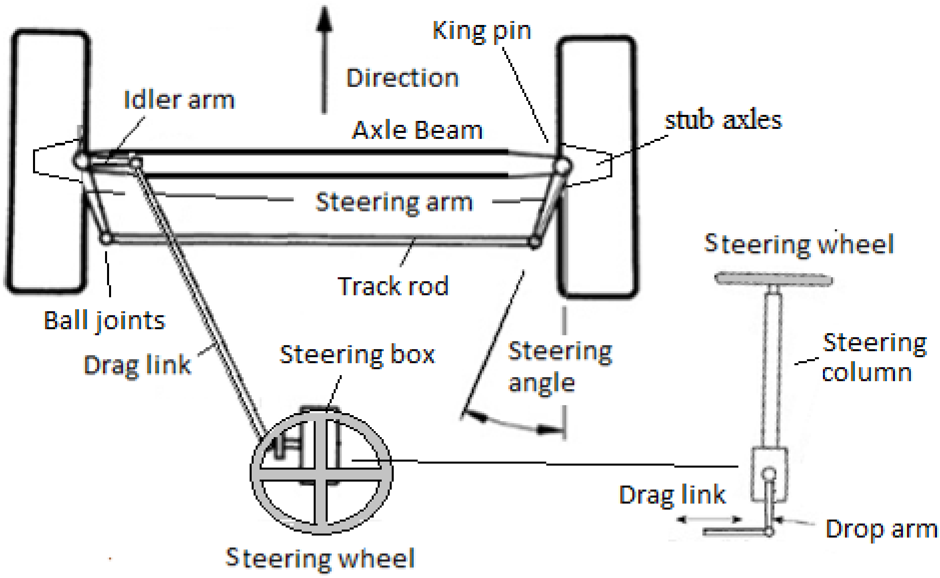

Source: Prepared by the Author.

The tractor wheels and tires have thereby the essential function of supporting the tractor and of converting torque in rotary motion and finally transform it in the desired linear motion of the tractor as a whole (Figure 54). The wheels have to support the weight of the tractor and transmit traction. They have to limit the compaction of the soil, the sinking into the soils surface and the resultant slip and rolling resistance (MACMILLAN, 2002).

Figure 54 – Tractor ground driving elements, tires, tracks and special wheels

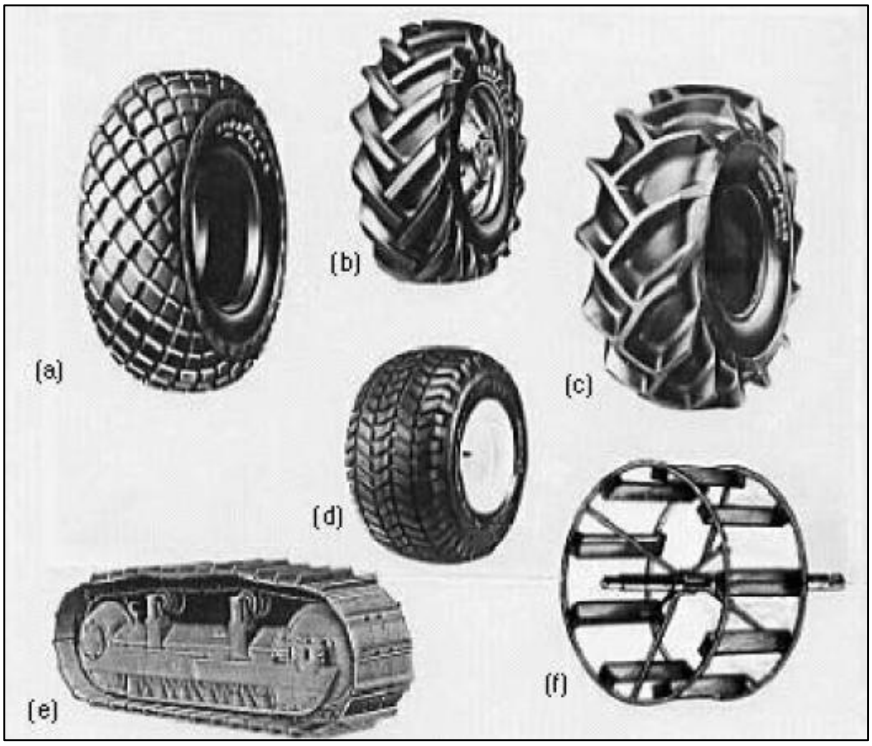

Source: Macmillan (2002).
Note: characteristics of the tires exhibited in this figure are shown in Table 5.

Table 5 – Surface and tread form characteristics of the tires exhibited in Figure 54

	Surface	Tread Form
(a)	Hard surfaces, such as roads	Large area, shallow tread with “high” pressure
(b)	Normal agricultural work	Heavy, intermediate depth tread
(c)	Soft, wet agricultural soils	Deep tread
(d)	Lawns, low sinkage is required	Wide, low pressure
(e)	Dry soil, heavy loads as in earthmoving	Tracks, as on a “crawler” tractor
(f)	Saturated, puddled soils	Metal cage, with angled lugs, alone or as extension to normal tires

Source: MacMillan (2002).

2.8.4 *Tractor performance*

The force sequence on a powered tractor wheel starts with the torque applied and the load (tractor weight) on it. Via the wheel radius, the torque generates a shear force between the tire and the soil. Since soil is compressible and the tire deforms under its load, this results in both a vertical and a horizontal offset (Equation 13), designated "e_v" and "e_h" (Figure 55). The actual amounts depend on the vertical dynamic reaction force (Wd), the tire loaded radius (slr) and on the motion resistance force (MR) (ZOZ and GRISSO, 2003).

$$e_h = \frac{(slr - e_v)(MR)}{W_d} \qquad (13)$$

where:

e_h = Horizontal offset (soft surface);
e_v = Vertical offset (soft surface);
slr = tire loaded radius;
MR = motion resistance force; and
W_d = Vertical dynamic reaction force.

Figure 55 – Deformable wheel on soft surface

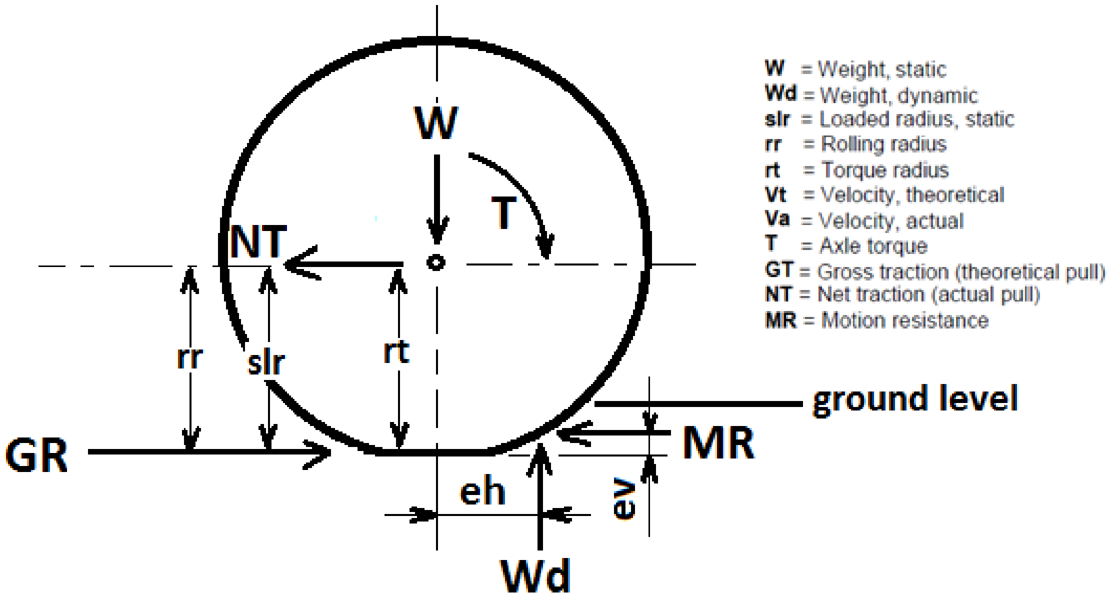

Source: Zoz and Grisso 2003

In Figure 55, *slr* is the *Static loaded radius*, distance from the axle centreline to a hard surface, used for force or moment calculations; *rr* is the *Rolling radius*, derived from the rolling circumference used for speed calculations; and *rt* is the *torque radius*, the effective radius where the gross traction (GT) and motion resistance (MR) forces act, which can be determined by back calculating using energy calculations[3].

When testing powered tractor wheels on a hard surface (ground not compressible) (Figure 56), the vertical reaction force (W_d) is not vertically aligned with the axle centerline; but since the soil in this case is not compressible only the tire deforms under the load. This results merely in a horizontal offset (Equation 14), designated "e_h". The offset amount (e_h) is solely a function of the motion resistance (MR), static load radius (slr) and dynamic weight (Wd) (ZOZ and GRISSO, 2003).

$$e_h = \frac{(slr)(MR)}{W_d} \tag{14}$$

where:

e_h = Horizontal offset (soft surface);
slr = tire loaded radius;
MR = motion resistance force; and
W_d = Vertical dynamic reaction force.

Figure 56 – Basic wheel forces on soft wheel and hard surface (not-compressible ground)

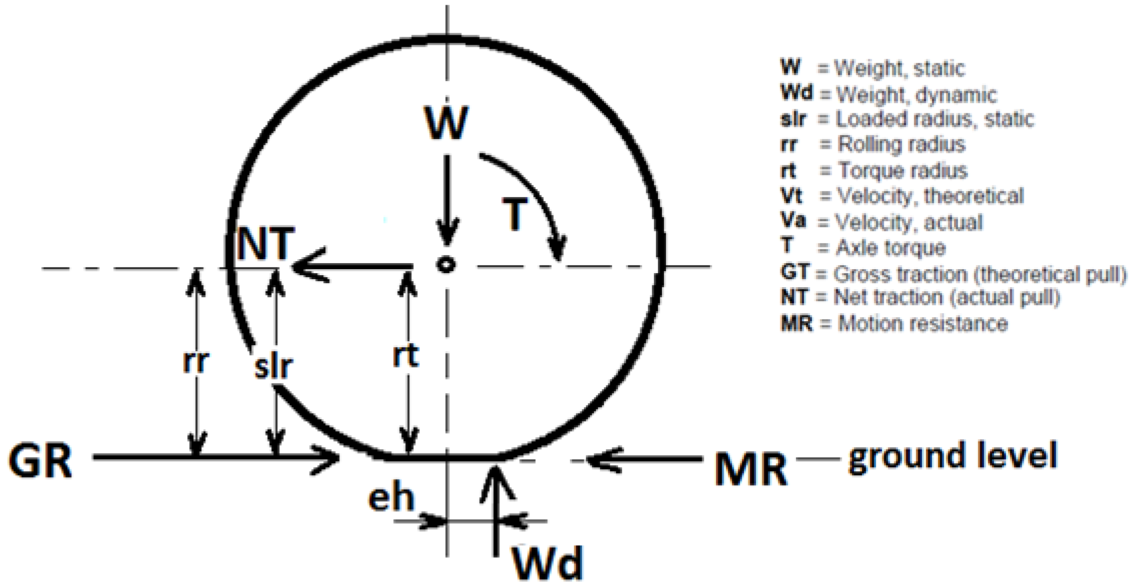

Source: Zoz and Grisso 2003

Draft Angle

[3] Note: Static loaded radius and rolling radius are not identical. The rolling radius is about 6% greater than the static loaded radius (ZOZ and GRISSO, 2003).

The vertical and horizontal offsets "ev" and "eh" result in a resistance opposing the forward movement effort of the wheel and consume in consequence part of the available energy of the advancing tractor.

The travel reduction ratio (TRR) or the slip is a result of flexion of the tractive device, the slip on the interface between tire and soil and the shear within the soil. It is a mechanical loss. Travel reduction (Equation 15) is the theoretical travel speed (Vt) not being completely transformed in forward movement (Va).

$$TRR = 1 - \frac{Actual\,Velocity}{Theoretical\,Velocity} \tag{15}$$

where:

TRR = Travel reduction ratio.

Alternatively, defined as slip of the driving wheels in % it is determined by (Equation 16):

$$\textit{Wheel or track slip (\%)} = 100\,(N_1 - N_0)/N_1 \tag{16}$$

where:

N_1 = sum of the revolutions of the driving wheels for a given distance with slip; and
N_0 = sum of the revolutions of driving wheels for the same distance without slip.

Travel reduction increases with the growing pull force of the tractor (BRIXIUS and WISMER, 1978).

Zero travel reduction is defined by the ASAE Standards, 2001b for self-propelled (zero net traction) condition on a non-deforming surface (ASAE, 2001). Zoz and Grisso (2003) confirm that the zero condition is used to define the rolling radius, since this method provides a repeatable test condition.

Theoretical speed (Vt)

The theoretical speed (Vt) of the tractive device is (Equation 17):

$$Vt = \omega * rr * 2\pi/60 \tag{17}$$

where:

Vt = Theoretical speed [m/s];
ω = Rotational speed (rpm); and
rr = Rolling radius (m).

The forward velocity (Va) of the tractor is measured by using an additional fifth wheel, a radar device, a GPS or is measured by the time needed to travel a defined distance.

Tractive Efficiency

The velocity loss and pull loss determine the tractive efficiency (Eq. 18):

$$TE = \frac{Output\ Power}{Input\ Power} = \frac{NT * Va}{Axel\ Power} \tag{18}$$

where:

TE = Tractive efficiency;
NT = Net Traction; and
Va = Velocity, actual.

Tractive Coefficient

The tractor's pull depends to a significant degree on its weight on the driving wheels. A useful expression to this is the non-dimensional drawbar pull - weight ratio, the Tractive Coefficient (Equation 19).

$$Tractive\ coefficent, \Psi = \frac{Drawbar\ pull}{Weight\ on\ drive\ wheels} \tag{19}$$

Gross Traction Ratio (GTR)

Gross traction (GT) is sometimes called the theoretical pull (not considering losses), as shown below, in Equations 20 and 21.

$$GTR = \frac{GT}{Wd} = \frac{T}{rt * Wd} \quad (20)$$

where:

GTR = Gross traction ratio;
GT = Gross traction (theoretical pull);
W_d = Vertical dynamic reaction force;
rt = Torque radius; and
T = Axle torque.

$$GTR = (NTR/TE)(Va/Vt) = (NTR/TE)(1 - TRR) \quad (21)$$

where:

Vt = Velocity, theoretical;
Va = Velocity, actual;
NTR = Net traction ratio;
TE (ratio) = Tractive efficiency; and
TRR = Travel reduction ratio.

The effective torque radius (rt) is then as shown in Equation 22:

$$\text{rt} = \frac{T}{(GTR) * (Wd)} \quad (22)$$

where:

GTR = Gross traction ratio;
W_d = Vertical dynamic reaction force; and
T = Axle torque.

Motion Resistance Ratio (MRR)

The Motion Resistance Ratio (MRR) is calculated by (Equation 23):

$$MRR = GTR - NTR \qquad (23)$$

where:

GTR = Gross Traction Ratio GTR; and
NTR = Net Traction Ratio.

2.8.5 *Tractor testing*[4]

The performance of a tractor depends on the performance of the engine, the transmission, the tires, the soil characteristic and the interaction between tire and soil (tire-soil interface). The tractor travel speed depends directly on the engine speed, the transmission ratio, effective tire diameter and on the wheel slip. The drawbar pull depends on the engine torque, the transmission ratio, mechanical losses, losses for auxiliary drives and on the rolling resistance. Drawbar power is defined by pull force and travel speed.

The performance of tractors is usually evaluated during practical experimental tests of the complete tractor-implement unit operating under controlled and repeatable conditions.

Comparative testing is also done with the tractor being operated on a firm surface at various travel speeds and at various drawbar loads. Regarding electric tractors, the transmission ratio (the gear) is fixed and the required torque is provided by controlling the current fed to the motor.

A tractor pulling a load experiences a dynamic weight transfer. A method must be used to determine the dynamic weight on the drive wheels.

During the test front (FWS) and rear (RWS) static weights are measured to obtain the correct weight on the tires and to assure the desired weight distribution (Figure 57). Drawbar height (Dh) and wheelbase (Wb) are determined for use in calculating dynamic weight transfer to the rear (dynamic weight (RWD)).

[4] According to ZOZ and GRISSO (2003).

Figure 57 – Two-wheel drive tractor used for tests

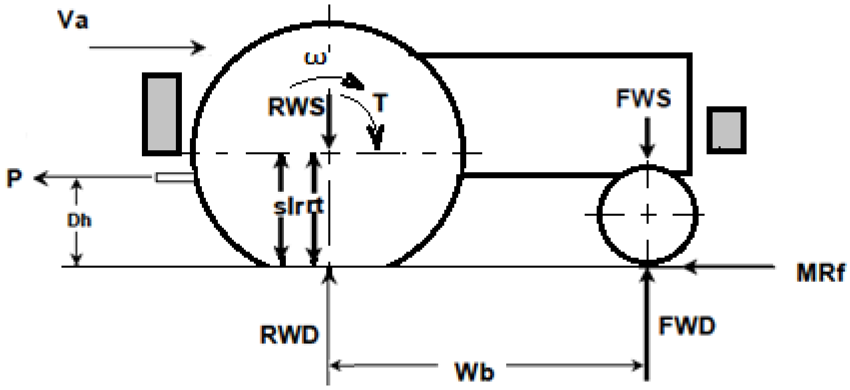

Source: Zoz and Grisso 2003

A second tractor with an implement (fig. 24) can be used to simulate the load. Zoz advises that travel speed of the load tractor (gear and engine speed, set at about 3/4 throttle to allow adjustment up and down) should be set to match the speed of the test tractor.

The implement is operated at a depth that the load tractor can pull, and the drawbar pull applied to the test tractor is adjusted using the throttle of the load tractor. When throttling back the load tractor the load on the test tractor increases respectively (MONTEIRO, 2011). By this, the test tractor is forced to pull more implement load (Figure 58).

Figure 58 – Test tractor with powered load tractor and implement as load

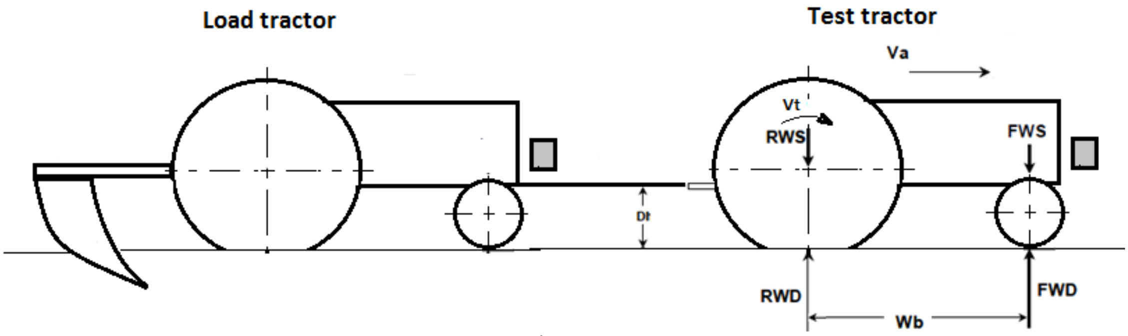

Source: Zoz and Grisso 2003

Testing the performance of tractors requires defined criteria and procedures. The Nebraska Tractor Test Law of 1919 played a pioneering role in regulating tractor testing and publication of test results.

Until today the Institute of Agriculture and Natural Resources of Nebraska Tractor Test Laboratory of the University of Nebraska–Lincoln is in charge for tractor testing in the US. Internationally, the Organization for Economic Co-operation and Development

(OECD) is the regulator of test codes for the twenty-nine countries adhering to the tractor test codes (UNIVERSITY OF NEBRASKA–LINCOLN, 2016).

The OECD Standard Codes for the Official Testing of Agricultural and Forestry Tractors – 2016 allows participating countries to perform tractor tests in accordance with harmonized procedures, and to obtain OECD official approvals (OECD, 2016).

The codes include the testing of:

1. *Tractor performance*: engine power output and fuel consumption; drawbar power; hydraulic power output; hydraulic lift capacity. Optional test procedures including: braking performance, turning area and turning circle; low temperature starting; center of gravity location; external noise level; axle power; engine (bench) test); waterproofing test; and performance at high ambient temperatures;
2. *Noise levels at driver's ear position*;
3. *Operator safety*: Roll-over Protective Structures (ROPS) and Falling Object Protective Structures (FOPS);

The OECD tractor performance test

The published specimen test reports include data such as test conditions, test results, optional test results, repairs, remarks and in its annex various curves.

Terms used in performance testing:

- *Rated Speed* - The motor/engine speed specified by the manufacturer for continuous operation at full load;
- *Engine Power* - Power measured at the output shaft/flywheel;
- *Belt Power* - Power measured at the belt dynamometer (not applicable);
- *PTO power* - Power measured at the shaft designed to be used as a power to take-off;
- *Power at the Drawbar* - Power at the drawbar, sustainable over a distance of at least 20 m;
- *Maximum Drawbar Pull* - The mean maximum sustained pull;
- *Power/Fuel Consumption* - Units of Consumption, specific fuel consumption, mass of fuel consumed per unit of work, specific energy; and
- *Emission Technologies* – e.g. particles, NO_x.

Definitions Relating to Dimensional Measurements and Checks:

- *<u>Preliminary definition: median plane of the wheel</u>* – The median plane of the wheel is the middle from the two planes containing the periphery of the rims at their outer edges;
- *<u>Definition of track (wheel/track)</u>* – The vertical plane through the wheel axis intersects its median plane along a straight line which meets the supporting surface at one point;
- *<u>For track</u>* – laying tractors, the track is the distance between the median planes of the tracks; and
- *<u>Additional definitions</u>*: Median plane of the tractor, Wheel base, Ground clearance, Length, Width, Height.

A table with the following results shall be presented in the report:

– Gear/speed designation;
– Drawbar power, kW;
– Drawbar pull, kN;
– Travel speed, km/h;
– Engine/motor speed, min^{-1};
– Fan speed(*), min^{-1};
– Slip, %;
– Hourly power consumption kWh and hourly fuel consumption, kg/h for a conventional tractor respectively;
– Specific power consumption kWh gross/kWh net, specific fuel consumption g/kWh;
– Fuel temperature(*), °C;
– Coolant temperature(*), °C;
– Engine oil temperature(*), °C;
– Atmospheric temperature(*), °C;
– Relative humidity(*), %; and
– Atmospheric pressure, kPa.

Permissible measurement tolerances (OECD, 2016)[5]:

- Rotational speed: ± 0.5%;
- Time: ± 0.2 s;
- Distance: ± 0.5%;
- Force: ± 1.0%;

[5] These values shall be used unless otherwise specified by a test procedure.
(*) Applicable only for a conventional tractor.

- Mass: ± 0.5%;
- Atmospheric pressure: ± 0.2 kPa;
- Tyre pressure: ± 5.0%;
- Hydraulic system pressure: ± 2.0%;
- Temperature of fuel, etc(*).: ± 2.0 °C; and
- Wet and dry bulb thermometers: ± 0.5°C;

2.9 Project Management

ZOPP is an acronym for the German term "Zielorientierte Projektplanung" which translated into English means "goal oriented project planning (GOPP)" (COMIT 1998). It is a methodology used for the planning of project related processes and the management of a development project throughout its life cycle.

MIT (2016) points out that it was initially called the 'Logical Framework Approach (LFA)' developed for the U.S. Agency for International Development (USAID) and it continues to be a project tool undergoing further refinement by various UN agencies. It has been widely used by multilateral organizations, such as AECID, GIZ, SIDA, NORAD, DFID, SDC, UNDP, EC and the Inter-American Development Bank (RENUCA, 2012).

This methodology is mainly used for designing, monitoring, and evaluating development projects. The planning assessment starts with the initial questions:

- What is the current status? (Initial problems, general conditions)
- What shall be achieved? (Objective)
- How to get there? (Required means and steps)
- What is the expected final outcome? (Hypothesis)

Project planning encompasses the following tasks:

a) Identification

The task of the first step at this stage is to understand the actual situation by evaluating the problems linked to social, environmental, economic and technical issues. The second step is an analysis of the potentials and risks associated with this project, and is concluded with a system of objectives. The project identification, objective and hypothesis definition is based on the problems evaluated in a cause-effect problem tree (Figure 59).

Figure 59 – Example of a cause-effect problem tree

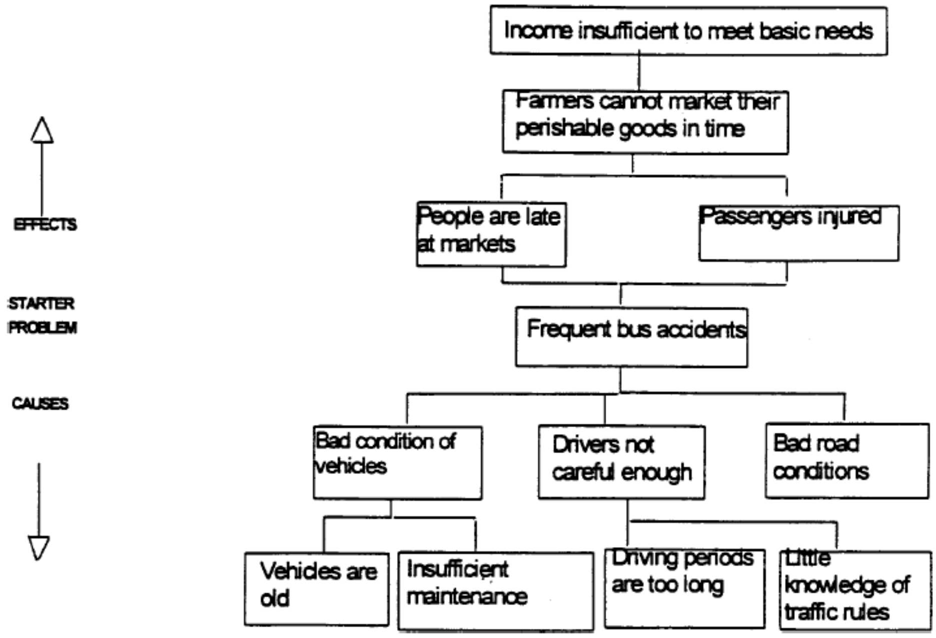

Source: COMIT (1998).

A hierarchy of objectives derived from the problem tree is the next step and the project main objective is determined depending on the scope and intention. The logical framework of cause and effect hypothesis is than the basis for the logical framework. It integrates the analysis of technical and economic feasibility.

b) Planning

This includes the overall project design, a set of milestones to be achieved for the expected outcomes, the main key activities and sub-activities, progress indicators (Figure 60), personal responsibilities and target costs. Objectively verifiable indicators have to be plausible and must target quantity, quality and time.

Figure 60 – Progress indicators

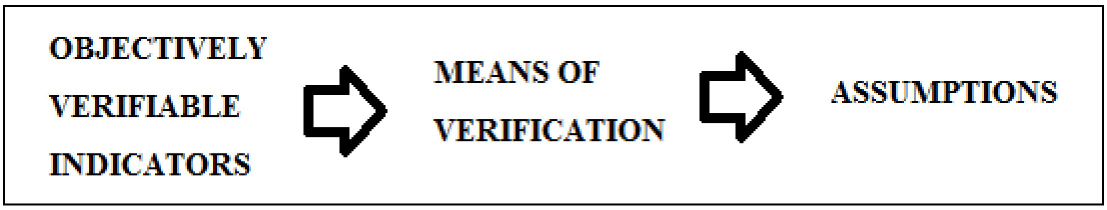

Source: Prepared by the Author.

c) Design

This stage outlines the project approach and defines the technical, organizational, financial, structural set up.

d) Implementation

This is a flexible process adapted to unexpected incidents during the project execution and includes operational planning, regular monitoring and organization of internal structure and external relations. It also includes adjustments and re-planning, and terminates with a report.

e) Final Evaluation

Finally, the evaluation is carried out by assessing the programs' and project's outputs and outcomes which will be reviewed and evaluated in the light of what was initially planned (MUGARUKA, 2014). During this stage deductive methods are applied to confirm (or not) the hypothesis as an indicator of feasibility and efficiency (CRAWFORD, 2003).

f) Review

Based on the review during final evaluation, a lessons learnt report will be produced (MUGARUKA, 2014).

2.10 Development and design

Any innovative design of new processes and products is an indicator of technical development. Technical development relies on proven design methods as key tools to enhance the process of implementing new solutions. Whenever an existing situation is considered as unsatisfactory, it is identified as a problem and becomes a matter of concern.

If it can be assumed that the existing situation can be changed with positive results, the basic process of redesign is started by identifying the root causes of the problem. It ends in case of a successfully conducted development process with the solution. On the way to the solution, a number of different phases have to be passed: From the global problem to the sub problems, to individual solutions for individual problems, to sub solutions and finally terminating with the global solution (Figure 61).

Figure 61 – Development model

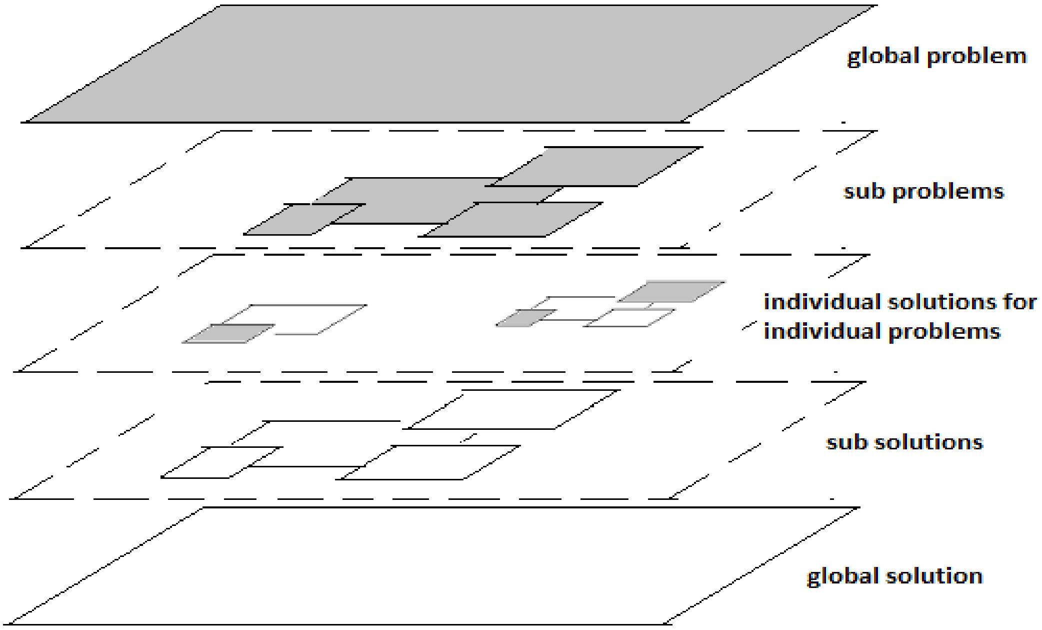

Source: Cross (1996).

Design methods guide the development process. VDI (1993) identifies the following sequence as main steps: Task, Specification, Concept, Preliminary layout, Definitive layout and Documentation. JANSCH and BIRKHOFER (2006) explain that “(...) the goal of this guideline is to propose a general methodology for designing technical systems and products and to support a methodical and systematic design process, in order to produce a more efficient working style”.

The process is highly flexible as it uses knowledge gained during the development process to flow back to adjust, upgrade and improve preceding steps. The sequence of the process together with the interactions between different activities is depicted in Figure 62:

Figure 62 – Guideline VDI 2222

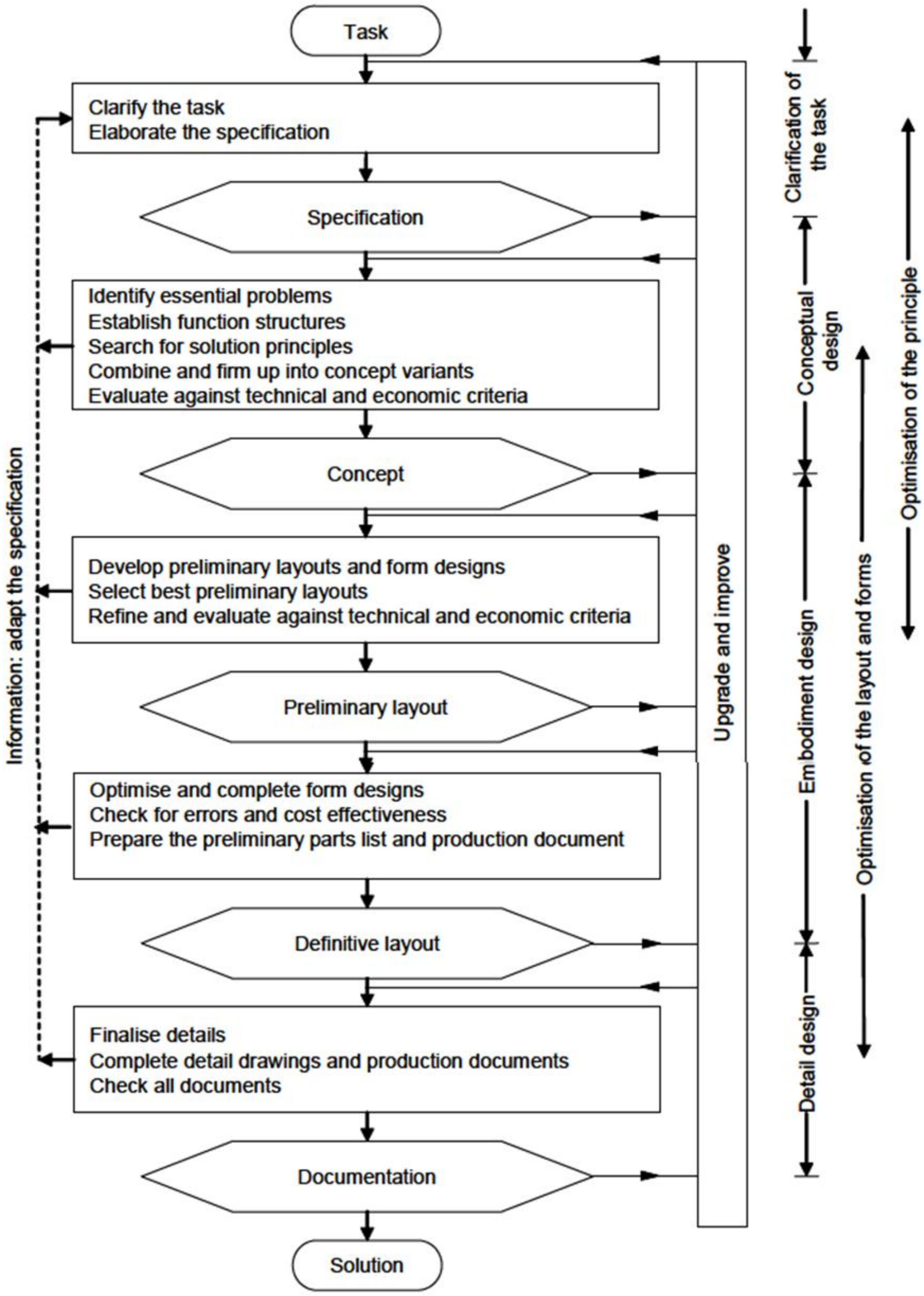

Source: VDI (1993).

In practice, the design process does not stop with the documentation and the definition of the solution. Depending on the complexity, market potential, the technical and economic shortcomings, it will reinitiate the design process to overcome bottlenecks and deficiencies. For innovative and safety sensible technologies a prototype test phase could reveal weaknesses beforehand.

2.11 Failure Mode and Effect Analysis

FMEA was developed by reliability engineers in the late 1950s to study failures that might arise from malfunctions of military systems. In 1963 NASA (National Space Administration) used it during the Apollo mission.

This method facilitates actions to reduce or eliminate the risk associated with those failures. Although the method was important to evaluate the potential failure of processes or systems, it was used in a larger scale by industry only from the year 1977 on, for example by the Ford motor Company for automotive manufacturing (PUENTE, 2002).

The Failure Mode and Effect Analysis is a preventive method and aims to ensure that during the product design potential failure modes and their causes and the associated mechanisms are considered (YUGI, 2006).

This method is used by engineers to ensure that all potential failures as potential effects of faults and potential causes of these failures are considered. It includes also methods to reduce the frequency of occurrence and preconditions for fault detection (TAN, 2003).

According to Liu *et al*. (2013), FMEA allows the identification of potential causes, the evaluation of the causes and effects for various component failures. Apart from that it allows to determine what could eliminate or reduce the possibility of failures. Analysts can identify and correct the failure modes and improve the performance of the product already during the production set up.

Pillay and Wang (2003) state that the failure mode can be understood as a failure category in which the process or product does not have satisfactory performance due to fatigue, collapse, decay, vibration, burns, break ups, etc. The authors also confirm that the potential cause of the deficiency refers to a failure mode and can be caused by incorrect material, corrosion, assembly, excessive heat or cold, improper maintenance, impurity in the material, misalignment etc.

To Albiero (2010), FMEA first identifies the potential failure mode during the product’s life cycle or of a process, and the effects of these failures and finally how critical the effects of these failures are for the product or process functionality.

According to Puente *et al*. (2002), FMEA has two stages: In the first stage it identifies potential failure modes of a product or process and its harmful effects, while in the second stage the effects are analyzed, especially with regard to risks, here namely the critical level of potential failures. Thus, the most critical failure has the first priority to be considered for improvement actions.

The FMEA method follows a logical and systematic sequence of evaluation to identify how a system or process is subject to fail. In this way it is possible to assess the severity of failures, how they may occur, and if so, how these failures may be detected before causing any harm. The method prioritizes failure modes with a greater risk (FERNANDE, 2005).

Thus, the fault priority classification uses three factors: the occurrence (O) which identifies the frequency of failure, the severity (S) which determines the effect of the fault and the form of detection (D) of the failure (LEAL, 2006).

According to Fernandes and Rebelato (2006), FMEA is developed in the following steps:

(1) *Identify potential failure modes and their effects* – all system functions, components, services or processes will be listed and will be identified for all potential failures that may occur during the operation of the product;

(2) *Quantification of the potential effects of failure* – After identifying the failure modes for each function, the effects caused by each potential failure will be determined. Subsequently, the corresponding failure mode will be classified according to the degree of severity. The severity can be classified through tables with pre-determined variation ranges, where 1 is no impact to the customer and 10 a botch;

(3) *Identify potential causes for each failure mode and its probability of occurrence* – Potential causes will be identified and the likelihood of occurrence of each cause will be categorized by means of tables with predetermined ranges ranging from 1 to 10 where 1 stands for are remote chance of occurrence and 10 for a high occurrence;

(4) *Identify what controls are currently in place and rates of likelihood of detection of failure* – The detection procedure allows the identification of faults present in the system design, product, process or service. The probability of detection will be classified by means of tables with predetermined ranges ranging from 1 to 10, 1 is for certain detection 10 and for a remote detection probability; and

(5) *Evaluate the potential risk for each failure mode and set measures to eliminate or reduce the risk of failure*.

The potential risk is associated to the impact, resulting from the combination of fault severity, probability of occurrence and possibility of detection. The risk potential number (RPN) can be calculated by multiplying the severity score values (S) by the occurrence (O) and detection (D) value. It can be classified by means of a scale ranging from 1 to 1000 points, where 1 is considered a very low risk and 1000 a critical risk. All risks exceeding a certain RPN require risk mitigation measures.

The Failure Mode and Effects Analysis can be incorporated into the Design – FMEA (DFMEA) – that aims to analyze and prevent failures in the product during the design process, while in the Process FMEA (PFMEA), the aim is to analyze and prevent failures such as planning errors (LEAL, 2008).

The main advantages in the use of FMEA are:

(1) Improves the quality, reliability and safety of products or services;
(2) Aids in the selection of alternative projects that promise better quality, increased reliability and higher levels of safety; improving the image and competitiveness of the company in the view of the customers;
(3) Is beneficial to improve customer satisfaction;
(4) Reduces the time and cost of developing systems, products, processes and services;
(5) Helps to determine redundancy requirements in the system, product, process or service;
(6) Supports fault diagnostic procedures;
(7) Defines priority actions in the project;
(8) Helps to identify critical features and their significance;
(9) Facilitates the analysis of new manufacturing processes or assemblies;
(10) Assists in establishing a systematic process to establish failure modes and aids to identify and prevent potential failures;
(11) Includes prioritization of corrective actions;
(12) Provides documentation and reference cases, helping future failure analysis; and
(13) Leads to recommendations covering risk reduction actions (mitigations).

2.12 Quality of measurement values and results

Each measurement of a physical quantity is linked with an error. It is therefore necessary to provide an error estimate for the measured value.

Beforehand, it is necessary to distinguish systematic and arbitrary statistical errors.

The systematic error is caused by the measuring system and is often identified by the fact that measured values are generally too large or too small when compared to theoretical calculated values or results of other measurement methods. To minimize systematic errors, the measurement system has to be improved or a numerical correction of the measured result has to be applied.

Statistical errors in contrast are caused by random positive and negative deviations. They are characterized by a probability distribution, indicating how likely a measured deviation from the exact and true value is. Statistics assists in the systematic reduction of variability, contributing to improve the fundamental quality of the measured value (RIBEIRO, 2011).

Mean, standard deviation and measurement uncertainty

In general, the more often a measurement is repeated, the more accurate the probability distribution and the lower will be the statistical uncertainty.

The first estimate of the probable value of a measured value **x** from **n** individual measurements $\mathbf{x_i}$ is obtained by calculating the arithmetic average $\bar{\mathbf{x}}$**,** the mean value (Equation 24).

$$\bar{x} = \frac{1}{n}\sum_{i=1}^{n} xi \qquad (24)$$

If the mean value $\bar{\mathbf{x}}$ is known, the differential amounts **|xi - $\bar{\mathbf{x}}$|** specify the deviations of the individual measurements from the mean. This demonstrates up to a certain degree the accuracy of the measurements.

For numerical reasons instead of using the deviations from the mean value one takes the sum of the squared differences **(xi- $\bar{\mathbf{x}}$)**^{2} from the mean and divides them by the count. This provides the variance. The root of the variance is defined as the standard deviation S (Equation 25) (STÖLZER, 2001):

$$s = \sqrt{\frac{\sum_{i=1}^{n}(\bar{x} - x)^2}{n-1}} \qquad (25)$$

The standard deviation indicates the average statistical deviation of a single measurement. The (positive) root is used with the aim to create a common comparable element for the standard deviation. The division by **n - 1** rather than **n** takes into account that for a single measurement (n = 1) no statistical statement can be made.

Very often, the measured values x_i are normally distributed, i.e.: their relative abundance is a so-called Normal or Gaussian distribution, as exemplified in Figure 63 (MOSTBÖCK, 2011).

Figure 63 – Shape of Normal (Gaussian) distribution

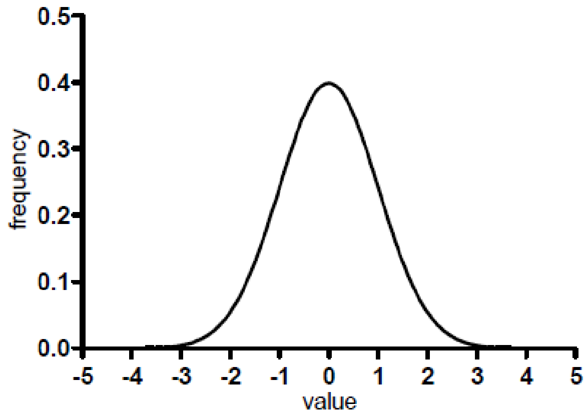

Source: Prepared by the Author

Linear regression focused on the conditional probability distribution of y given X

Often in Physics, a relationship between two variables *x* and *y* is linear (a linear relationship), as shown in Equation 26:

$$y = a + bx \tag{26}$$

Recalling that each measurement is subject to an error, the measured values (x_i, y_i) and the graphical representation of $y_i = f(x_i)$ are measuring points scattered around a line. In this case the search is for a line that eliminates the deviations as good as possible.

The constants *a* and *b* of the linear equation can be calculated by the method of least squares of errors. For this, it is evaluated which constants (*a* and *b*) of the expression represent a (absolute) minimum (UNIVERSITÄT DUISBURG-ESSEN, 2016), as shown in Equations 27 to 34.

$$\Sigma(a + bx - y)^2 \tag{27}$$

In this case, the constants then satisfy the condition:

$$\vartheta/\vartheta a \Sigma\ (a + bx - y)^2 = 0 \tag{28}$$

$$\vartheta/\vartheta b \Sigma\ (a + bx - y)^2 = 0 \tag{29}$$

Differentiation provides the Equations 30 and 31:

$$.\ a\, n + b \Sigma x = \Sigma y \tag{30}$$

$$.\ a \Sigma\, x + b\ \Sigma x^2 = \Sigma xy \tag{31}$$

With the solution shown through Equations 32 and 33:

$$a = \frac{\sum y \sum x^2 - \sum x \sum xy}{n \sum x^2 - (\sum x)^2} \tag{32}$$

$$b = \frac{n \sum xy - \sum x \sum y}{n \sum x^2 - (\sum x)^2} \tag{33}$$

For a best fit line, which is to pass through the origin (a = 0), that is y = b x the appropriate solution is (Equation 34):

$$b = \frac{n \sum xy}{\sum x^2} \tag{34}$$

2.12.1 ***Sample Outlier - Detecting outliers***

Statistics offers several ways to detect outliers (see Figure 64). One of the methods is the so-called ESD method (extreme standardized deviate) also called Grubbs' test[6].

---

[6] More info on Grub’s Test is available at: <http://www.graphpad.com/quickcalcs/Grubbs1.cfm>.

Figure 64 – Outliers in a reference distribution

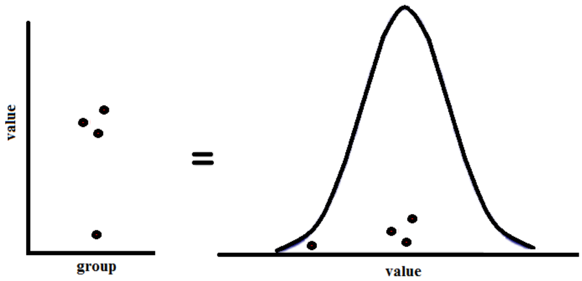

Source: Prepared by the Author

The first step in this methodology is to quantify how far the outlier is from the others. Calculate the ratio Z as the difference between the outlier and the mean divided by the SD (Standard Deviation). If Z is large, the value is far from the others. Note that one has to calculate the mean and SD from all values, including the outlier (Equation 35).

$$Z = (mean - value) / SD \tag{35}$$

When analyzing experimental data, the SD of the population is not known. One calculates the SD from the data. The presence of an outlier increases the calculated SD. Since the presence of an outlier increases both the numerator (difference between the value and the mean) and denominator (SD of all values), with a sample of N observations, Z can never get larger than (N-1) √ N if N=3, Z cannot be larger than 1.155 for any set of values.

If the calculated value of Z is greater than the critical value of the calculated Z, then the P value is less than 0.05. This means that there is less than a 5% chance that an outlier would be encountered so far from the others (in either direction) by chance alone, if all the data are sampled from a single Gaussian distribution.

If that is the case, the question is: “Is this an outlier or is this a value of the population?” The simplest case is a value that lies outside the technical reasonability or which could also be the result of an error in the method. In such a case one has to confirm the technical reasonability and the method.

But if both criteria are satisfied, the value that is just quite high or low could simply be a value from the edge of the normal distribution. Such a value should remain in the analysis! To analyze that, Mostböck (2011) recommends using the Grubbs' Test.

2.12.2 *Analysis of Variance ANOVA*

Analysis of Variance (ANOVA) investigates a relationship between a group of variables and groups of independent variables (qualitative – metrical).The question is: Is there an influence or correlation between these groups?

In effect it tests equality of population means to confirm or reject the null hypothesis which states that the mean between groups of the population is equal. This is to authenticate or discard the hypothesis (H_0 = Null Hypothesis = $\bar{x}_1 = \bar{x}_2 = \bar{x}_3 \ldots = \bar{x}_a$) i.e. that there is no cause-effect significance.

In this respect ANOVA is a cause-effect relevance evaluation to validate or reject the significance of statistical findings.

This is achieved by calculating the Sum of Squares Between groups (SSB) and the Sum of Squares Within groups (SSW). Subsequently, each of these two values is to be divided by its degree of freedom [df]. The result obtained is called numerator and denominator respectively. Division of the numerator by the denominator provides a score of the [F] ratio which leads to acceptance or rejection of the hypothesis considering the standard deviation of the Gaussian distribution.

The actual mathematical process for One-Way ANOVA develops in the following steps:

Definition of the Null Hypothesis H_0

As there is no difference between the means of the groups (Equation 36):

$$\bar{x}_1 = \bar{x}_2 = \bar{x}_3 \ldots = \bar{x}_a \qquad (36)$$

Sum of Squares Within Groups SSW (Equations 37, 38 and 39).

$$\text{Mean of each individual group} = \bar{x} = 1/n \sum_{i=1}^{n} xi \qquad (37)$$

$$\text{Sum of squares of each individual group} = \sum_{i=1}^{n} (xi - \bar{x})^2 \qquad (38)$$

$$SSW = SSG_1 + SSG_2 + \ldots + SSG_a \qquad (39)$$

where:

SSW = Sum of Squares Within Groups; and
SSG = Sum of square group.

Sum of Squares Between Groups SSB (Equation 40).

$$SSB = ((\bar{x}1 - \bar{x}total)^2 + (\bar{x}2 - \bar{x}total)^2 + \dots + (\bar{x}a - \bar{x}total)^2) \times n \quad (40)$$

Then the Total Sum of Squares (SST) is the Sum of Squares Between groups (SSB) plus the Sum of Squares Within Groups (SSW), as shown in Equations 41, 42 and 43:

$$SST = SSB + SSW \quad (41)$$

$$\text{Mean of all observations in all groups} = \bar{x}_{total} = 1/N \sum_{i=1}^{N} xi \quad (42)$$

$$SST = \sum_{i=1}^{N} (xi - \bar{x}total)^2 \quad (43)$$

Final calculations (Equations 44 and 45)

$$\textit{Degrees of freedom SSB} = \textit{number of groups} - 1 \quad (44)$$

$$\textit{Degrees of freedom SSW} = \textit{number of total observations} - \textit{number of groups} \quad (45)$$

Thus, the score ratio F equals (Equation 46):

$$F = \frac{SSB/degrees\ of\ freedom\ numerator}{SSW/degrees\ of\ freedom\ denominator} \quad (46)$$

where:

SSB = Sum of Squares Between groups; and
SSW = Sum of Squares Within Groups.

Confirmation or rejection of the Null Hypothesis

With degrees of freedom numerator and degrees of freedom denominator the critical value is determined with the help of a table (see sample in annex).

Figure 65 – Conditions to confirm or reject the Null Hypothesis

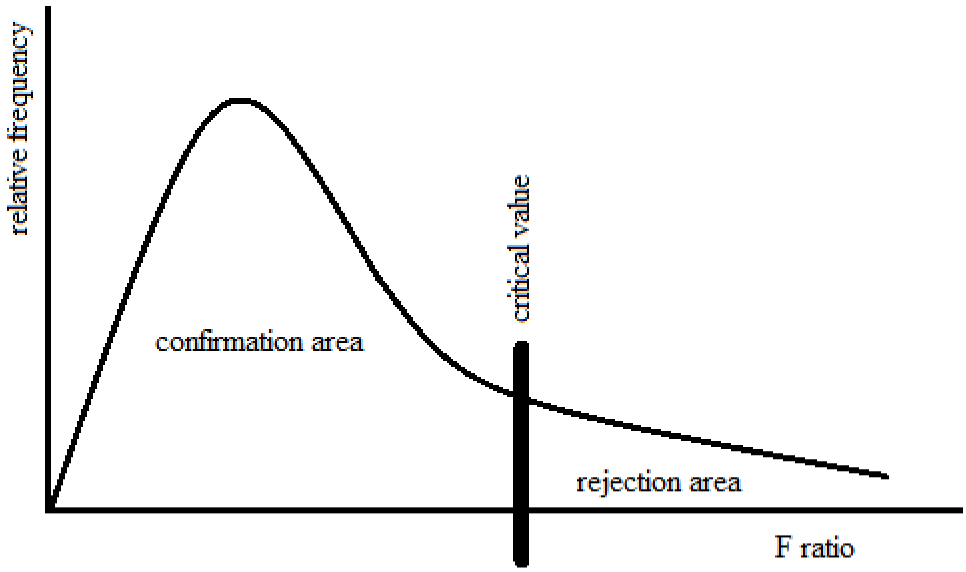

Source: Prepared by the Author

The Null Hypothesis is confirmed if the score ratio F is smaller than the critical value (Figure 65).

This means that there is no relevance between the statistical findings of the groups.

The Null Hypothesis is rejected if the score ratio F is bigger than the critical value. This means that there is relevance between the statistical findings of the groups.

SST = Total Sum of Squares
SSB = Sum of Squares Between Groups
SSW = Sum of Squares Within Groups
N = number of total observations in the experiment
n = number of observations in each individual group
a = highest group ordinal number
x = individual observation
F = ratio

2.13 Commercial value evaluation

A common form of a commercial value evaluation is a cost benefit analysis to evaluate all the potential costs and revenues that may be occur over a given period of time. The outcome of the study will determine whether the project is economically feasible and what the expected gains could be. Costs include mainly direct and indirect costs, and the cost of potential risks. Benefits should include all direct and indirect revenues (MISHAN, 1976).

If the available data are insufficient for a cost benefit analysis, an alternative costs comparative study can show how competitive a new project is in relation to a common reference product used to achieve the projects aims. In this case the relevant technical and commercial properties are compared and weighted with the objective to determine commercial advantages and disadvantages to the common product.

For an agricultural tractor the cost breakdown has to include:

A. Investment costs; and
B. Hourly operating costs.

Costs considered in determining the hourly operating costs:

A. Fixed costs
   i) Depreciation cost; and
   ii) Insurance cost.

B. Variable costs
   i) Repair and maintenance costs;
   ii) Fuel cost or alternatively battery cycle cost; and
   iii) Oil cost, if applicable.

By comparing the hourly operating costs of the two alternatives a measure is obtained for judging the competitiveness of the electric tractor system *versus* a reference tractor.

3 MATERIALS AND METHODS

3.1 Project development method

The overall project starts with the project identification, its characterization and the project planning. The method used for this initial phase is the *Objective Orientated Project Planning.* In this stage the social, technical, and economical, situation is analysed with the aim to identify the central problem. The results of this process are the definition of the project objective and the project hypothesis.

The scientific method to be applied is *Deductive Reasoning* with the aim to falsify or confirm the project's hypothesis. The project implementation method is the combination of the engineering, and the research method.

The engineering method is the *Design method* defining concepts and developing the hardware. The research methods comprise the *Tractor test method*, the *Noise determination method* and the *Cost evaluation method.*

The latter is intended to evaluate the test data and the design with respect to performance and commercial viability.

In the project method scheme (Figure 66), the interaction of the applied methods is shown. It starts with the planning process and concludes with confirming or falsifying the hypothesis.

Figure 66 – Project method scheme

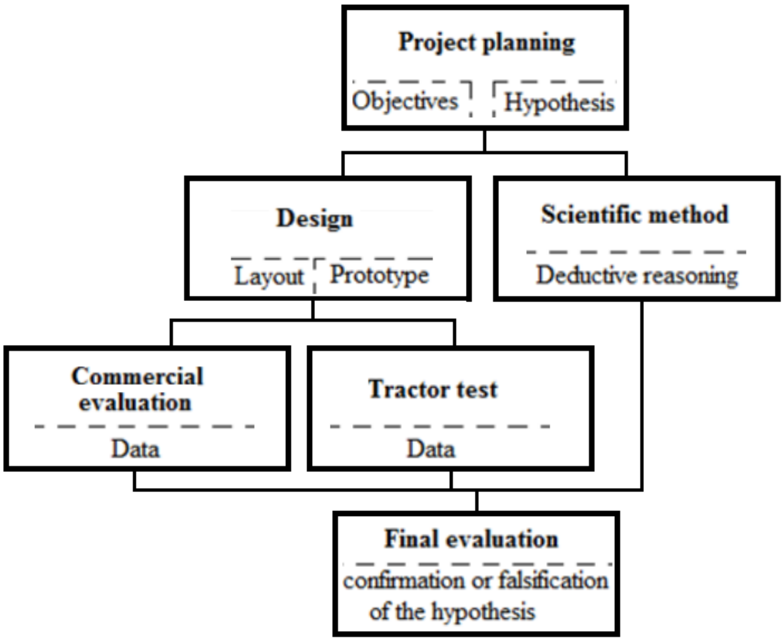

Source: Prepared by the Author

3.2 Prototype tractor

The electric tractor which is used for the experimental test runs is of a prototype design (Figure 67). A sub-objective of the project is to develop a micro electric tractor capable to operate seeding and harvesting implements specifically developed by UFC – DENA for small scale semiarid family farming.

The following programs/methods were used during the design stage of the prototype tractor: Conventional design methods, Computer Aided Design (CAD) and Tabellen dokument (Open Office) for calculations.

Figure 67 – Prototype tractor

Source: Prepared by the Author

The prototype tractor is designed to evaluate the electrically powered drive system and its traction characteristics.

Prototype tractor specification:

Motor data:

- Type: Three phase induction motor
- Designation: Motor Especial 100L IP55
- Manufacturer: WEG
- Nos: 2 motors one for each traction wheel
- Rated Power: 9 kW (two motors with 4.5 kW each)

- Rated voltage: 38 V
- Rated motor speed: 1715 rpm
- Electronic control of motor: WEG Inverter CVW300, 400 A

Inverter data:

- Type: Solid state
- Designation: CVW300, Conversor Veicular WEG,
- Manufacturer: WEG DRIVES & CONTROLS - AUTOMACAO
- Model: CVW300A0400D0NB66
- Rated input voltage: 24-72 V CC
- Rated current at 45 °C: 200 A
- Maximum current for 2 min: 400 A

Battery data:

- Type: Lead acid
- Configuration of battery pack: 4 batteries each with 6 cells
- Rated voltage: 12 V per battery
- Rated capacity: 200 Ah per battery
- Arrangement: serial

Transmission type

- Two stage chain transmission
- Transmission ration
  (gear teeth 10 – 75) = 1:7.5
  (gear teeth 13 – 60) = 1:4.6
  Total transmission ration = 1:34.6

Brakes

- Regenerative braking by the electric motors
- Conventional mechanical drum brake

Steering:

- Mechanical steering gear acting on front axle

Chassis

- Ladder type frame made of 100 mm steel channel

Dimensions

- Wheelbase: 1700 mm
- Overall width: 1400 mm
- Overall length: 2000 mm
- Overall height (driver excluded): 1100 mm
- Ground clearance: 280 mm

Tire sizes

- Front 13 175/70 (with 45 cm outer diameter)
- Rear 295/75 R15 (with 75 cm outer diameter)

Weights and balances[7]*

- Total weight 700 kg (with batteries)
- Front axle 300 kg (150 +150)
- Rear axle 400 kg (200 + 200)

Theoretical speeds and traction forces

- Theoretical speeds and traction forces (not considering mechanical losses)
- Nominal speed (at nominal motor rotation speed) = 6.3 km/h
- Travel speed (at 3 times nominal motor rotation speed) = 19 km/h
- Traction force[8] at nominal motor torque (2 motors x 2316 N) = 4632 N
- Maximum traction forces at 330% maximum permitted motor torque for maximum of 2 minutes = (2 motors x 7643 N) = 15286 N

3.3 Tractor prototype test

3.3.1 *Test location*

The tractor prototype test runs were carried out at the Laboratory of Electronics and Agricultural Machinery, which belongs to UFC-DENA (Department of Agricultural Engineering of the Federal University of Ceará), and is located in Fortaleza, Ceará, Brazil.

The tests are performed on concrete surfaces. This test track is especially dedicated to agricultural machinery. The concrete paved test track is designed as an elliptic

[7] Libra equipment used: NUTEC Fortaleza, during the month of September, 2017.
[8] Traction forces are theoretical values not considering mechanical losses.

round course according to OECD-Code 2 (2008) with a width of 4 meters and a total length of two times 75 meters. (Figures 68)

Figure 68 – DENA test track at UFC Fortaleza

Source: Prepared by the Author.

The test track has the following geographical coordinates, 03º43'02 "S, 38º32'35" W with an average altitude of 19 m.

3.3.2 *Tractor traction measuring devices*

Load cell:

For the tractor traction test, a load cell is used (Model: HBM; RSCC), with a maximum permitted tensile load of 10 kN, as shown in Figure 69.

Figure 69 – Load cell, Model: HBM, RSCC

Source: Prepared by the Author

The load cell measures the traction force between the tractor and the tracking load. The signals are transmitted to a HBM data acquisition logger, Quantum X MX804A, shown in Figure 70. The logger is connected to a portable computer and readings are monitored and recorded in real time.

Figure 70 – Data logger, HBM Quantum X MX804A

Source: Prepared by the Author.

3.3.3 *Noise measuring devices*

To protect humans from noise-induced hearing loss the IEC 61672-1:2013 mandates the use of frequency weighting for working places in noisy environments.

The A-frequency-weighting is used since this is what humans are physically capable of hearing (Figure 71). Equal sound pressure is the Z-Weighting line and the C-Weighting line is what humans hear when the sound power is increased (NTI-AUDIO, 2018).

Figure 71 – Frequency A, C and Z weighting of noise

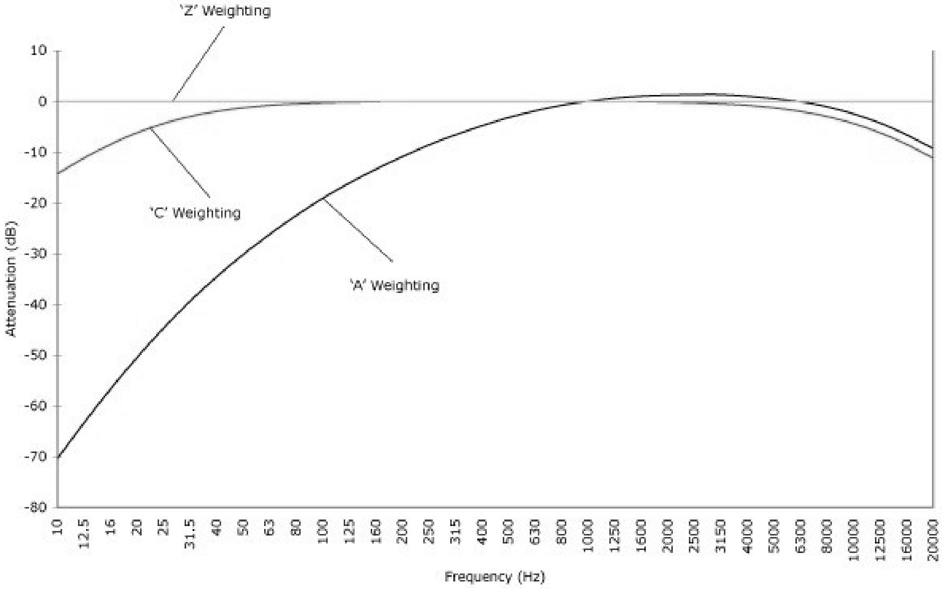

Source: Tingay (2016).

Measuring of the noise to which the driver of the tractor is exposed to is conducted with a personal sound exposure meter (PSEM) in accordance with International standard IEC 61252.

Technical data of the available sound exposure meter:

- Make: VOLTCRAFT SL-200 Sound level meter, Noise meter 31.5 Hz - 8 kHz
- Model number: 411/18
- Applicable Standards: EN 60651 Class 2 and EN 61672 compliant
- Accuracy: ± 1.5 dB (1 kHz)
- Measuring range:30 bis 130 dB A/C
- Frequency range: 31.5 to 8000 Hz
- Sound level resolution: 0.1 dB
- Sound level meter class 2

3.3.4 *Tractor test method*

In order to obtain comparable results, the method used for the drawbar tests is based on the CODE 2document (OECD, 2008). The acquired test data are input to a logger data recording system.

Traction drawbar tests

The signals generated by the load cell are fed into the data recording system. The analysis uses Equation 47 to calculate the mean traction force.

$$NTm = \frac{\sum_{i=1}^{n} Fi}{tp} \tag{47}$$

where:

Fi = Instant measured force at load cell over the time interval between actual and last measurement [kN.s^{-1}];
NTm = Mean net traction force [kN]; and
tp = Test run time on the test track section [s].

Test run velocity

The mean velocity is determined by measuring the time required to cover each test track section of 30 meters in length. The mean velocity is calculated according to Equation 48, where Velocity is expressed in km.h^{-1}.

$$Vm = \frac{s}{t}\ x\ 3.6 \tag{48}$$

where:

Vm = Mean velocity [km h^{-1}];
s = Runway section length [m];
t = Test run time on the test track section [s]; and
3,6 = Conversion factor.

Tractor Wheel slip

By processing signals received from the pulse generators installed on the rear wheel and entering them into Equation xx, it is possible to determine the tractor wheel slip (Equation 49). The wheel slip is determined for the tractor with and without traction load.

$$Slip = \frac{N1 - N0}{N1}\ x\ 100 \tag{49}$$

where:

Slip = Slip at drive wheels;
N0 = Number of pulses without traction load; and
N1 = Number of pulses with traction load.

Drawbar power

The available drawbar power is a function of traction force and velocity and calculated as defined in equation 50:

$$Pd = \frac{Fm \; x \; V}{3.6} \tag{50}$$

where:

Pd = Drawbar power [kW];
Fm = Mean traction force [kN]; and
V = Velocity (km h^{-1}).

Drawbar efficiency

Drawbar efficiency is determined according to equation 51:

$$Ed = \frac{Pd}{Pm} \; x \; 100 \tag{51}$$

where:

Ed = Drawbar efficiency [%];
Pd = Drawbar power [kW]; and
Pm = Motor power [kW].

Traction coefficient

Tractive coefficient Ψ= (Drawbar pull)/ (Weight on drive wheels) is determined according to equation 52:

$$\Psi = \frac{Fd}{Mt} \tag{52}$$

where:

Ψ = Traction coefficient;
Fd = Drawbar pull [kN]; and
Mt = Weight on drive wheels [kN].

Evaluation of the tractor test run results

Processing of the traction and speed data was carried out by using the basic statistic tools of mean and standard deviation.

After concluding the test runs, the arithmetic average, the mean and standard deviation are to be calculated to obtain reliable results to determine the linear regression.

In order to investigate the torque reserve characteristic further tests will be required.

3.3.5 *Noise test method*

Noise determination measurement will be in accordance with the CODE 5, the standard code for the official measurement of noise at the driving position on agricultural and forest tractors (July, 2012).

Two different values are measured:

1. *Continuous sound level*

   This is the time average sound level, usually called the 'equivalent continuous sound level' described in paragraph 3.9 of IEC 61672-1.

2. *Peak sound pressure level*

   This is the absolute peak value to be measured which is relevant for protecting worker’s hearing ability against sudden large pressure peaks using either 'C' or 'Z' frequency weighting.

3.3.6 *Technical evaluation method*

The processing of the traction-speed data will use basic statistic tools, such as mean and standard deviation (SD).

Since the torque characteristic of electrical motors are linear, from 0 to nominal speed, the expected traction on a concrete surface is to be linear too and nearly constant from 0 to nominal speed. This is because mechanical friction losses are limited, especially due to mechanically efficient the chain drive and the tire-soil interaction on the test track.

So, determining the arithmetic mean and the standard deviation is expected to give reliable results in order to determine the linear regression.

3.3.7 *Failure Mode and Effect Analysis method*

To reduce or eliminate the risks associated with functional faults, the Failure Mode and Effect Analysis is applied FMEA. The method determines how critical the effects of failures are for the product functionality and the operator's safety.

In the first stage, it identifies potential failure modes of the tractor and its possible harmful effects, in the second stage, the effects are being analyzed with regard to potential risks and in the third stage remedial actions are proposed.

FMEA systematic is utilized to suggest corrective measures in order to prevent failures when operating the device. For each detected failure mode, a classification in accordance with the tables below is carried out. This encompasses the severity of failure (Sv), the occurrence of failure (Oc) and the probability of detection (Dt). Subsequently, these values are multiplied as given in the following equation 48:

$$RPM = Sv * Dt * Oc \tag{53}$$

where:

Sv = Severity of failure;
Dt = Detection of failure;
Oc = Occurrence of failure; and
RPN = Risk priority number.

The following tables (Tables 6, 7 and 8) provide the criteria for the determination of the values for Sv (severity of failure), Oc (occurrence of failure) and Dt (detection of failure).

Table 6 – Severity of failure (Sv)

Indexes	Severity	Description
1	Mini	Almost impossible to note
2-3	Small	Functioning slightly affected
4-6	Moderate	Functioning severely affected
7 -8	High	Total failure of system
8-10	Very high	Failure of system including safety risks

Source: Albiero (2010).

Table 7 – Detection of failure (Dt)

Indexes	Severity	Description
1	Mini	Easy to notice
2-3	Small	High probability to notice
4-6	Moderate	Chances of not being noticed
7 -8	High	Very likely not being noticed
8-10	Very high	Certainly not being noticed

Source: Albiero (2010).

Table 8 – Occurrence of failure (Oc)

Indexes	Severity	Possibility of failure occurrence
1	Mini	1 in 1,500,000
2	Small	1 in 150,000
3	Small	1 in 15,000
4	Moderate	1 in 2000
5	Moderate	1 in 400
6	Moderate	1 in 80
7	High	1 in 20
8	High	1 in 8
9	Very high	1 in 3
10	Very high	1 in 2

Source: Albiero (2010).

The multiplication of the three Indexes gives the *risk priority number* (RPN). The potential failure is then classified as shown in Table 9:

Table 9 – RPM, Priority and Class

RPM	Priority	Class
01 – 207	No priority	NP
208 – 407	Low priority	LP
408 – 607	Medium priority	MP
608 – 807	High priority	HP
808 – 1000	Top priority	TP

Source: Albiero (2010).

3.4 Energy propulsion system simulation method

The energy system simulation system is a virtual – computer generated system to evaluate the various operating scenarios and cost characteristics.

The design of the system relies on commercially available equipment. It simulates the energy storage system with the batteries, converters and controls. The battery system is designed to store all captured renewable energy that is not instantly consumed.

The layout of the electric transmission system simulates the use of a pivot system fitted with a flexible power cable to hook up the tractor when operating at the fields, thus enabling the tractor to operate with continuous external power supply within the range of this system.

3.5 Tractor cost comparative method

A direct cost-benefit analysis of the electric tractor operated under semiarid conditions by family farms is not included in the scope of this project since reliable data on expenditures and earnings of such farms are not available. Alternatively, a cost study comparing the proposed electric tractor system with a common - commercially available combustion engine micro tractor for agricultural family farming was chosen to assess the economic efficiency of the electric tractor system.

The method is based on the conversion of investment costs and specific operating costs into total hourly operating costs of the two tractor alternatives.

This study determines the complete system costs comprising PV-generator, transmission and storage system, installation and based on the design data the investment costs of the electric tractor. Further includes the purchase price for the system's components and the costs for assembly, debug and start up.

For the combustion engine micro tractor, the base is the market purchase price and the fuel cost. Overheads, like insurance and maintenance, are considered also for the two alternatives as percentage of the investment cost and the period of use (see Figure 72).

Figure 72 – Method scheme of the comparative study

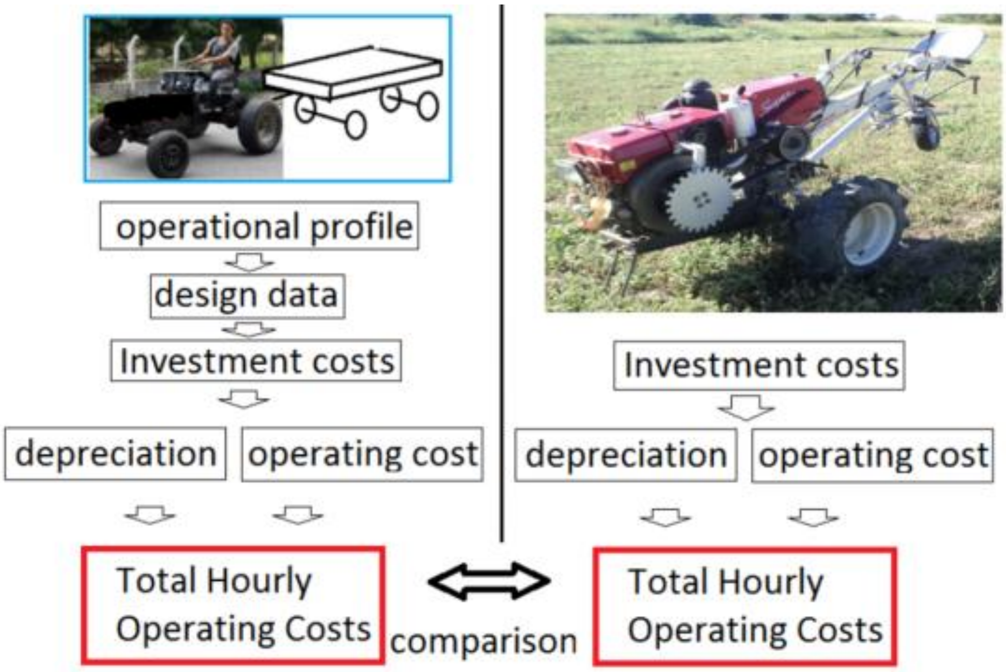

Source: Prepared by the Author

The cost breakdown includes:

A. Investment costs; and
B. Hourly operating costs.

The considered costs were the following:

A. Fixed costs

i) Depreciation cost; and
ii) Insurance cost.

B. Variable costs

i) Repair and maintenance costs;
ii) Cycle cost for the batteries of the electric tractor system; and
iii) Fuel cost of the combustion engine tractor.

The calculation of the hourly operating costs of the electric tractor considers different types of electric tractor system configurations (Figure 72) and the tractor utilization costs based on one to four users (semiarid family farms).

The hourly operating costs are meant to serve as an indicator of the competitiveness of the electric tractor system in relation to a combustion engine micro tractor. They are computed considering the different electric tractor system configurations and the yearly and daily tractor working hours of the two tractor alternatives.

The electric power generation using PV systems brings with it environmental benefits in comparison to a combustion engine powered tractor. However, even though these benefits are important for the world society as a whole, they are of no commercial relevance to the individual farmer. Hence, this aspect has not been considered in this comparative cost study.

3.6 Costs calculation method

The suitability and efficiency of a tractor to carry out agricultural tasks at a plantation is of prime importance for the farmer. In parallel the hourly operating costs are a crucial economic factor.

The hourly operation cost generally depend on the type of tractor, type of motor, type of energy and the operating profile on the farmland.

Since the tractor of this project is designed for semiarid family farming, different alternatives operating profiles are considered with different maximum daily and yearly tractor working hours for the use by one farming family or by a collective of several families.

The cost calculation considers the tractor, the trailer, the cable feed system (Configuration C and D only, Figure 88 and 89) and the PV- Generator as investment that gradually loses its value over a period of time according to a linear depreciation. The batteries in contrast, lose their initial value with the amount of the charge-discharge cycles and the depth of the discharge. Hence, the cost of batteries is included in the direct operational costs (similar to the fuel burn of the combustion engine tractor in the total hourly operating costs.

The applied depreciation calculation for the time dependent components is as follows.

Yearly depreciation (Equation 54)

$$DY = \frac{IIC - RV}{DPY} \tag{54}$$

where:

IIC = Initial investment costs (for the electric tractor this includes PV - energy generator);
RV = Residual value at the end of the depreciation time;
DPY = Depreciation period in years; and
DY = Depreciation per year.

Hourly depreciation (Equation 55)

$$HD = \frac{DY}{UHY} \tag{55}$$

where:

UHY = Utilization hours' yearly; and
HD = Hourly depreciation.

The hourly fixed costs (Equation 56) are calculated as:

$$HC_{fix} = HD + Ov \tag{56}$$

where:

HC_{fix} = Hourly fixed costs; and
Ov = Overheads (Insurance and maintenance).

The Battery cycle costs are derived from the number of cycles and the depth of discharge (Equation 57):

$$CC = \frac{BIC}{NC * DD} \tag{57}$$

where:

BIC = Battery investment cost per kWh storage capacity;
CC = Cycle costs (per kWh);
NC = Number of cycles during useful battery life; and
DD = Depth of discharge.

The cost for one-hour tractor operation at an average power level of the nominal tractor power (Equation 58):

$$BC = HRE * CC * APL \tag{58}$$

where:

HRE = Hourly required energy for the electric tractor operation at nominal power[kWh]; and
APL = Average Power Level.
BC = Battery Cost per tractor working hour

The tractor hourly cost (Equation 59) is than the sum of the hourly cost plus the battery cost (Figure 73):

$$THOC = HC_{fix} + BC \tag{59}$$

where:

HC_{fix} = Fixed Hourly costs; and
THOC = Tractor hourly operation cost (at average power level).

Figure 73 – Cost Calculation method scheme of the electric tractor system

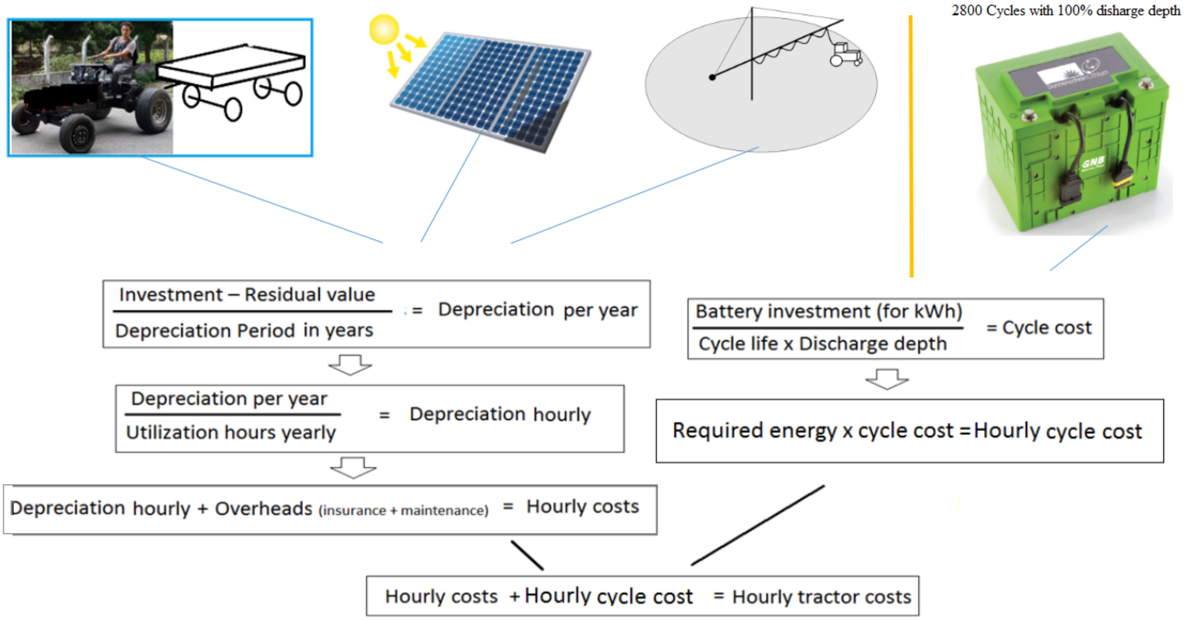

Source: Prepared by the Author

For the comparative - common combustion engine micro tractor, the hourly operation costs are calculated in the same manner. The only difference is that the fuel costs enter the equation (Eqs. 60 and 61), instead of the battery cycle costs (Figure 74).

$$HFC = HFC_{on} * FC \tag{60}$$

where:

HFC_{on} = Hourly fuel consumption;
FC = Fuel costs; and
HFC = Hourly fuel cost.

$$ThC = HC + HFC \tag{61}$$

where:

HC = Hourly costs; And
ThC = Tractor hourly cost.

Figure 74 – Cost Calculation method for the Common Comparative tractor

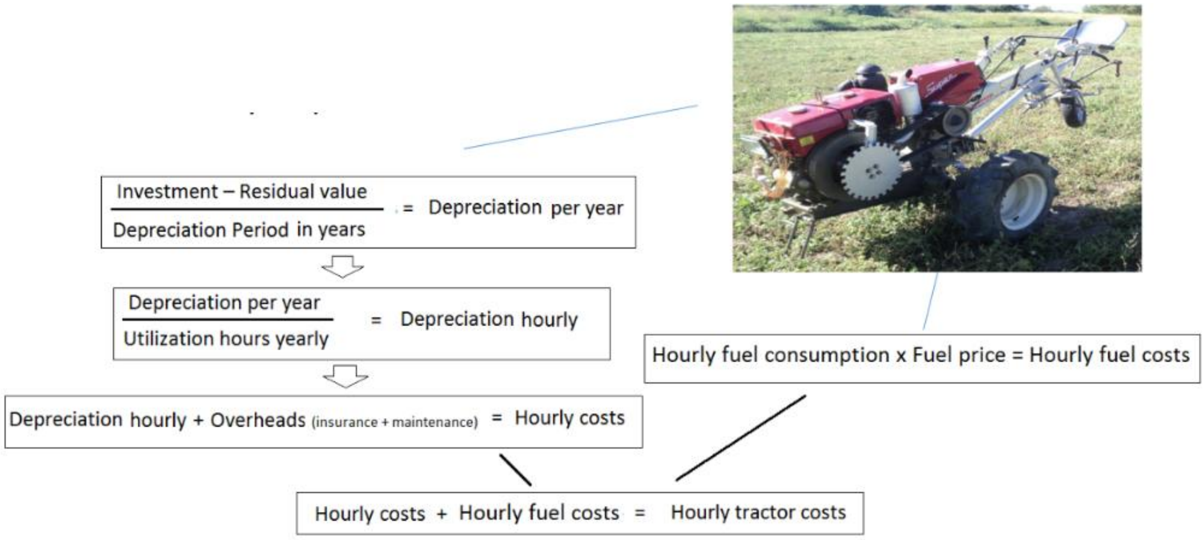

Source: Prepared by the Author

4 DEVELOPMENT

4.1 Project planning

The project conception is based on the assessment of the living conditions and the working environment of semiarid farming families in the Northeast of Brazil. Based on this analysis of the present situation, a list of socioeconomic key points has been elaborated:

- ✓ *Rural exodus* – young people migrate to urban centers in search of better living conditions;
- ✓ *Poor (or extremely poor) families* – subsistence farming makes adequate housing unaffordable (often make-shift houses made of clay and wooden sticks);
- ✓ *Lack of human resources* – labor intensive manual planting and harvesting methods require excessive manpower;
- ✓ *Unaware of efficient farming methods* – as access to appropriate training institutes is limited (available places and costs);
- ✓ *Low productivity* – lack of motorized implements, fertilizers, high yielding seeds and agrochemicals preclude the potential yield of modern agriculture;
- ✓ *Waste of agricultural resources* – heavy losses due to weeds and pests, no cooling facilities, long transport times to markets etc.;
- ✓ *Inappropriate infrastructure* – poorly developed and maintained access roads, insufficient and water wasting irrigation systems, no or limited access to safe drinking water; and
- ✓ *No specifically adapted machinery for semiarid family farming* – low income farmers represent no business case for industry, renewable energy was economically not feasible.

Unfavorable environmental conditions:

- ✓ Regular droughts; and
- ✓ Hot equatorial climate with high evaporation rate.

The cause-effect hierarchy tree as depicted below represents a conversion of the above listing of relevant circumstances (Figure 75).

Figure 75 – Cause-effect hierarchy semiarid farming families' problem tree

Source: Prepared by the Author

Since detrimental effects such as lack of human resources, transfer of knowledge, inadequate professional skills and the drought that regularly afflicts the semiarid farming region cannot be resolved by resources available for this project, the specific problem of "No machinery adapted for semiarid family farming available" had to be selected as the one to be worked on. Consequently, it is transformed into an objective: "Machinery adapted for semiarid family farming".

Thus, the overall scope of the project is to investigate and qualify powering and mechanization techniques for small-scale farming in semiarid regions.

A crucial and decisive factor for introducing mechanization is the availability of energy in the appropriate form and at economic terms.

In connection with renewable solar energy in the targeted region, the following boundary conditions play a decisive role:

1. The availability of a median irradiance of >5kWh per square meter per day;
2. That Photovoltaic electric energy production is a competitive form of usable energy; and

3. That in the future mechanization has to be based on nonpolluting energy sources.

Hence, the specific objective relating to the type of energy to be used for mechanization is defined as clean energy from renewable sources – particularly solar energy which is extensively available in the region. The intent is to convert it locally into electric energy by photovoltaic panels.

The system as a whole with its various components is intended to generate, store and transfer electric energy to the consumers, thus enabling the farmer to propel a micro farm tractor for soil preparation, cultivation and harvesting. Furthermore, the collected surplus energy (not consumed by the tractor) will serve to operate other electric consumers of the community for the purpose of water pumping, lightning, communication, refrigeration and processing and/or will be commercialized if there is an opportunity.

In general, the design of the energy system will include the following subsystems:

1. Clean energy generation system;
2. Storage system for balancing energy generation and consumption;
3. Transmission system; and
4. Appropriate electric energy consumers with emphasis on powering an electric tractor.

Since implements for the use on semiarid family farms are in development by the Federal University of Ceará (UFC), the genuine intend of the project is therefore to fill the gap by developing a tractor tailored for the specific climatic and farming conditions of the semiarid family farms in the northeast (Figure 76).

Figure 76 – The genuine intend of the project

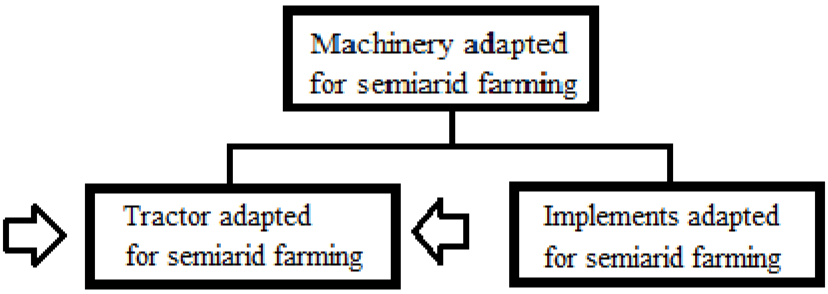

Source: Prepared by the Author.

The particular pioneering purpose to be accomplished and to be evaluated is a technically and economic feasible layout of a local renewable energy system that allows propelling an electric micro tractor in conjunction with the development and testing of a prototype electric micro tractor to operate implements specifically designed for small scale semiarid family farming.

The required steps to get there are:

1. Definition of project scope;
2. Planning of activities and methods to be applied;
3. Layout of the renewable energy system;
4. Development of a prototype electric micro tractor;
5. Testing of the prototype electric micro tractor;
6. Evaluation of the prototype tractor; and
7. Evaluation of the integral system in terms of its technical and economic feasibility.

The layout of the renewable energy system is elaborated in accordance with the following steps:

1. Conception of possible layouts for generation, storage and transmission of electric energy; and
2. Technical design of the selected renewable energy system.

The development of a prototype electric micro tractor will include:

1. Determination of required performance and capabilities (datasheet);
2. Selection of tractor main components: onboard energy storage, motor, mechanical, electric and electronic components;
3. Design of the electric and- electronic tractor subsystems;
4. Layout of drive train;
5. Layout of chassis with optimized weight balance, controls and safety features;
6. Manufacture of a prototype tractor; and
7. Preliminary function and safety tests.

The activity planning is exhibited in Table 10, and the cost sheet for the prototype tractor in Table 11 (below).

Table 10 – Activity planning for the period 2017-2018

No.	Main steps	Activity	Location	Time schedule 2016	2017	2018	Costs (Euro)
1	**Energy system**						
		Concept layout	Fortaleza	XX----	--------	--------	none
		Physical layout	Wuppertal	----XX	--------	--------	none
2	**Tractor prototype**						
		Required performance	Fortaleza	XX----	--------	--------	none
		Selection of components	Fortaleza	----XX	--------	--------	none
		Electric layout	Fortaleza	----XX	--------	--------	none
		Drive train layout	Fortaleza	----XX	--------	--------	none
		Chassis design	Fortaleza	----XX	--------	--------	none
		Manufacture	Fortaleza	------X	XX----	--------	11,892
		Function test	Fortaleza	--------	----XX	--------	none
3	**Evaluation**						
		Method definition	Fortaleza	XX----	XX----	--------	none
		Tractor test runs	Fortaleza	--------	------X	X------	"
		System evaluation	Fortaleza	--------	XXXX	X------	"

Source: Elaborated by the Author.

Table 11 – Cost sheet for the prototype tractor

Description	Quantity	Costs (in Euro)
Motor	02	1,351
Inverter	02	3,784
Mechanic Material	-	1,622
Electric Material	-	2,838
Service and Installation	-	2,297
	TOTAL	**11,892**

Source: Elaborated by the Author.

4.2 Electric tractor propulsion system

In this chapter, conceptual considerations for the energy generation, storage and transmission systems are presented. In general, commercially available equipment is being considered for the energy generation system (Figure 77). For semiarid family farming, conversion of solar power by means of the photovoltaic principle is favored. (For other regions and agricultural societies alternative renewable energy sources like wind and biogas generation could be considered).

The technical and economic viability of the system depends on the assessment of specific local conditions such as, meteorology, topography, land use and availability, types of consumers, grid connection etc.

Where grid connection is available locally produced renewable surplus energy can be injected into the grid and recovered from there when necessary. Thus the grid assumes the function of a virtual energy storage system.

Figure 77 – Local grid for sustainable semiarid family farming

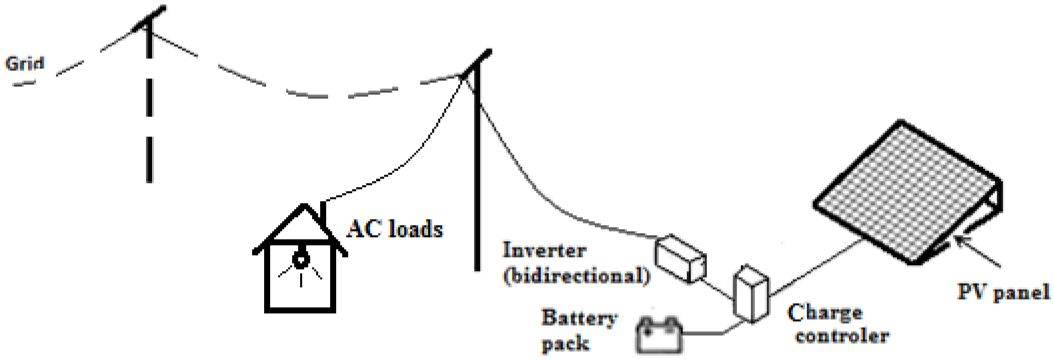

Source: Prepared by the Author.

4.2.1 *Electric tractor energy provision model*

For the electric tractor to move independently, the crucial challenge is (as with other electric vehicles) to store sufficient electrical energy onboard for an extended operating time. The energy storage system is a combination of base – and tractor onboard battery packs.

The concept is based on exchangeable battery packs in order to enable the tractor to operate in plantations for an extended period. Basically, the tractor runs on the onboard battery pack and whenever the battery pack is exhausted it is exchanged for a fully charged one (Figure 78).

Figure 78 – Exchangeable battery packs

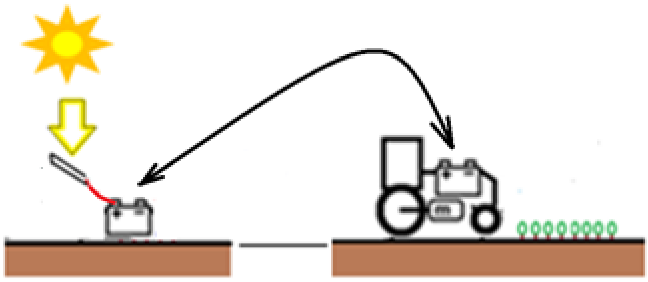

Source: Prepared by the Author.

If a grid connection is available, the grid will assume partly the electrical energy storage function from the base battery. In this case locally produced renewable energy that surpasses the consumption will be injected into the grid and will be recovered later when consumption needs are surpassing the local generation.

Based on an analysis of the flow of energy between the electricity generation system at the home base and the tractor, two principal scenarios are here considered:

I. *Battery charge and battery swap at the home base*

By exchanging the discharged battery on the tractor at the base, the tractor runs exclusively on the (exchangeable) onboard battery (Figure 79).

Figure 79 – Battery swap at the home base

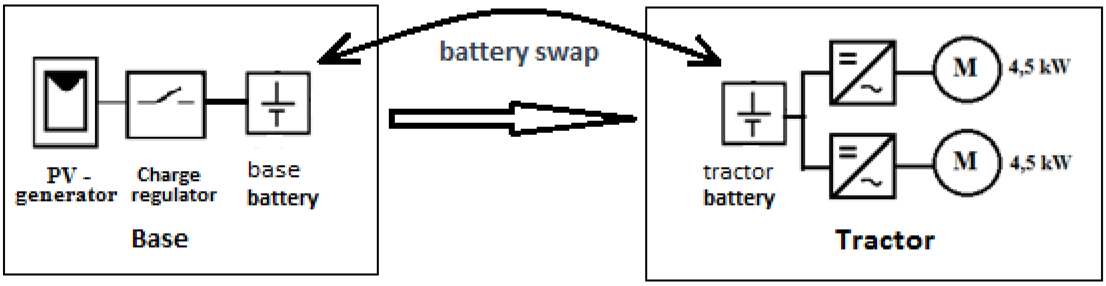

Source: Prepared by the Author.

II. *Energy transmission to tractor via cable feed system*

When transiting or working outside the range of the cable feed system, electric energy flows from the tractor's onboard battery via the onboard inverters to the motors.

Working inside the range of the cable feed system and being hooked up, the energy flows from the stationary battery via a cable and an inverter to the tractor´s motors (Figure 80). In this case the tractors onboard batteries are being charged simultaneously.

Figure 80 – Cable system with pivot and boom suspended cable

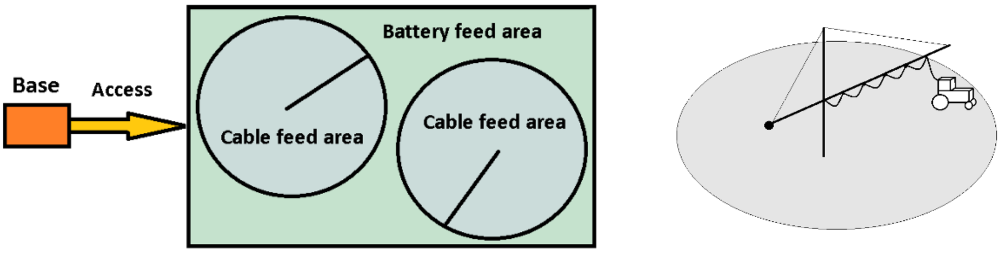

Source: Prepared by the Author.

When the tractor is supplied with electrical energy via a cable over a longer distance, the energy transmission from the stationary battery to the tractor's onboard battery represents a challenge with respect to conceiving a technically feasible design. Electrical conductors represent an ohmic resistance that neutralizes part of the flowing energy in form of heat.

Figure 81 – Energy transmission to tractor via cable feed system

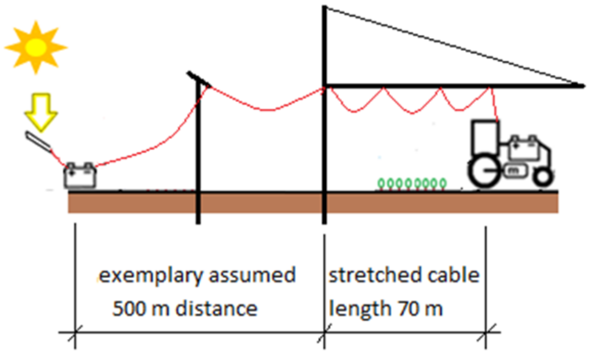

Source: Prepared by the Author.

The peak power demand of the tractor hooked up by cable has two components. One is the tractor's motors drawing 9 kW power at full load and the other one is the power consumption of 3 kW for charging the tractor's onboard batteries. This adds up to a total power demand of 12 kW at the tractor's terminals for which the electrical supply system has to be designed.

A typical distance (Figure 81) could be 500 m from the cable suspension system to the home base plus the length of the hook up cable of 70 m for a 50 m boom range.

Assuming a direct DC power transfer from the stationary battery to the tractor's onboard 72 V battery via a cable of 300 mm2 cross sectional area (Figure 82), a total power input of 14000 W and an amperage of 163 A requires 86 V at the cable input terminals to provide an electric power of 12 kW with a voltage of 74 V on the tractor's terminals.

Figure 82 – Power transmission by direct current

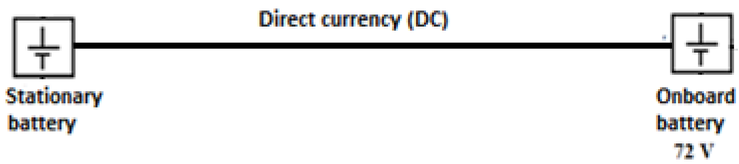

Source: Prepared by the Author.

For economic reasons a cable of 300 mm2 cross sectional area and a power loss of 1.9 kW (13.9%) is not acceptable. Furthermore, a cable of 300 mm2 cross sectional area is difficult to handle for its weight and stiffness and thus does not meet the technical flexibility requirements of the application.

A technically more feasible approach to reduce this significant power loss and the resulting excessive cable cross sections is to increase the transfer voltage. This could be put into effect in a DC or an AC system. According to physics, the lower the amperage, the lower is the power loss (on a physically and geometrically equal conductor).

Two configurations are technically, economically and from safety point of view feasible for the required electric energy transfer over a distance of 570 m, a 400 V DC and a three-phase 400 V AC transmission line.

The electrical power transfer from the stationary battery is implemented by means of a boost converter which increases the batteries low DC voltage to 400 VDC (+ 200 V vs. – 200 V) to pass the 570 m cable length (Figure 83). The result is an acceptable power loss of 4.5% for a 35 mm^2 cable. At the other end of the cable, the voltage is reduced by a buck converter to the tractor's onboard 72 V battery voltage. A power input of 12566 W with an amperage of 30 A is required on the stationary battery side to provide an electric power of 12 kW on the tractor.

Figure 83 – Power transmission by two-phase direct current 400 V DC

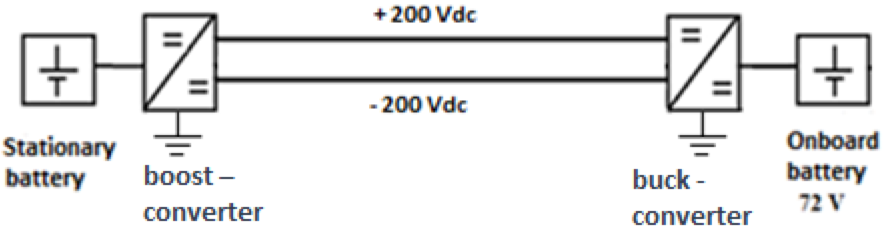

Source: Prepared by the Author.

In terms of operational safety, the bipolar design of +200 V and – 200 V would be comparable with the normal household installation of 230 V AC system in Europe or South America.

The most feasible alternative (technically, economically, and also in terms of safety) is the three-phase power supply with 400 V AC (Figure 84).

Figure 84 – Power transmission by three-phase alternating current 400 V AC

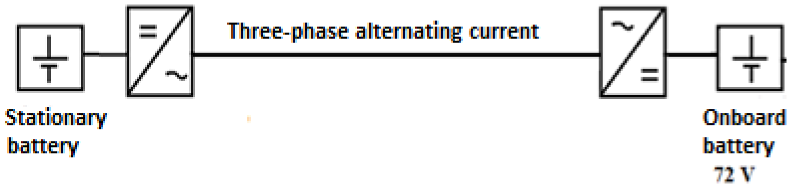

Source: Prepared by the Author.

This results in a (three phase) cable of 16 mm^2 cross-section per conductor in order to keep power losses at 5,52%.

The conclusion is that transfer voltages of at least 400 V (DC or AC) are required in order to keep power losses around 5% and to limit conductor cross-sections to a maximum of 35 mm^2 (Table 12). The system chosen to simulate the tractor's hourly operation cost is a three-phase power supply with 400 V AC.

Table 12 – Transmission parameters

Parameter	**Mono-phase 72 V DC**	**Bipolar +200-200V DC**	**Three-phase 400 V AC**
Cable cross section [mm^2]	300	35	16
Current [A]	162.79	29.99	20.4
Outgoing on stationary battery side			
Power [W]	14000	12566	12720
Voltage per phase to GND [V]	86	209.5	230
Incoming on the tractor			
Power [W]	12053	12028	11903
Voltage per phase to GND [V]	75	209.5	217
Power loss [W]	1849	538	816
Power loss [%]	13,21	4.28	6.42
Power loss per meter cable [W/m]	3.24	0.94	1.43
Copper material costs [Euro]	15406	2696	1643

Source: Prepared by the Author.

4.2.2 *Electrical energy generation and transmission configurations*

There are different configurations of the energy generation and transmission system possible depending on the conditions at the place of application. The architecture of the proposed energy system has two main components: firstly, the home base with the generation and charging system and an optional stationary battery, and secondly, the tractor as mobile unit with the onboard battery pack and the drive train (Figure 85).

Figure 85 – Stationary battery exchangeable (Configuration A, B, und D)

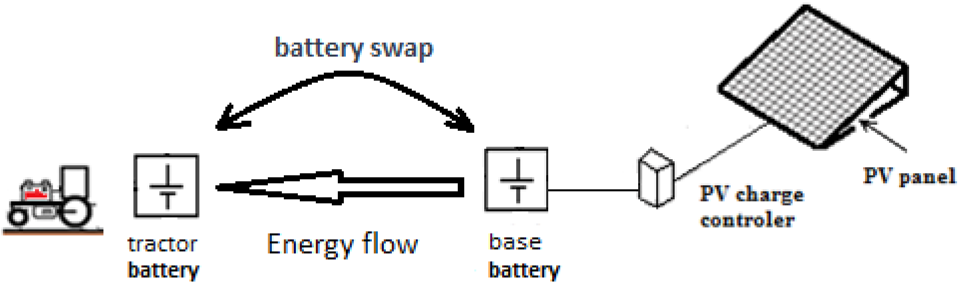

Source: Prepared by the Author.

The locally generated energy is temporarily stored by means of batteries (both generation and battery charging system normally located at the farm premises). The tractor's onboard battery has to enable the tractor to cover the distance to- and from the work area (transit phase) and to do the agricultural work at the crop fields.

This onboard battery storage represents a challenge for an all-electric tractor (as for any electric vehicle). The reason is that the presently dominating technology of storing electrical energy in a battery is marked by a very low energy density in terms of weight and space (compared with fossil fuels such as petrol and diesel). An objective of this project is therefore, to develop and evaluate different strategies and techniques in an attempt to alleviate this drawback.

A typical characteristic of farming activities is that during certain periods of the planting, cultivation and harvest sequence the tractor has to work 10h or more in a row. Thus, the onboard battery, even the one with the highest energy density and largest technically feasible capacity cannot sustain continuous energy supply. In consequence, additional strategies and techniques are proposed to ensure continuous energy supply during extended operating intervals of the tractor. Taking into account this basic requirement, the following strategies and techniques are considered:

Configuration A: Tractor operating on its onboard battery only. Transiting and field work is done until completion or until battery charge is down to a minimum for secure return to the home base (Figure 86). In this case, the tractor returns to the home base, to exchange the battery for a charged one.

Figure 86 – Tractor operating using onboard battery only

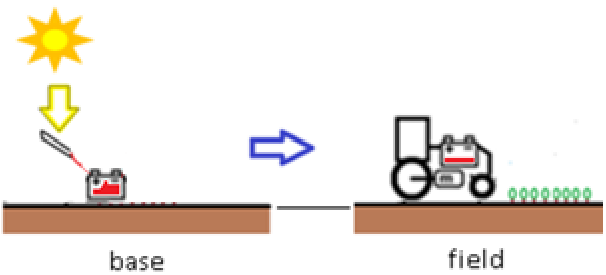

Source: Prepared by the Author.

<u>Possible variant</u>: Additionally, a small capacity photovoltaic system can be mounted on the tractor to extend the operating time until the tractor has to return to the home base and as an emergency battery charging device if the tractor runs out of battery power in a remote area away from the home base.

<u>Configuration B</u>: Tractor operating on exchangeable battery packs. The tractor while transiting to work in the fields tows a trailer with mobile exchangeable battery packs (Figure 87) on it. In this case the tractor uses its onboard battery for transiting and doing field work until the onboard battery pack is down. Subsequently, the driver exchanges the battery pack against a fully charged one until work is done or the last battery pack is down on its limit for secure return to the base. Variant: When the tractor takes a trailer with exchangeable battery packs with it, a second trailer with battery packs remains at the home base to be charged.

Figure 87 – Tractor operating using onboard battery and quickly exchangeable spare battery packs for battery-swapping

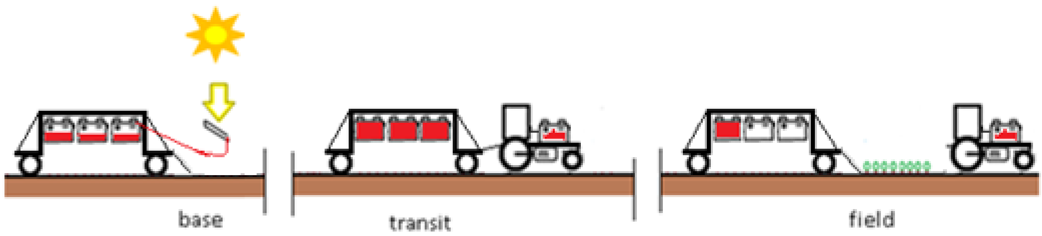

Source: Prepared by the Author.

<u>Configuration C</u>: Tractor working on a cable feed system linked to the home base. In this case the tractor uses its onboard battery for transiting. While carrying out field work, the tractor can operate in two modes: inside and outside of the cable feed system. Outside the cable feed system, it draws the energy from the onboard battery. When operating within the reach of the cable feed system the tractor hooks up to the cable and receives energy via cable directly from the stationary battery at the home base (Figure 88). Working hooked up to the cable, the tractor's onboard battery is being recharged in parallel. Note: the energy transfer via cable over a longer distance needs an appropriate electric architecture to minimize the ohmic losses in electric conductors.

Figure 88 – Cable feed system provides a link to the home base

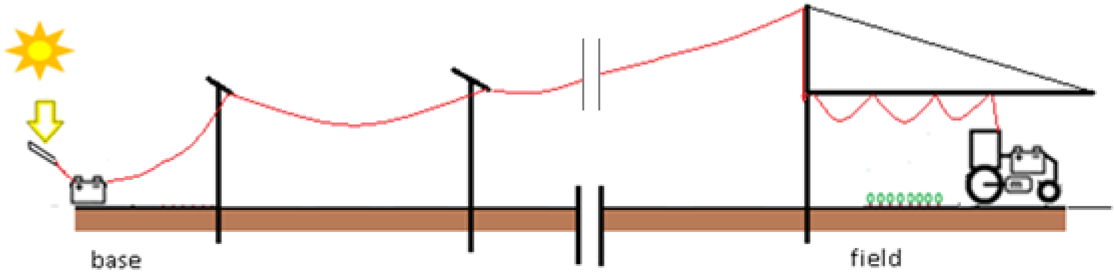

Source: Prepared by the Author.

Configuration D: Tractor working on a cable feed system linked to mobile battery packs on a trailer. The tractor when transiting to work in the fields tows a trailer with mobile battery packs on it. At the field the mobile battery packs on the trailer are linked to the cable feed system. The tractor, when hooked up and working inside the range of the cable feed system, draws the energy from battery packs mounted on the trailer. The advantage is the short distance between battery packs and the tractor's motors, minimizing the ohmic losses especially when working at low tension (Figure 89). Furthermore, a second set of battery packs can simultaneously be charged at the home base (similar to Configuration B).

Figure 89 – Cable feed system is not linked to the home base using a transportable battery package

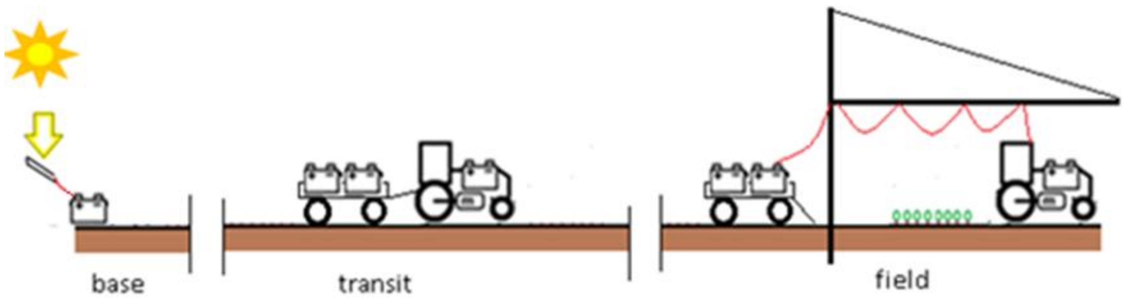

Source: Prepared by the Author.

Possible variant: A mobile energy generating system which will be temporarily installed at the cable feed system.

Generally, a combination of the operational profiles is possible. Especially a combination of the cable feed system and the exchangeable battery pack technique could extend operational endurance to a maximum.

4.2.3 *Open issues on electrical energy generation and transmission configurations*

Open issues and hypothec pros and cons in relation to the use of Li-ion batteries on agricultural micro tractors and questions in relation to the functional viability and safety of the Configuration A, B, C and D that need to be evaluated in a field test are:

I. **Li-ion batteries**: For all 4 configurations Li-ion batteries are assumed for energy storage. The operational behavior of these new type of batteries has some unknown aspects when used on electric tractors:

- Recharging time required;
- Susceptibility to operating conditions (temperature, vibrations etc.);
- Degradation and service life under real operating conditions; and
- Safety concerns (e.g. fire hazard).

II. **Configuration A**: This configuration is intended for a single semiarid farmer:

Pros:

- Lowest investment costs of all configurations;

Cons:

- Time wastage due to in between transit to home base for battery exchange;

Other aspects:

- Small fields (typically not bigger than 5 ha);
- Distance to home base not exceeding 2 km;
- Duration of heavy duty work at 80% power rating up to 6 hours over the whole day; and

- Energy consumption for transit to and from the field to be deducted from the available battery capacity.

Remark: Under favorable conditions, e.g. light or medium duty work and a short distance between home base and field, a substantial extension of the operation duration is to be expected. However, this needs verification during the field testing stage.

III. **Configuration B**: This configuration allows heavy duty tractor operation for up to 15 hours and is intended for larger farming cooperatives because the increase in capability requires a correspondingly higher investment:

Pros:

- Long operating endurance;
- Flexibility regarding location of fields; and
- High battery capacity would be beneficial for supporting a micro grid.

Cons:

- Substantially higher investment costs, especially for batteries; and
- Energy and time wastage for transit to and from the field (tractor pulling a trailer).

Other aspects:

- For larger fields and or fields which are some distance away, typically not more than 4 km;
- Tractor operation beginning and ending before and after daylight;
- Power consumption for tractor lights in the order of 0.5 kWh per day to be taken into account;
- Option to optimize (reduce) battery capacity if the tractor returns to the home base in the course of the day to exchange batteries (small reduction in capability, but significant reduction of investment costs); and
- It is presumed that a mobile PV-System increases the efficiency of this configuration.

IV. **Configuration C**: This configuration requires that the field is close to the home base (500 m) and that during the growing season the particular field requires an intensive use of the tractor.

Pros:

- Best suited for heavy operation due to continuous power supply from home base;
- Less dependent on system battery capacity; and
- No time wastage for battery swapping and no in between transit to home base required.

Cons:

- High Investment costs due to transmission line, i.e. max. distance to the field is limited (in the worst case economic viability depends on the yield of a single small field);
- Only suitable for land with a very small slope gradient;
- Very limited flexibility to shift from one field to the other, hence low utilization rate of system;
- Complicated tillage of field (first in circles, remaining area requiring extensive maneuvering);
- Soil compaction due to maneuvering in corners of the field;
- Significant energy loss in power transmission line;
- A small system battery capacity would have a negative impact on a micro grid;
- Technical risks due to unproven design e.g. forces and moments exerted on boom and pivot difficult to assess (moving tractor, wind, moments of inertia etc.), wear and tear on cable and cable suspension system; and
- Large effort required to put up the system (mobilization).

Other aspects:

- Possibility to optimize battery capacity (PV directly feeds power to the tractor during day time) to compensate for costs of transmission line.

Remark: It has to be investigated which effort is required to reroute the transmission line to other fields (incl. relocation of pivot) during the growing season or whether branches from the main transmission line are feasible. And it is presumed that a mobile PV-System increases the efficiency of this configuration.

V. **Configuration D**: With this configuration deployment of the tractor on a somewhat remote field is possible.

Pros:

- Option to connect a large capacity battery so that tractor operation is possible throughout the day without an interruption for battery exchange or to return to home base for exchanging batteries; and
- Reduced energy losses due to short distance between source of power and consumer (tractor).

Cons:

- High Investment costs due to large capacity batteries and pivot and boom structures (in the worst case economic viability depends on the yield of a single small field);
- Only suitable for land with a very small slope gradient;
- Limited flexibility to shift from one field to the other, hence low utilization rate of system;
- Complicated tillage of field (first in circles, remaining area requiring extensive maneuvering);
- Wastage of time and energy if a return to the home base for a battery exchange is required; and
- Technical risks due to unproven design e.g. forces and moments exerted on boom and pivot difficult to assess (moving tractor, wind, moments of inertia etc.), wear and tear on cable and cable suspension system.

Other aspects:

- Power consumption for tractor lights in the order of 0.5 kWh per day to be taken into account.

Remark: Flexibility of this configuration has to be proven. It is presumed that a mobile PV-System increase the efficiency of this configuration.

4.2.4 *Layout of Energy storage*

The computation of the investment cost requires to determine the storage capacity for the batteries and the generation capacity of the PV- Generator. Those values depend on the tractor's daily operating hours, the average power level during tractor operation, the transmission loss between the battery and the tractor's motors and the transmission loss between the PV- generator and the batteries.

Remark: The capacity of the batteries has been determined based on a conservative approach. As already indicated in the item 4.2.3, there is depending on the local conditions an opportunity to reduce the capacity of the battery without significant deterioration of the system performance.

The tractor is equipped with two 4.5 kW electric motors with a total potential of 9 kW. The average power level considered for tractor operation is 80%, which results in 7.2 kW of average tractor power.

The tractor average power level is given by Equation 62:

$$A = P_{nom} * APL \tag{62}$$

where:

P_{nom} = Tractor nominal power [kW];
P_{av} = Tractor average power level [kW]; and
APL = Average tractor power [%].

The transmission efficiency values of the tractor's components are:

~ 55% tractors mechanical minimum efficiency between motor and draw bar
~ 95.3% Motor
~ 93% Inverters
~ 84.5% Onboard battery

The transmission efficiency values of the electrical components at the home are:

~ 17% PV- generator solar panel

~ 90% Battery charger
~ 84.5% Base Battery

In case of the cable feed system with pivot and boom suspended cable, the following efficiency values are assumed:

~ 93% Inverter
~ 95% Line (cable transmission between base and pivot)
~ 90% Battery charger

The listed efficiency values refer (Figure 90) to the actually considered electric components (see annex) or are values documented in the literature (see References: Fakten-Check Mobilität and Batterie Elektrische Fahrzeuge in der Praxis).

Figure 90 – Efficiency of System Components

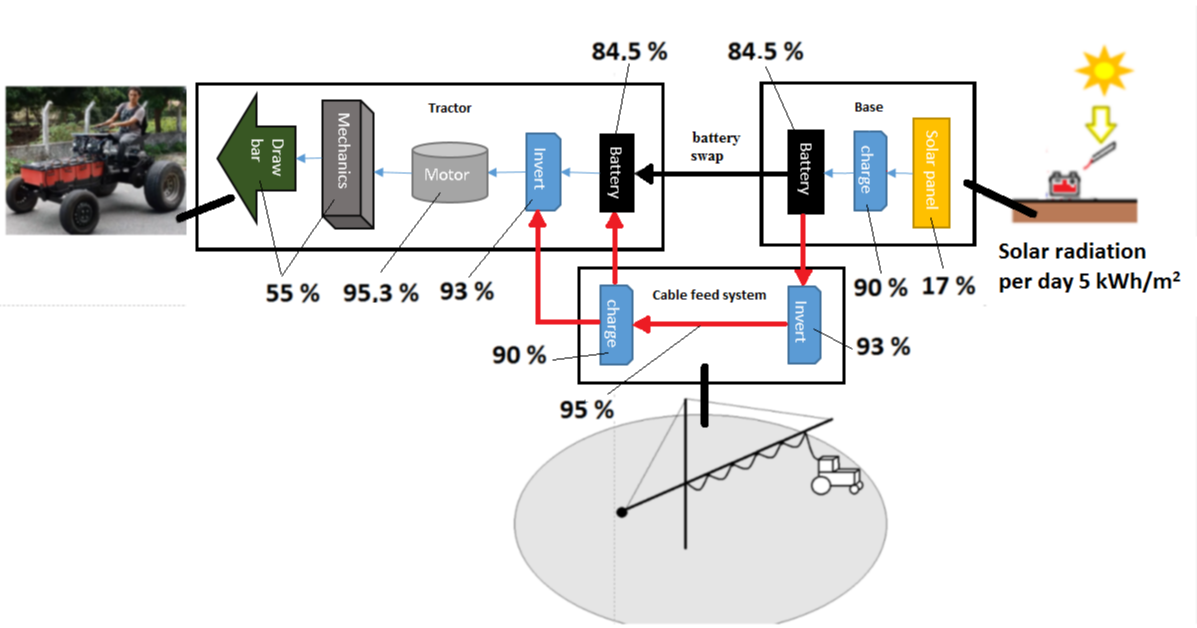

Source: Prepared by the Author.

As far as the design of the battery backup and photovoltaic system is concerned, the capacity shall be tailored to the maximum intended daily tractor operating time of 15 h (or alternatively 6 h), as shown in Equation 63.

$$E_{ht} = P_{apl} * t \quad (63)$$

where:

P_{apl} = Tractor average power level [kW];
t = time [h]; and
E_{ht} = Energy consumption [kWh].

Battery capacity requirements is in Equation 64:

$$TBSC = E_{th} * \eta_{total} \quad (64)$$

where:

TBSC = Tractor battery storage capacity [kWh]; and
η_{total} = total efficiency [%]; and
E_{ht} = Energy consumption [kWh].

Note: Total efficiency is the combined efficiency of motor, inverter and tractor battery- of the electric tractor. In case of battery swap, the tractor battery efficiency does not have to be considered since it is already included as base battery efficiency in Equation 65.

$$PV_{pa} = TBSC * \eta_{total} \quad (65)$$

where:

PV_{pa} = PV panel area [m^2]; and
η_{total} = total efficiency [%].

Note: Total Efficiency η_{total} is the combined efficiency of PV panel, charger and base battery, PV generator and storage battery. The combined efficiency η_{total} of configuration C with cable transmission has additionally to include the 3-phase 400V inverter, the cable transmission proper and the charger efficiency.

The resulting capacity requirements for battery and PV panel are listed in Table 13:

Table 13 – Capacity requirements for Battery and PV panel

Electric Tractor System Configuration	Tractor maxim Endurance [Hours per day]	Necessary PV Panel Area	Battery Capacity
A 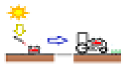	6h	75 m^2	58 kWh
B 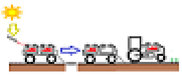	15h	189 m^2	144 kWh
C 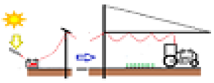	15h	221 m^2	101 kWh
D 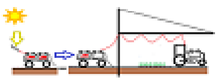	15h	189 m^2	144 kWh

Source: Prepared by the Author.

Note: The battery capacity considered for configuration C is 9 h. The reason being that the PV system supplies the energy directly to the tractor during the strong daily sunshine hours from 9 h to 15 h. During this period the energy needs not to be stored since it is consumed instantly.

4.2.5 *Energy management system*

The objective of the energy management system is to maximize autonomy and efficiency and ensure a high degree of energy availability while minimizing the necessary storage and generation capacity.

The energy system designed for semiarid farming families comprises various system modules/components such as: generation system, base battery, energy transmission system, onboard battery and finally the tractor's drive train and controls. All systems modules have their specific characteristics (Figure 91).

Then there is the farmers working and planting environment characterized by: seasonal planting and cultivation patterns, agricultural planting area, distances, location, topography, weather conditions.

Figure 91 – Energy management schema

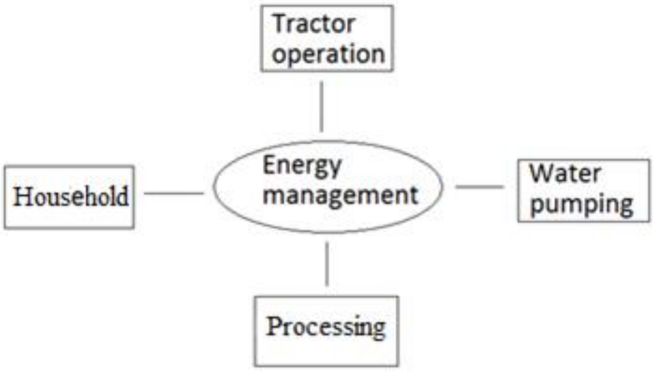

Source: Prepared by the Author.

The system proposed is a simple planning scheme for the semiarid farmer in the form of a white board with magnetic symbols which represent the energy consumers, the amount of energy to be consumed on this particular day and during the week ahead, always taking into account the expected weather conditions in this period.

Using this tool (see Figure 92), the farmer is in a position to plan his activities in accordance with the energy needed to carry out the agricultural works, and to operate the household consumers.

Figure 92 – Farmers energy usage planning board

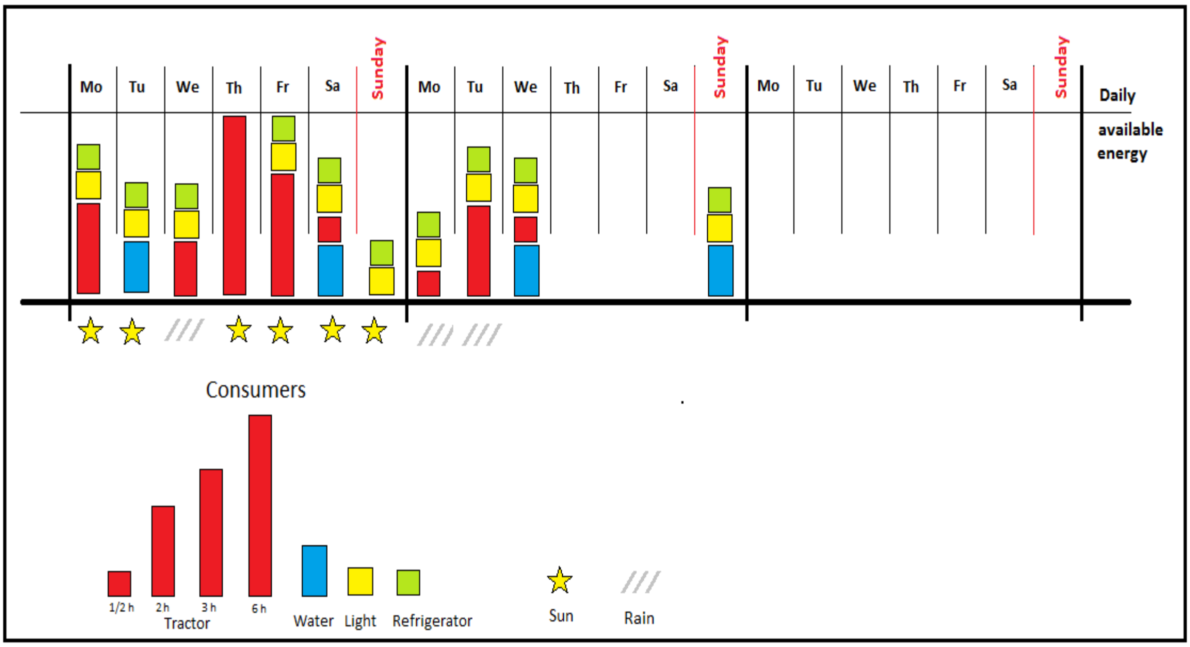

Source: Prepared by the Author.

The diversity of the consumers depends on the needs of the farmer and the extend of usage of the tractor by one or up to four farmer families. The purpose is to keep the system simple to operate for the farmer, and also flexible to adapt to changing conditions.

4.3 Prototype Tractor

4.3.1 *Power requirements*

The use of electric motors as prime movers for an agricultural tractor necessitates a different configuration of the drive train, the PTO (power take off) and the lifting mechanism of the three-point hydraulic hitch (as compared to a common combustion engine driven tractor).

Apart from that, for a tractor which shall serve semiarid family farmers, the limited availability of electrical, mechanical and hydraulic system components and the lack of technical support in rural areas of Brazil has to be taken into account. Generally, the cost of imported equipment is significantly higher and after sales service is usually poor.

Furthermore, procurement of spare parts for imported equipment is difficult and may lead to long outages and high expenditures. To eliminate these risks for the farmer of a semiarid farm, only products with proven reliability and assured local availability are considered for the electric tractor.

The tractor's maximum power requirements for pulling a seeder (MELO, 2017) were determined by considering data generated by research projects dealing with agricultural implements which in this case is the UFC research group GEMASA (Energy and Machines for Semi-Arid Agriculture).

As a result of these efforts it was established that the required traction force of 2656 N has to be produced at a speed of 5 km/h which leads to a minimum net power requirement of 3.7 kW (3689 W) for traction (Equation 66).

$$P = F * v \tag{66}$$

where:

P= Power [W];
F = Force [N]; and
v = Speed [m/s].

Based on a 45% maximum power loss between the motor and the drawbar due to mechanical friction in the drive train and an unavoidable margin for tire resistance and slip (on soft agricultural soil), the minimum total gross power requirement for the prototype's motors was computed to be 6.7 kW (6707 W) (ASABE, 2006).

4.3.2 *Drive train*

In the process of establishing a suitable drive train configuration, six alternative drive train configurations where evaluated by considering different electrical, mechanical and hydraulic options. An illustration of the six different drive train alternatives is provided in Appendix.

The selected drive train configuration for the prototype of the tractor comprises two drive motors, each dedicated to one of the rear drive wheels (Figure 93). A mechanical lock (type of differential lock on a conventional tractor) between the two parallel power trains ensures full power at that wheel with traction to the ground when the other side is slipping (reduced traction).

Figure 93 – Powertrain configuration intended for the first prototype

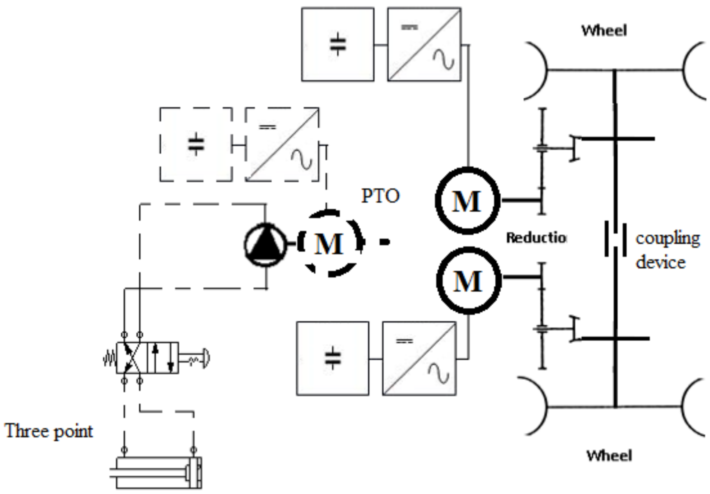

Source: Prepared by the Author.

4.3.3 *Electromechanical layout of prototype drive train*

A product search in the Brazilian market produced locally manufactured motors for the envisaged twin motor configuration. The motors manufactured by WEG are designed as three phase induction motors with a squirrel-cage rotor - for further details of the motor pl. refer to Technical Data (Table 14). The rated torque of each motor is 25.1 Nm and the maximum torque that can be sustained for a limited time of two minutes is 330% of the nominal torque. Consequently, the maximum peak torque to be considered as input in the mechanical design calculations is 82.83 Nm for each motor.

One of the advantages of this motor is that WEG offers an inverter capable to draw power from batteries with a voltage at the battery terminals between 36 V and 72 V. The inverter can be programmed to control speed and torque by means of an accelerator potentiometer as used in today's cars (Table 15).

For a detailed assessment of motor and converter see the following chapter: Tractor motor and converter.

A revised cost calculation revealed that a power train with a gearbox costs at least 300% more than a chain drive. Thus, a drive train design based on a chain drive layout was adopted for the first prototype (Figure 94).

Figure 94 – Two-stage chain drive layout of the prototype

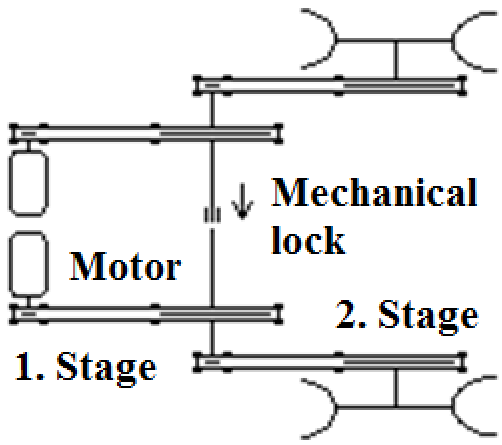

Source: Prepared by the Author.

The designation of the selected tire for the rear drive wheels is 295/75 R15 (with 750 mm outer diameter).

In designing a chain drive, a number of mechanical parameters (diameter and number of teeth of sprocket wheels, sizes of roller chains, pitch, etc.) have to be checked. The applicable standards are: ASME/ANSI B29.1-2011 Roller Chain Standard Sizes and ISO 10823:2004, Guidelines for the selection of roller chain drives

For the prototype the following chain and sprocket wheel combinations were selected (Table 14):

Table 14 – Chain drive transmission ratios

Stage	**Chain**	**Driving Sprocket**		**Driven Sprocket**	
	Pitch [mm]	**Teeth**	**Pitch ∅ [mm]**	**Teeth**	**Pitch ∅ [mm]**
1. Stage	12.7	10	41	75	307.5
2. Stage	19.5	13	78	60	360

Source: Prepared by the Author.

The above given data of the chain drive result in a total transmission ratio of 34.6. This gives at the motor's nominal rotational speed of 1715 rpm a rotational speed of 49.5 rpm at the driven wheel.

To calculate the tractor´s pull force the effective torque radius of the tire is to be considered. It is the distance from the tractor wheel axle centerline to the soil surface and it differs from the radius of the unloaded tire. For the initial calculation, a 9% deformation of the tractor tire is to be taken in to account in Equation 67.

$$\textit{Torque radius} = (\textit{Tire diameter}/2) - \textit{Tire deformation} \tag{67}$$

For a tire radius of 375 mm with 9% deformation the torque radius to be considered is 337.5 mm. This gives a rotational speed of the wheel of 49.5 rpm or a speed of 6.3 km/h (not considering slip).

Considering the above parameters, the following theoretical speeds and traction forces (not considering mechanical losses) are obtained:

- Nominal speed (at nominal rotational speed of the motor) = 6.3 km/h;
- Travel speed (at 3 times nominal rotational speed of the motor) = 19 km/h;
- Traction force at nominal motor torque (2 motors x 2316 N) = 4632 N; and
- Maximum traction force at 330% maximum permitted motor torque for a maximum of 2 minutes = (2 motors x 7643 N) = 15286 N

4.3.4 *Tractor motor and converter*

Generally, prime movers for agricultural tractors are of the internal combustion engine design. This engine design needs a sophisticated gearbox in order to cope with its specific torque – power characteristic. Induction squirrel cage electric motors (Table 15) controlled by inverter (Table 16) in contrast have an entirely different torque – power characteristic by producing a constant torque from 0 (zero) rpm up to nominal rotational speed (Figure 31).

On the other hand, the power increases linear from 0 (zero) rpm up to nominal speed and then stays constant up to maximum speed. The maximum rotational speed depends on the motor's characteristic and can reach up to 7 (seven) times the nominal speed. This torque-power relation allows different layouts of the drive train that transmits the motor power to the drive wheels.

Table 15 – Technical data of motor

Technical data of the selected motor	
Type of motor	Three phase induction motor – Squirrel cage rotor
Manufacturer	WEG DRIVES & CONTROLS – AUTOMAÇÃO
Frame size	100L
Power rating	4.5 kW (6 HP-cv)
Frequency	60 Hz
Number of poles	4
Nominal speed	1715 rpm
Slip	4.72 %
Rated voltage	38V
Rated current	115 A
Excitation current	61.0 A
Rated torque	25.1 Nm
Maximum torque	330%
Insulation class	H
Max. permitted temperature rise	125 K
Max. surrounding temperature	40°C
Max. altitude without derating	1,000 m
Protection	IP55
Direction of rotation	both
Weight	38 kg
Moment of inertia	0.0097 kgm^2

Source: Prepared by the Author.

Table 16 – Technical data of inverter

Technical data of the selected inverter	
Type of motor	CVW300, Conversor Veicular WEG
Manufacturer	WEG DRIVES & CONTROLS – AUTOMAÇÃO
Model	CVW300A0400D0NB66
Rated input voltage	24-72V CC
Lower and upper voltage limit	18-90V CC
Rated current at 45°C	200 A
Maximum current for 2 min.	400 A
Interfaces	
Digital Inputs	8
Analog Inputs	2 (±10 V)
Digital Outputs	4
Relay Digital Outputs	1
Analog Outputs	2 (0 - 10 V)
Temperature Sensor	PTC 1
Input for incremental encoder	1
Port RS485	1
Operating interface	IHM 1

Source: Prepared by the Author.

Figure 95 – Tractor motor control with inverter and battery

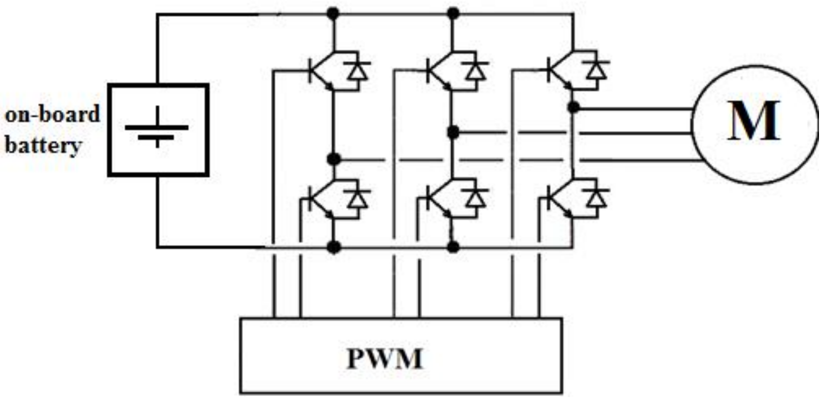

Source: Prepared by the Author.
Legend: PWM = Pulse Width Modulation.

For the configuration using a cable feed system, the electric tractor has to be able to operate alternately in an onboard-battery and cable mode. With this configuration the tractor's battery is charged, whenever the tractor is hooked up by cable. The electrical architecture of the charging configuration is shown in Figure 96.

Figure 96 – Architecture of the motor control and alternative energy supply

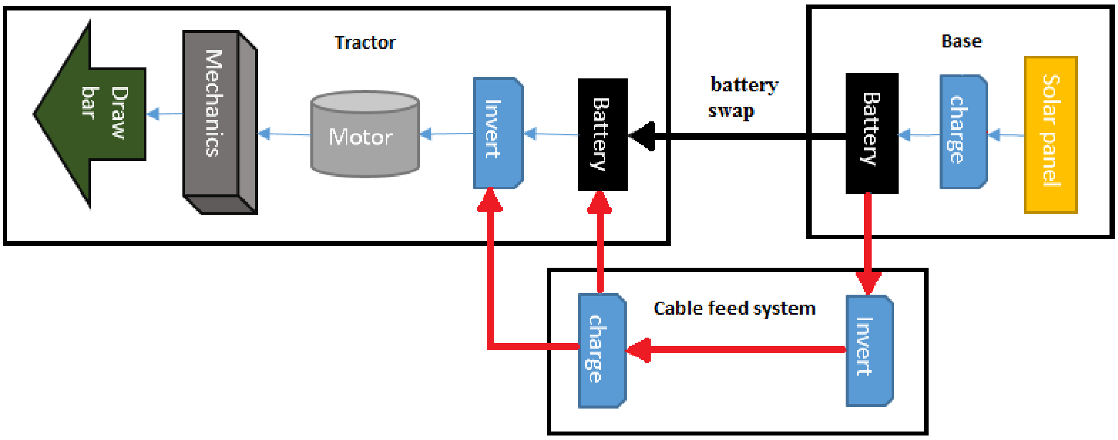

Source: Prepared by the Author.

4.3.5 *Weight distribution alternatives for the prototype*

The weight balance between the front and the rear axle is a key factor determining the tractor´s traction efficiency. For a rear axle driven tractor a 40% (front axle) and 60% (rear axle) weight distribution is considered as an optimum balance with respect to traction performance and safe handling.

For arranging the main components, i.e. motors and battery pack, different alternatives exist. In the first step the alternative motor arrangements are assessed, taking into consideration restrictions imposed by the chain drive. Feasible arrangements with the motors placed in forward and backward position are shown in Figure 97.

In contrast to the drive train, there is more flexibility in locating the batteries.

For the complete power train, the following arrangements are considered:

Arrangement a: Both motors are located above the rear drive axle. Driver positioned at the centerline on top of the drive axle. 4 Batteries at the front of the tractor.

Arrangement b: Both motors are located in front of the driver and in front of the rear drive axle. Driver positioned at the centerline on top of the drive axle. 4 Batteries located at the front of the tractor.

Arrangement c: One motor located in front and one above the rear drive axle. Driver positioned at the centerline on top of the drive axle. 4 Batteries positioned at the front of the tractor (Figure 98).

Figure 97 – Possible alternatives for arranging the motors on the prototype

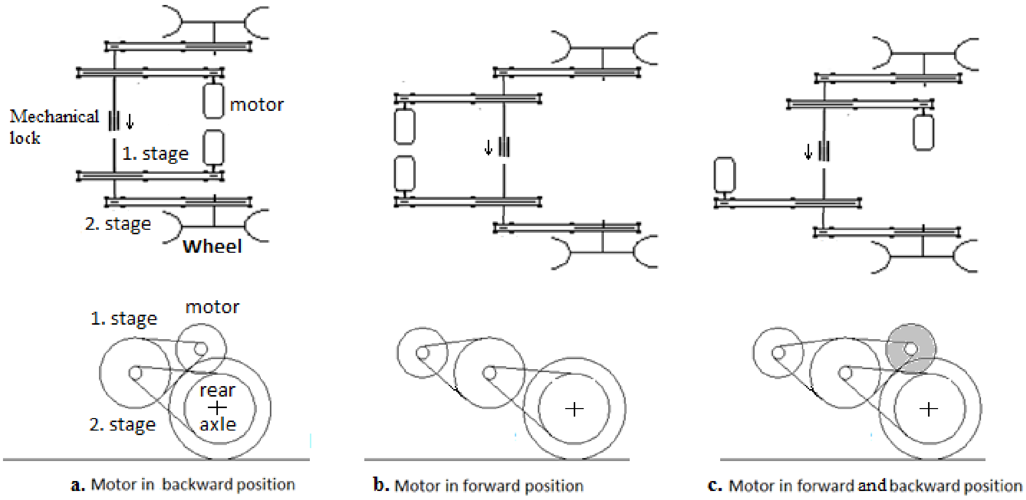

Source: Prepared by the Author.

Figure 98 – Illustration of alternative arrangements for motors and driver. Batteries in front

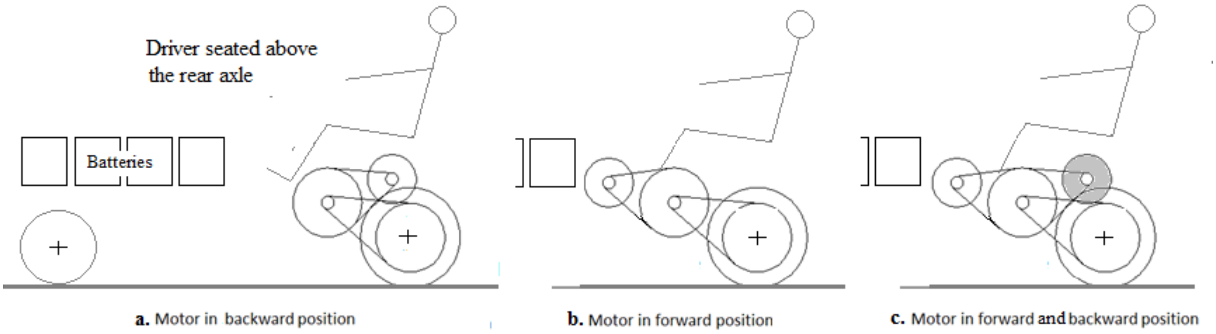

Source: Prepared by the Author.

The masses considered as locatable in terms of fixed position on the prototype are the driver considered with a total weight of 100 kg, batteries each with 57.8 kg and two motors each with a weight of 38 kg.

The optimized arrangement was evaluated by taking the positioning of the batteries in the front as fixed. The considered positions are 0.3 m for batteries, 1.3 m and 1.7 m alternatively for the motors and 1.7 m for the driver behind the front axle right over the rear axle (Figure 99).

The various weight distribution alternatives are listed in Table 17 (see below).

Figure 99 – Positions of the main tractor components in relation to the forward axle

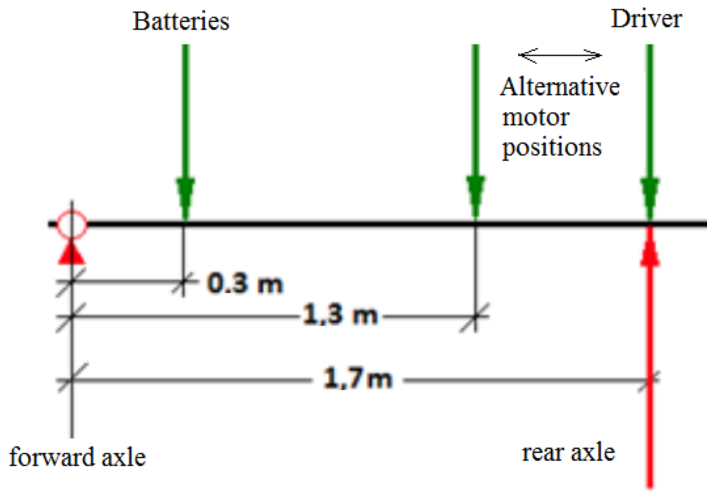

Source: Prepared by the Author.

Table 17 – Weight distribution alternatives

Arrangement	Position of center of gravity relative to front axle [m]				Weight distribution	
	Batteries	Driver	Motor 1	Motor 2	Front axle	Rear axle
A	0.3	1.7	1.7	1.7	40.9%	59.1%
B	0.3	1.7	1.3	1.3	46.0%	54.0%
C	0.3	1.7	1.3	1.7	50.2%	49.8%

Source: Prepared by the Author.

Since Arrangement A represents an almost ideal distribution of masses, the prototype features two motors with the driver located above the rear axle. With all three designs, the batteries are located 0,3 m behind the front axle. Figure 100 illustrates the resultant geometrical tractor configuration based on alternative A.

4.3.6 *Prototype overall mechanical layout*

The overall mechanical layout chosen for the prototype is based on the electromechanical layout of prototype drive train, the weight distribution and the dimensional requirements of semiarid family farming (Figure 100). Figure 101 indicates the principal prototype tractor overall dimensions (in mm).

Figure 100 – Three dimensional representation of resultant prototype tractor geometrical configuration

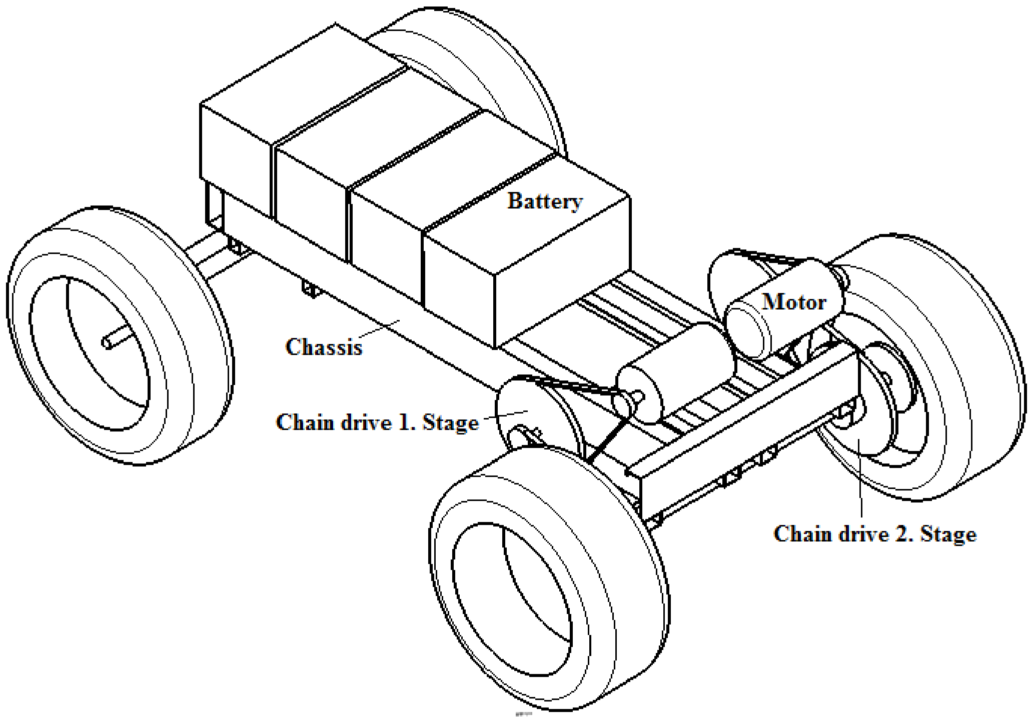

Source: Prepared by the Author.

Figure 101 – Principal prototype tractor overall dimensions [mm]

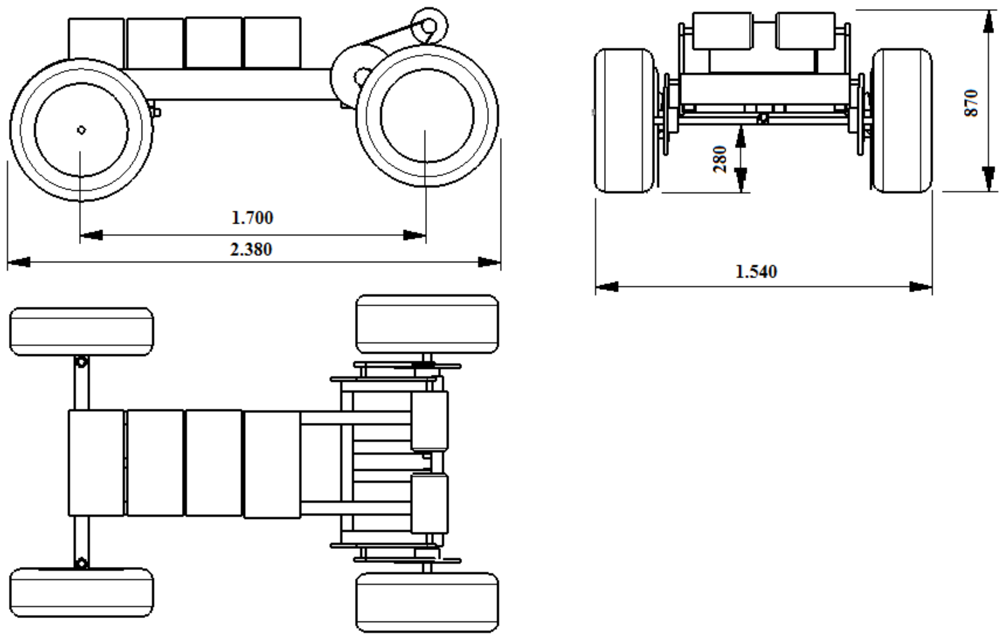

Source: Prepared by the Author.

4.3.7 *Chassis and axles*

The requirement to fabricate the chassis in a local workshop is met by a ladder type frame made of 100 mm steel channel as basic layout (Figure 102a). Two sub frames, one for the front swing axle and one for the drive train rear axle are mounted underneath the main chassis structure (Figure 102b).

Figure 102 – (a) The main chassis structure, and (b) front and rear sub frames

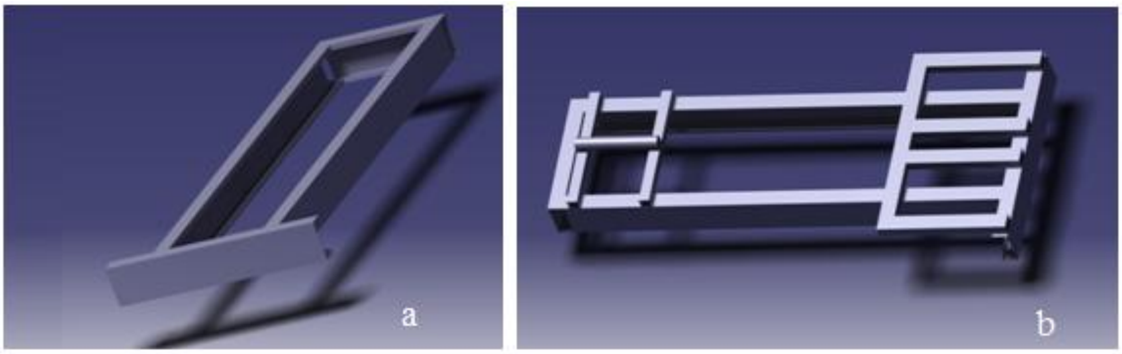

Source: Prepared by the Author.

The swing axle at the front is designed as a rectangular tube of a square cross section of 70 x 70 x 3 mm. It is connected to the front sub frame of the main chassis structure by means of a tube that functions as pivot to allow the axle to swing transverse to the longitudinal tractor axis (Figure 103).

Figure 103 – Front axle of prototype tractor

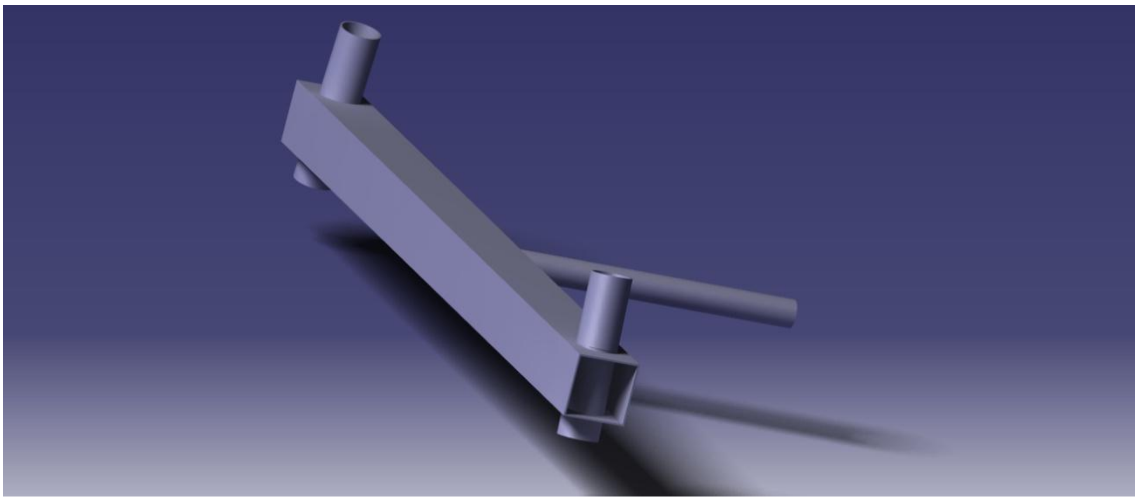

Source: Prepared by the Author.

The steering system on rigid axles needs to allow rotation of the front wheels' steering kingpins around a vertical axis. To this end, two inclined tubes are provided on the front axle outer ends (Figures 104 and 105).

Figure 104 – Front axle mounted to the main chassis[9]

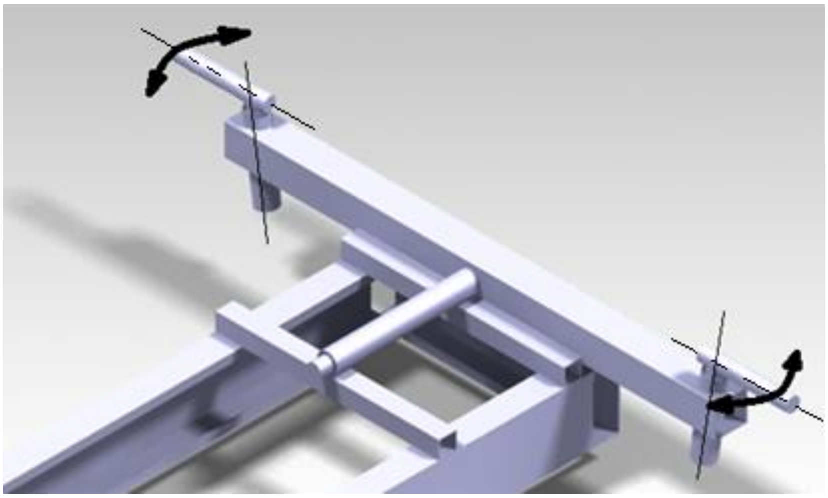

Source: Prepared by the Author.

Figure 105 – Picture of the front axle on the prototype with wheels mounted

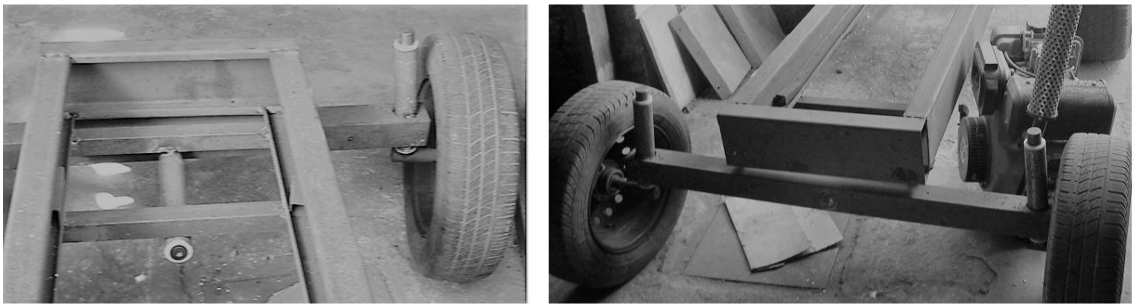

Source: Prepared by the Author.

The rear axle is fixed onto the rear sub frames of the main chassis structure by means of 4 bearing blocks. It consists of two half shafts (Figures 106 and 107).

[9] The figure shows the front axle upside down.

Figure 106 – Rear axle with support structure mounted to the main chassis[10]

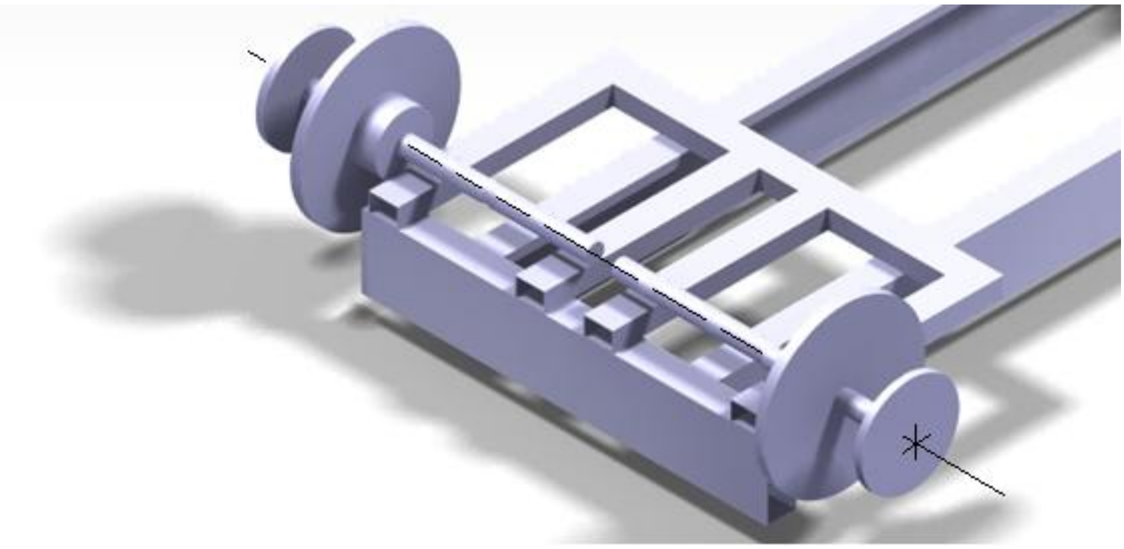

Source: Prepared by the Author.

Figure 107 – Rear axle with support structure mounted to the main chassis

Source: Prepared by the Author.

The complete chassis, with front and rear axle mounted and the prototype's chassis are shown in Figure 108.

Figure 108 – Assembled chassis with front and rear axle a. top view and b. bottom view

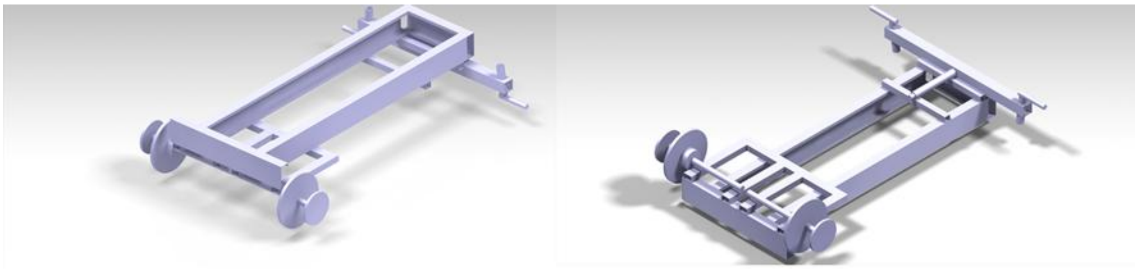

Source: Prepared by the Author.

[10] The figure shows the chassis upside down. Journal bearings are not shown.

4.3.8 *Motor and drive train lay out*

To optimize the tractors weight balance, the motors had to be arranged on top of the rear axle below the driver's seat. This increases the weight on the driven wheels of the rear axle and thus the maximum possible traction force of the tractor (Figure 109).

Apart from that this arrangement provides space for the driver's legs and feet, the brake pedals and the accelerator and does not obstruct entering and exiting of the driver. Furthermore, the open space around the motors ensures sufficient ventilation for dissipation of heat generated in the coils of the motors. The electric cabling connecting the motors with the inverters is routed through the interior of the chassis (see figure below).

Figure 109 – Motors on top of the rear axle below the driver's seat

Source: Prepared by the Author.

The two drivetrains which transmit the motor power to the rear axle are designed as a two stage chain drive and are placed on both sides lateral to the driver's seat position. A separation cover serves as protective device for the driver by preventing inadvertent contact with the chain drive components (Figure 110).

The intermediate axle is split in two half shafts so that the right and left drive train are mechanically separated (Figure 111). A mechanical lock can couple the two half shafts together to get the full power of the two motors on one of the drive wheels in case that the other one loses traction and slips.

The intermediate half shafts have four bearing blocks (two on each shaft). Each half shaft is equipped with a separate brake drum (for separate left and right side braking of the drive wheels). A mechanical lock enables the driver to couple the two half shafts (type of differential lock). To each intermediate half shaft a big and a small sprocket wheel is fitted.

Figure 110 – Two stage chain drive (guards removed)

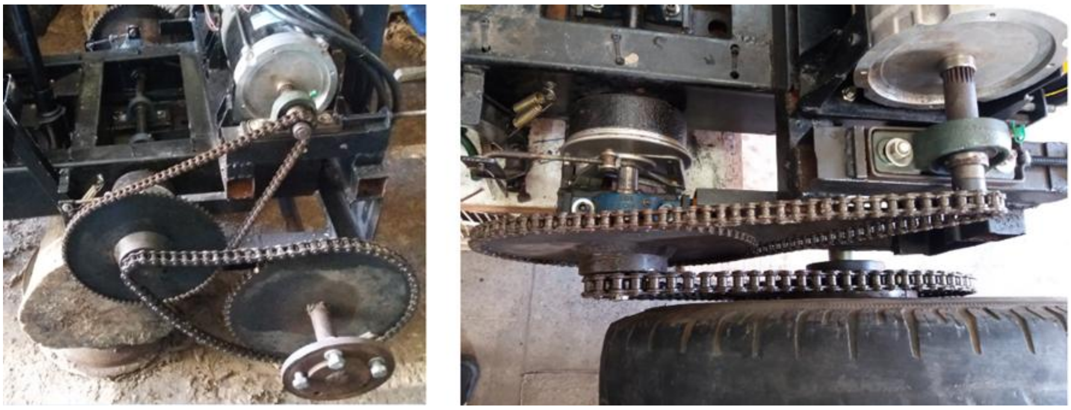

Source: Prepared by the Author.

The big sprocket wheel is part of the first stage (chain coming from the motor) and the small sprocket wheel is part of the second stage of the chain drive (chain going to the wheels). The main functional requirement of the half shaft is to withstand the bearing, brake, chain- and torque forces. Furthermore, by displacing (adjusting the position) the intermediate shaft, the tension of the chain can be adjusted.

To minimize the wear of the open chain drive regular lubrication of the chain drive components is required. By doing so it is expected that the life expectancy of these components meets the requirements of a tractor designed for a yearly utilization of up to 1200 hours.

Figure 111 – Intermediate shaft of prototype electric tractor

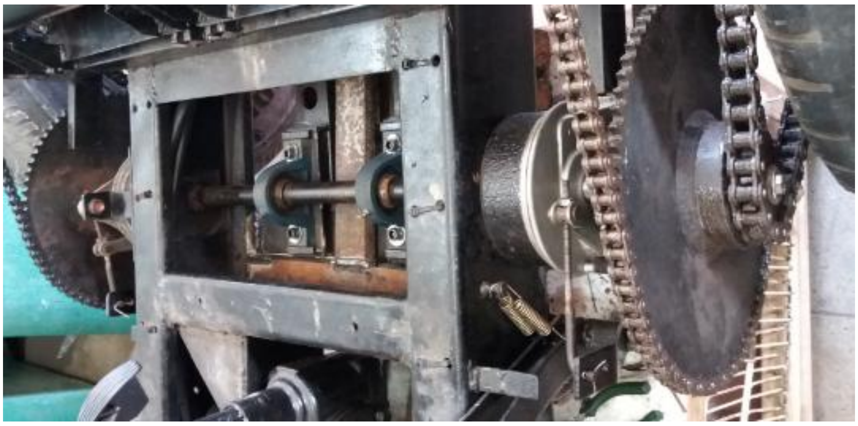

Source: Prepared by the Author.

The brake pedals for the left and right side are grouped together on the drivers left feet side and can be activated simultaneously or individually by the driver's left foot.

4.3.9 *Front mounted battery to facilitate battery pack exchange*

To achieve feasible operating times, the frequent battery exchanges in the the course of the tractor's working day have to be carried out in the shortest possible time. By mounting the battery packs at the front an unobstructed access (Figure 112) is provided, thus, allowing a quick exchange of discharged battery packs against charged ones.

It worths mentioning that the swap mechanism is not included with the prototype (batteries are fixed mounted). The swap mechanism has to be developed in a further project.

Figure 112 – Battery packs at the front of prototype electric tractor

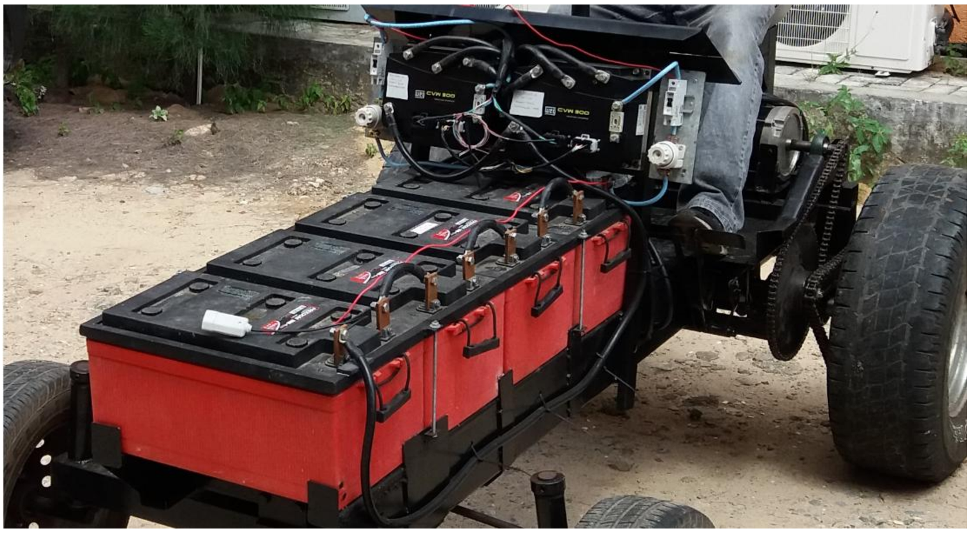

Source: Prepared by the Author.

4.3.10 *Steering*

The steering system is a conventional mechanical system for rigid axle beams (Figure 113).

Figure 113 – Steering system of prototype electric tractor

Source: Prepared by the Author.

4.3.11 *Brakes and accelerator*

Brakes and accelerator are positioned to the left and right side of the steering column (Figure 114).

Figure 114 – Brakes and accelerator of prototype electric tractor

Source: Prepared by the Author.

4.3.12 *Panel*

The main switch, the emergency button and the selection switch for forward or backward motion is positioned on the tractor's instrument panel (Figure 115).

Figure 115 – Main switch, forward – rear selection switch, and the emergency button

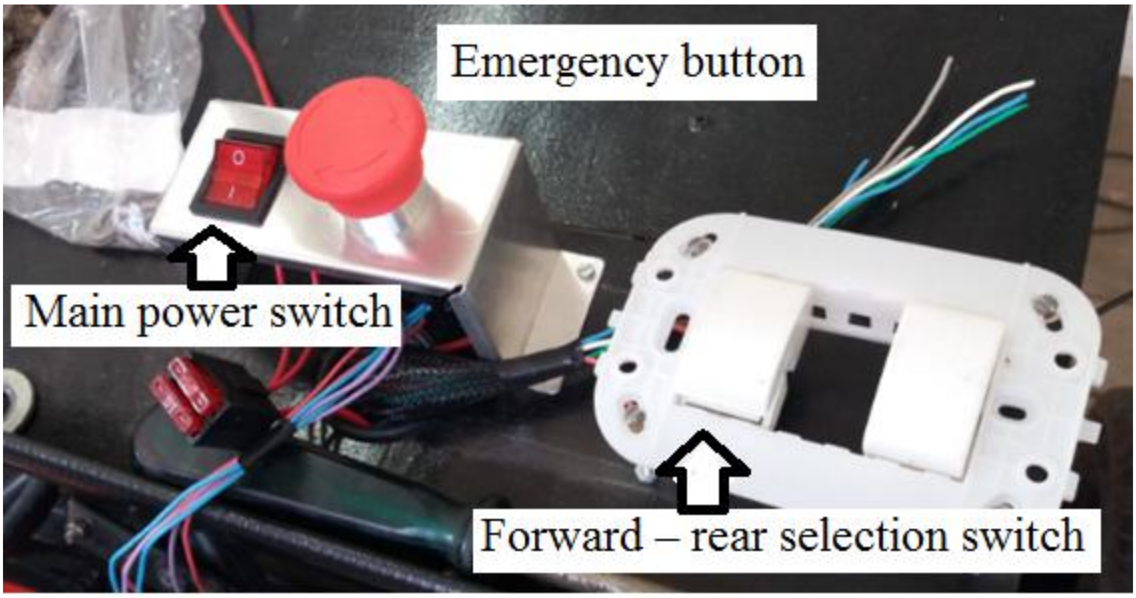

Source: Prepared by the Author.

4.3.13 *Electric prototype tractor tests*

The method used for the pull test on the drawbar is based on the CODE 2 document issued by international organization OECD in 2008. This standard defines the test procedure for farm tractors featuring combustion engines as prime movers and including the following features: specifically designed tractor tires, a tractor hydraulic system, a three-point hitch and a power take-off shaft.

The electric prototype tractor presented in this document has none of those features! However, the main purpose of CODE 2 is to verify the performance of the tractor under defined operating conditions, focusing on traction force in relation to the traction speed and the associated energy consumption.

The testing procedure outlined below aims to determine these performance data of the electric prototype tractor developed in connection with this project and a comparative combustion engine tractor.

In order to obtain reliable test results the following data will be recorded[11]:

1. Traction force on the draw bar measured by means of a load cell;
2. Theoretical speed and ground speed under traction conditions:

   a. The tractor's actual speed V_a . This is the tractor's speed relative to the test track under load, measured by taking the time to cover the distance between the starting point and the end of the defined length of 75 m on the test track; and

   b. The theoretically obtainable speed V_t as basis to determine the TRR Travel reduction ratio and the wheel or track slip.

3. Motor rotational speed;
4. Hourly specific energy consumption (based on fuel or electricity consumption);
5. Temperature of engine/motor, batteries and inverter during tests;
6. Tractor load on rear and front axle (empty weight measured before the test at NUTEC facilities); and
7. Temperature, humidity and air pressure on the day of the tests[12].

The test is to determine the following parameters:

- Rated Speed
- Power at the Drawbar
- Drawbar Pull
- Fuel Consumption
- Slip
- Ballasted Mass

The tractor test is conducted to record the tractor's configuration parameters, the environmental data, test conditions and results.

A. SPECIFICATIONS OF ELECTRIC TRACTOR TO BE TESTED

- Motor data
- Inverter data
- Battery data
- Transmission type

[11] The reader may be willing to read part of the doctoral thesis of Professor Leonardo: 5.2.3 OECD-Code test 2 page 38.

[12] Data available on the Internet at <www.funceme.br>.

- Brakes
- Steering
- Chassis
- Dimensions
- Tire sizes
- Weights and balances

B. TEST CONDITIONS

- Test track geographical data (location / elevation)
- Track dimensions
- Test track type and category (concrete)
- Type of Tractor to be dragged
- Environmental conditions (track and air temperature / humidity / wind / rain)

C. TRACTOR’S CONFIGURATION AND PHYSICAL PARAMETERS

- Relevant tractor main component temperatures before test
- Ballasted Mass
- Centre of Gravity
- Battery charge level

D. TEST DATA DOCUMENTATION

- Data sheet with registration number
- List of data to be recorded during the test by the monitoring system
- Record of testing equipment
- Configuration of monitoring system
- List of sensors connected to the monitoring system
- List of data to be recorded with separate apparatus (chronometer, sound exposure meter)
- Miscellaneous documents (photos / video clips)

E. TEST RUNS

During the test runs, all relevant data are entered in the test data sheet such as, inter alia, temperatures of the tractor components, battery charge status together with various manually recorded values. The data registered on the monitoring system are processed and a graphical presentation of the results is generated.

F. FINAL TEST REPORT (INCLUDES THE FOLLOWING DOCUMENTS):

- Data sheet filled in and certified

G. TEST TRACK PATTERN DIMENSIONS

Figure 116 shows a simplified scheme of the test track dimensions.

Figure 116 – Dimensions of the test track

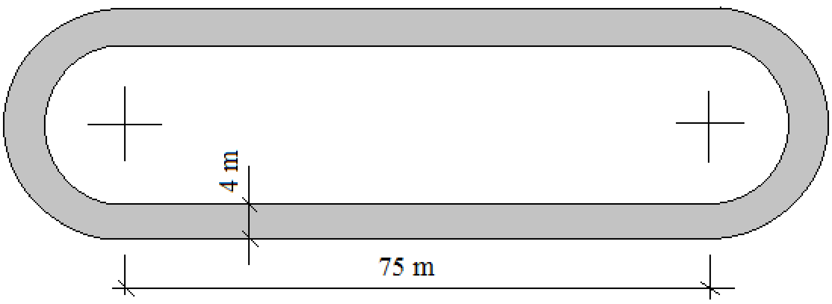

Source: Prepared by the Author.

H. TEST SHEET

The test sheet is filled in for each test run and documents all relevant data (Figure 117). The complete test sheet in available for consultation in the Appendix.

Figure 117 – Tractor test sheet

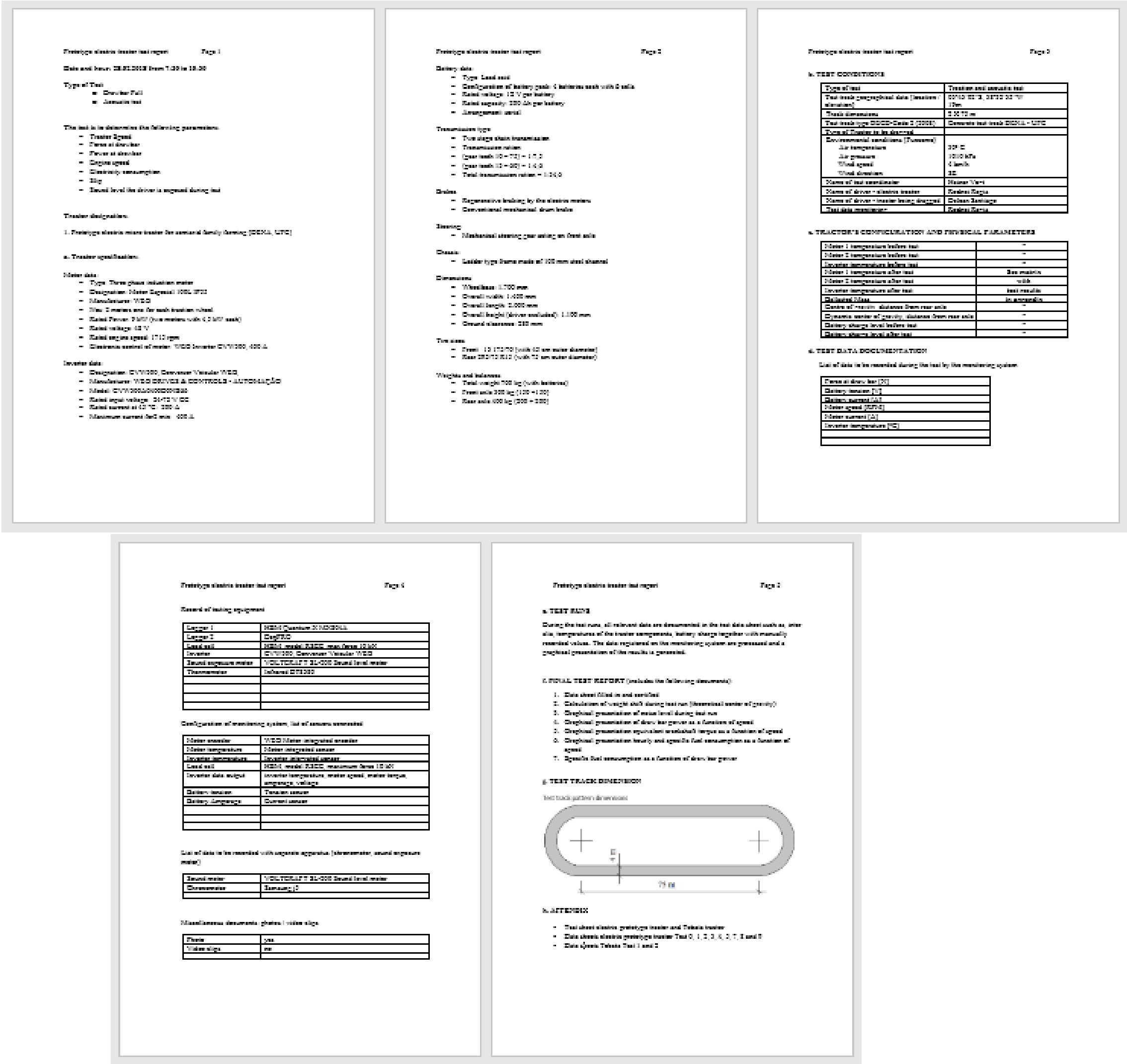

Source: Prepared by the Author.

4.4 Prototype test

4.4.1 *Test configuration*

The electric prototype tractor and the reference Tobata tractor were subjected to various tests at the DENA-UFC test track, located at *Campus* do Pici, Fortaleza, Ceará. The geographical coordinates of the test track are: 03º43’02”S and 38º32’35”W. It is a round track with two 75-meter-long straight stretches. The measurements were performed on the straight sections of the test track.

The weather conditions on February 28th, 2018 were as follows: dry, average temperature 30°C, air pressure 1010 hPa, and wind speed of 4 km/h. These data were collected from the website of FUNCEME. For more detailed information, see the section "Test sheet electric prototype tractor", available in the Appendix.

The load to be dragged both by the electric prototype tractor and the reference Tobata tractor was another tractor, a Valtra A Series one, and also a two axle trailer hooked up to it (Figure 118).

Figure 118 –Test train with prototype electric tractor dragging a Valtra A Series tractor and a two axle trailer as its load

Source: Prepared by the Author.

Eight test runs were completed with the electric prototype tractor, and two with the reference combustion engine powered, Tobata tractor.

For reasons of comparability, the two test runs with the Tobata were conducted with the same traction load. To permit the evaluation of higher loads and the determination of the upper traction limit of the electric tractor, the test driver of the load tractor applied the brakes at the 8th test run up to a point at which the wheels of the electric tractor started slightly visually slipping.

A data monitoring system was used to record data of the load cell, the inverter, the motor encoder, and the voltage and current sensors of the battery. The voltage and current data of the battery were registered on the DagPRO logger. The inverter communicated the rotational motor speed, the motor current and the inverter temperature directly to the personal computer. Load cell data were transmitted via Quantum X to a computer connected to the system components, which was used to perform the data processing. Figure 119 shows the architecture of the monitoring system.

Figure 119 – Architecture of the data acquisition system

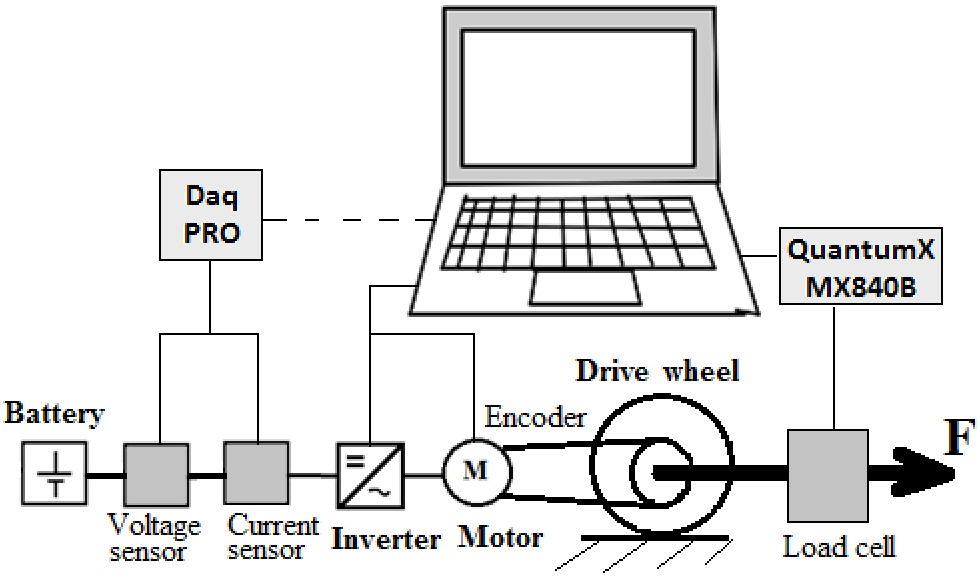

Source: Prepared by the Author.

4.4.2 *Specific objectives of the test*

The main objective of the test was to evaluate the electric tractor's tractive characteristics. Since the electric induction motor's torque characteristic is different from that of a combustion engine powered tractor, it was necessary to evaluate its tractive force and its tractive behavior. Furthermore, the temperature rise of the motors and the inverter was measured, and the controllability of the electric tractor motors by means of an accelerator potentiometer was assessed by the driver.

The complimentary purpose of the test was to compare the tractive force and the tractive characteristics of the prototype electric tractor, with the Tobata tractor serving as a reference. Both tractors have almost the same engine power; the electric tractor has 9 kW and the Tobata has 10.4 kW motor power.

The sound level was monitored on all test runs of the electric prototype tractor and the Tobata tractor, in order to determine the noise level the driver is exposed during operation.

4.4.3 *Test boundary conditions for electric tractor*

The first test run of the electric prototype tractor (Test 0) was conducted with only 8 kg of ballast. During this test run, excessive slip occurred, hence, the following 7 test runs were conducted with 99 kg additional ballast (with a second person on the tractor).

During the electric tractor prototype test, the minimum traction necessary to pull the load was 1770 N and resulted in a speed of 5.5 km/h. The maximum traction achieved with the electric tractor was 4750 N at a speed of 4.8 km/h. To evaluate higher traction forces, and to find the upper traction limit of the electric tractor, the test driver of the load tractor applied the brakes. During the test, the medium and the maximum sound levels, battery voltage, and the temperatures of motor and inverter were recorded.

4.4.4 *Test boundary conditions for reference Tobata tractor*

The minimum tractive force necessary to pull the load by the Tobata tractor was 1404 N, at a speed of 1.7 km/h. During this test, the first gear was engaged. The maximum pull of 2365 N was achieved in third gear, at a speed of 0.82 km/h.

During the test, the medium and the maximum sound levels were also recorded.

4.4.5 *Test results*

The electric prototype tractor achieved steady tractive forces ranging from 1770 N (Test 1) up to 4754 N (Test max).

In Pre-test 0, with only 8 kg ballast weight excessive slip occurred. The results of Test 0 were therefore considered as *not* valid. All following tests were carry out with an extra passenger, with a weight of 99 kg, as ballast on the tractor.

During Test 1, the mean force at the draw bar was 1956 N with a slip of 12.3% and a measured speed of 4.74 km/h on the demarcated test track part. The resultant power at the draw bar was 2673 W. The power provided by the batteries was 3998 W, which represents an efficiency of 64.78% between battery and draw bar. The measured medium sound level was 77 dB(A). Acceleration of the whole test train (Figure 120) lasted around 3 seconds, and produced for a moment a draw bar power of up to 5000 N, which required for an instant pike power of up to 7500 W from the battery.

Figure 120 – Drawbar force and battery power during Test 1

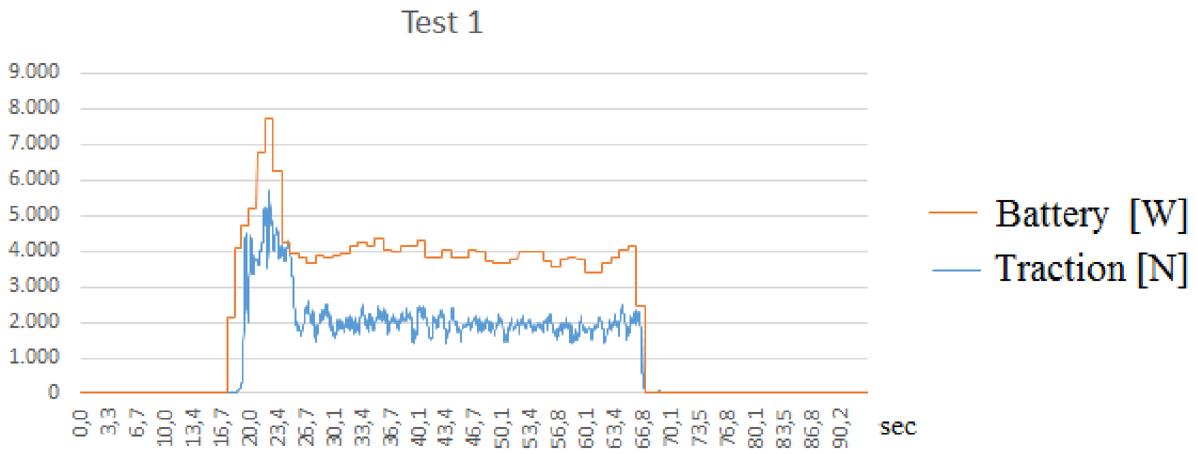

Source: Prepared by the Author.

In the following tests, from 2 to 6, the traction load was varied and reached up to 2926 N continued mean traction force in Test 6. The complete test results of all tests at Table 18 (see below). The slip in Test 6 was 14.1% and the measured speed on the demarcated test track part was 4.72 km/h.

The resultant power at the draw bar was 3840 W. The power provided by the batteries was 5915 W, which represents an efficiency of 64.92% between battery and draw bar. The measured medium sound level was 79 dB(A). Acceleration of the whole test train (Figure 121) lasted around 3 seconds, produced for a moment a draw bar power of up to 6000 N, which required an instant pike power from the battery of 7500 W.

Figure 121 – Drawbar force and battery power during Test 6

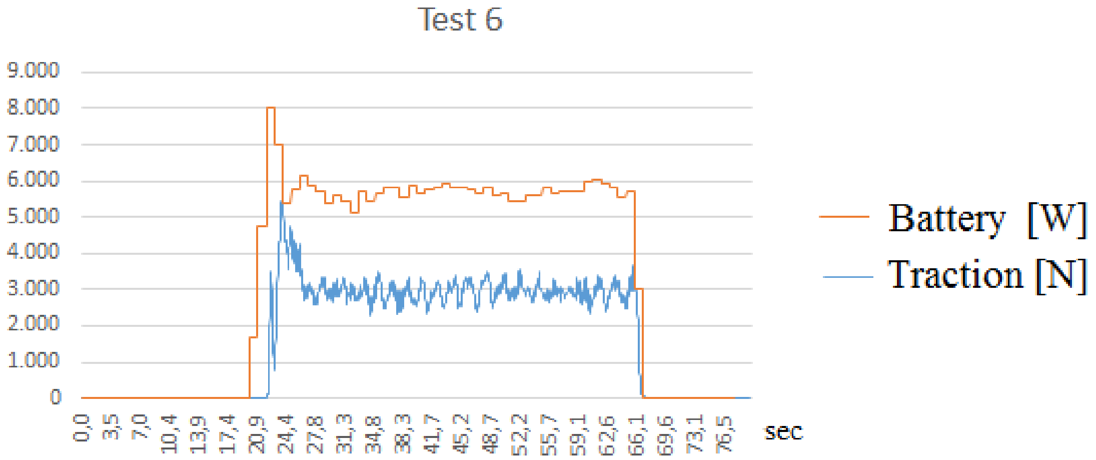

Source: Prepared by the Author.

The electric prototype tractor maximum continued traction force achieved was 4750 N in the “max” test (see Figure 122). During that test, the driver of the load tractor, Mr. Delean Santiago, carefully pressed the brakes of the load tractor until the wheels of the electric prototype tractor were visually slightly slipping. Consequently, the tire slip in test “max” was much stronger than in the previous Tests 1 to 6, with 35.79%. The speed decreased significantly to 3.08 km/h (compared to Tests 1 to 6) because of the heavy load.

The resultant power at the draw bar was 4082 W. The power provided by the batteries was 7145 W, which represents an efficiency of 57.13% between battery and draw bar. The measured medium sound level was 79 dB(A). In the acceleration phase, for a maximum of two seconds, the load tractor used its own motor to accelerate itself and the trailer.

Figure 122 – Drawbar force and battery power during test "max"

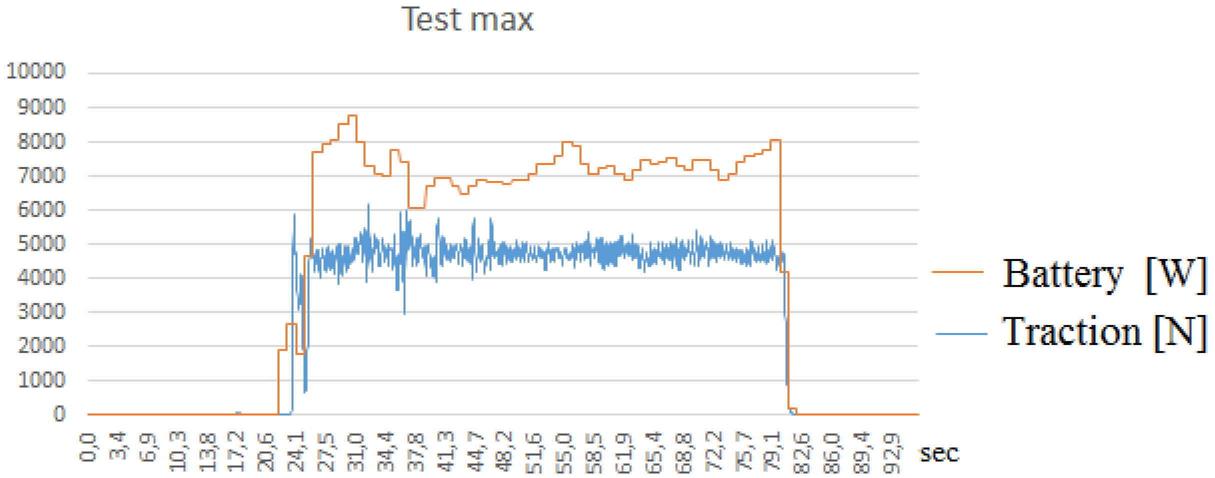

Source: Prepared by the Author.

Summarizing, the power at the draw bar ranged from 2423 W to a maximum of 4082 W. The overall efficiency based on the power provided by the batteries and the power at the drawbar was in the range of 54.53% to 64.92%. The speed ranged from 3.08 km/h to 4.76 km/h.

The overall theoretical efficiency value computed on the base of the individual efficiency values of the tractor components were: inverter 96%, motor 83%, chain drive stage 96%, and the efficiency between tire and concrete surface as defined by ASAE (2003) of 87% comes to 66.5% (Figure 123), which is not fully match by the 64.92% measured during the test runs. The reason was that the ohmic resistance losses in the cables were not considered in this calculation.

Figure 123 – Individual efficiency values of drive train from battery to draw bar

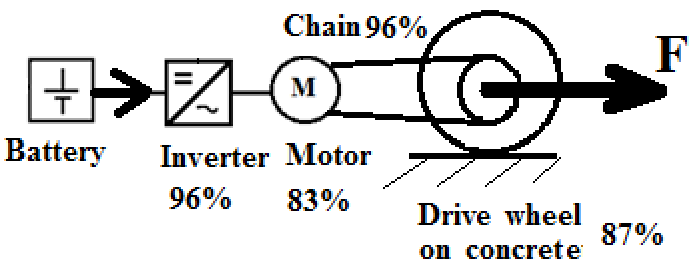

Source: Prepared by the Author.

The maximum recorded sound level during the sound test was 79 dB(A), which was in accordance with the Walsh-Healy Act, well below the level that the driver can be exposed to for more than 8 h per day (see Table 3, “Occupational Safety and Health Act Noise Criteria”).

The controllability of the electric tractor motors by means of an accelerator potentiometer, as used in modern passenger vehicles, was according to the driver satisfactorily functioning.

The complete overview of all test data is provided in Table 18.

Table 18 – Tractor test results

	Electric tractor prototype							Tobata	
Test number	1	2	3	4	5	6	max	Tobata 1	Tobata 2
Date				28.02.2018				28.02.2018	
Test coordinator				Heiner Vogt				Heiner Vogt	
Test data monitoring				Rodnei Regis				Rodnei Regis	
Test driver test tractor				Rodnei Regis				Sandoval J. Bezera	
Test driver load tractor				Delean Santiago				Delean Santiago	
Pre-test motor temperature [C°]	35	36	36.5	39	40	40	40	Gear	Gear
Post-test motor temperature [C°]	36	36.5	37	40	40	40	40	1	3
Pre-test inverter temperature [C°]	31	32	33	34	35	35	35		
Post-test inverter temperature [C°]	32	32	33	35	35	35	35		
Driver over rear axle [kg]	91	91	91	91	91	91	91		
Weight of passenger over rear axle [kg]	99	99	99	99	99	99	99		
Ballast rear axle [kg]	8	8	8	8	8	8	8		
Static empty weight forward axle [kg]				300					
Static empty weight rearward axle [kg]				400					
Dynamic reaction force forward axle [N]	2253	1871	2281	2293	2294	1910	1260		
Dynamic reaction force rearward [N]	6557	6938	3585	6516	6516	6899	7549		
Traction coefficient [Ψ]	29.82%	43.77%	52.30%	28.28%	28.24%	42.41%	63.16%		
Dynamic center of gravity x [m]	0.39	0.34	0.40	0.40	0.35	0.24	0.24		
Pre-test battery tension [V]	51	51	50.8	50.7	50.6	50.5	50.4		
Post-test battery tension [V]	51	50.8	50.7	50.6	50.48	50.4	50.3		
Medium sound level [dB(A)]	77	78	76	78	76	79	79	82	84
Maximum sound level [dB(A)]	80	82	81	81	80	83	83	85	86
Test run time (50m) [sec]	38	41	38	37.9	37.8	38.1	58.4	220	106
Speed [m/s]	1.3	1.2	1.3	1.3	1.3	1.3	0.9	0.2	0.5
Speed [km/h]	4.7	4.4	4.7	4.7	4.8	4.7	3.1	0.8	1.7
Theoretical speed [km/h]	5.4	5.1	5.4	5.5	5.5	5.5	4.8		
Slip [%]	12.28	13.92	12.28	13.65	13.42	14.10	35.79		
Power at draw bar [W]	2,573.2	3,704.2	2,467.02	2,429.4	2,433.9	3,839.9	4,082.2	538	646
Battery power [W]	3,998	5,900	3,880	3,795	3,685	5,915	7,145		
Efficiency Battery - Draw Bar [%]	64.36	62.78	63.58	64.02	66.05	64.92	57.13		
Mean force at draw bar [N]	1,956	3,037	1,875	1,841	1,840	2,926	4,768	2,365	1,370

Source: Prepared by the Author.

Note: Test sheets with results and curves can be found in the Appendix.

The dynamic center of gravity is recorded as distance “x” in front of the rear axle in meter (Table 18). The scheme of forces on the operating tractor is shown at Figure 124. The dynamic center of gravity [x] ranged from 0.24 m to 0.4 m. For possible further heavier traction test, it is advisable to install front ballast, in order to avoid accidentally lifting of front during tests.

Figure 124 – Scheme of forces on the dragging tractor

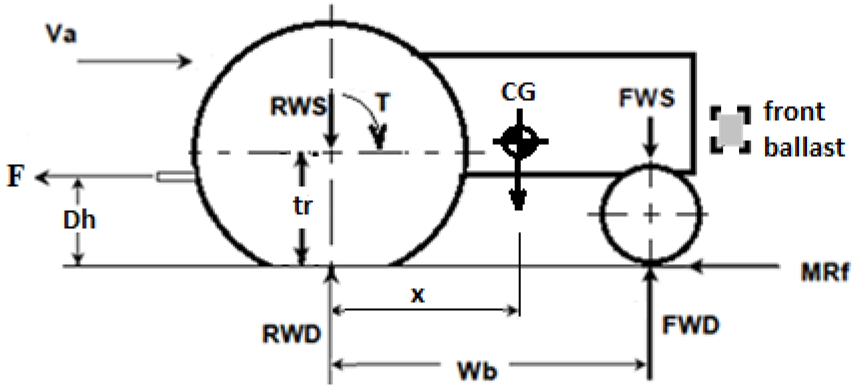

Source: Prepared by the Author.

Legend: FWS: Static load on forward axle; RWS: Static load on rearward axle; FWD: Dynamic reaction force forward axle; RWD: Dynamic reaction force rearward axle; Dh: Draw bar height; CG: Center of gravity; F: Traction force at draw bar; MRf: Motion resistant force; rt: Torque radius; T: Torque on drive wheels; Va: Velocity (speed); and Wb: Wheel base.

Motor and inverter temperature raised slightly during the tests, and then remained constant. Outside motor temperature raised from 31°C (Test 0) to 40°C (Test 4), and also remained stable at that level, until the last max test. Outside inverter temperature raised from 30°C (Test 0) to 35°C (Test 4), and remained stable at that level until the last max test.

For statistical purposes, the following values for the draw bar force were determined: sum of all sample, number of samples, mean value, median, minimum and maximum, range, variance, variance coefficient, mean deviation, lower quartile, upper quartile and interquartile range. In the Gruber test, no outliers have been detected for Tests 1 to 6 and for the Tobata tests (see all statistic test figures in the Appendix). Consequently, the results can be considered to be reliable.

4.4.6 *Electric tractor versus Tobata reference tractor*

The comparative Tobata tractor achieved constant traction forces of 2365 N with a speed of 0.82 km/h compared to the electric prototype tractor with 4750 N with a speed of 3.08 km/h.

The Tobata continued sound level was up to 84 dB(A). Compared to the electric tractor with a maximum sound level of 79 dB(A), the sound level of the Tobata was notable higher, since sound pressure doubles with every 6 dB, and sound power doubles already with every 3 dB.

Table 19 presents the basic descriptive statistics of the two alternatives' behavior during traction Test 5 of the electric tractor and traction Test 2 of the Tobata tractor.

Table 19 – Descriptive statistics of the two alternatives behavior during traction test

Statistic Measures	**Electric tractor Test 5**	**Tobata Test 2**
Sum X	**918.293**	**683.800**
$\sum X^2$	1.723.848.111	1.250.964.786
Samples	499	499
Median	1.840	1.370
Mean value	1.850	1.404
Minimum	1.142	69
Maximum	2.375	2.957
Range	1.233	2.888
Variance	68.025	315.436
Variance coefficient	14%	40%
Mean deviation	261	562
Lower quartile	1.686	1.190
Upper quartile	2.027	1.613
Interquartile range	341	423

Source: Prepared by the Author.

In terms of traction force oscillation, there was as well a notable difference comparing the 5th electric prototype tractor test with a medium traction force of 1850 N, and the 2nd Tobata tractor test with a medium traction force of 1370 N. In those tests, the samples of the traction measurement ranged for the electric prototype tractor from a minimum of 1142 N to a maximum of 2375 N.

This result is in a range for the electric prototype tractor of Δ 1233 N. For the Tobata, the minimum was 69.18 N and the maximum 2957 N, with a range of Δ 2888 N. This means the electric tractor was 2.49 times more stable in its traction force oscillation during these tests than the reference Tobata tractor. Evaluating the comparative tractor test analysis of variance rendered the results listed in Table 20.

Table 20 – Analysis of variance for the comparative tractor test

Source	SS	*df*	F	$F_{critical}$	*p*
Between-groups	55440618.78	1	287.94	6.69	0.0001
Within-groups	192544.79	996			
Total	55633163.57	997			

Source: Prepared by the Author.

The f-ratio value was 287.94. The critical F-ratio is 6.69 and the p-value is <0.00001. The result is significant at p<0.05. The control charts of this comparative tractor traction tests are presented in Figures 125 and 126.

Figure 125 – Control charts electric tractor Test 5

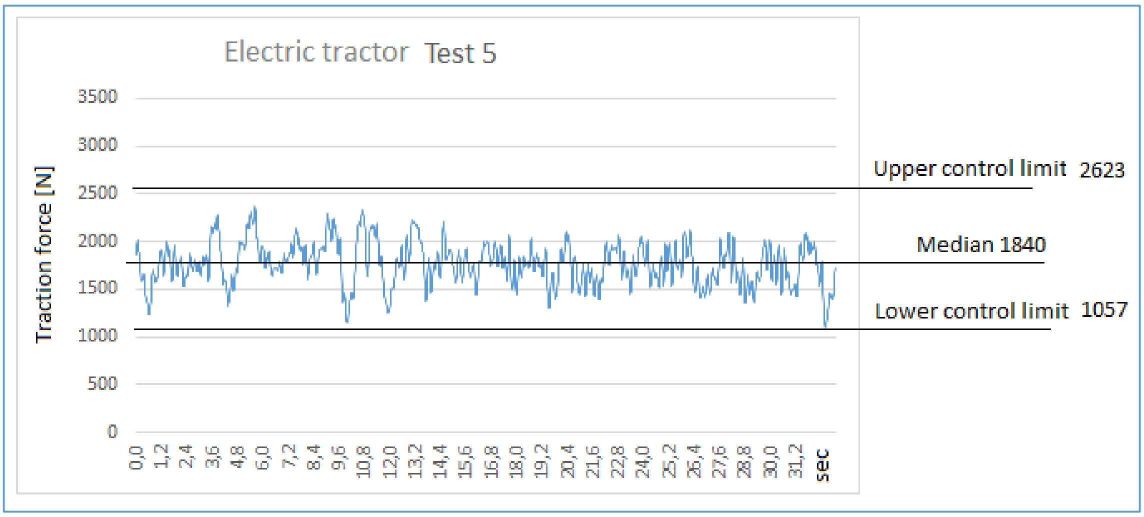

Source: Prepared by the Author.

Figure 126 – Control Tobata tractor Test 2

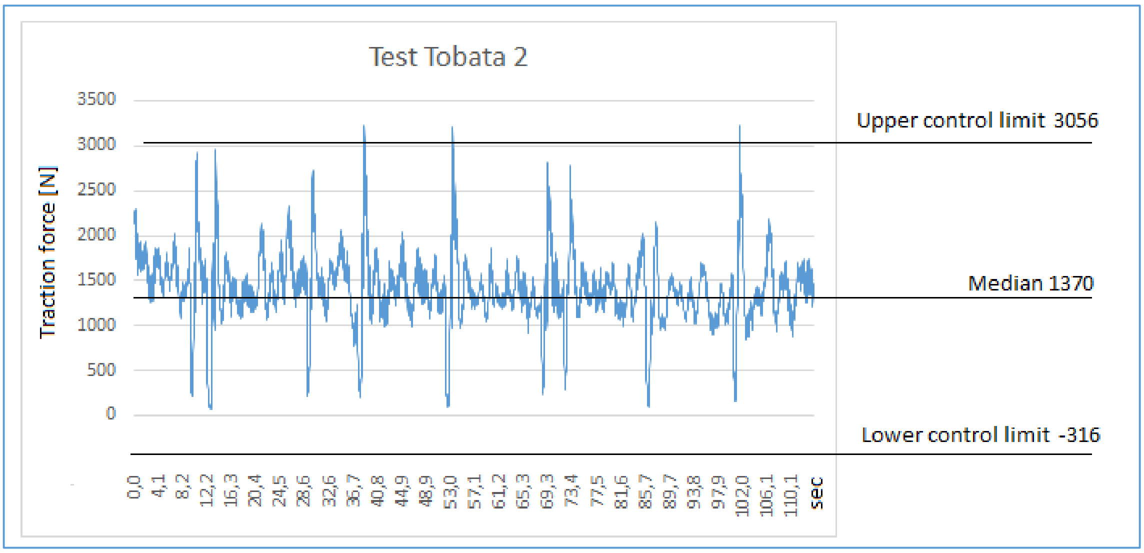

Source: Prepared by the Author.

The control charts shown in Figure 125 and Figure 126 point that, to the Tobata Test 2, several points are outside the upper control limit. This indicates an unstable process. However, as Albiero *et al*. (2012) highlight, two considerations must be fulfilled: the first is that control charts are not recommended by Montgomery (2004) for non-normal processes; and the second is that agricultural processes are now far from the ideal of industrial control.

Summarizing, the electric tractor was more powerful and faster on the drawbar, produced a lower noise level, and the traction process had a higher stability than the Tobata tractor. But one has to bear in mind that tests were carried out with a first-conception prototype of the electric tractor on a concrete test track, which is not the common ground for an agricultural tractor. Consequently, future projects will have to prove in field tests the measured capabilities of the electric tractor in real agricultural application.

4.4.7 *Failure Mode and Effect Analysis of prototype tractor*

As posited by Albiero (2010), the FEMA process comprises 11 stages:

1. Define the scope of the analysis
2. Prepare a flowchart of the process
3. Identify potential failure modes and their effects
4. Quantify the potential effects of failure
5. Identify potential causes for each failure mode and its probability of occurrence

6. Classify the severity
7. Classify the occurrence probability
8. Identify what controls are currently in place and the rates of likelihood of detection of failure
9. Calculate the RPM (risk priority number)
10. Evaluate the potential risk for each failure mode
11. Set measures to eliminate or reduce the risk of failure.

a. ***Scope of the analysis***

The process to be analyzed is the electric tractor operation spanning from early morning pre-start activities, operating phase at the plantation including transit from and to the base and ending with preparations for the next day. The particular working process steps are (exemplary for configuration A or B):

1. Check tractor battery charge level – swap batteries for charged ones if required
2. Check tractor ballast – adjust ballast
3. Check tractor tire pressure – adjust tire pressure
4. Check visually tractor mechanical and electrical components – if necessary repair
5. Calculate necessary battery capacity for transit and actual work – If onboard battery pack charge is not sufficient load trailer with sufficient (charged) battery packs
6. Hook up implement and trailer
7. Check if battery packs on second trailer are hooked up to the charger – if necessary hook up second trailer to charger
8. Prepare tractor operation by: Close circuit breakers, turn main switch on, check emergency button for unhooked position and select forward or reverse drive
9. Drive to work destination/ work
10. Low tractor battery indicator alarm – stop tractor operation - swap battery packs
11. If last battery pack swapped on tractor – set alarm for battery minimum for secure return to base
12. If battery alarm for secure return to base rings – stop work, return home to base
13. At base swap battery packs – discharged one against charged one
14. Hook up discharged battery packs on charger
15. If required return to the field and complete the work
16. Park tractor, main switch off, take circuited breakers out
17. Visual check of tractor mechanical and electrical components – if necessary repair

b. ***Flow chart***

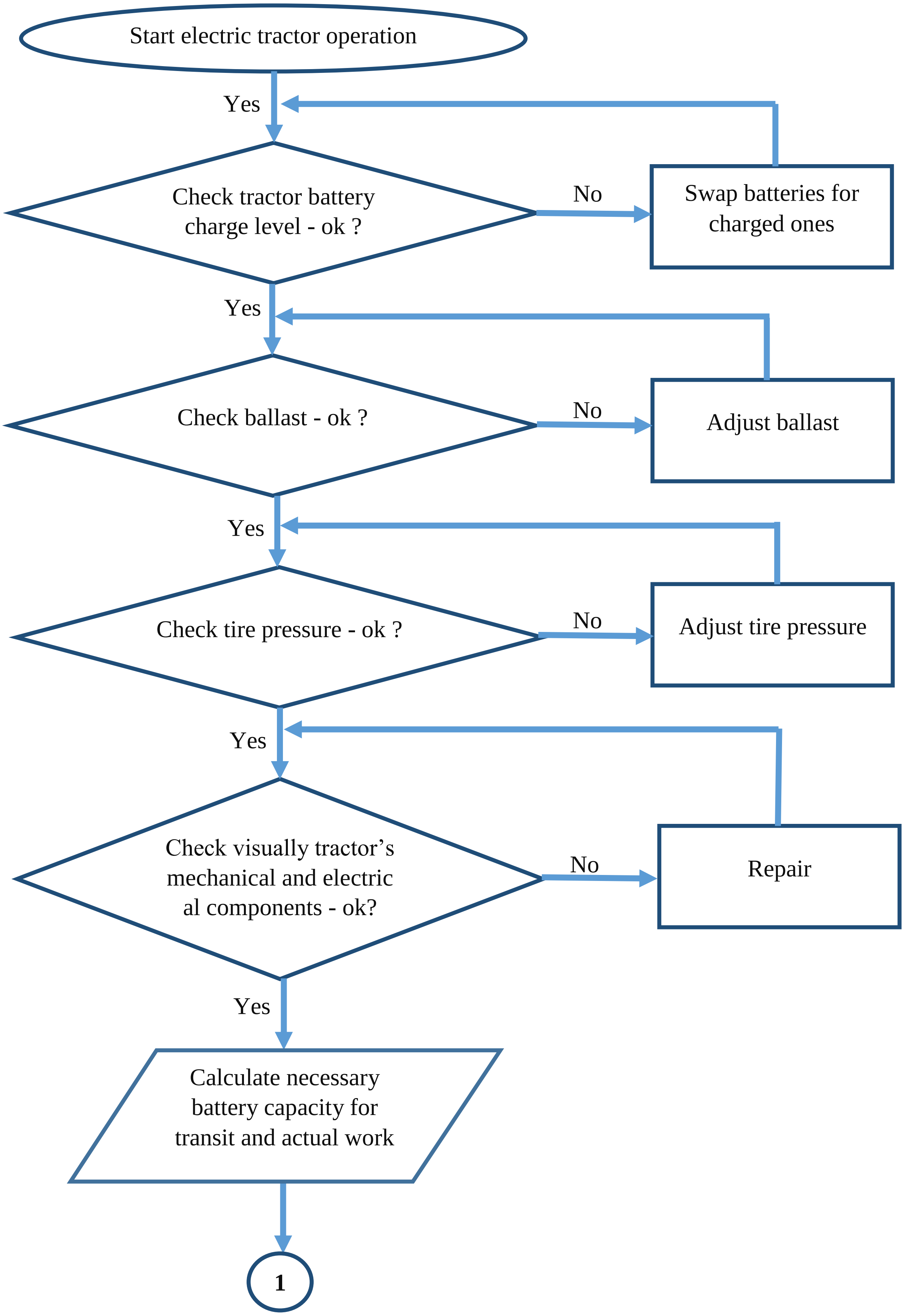
Start electric tractor operation
Yes
Check tractor battery charge level - ok ?
No
Swap batteries for charged ones
Yes
Check ballast - ok ?
No
Adjust ballast
Yes
Check tire pressure - ok ?
No
Adjust tire pressure
Yes
Check visually tractor's mechanical and electric al components - ok?
No
Repair
Yes
Calculate necessary battery capacity for transit and actual work
1

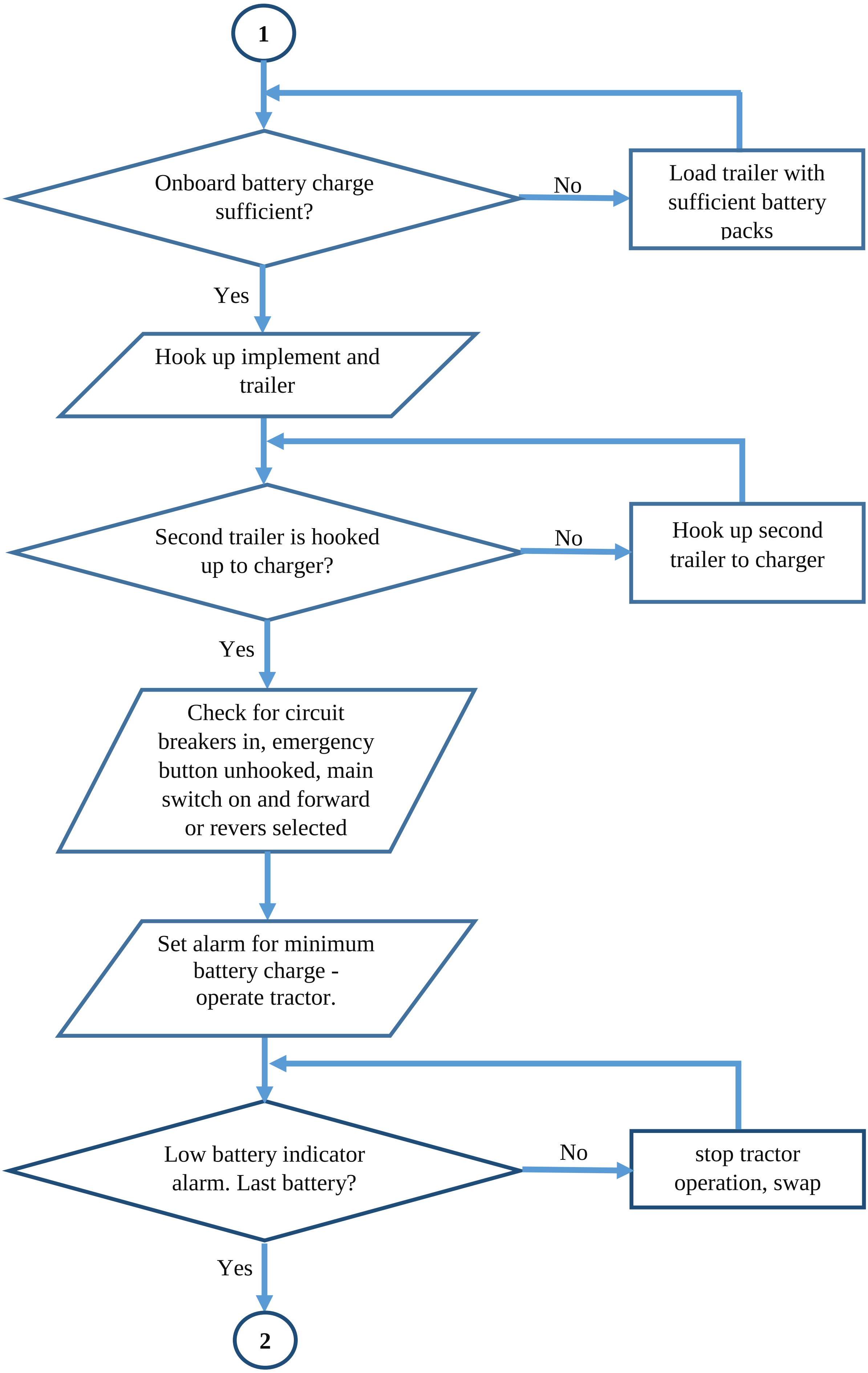
1
Onboard battery charge sufficient?
No
Load trailer with sufficient battery packs
Yes
Hook up implement and trailer
Second trailer is hooked up to charger?
No
Hook up second trailer to charger
Yes
Check for circuit breakers in, emergency button unhooked, main switch on and forward or revers selected
Set alarm for minimum battery charge - operate tractor.
Low battery indicator alarm. Last battery?
No
stop tractor operation, swap
Yes
2

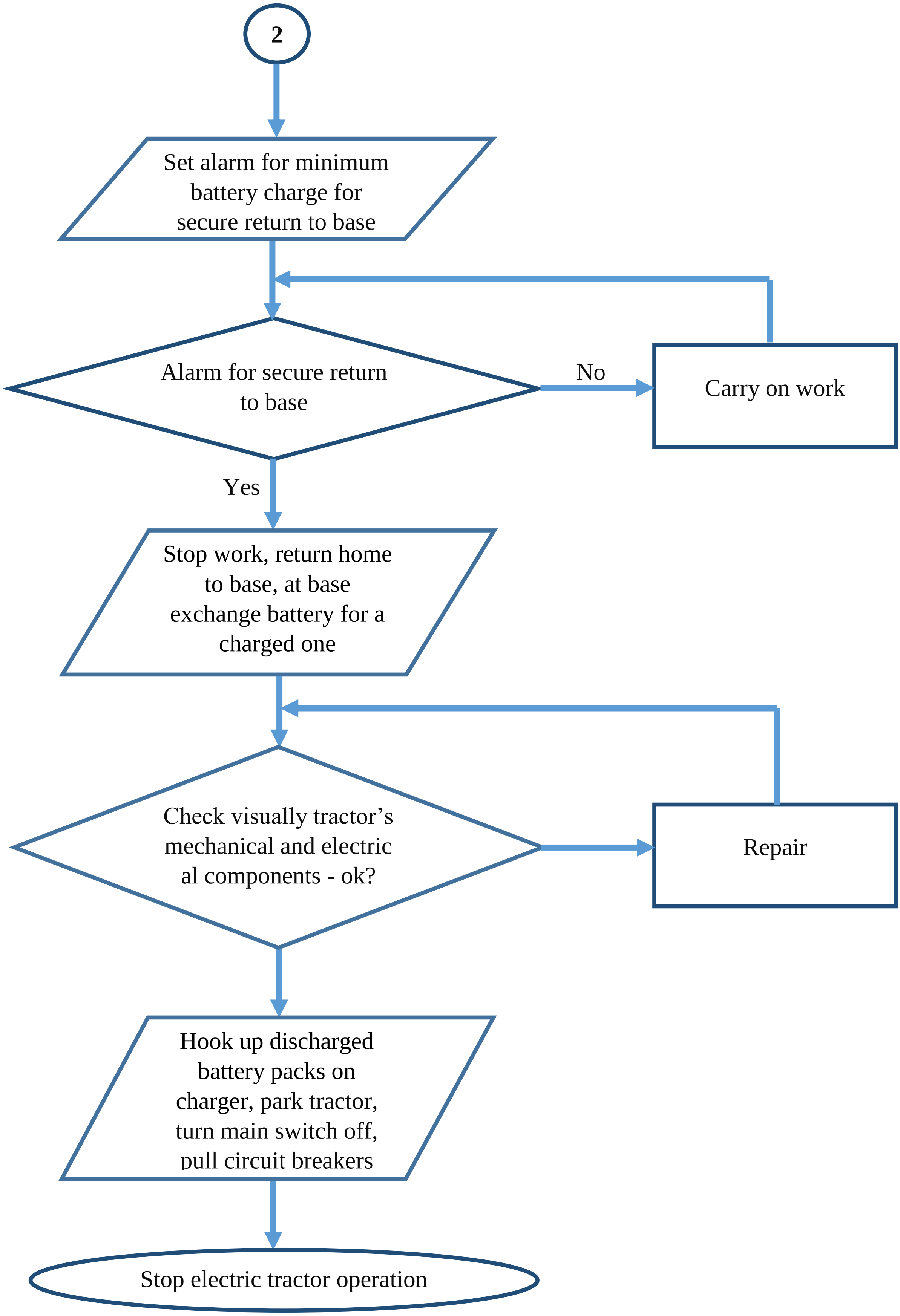
2
Set alarm for minimum battery charge for secure return to base
Alarm for secure return to base
No
Carry on work
Yes
Stop work, return home to base, at base exchange battery for a charged one
Check visually tractor's mechanical and electric al components - ok?
Repair
Hook up discharged battery packs on charger, park tractor, turn main switch off, pull circuit breakers
Stop electric tractor operation

c. *Potential failures and their effects*

The purpose of this process is to compute a risk priority number (RPN) as a quantification of the potential effects of a failure by evaluating the following criteria: identified potential causes, probability of occurrence and their classification of severity, identified control measures already in place and the rates of likelihood of detection of failure. Table 21 lists the potential tractor operating risks classified as top, high and medium priority.

Table 21 – Risk failure potential of tractor operation

Serial No.	**Risk description**	**Potential effects**	**Risk failure potential**	**Mitigation**	**RPN** (risk priority number)	**Class**
1.	Parking brake fails	Uncontrolled rolling of tractor	Fatal injuries to others, property damage	Inspect/test at regular intervals	897	TP
2.	Chain drive	Limbs get entangled	Fatal injury	Fitting of guards and warning labels	870	TP
3.	Tractor roll over	Operator may not be able to leap off	Fatal injury or property damage (tractor)	Roll over protection bars to be fitted.	833	TP
4.	Foreign object short circuiting battery terminals	Batter conflagration	Property damage (destruction of battery)	Cover to be installed	770	HP
5.	Short circuit	Battery may overheat and cause a fire, spillage of chemicals	Property damage, contamination of environment	Install main fuse close to battery terminals	630	HP
6.	Chain of second stage snaps	Brakes ineffective	Fatal injury, Property damage	Regular inspection, elongation test	450	MP
7.	Battery discharged at field	Tractor cannot return to base	Tractor abandoned at the field	PV charge device on tractor	423	MP
8.	Low sound level	Other traffic participants are not alerted	Collisions	Fit horn	420	MP
9.	Unsafe battery handling	Battery drops to the ground	Sever injury, property damage	Elaborate procedures and provide suitable tools and tackles	380	MP

Source: Prepared by the Author.

General Remark: All operators of the tractor will be trained and made aware of the risks associated with operation of the tractor.

The classification of potential failures is made according to the intervals:

408 – 607 RPN	= medium priority	(MP)
608 – 807 RPN	= high priority	(HP)
808 – 1000 RPN	= top priority	(TP)

4.5 Cost comparison of electric tractor systems *versus* common tractor with combustion engine

For the cost study family farming in the northeast of Brazil is a favorable scenario for the implementation of an electric tractor system. The main reasons are that there is abundant solar irradiation exceeding >5 kW/h per square meter per day basically throughout the year (see Figure 8) and that small scale farms play a dominating role.

The comparative cost study based on the electric tractor system and a common combustion engine tractor of approx. same power rating is favored to a direct cost-benefit analysis since reliable data on expenditures and earnings are not available for such farms in this region.

The applied method bases upon the conversion of investment costs and direct operating costs into total hourly operating costs of the two alternatively powered tractors. For the combustion engine powered micro tractor, the costs considered are the market purchase price and the fuel cost. Overheads, like insurance and maintenance are considered for both alternatives as percentage of the investment cost and the period of use (Figure 127). The electric tractor is equipped with a 9 kW and the combustion engine tractor with a 10.3 kW motor.

Figure 127 – Representation of the two tractors systems of the comparative cost study

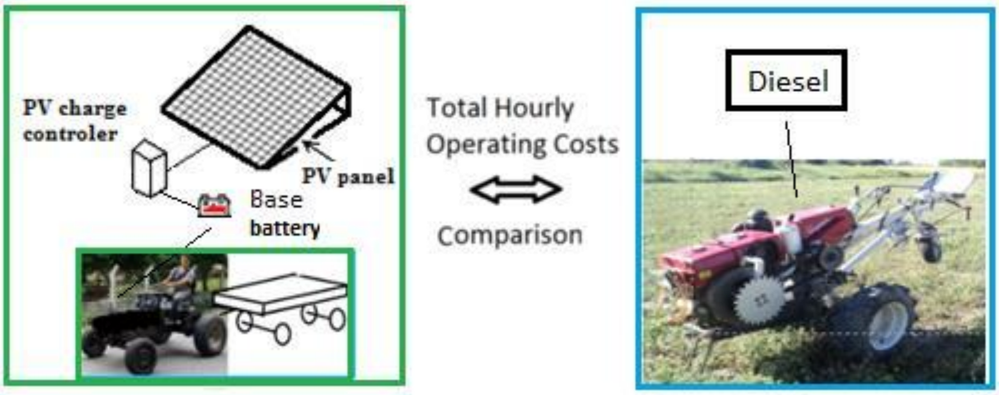

Source: Prepared by the Author.

Battery costs enter the calculation process as operational costs since the degradation occurs in proportion to the number and depth of the charge – discharge cycles. For the electric tractor Li-ion batteries were considered based on an expected future price level of 120 US$ per kWh storage capacity from the year 2020 and on (Figure 128).

Figure 128 – Evolution of battery energy density and cost

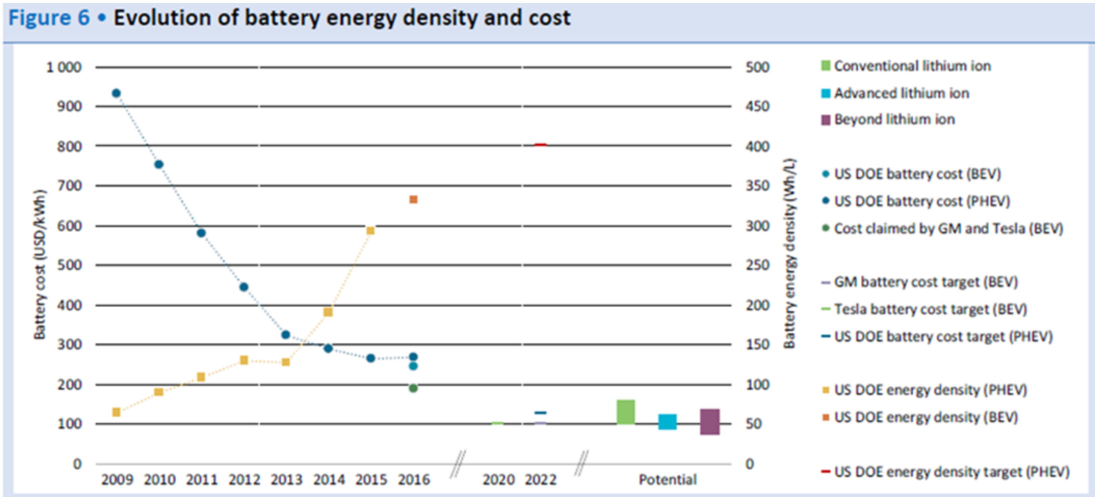

Source: Global EV Outlook (2017).

The investment cost per kWh storage capacity are:

~ Lead-acid	on 2017 price level	148 US$
~ Li-ion	on 2017 price level	220 US$
~ Li-ion	on 2020 price level	120 US$ (predicted)

It is assumed that the battery can sustain 2800 charge-discharge cycles at 100% depth of discharge each time (SONNENSCHEIN, 2014) until the batteries storage capacity is reduced to 80%. This leads to a cycle price of 0.04 Euro kWh/cycle. In comparison, the calculated cycle costs of a lead-acid battery based on the 2017 price in Brazil and with 700 cycles at a discharge depth of 75%, are 0.24 Euro kWh/cycle which is six times higher (Figure 129).

Figure 129 – Battery cycle costs for lead-acid and Li-ion at 2017 prices and predicted price level for 2020

Source: Prepared by the Author.

The assumed yearly operating times of the tractor for 1 to 4 semiarid family farms are: 250 h, 500 h, 750 h, and 1000 h. It is important to mention that these yearly operating times apply also to the trailers and the PV – generator.

The assumed yearly operating time of the cable feed system is 221 h. The reason behind this reduced number of hours (compared to the yearly tractor operating hours) is that the area covered by the system using a 50 m boom is 0.78 ha (7800 m^2). For the determination of this value pl. refer to the annex.

The electric tractor system configurations considered are shown in Figure 130. Detailed description of all configurations can be found on item 4.2, Energy systems (transmission).

Figure 130 – Electric tractor system configurations

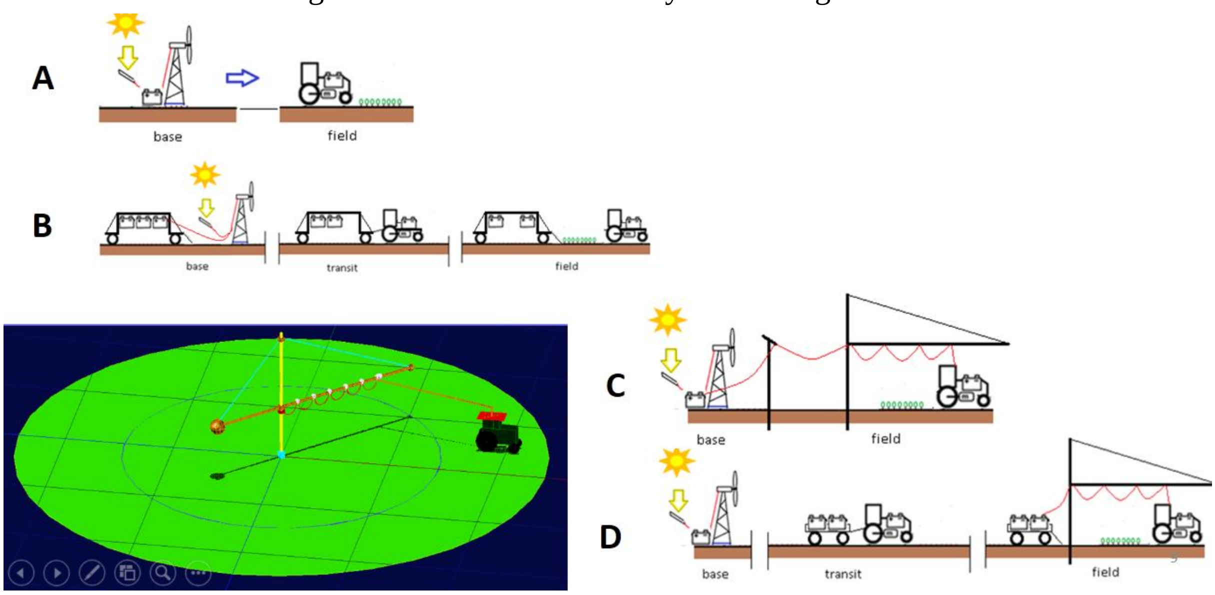

Source: Prepared by the Author.

With respect to the energy transmission system comprising a pivot and a boom according to configuration C, the calculation bases on a three phase 400 V transmission line of a length of 570 meters between the home base battery and the field. These design parameters represent an optimum regarding cable cross-sections, operational safety and availability of equipment (Table 11).

The electric architecture options of transmission via battery swap and via cable and pivot and boom are shown in Figure 131.

Figure 131 – Electric architecture options of transmission via battery swap and via cable, pivot and boom

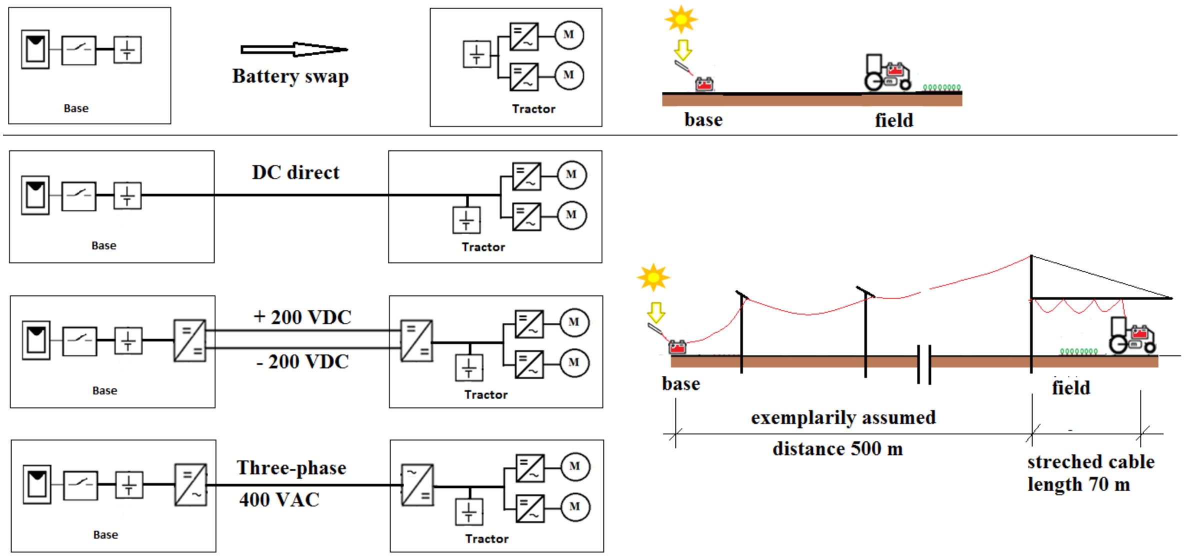

Source: Prepared by the Author.

The complete electric tractor system from PV-generation to the tractor linked to the base battery via pivot and boom is shown in Figure 132.

Figure 132 – Electric tractor system from PV-generation to the tractor linked to the base battery via pivot and boom

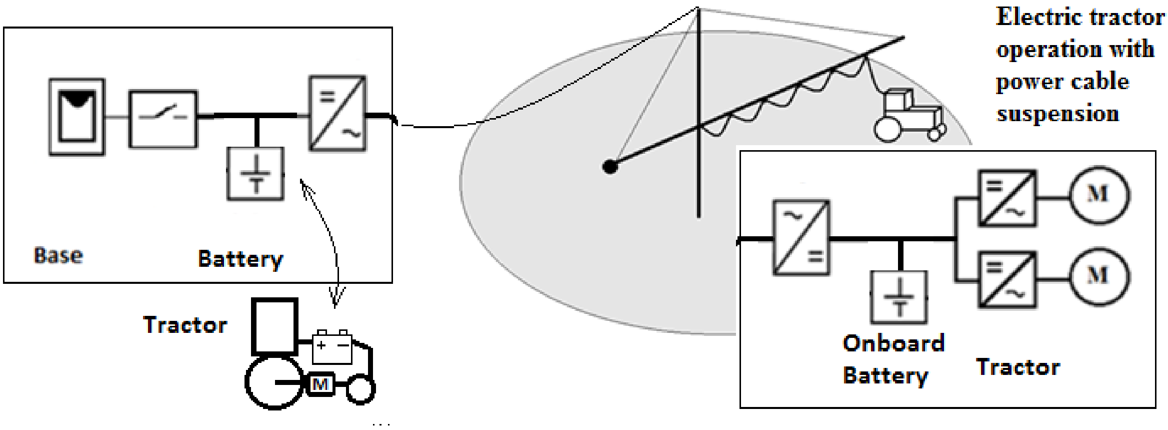

Source: Prepared by the Author.

Costs are based on the 2017 Brazilian market prices for locally available products. Imported equipment (and re-conversion of Real in Euro) is factored in with an exchange rate of 3.7 Real for 1 Euro or 3.1 Real for 1 US$ (Exchange rates from 04th September 2017).

For calculating the depreciation of the equipment value, the following periods are considered: 12 years for the tractor including trailer, cable system with pivot and boom and 25 years for the PV-panels (Figure 133).

Figure 133 – Tractor hourly operating cost parameter

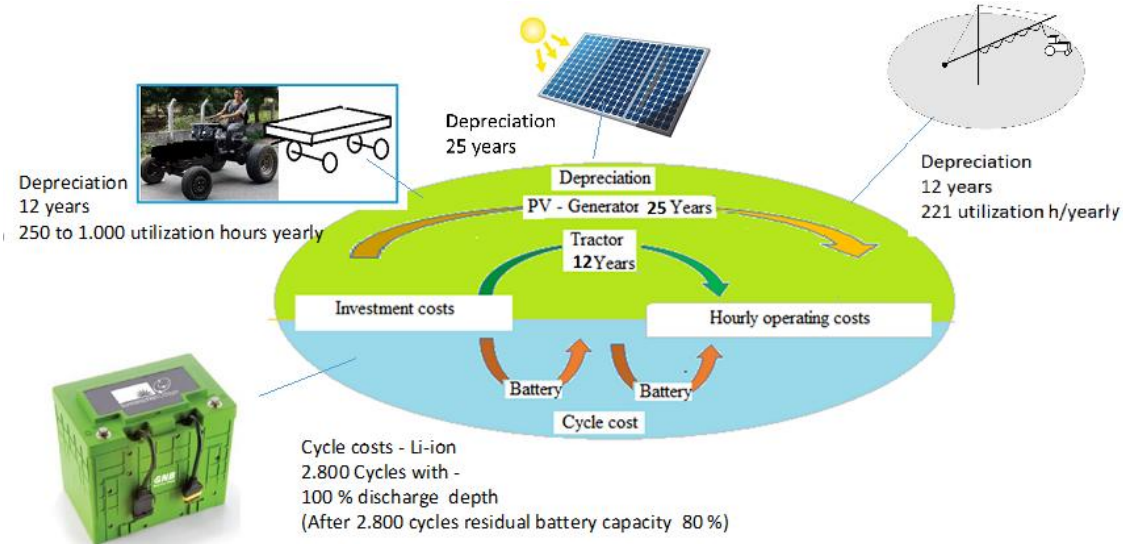

Source: Prepared by the Author.

Yearly Insurance costs are included with 1.5% on the initial investment and maintenance costs with 0.5% per 100 tractor operating hours. Interest rates are not taken into account.

The cost calculation method to determine the hourly operating cost of the electric tractor system and that of the common combustion engine tractor is outlined in chapter 3.12. Cost Calculation Method.

The determination of the electrical system's generation and storage capacity takes into account the efficiency of all system components (Figure 90). The maximum daily energy consumption is based on a maximum of 15 (and alternatively 6 h) tractor working hours at 80% power level (of the rated tractor power).

The capacity determination of battery and PV generator is based on the power requirements of the tractor's motors. In addition, the component efficiencies are considered for computing the capacity of the battery and finally that of the PV generator Figure 134.

Figure 134 – Capacity determination of battery and PV generator

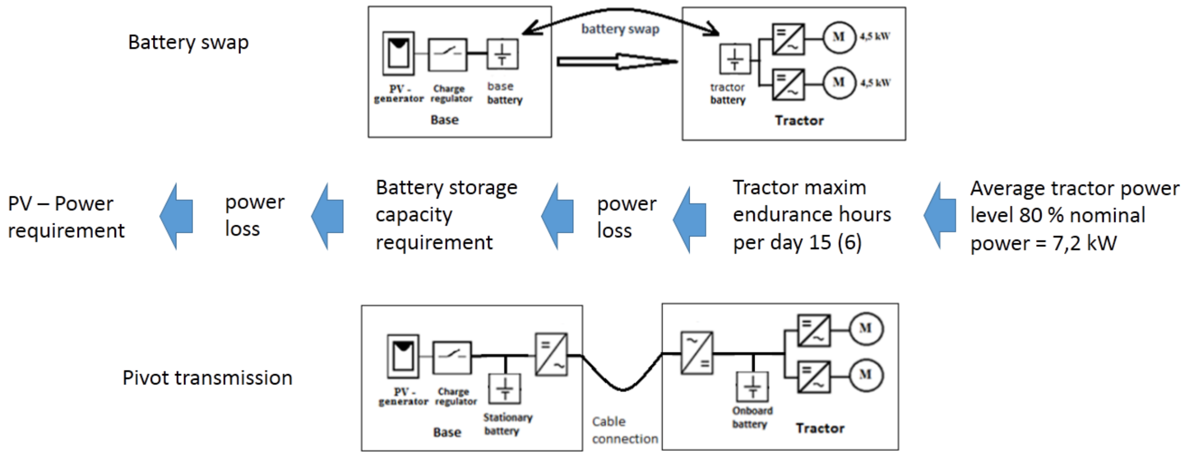

Source: Prepared by the Author.

As far as the design of the battery backup and photovoltaic system is concerned, the capacity is tailored to the maximum intended daily operating time of the tractor. When the tractor is used on consecutive days at an average of 80% of its nominal power for 15 h (or alternatively 6 h), then all of the energy generated during this period would be consumed by the tractor.

For calculating the total hourly operating costs, the following assumptions have been taken:

- Li-ion battery 2020 prices forecast of 120 US$ / kWh
- 2800 cycles with 100% discharge depth
- Insurance 1.5% of investment costs yearly
- Maintenance 0.5% of investment costs per 100 tractor hours
- Exchange rates: US$ - Real 3.1; Euro - Real 3.7
- Tractor, trailer and pivot depreciation period 12 years
- PV depreciation period 25 years
- Average tractor power level 80%
- Reference tractor: Yanmar Agritech TC14S, Real 22000 with a fuel consumption of 3-liter diesel per tractor hour
- Fuel cost per liter diesel 3.20 Real

Not considered:

- Battery residual value with a storage capacity of 80% after 2800 cycles
- Economies of scale cost benefits
- Reduced maintenance cost inherent to electric vehicles (compared to a combustion engine driven vehicle)
- Surplus energy (refer to separate chapter)
- Environmental benefits

Based on the above boundary conditions the required capacity of the battery packs and the PV-System is calculated. The results are given in Table 12 Capacity Requirements for Battery and PV – Panel, shown in item 4.3, Determination of battery storage- and PV-generation- capacity.

In order to implement an electric tractor system of the capacity indicated above, investment costs amounting to the figures below are predicted (Table 22).

Table 22 – Investment for electric tractor system configurations (in Euros)

	Tractor	**Trailers (two)**	**Battery**	**PV panel**	**Pivot**	**TOTAL**
A	€ 10,746		€ 5,801	€ 8262		€ 24,809
B	€ 10,746	€ 3,784	€ 14,502	€ 20,654		€ 49,686
C	€ 10,746		€ 10,177	€ 24,156	€ 17,181	€ 62,260
D	€ 10,746	€ 3,784	€ 14,601	€ 20,795	€ 3,223	€ 53,150

Source: Prepared by the Author.
Note: Pivot includes structure, electric components and power electronic.

The common tractor used for comparison purposes is a Yanmar Agritech TC14S single axle micro tractor powered by an internal combustion 4-stroke diesel engine (10.3 kW, 2,400 rpm, Weight 433 kg [10]) with a market price of 5,964 Euro plus a diesel storage tank at a cost of 535 Euro. This makes a total of 6,481 Euro for the combustion engine tractor.

Table 23 – Investments electric tractor system *versus* common tractor

Electric Tractor System Configuration	Investment	
	Electric Tractor System	Comparable Common Tractor
A 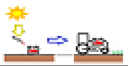	€ 24,809	€ 6,481
B 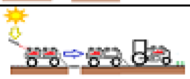	€ 49,686	€ 6,481
C 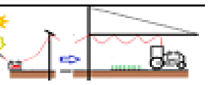	€ 62,260	€ 6,481
D 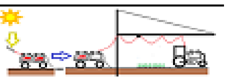	€ 53,150	€ 6,481

Source: Prepared by the Author.

By using the values in Table 20 as input for calculating the total hourly operating costs, the values as shown in the table below are obtained (Table 24). With respect to the common tractor, a fuel price of 3.2 Real (0.865 Euro) per liter of diesel (Price base as of November 2017) and a fuel consumption of 3 liters per hour were considered (NASCIMENTO, 2012).

Table 24 – Tractor total hourly operating costs [EURO/h]
(not considering surplus energy benefit)

Electric Tractor System Configuration	Utilization per year in Hours	Maximum Daily Tractor Hours	Hourly Electric Tractor Cost	Comparable Common Tractor
A 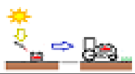	250	6	€ 6.43	€ 5.23
	500	6	€ 3.66	€ 4.06
B 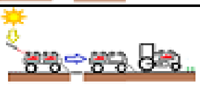	750	15	€ 3.89	€ 3.67
	1000	15	€ 3.14	€ 3.48
C 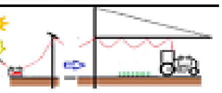	750	15	€ 10.13	€ 3.67
	1,000	15	€ 9.45	€ 3.48
D 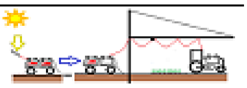	750	15	€ 5.11	€ 3.67
	1,000	15	€ 4.36	€ 3.48

Source: Prepared by the Author.

The results show that the electric tractor system according to configuration A with 500 yearly tractor working hours and 6 h maximum per day and according to configuration B with 1000 yearly tractor working hours and 15 h maximum per day, is competitive with a common combustion engine tractor.

Surplus energy

The capacity of the energy generation and storage system is designed to provide energy for the tractor for an unlimited duration of consecutive days either for15 (or 6) working hours per day.

Hence, in periods of times when the agricultural farming activities are demanding the full tractor potential (in power and operating time) on a number of consecutive days, the capacity of the generation and storage system is fully used for tractor operation. Such a situation occurs mainly in planting and harvesting periods. But looking at it over the course of a year such an intensive utilization is not likely to happen very often. Normally, there is surplus energy left unexploited. However, the amount of energy in surplus will vary greatly depending on the utilization of the tractor, i.e. whether it is idle, in part time or in full time use (Figure 135).

Figure 135 – Energy Use and Surplus Energy Availability

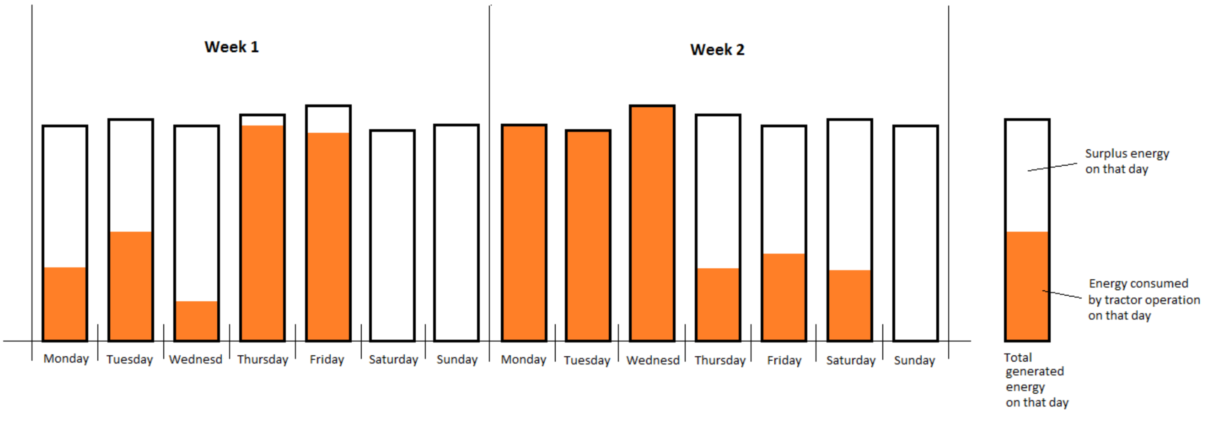

Source: Prepared by the Author.

The amount of surplus energy is significant. This shall be demonstrated on an example based on 1000 yearly tractor working hours with a daily maximum tractor working time of 15 hours. The energy generation and storage system is designed to provide the necessary energy for 15 tractor working hours on every day of the 365 days of the year.

Thus, 1000 yearly working hours divided by 15 working hours daily result in a total of 66.7 tractor working days (if the tractor would work continually the full working hours daily). This means that the capacity of the generation and storage equipment is 5.47 times higher as the summed up energy required for the tractor operation over the full year (with 365 days).

This is a commercially interesting opportunity as in times when the tractor is used only a few hours per day (Figure 136) or is standing idle, the amount of this surplus energy could be used for other purposes such as for domestic applications (lightning, refrigeration, communication entertainment), for water pumping or processing of agricultural products. To do so an appropriate micro grid would be necessary.

Furthermore, many semi-arid families (over 80%) are connected to the grid and the Brazilian law permits to inject surplus energy into the grid. The connection to the grid (officially 230 V with 15 A) is however of a low power rating and in most cases a substantial voltage drop occurs across long cables transmitting the power to the end consumer. Given these circumstances, a future investigation would be required in order to determine whether the alternative of feeding surplus energy into the grid would make economic sense.

The effective use of surplus energy requires an energy management system and a separate infrastructure (a micro grid for domestic consumers and/or a feed in connection to the public grid). The objective of the energy management system would be to ensure that the consumption of power of other flexible consumers is scheduled such that operation of the tractor is not disturbed.

In practice this would mean that power for other consumers is only available when the tractor is idle or used for field work requiring a low power output. This of course is not acceptable since certain consumers related to conservation and safety cannot be turned off, therefore, a micro grid has to include a separate energy storage device for these essential consumers (Figure 136).

On the other hand, an additional trailer with battery packs as energy buffer could be used to cover these periods. This should be investigated in a further project.

Figure 136 – Side Benefits for joint Energy Use

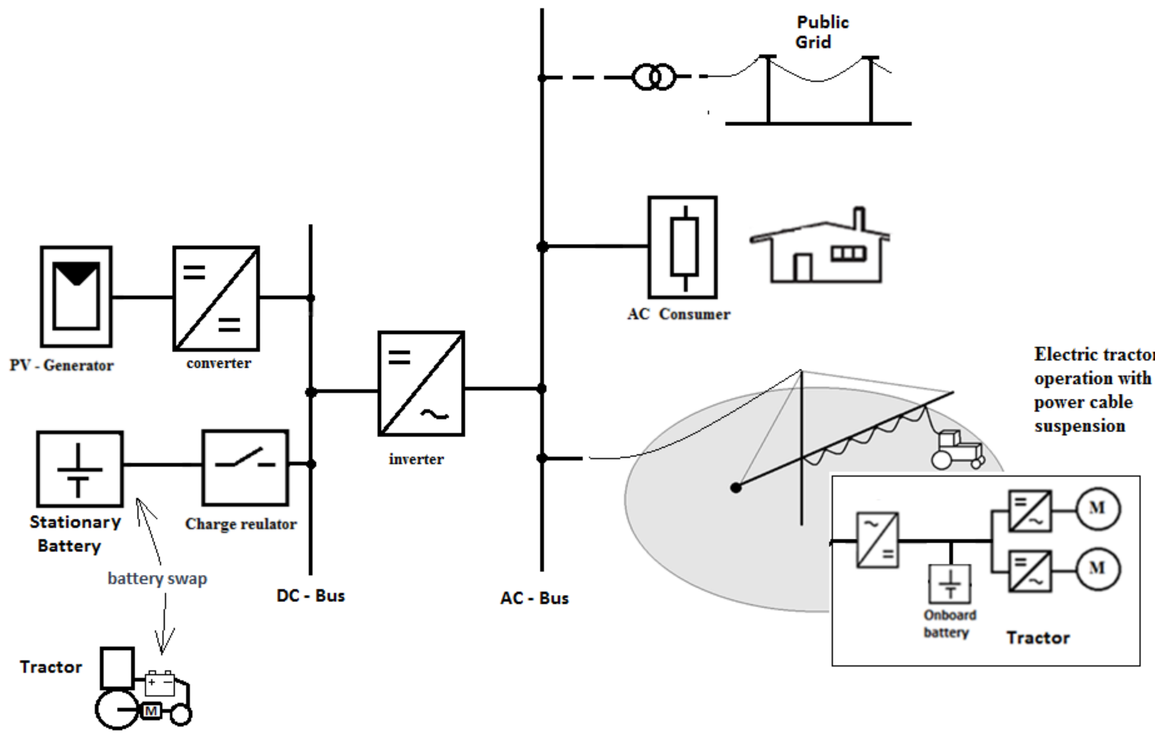

Source: Prepared by the Author.

In order to configure such a micro grid, one would have to carry out an investigation of the load pattern required by any potential consumers. As this goes beyond this project, the requirement has been put in the future task list. However, as this aspect is essential for an evaluation of the economic viability of the electric tractor system, deliberately low end user prices have been assumed for determining the benefit in order to be on the conservative side.

To consider the economic potential of this energy surplus, a second Hourly Operating Cost calculation of the electric tractor system considers a kWh price of 0.03 Euro for the surplus energy. This is far less than the normal price per kWh of 0.15 Euro but it represents a cost figure that is comparable to the subsidized kWh- price poor people pay in the northeast of Brazil. Families, which are considered poor (low income), pay a government subsidized price of about 0.05 Euro per kWh.

By including the energy surplus as an economic benefit, the result of this calculation is that the electro tractor system is matching the hourly operational cost of the common combustion engine tractor for the configurations A, B and D (Figure 130).

Taking the benefit of this surplus energy into account, the total hourly operating costs of the electric tractor system drop to the values listed in Table 25.

Table 25 – Tractor total hourly operating costs [EURO/h]
(considering surplus energy benefit at 0.03 Euro/kWh)

Electric Tractor System Configuration	Utilization per year in Hours	Maximum Daily Tractor Hours	Surplus Energy Compensator	Hourly Electric Tractor Cost	Comparable Common Tractor
A 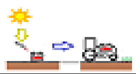	250	6	€ 1.22	€ 5.22	€ 5.23
	500	6	€ 1.22	€ 2.44	€ 4.06
B 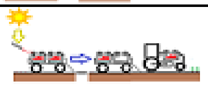	750	15	€ 1.84	€ 2.05	€ 3.67
	1,000	15	€ 1.38	€ 1.76	€ 3.48
C 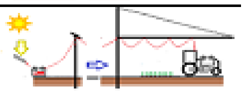	750	15	€ 2.15	€ 7.98	€ 3.67
	1.000	15	€ 1.61	€ 7.84	€ 3.48
D 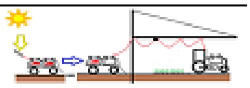	750	15	€ 1.84	€ 3.27	€ 3.67
	1,000	15	€ 1.38	€ 2.89	€ 3.48

Source: Prepared by the Author.

The cost reduction potential of the electric tractor system does not yet consider other opportunities of cost degression such as in-series production of the electro tractor, the residual value of the tractor batteries that are passed out after 2800 cycles at 80% of their original storage capacity (they could be used as stationary batteries) and the cost advantages in the maintenance of electric vehicles (compared to combustion engine ones).

This cost comparative study (Table 26) was elaborated to the best knowledge of the authors for the conditions in the semiarid region in the northeast of Brazil. Some component prices had to be estimated.

Residual values for tractor, pivot, trailers and batteries, benefits of an in-series production of the electric tractor system and especially environmental benefits were not considered. Also not considered were interest rates since they are actually zero (in the Euro zone) and since it is presumed that this kind of investment would benefit from agricultural development programs for the region. The complete study with all relevant sources, references and documents will be available and publicized as soon as the project is concluded.

Note: The pivot system, configuration C, will most probably be competitive in case of a three phase 400 V AC grid connection on the farm. This will be occasionally the case in bigger farms and it is not considered in this study.

Table 26 – Results: electric system *versus* common tractor

Electric Tractor System Configuration	**Utilization per year in Hours**	**Maximum Daily Tractor Hours**	**Hourly Electric Tractor Cost**	**Comparable Common Tractor**
A 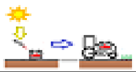	250	6	€ 5.22 to € 6.43	€ 5.23
	500	6	€ 2.44 to € 3.66	€ 4.06
B 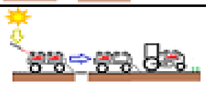	750	15	€ 2.05 to € 3.89	€ 3.67
	1,000	15	€ 1.76 to € 3.14	€ 3.48
C 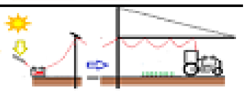	750	15	€ 7.98 to € 10.13	€ 3.67
	1,000	15	€ 7.84 to € 9.45	€ 3.48
D 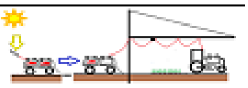	750	15	€ 3.27 to € 5.11	€ 3.67
	1,000	15	€ 2.98 to € 4.36	€ 3.48

Source: Prepared by the Author.

5 RESULTS

5.1 Results in relation to the objectives (including confirmation of hypothesis)

1. Requirements were defined of an electric micro tractor capable to pull implements as used for small scale semiarid family farming. (Chapter 4.3.).
2. Four alternatives configurations were elaborated for renewable energy conversion system based on the operational data of the electric micro tractor utilizing locally renewable energy resources (Chapter 4.2.).
3. In initial test runs the prototype electric micro tractor has been technically evaluated for its pull performance on the DENA/UFC test track (Chapter 4.3.13)
4. A comparative cost comparison study of electric tractor systems versus common tractor with combustion engine has been accomplished (Chapter 4.4.)
5. And as the last of the defined objective the hypothesis “*An electric micro tractor propelled by locally available renewable energy, designed to operate implements specifically designed for small scale semiarid family farming is technically and economically feasible and viable in terms of performance, operational costs, noise generation when compared to common combustion engine powered micro tractor*” has been confirmed.

5.2 Scientific result

The scientific result obtained in connection with this project is an increase of knowledge with respect to the pros and cons and the economic viability of an electric tractor system powered by renewable energy. To overcome the obvious drawbacks of electrically powered vehicles, innovative concepts were developed in order to render the system viable for small scale family farming in semiarid regions of the northeast of Brazil.

The results were elaborated in cooperation between the Universidade Federal de Ceará in Fortaleza, Brazil and the Bergische Universität Wuppertal, Germany.

5.2.1 *Knowledge gains*

- The electric tractor drive train lay out with induction motor controlled by inverters and the development of a low cost chain drive transmission system including prove of concept by test runs at UFC test track. (Chapter 4.3.2.)
- An economic evaluation of the feasibility of specific electric tractor system configurations (Chapter 4.4.)

5.2.2 *Innovative gains*[13]

- Design and fabrication of an electric tractor based on locally available components (Chapter 4.3.1. to chapter 4.3.12.)
- The conceptual development of different configurations to transmit power from the PV generator to the moving tractor; especially a pivot type cable suspension system for movable objects (Chapter 4.2.)

5.2.3 *Cooperation*

In result cooperation was essential basis for this multidisciplinary project, encompassing agricultural, mechanical, power electronics and electrical engineering, implementation of mobile electric power and renewable energy systems.

The cooperation agreement with Bergische Universität Wuppertal, Germany offered access to a wide pool of engineering resources in electric mobility, ensuring quality and progress to the electric designs.

In particular, the author wants to highlight the participation of the experts listed below, who provide the project with the necessary essential expertise and continuous constructive support: Prof. Benedikt Schmülling, Department of Electric Mobility, at Bergische Universität in Wuppertal, Germany, Prof. Sérgio Daher, expert in inverter techniques, Department of Electrical Engineering at UFC, Mr. Rodnei Regis (Doctorate student, supervised by Professor Fernando Luiz Marcelo Antunes at UFC) and Heribert Luegmair, Germany.

[13] Note: For both mentioned innovations, patent applications are pending at the INPI (See patents abstracts in Appendix).

6 CONCLUSIONS

For agricultural applications in remote areas without (or with) access to the grid, the electric tractor system provides the option to utilize locally generated renewable energy. In equatorial regions with a reliable and low-cost energy source in the form of a PV-plant, the concept of an electric tractor represents already today an economic and technical feasible solution using the technique of exchangeable battery packs.

The most remarkable result is that in equatorial regions electric energy generated by a photovoltaic system would not only sustain the electric tractor operation but could in parallel contribute to recover the investment for it and provide an extra income to the semiarid family farmer (if a way is found to commercialize the surplus energy).

Apart from that, the performance of an electric tractor is in some aspects superior to the common combustion engine tractor. The rated power is with 9 kW less than the 10.3 kW of a comparable combustion engine tractor, but the pull force with 4750 N (plus the 330% torque reserve for two minutes) substantially exceeds the 2600 N of the combustion engine tractor measured at test runs of both alternatives.

On the other hand, there are up to 10 times higher investment costs to be encountered for implementing the electric tractor system (49686 Euro and 69045 Euro respectively compared to 6481 Euro for the combustion engine tractor). But one has to bear in mind that the electric tractor investment includes the energy capture and transformation system, costs that are hidden in the diesel fuel price.

And last but not least, it should also not be forgotten that with this change of technology significant benefits will be expected for the environment in addition to economic opportunities for the local population.

6.1 Proposal for further development

To develop the systems and the tractor to a level for in-series production further development and research is necessary, for example:

- The operational behavior of Li-ion batteries used for tractor operation has to be verified regarding the following main aspects: (pl. refer to 4.2.3).
  - Recharging time required;

- Susceptibility to operating conditions (temperature, vibrations etc.);
- Degradation and service life under real operating conditions; and
- Safety concerns e.g. fire hazard.

- Develop supervisory system controlling the motor inverters (in development by PhD UFC student Rodnei);
- Review electric – electronic architecture;
- Review safety, reliability and maintenance requirements of the electric tractor fulfilling the law;
- Review drive train layout of the electric micro tractor using adjustable ratio transmission belts for higher and variable traction forces (Figure 137);
- Conceive battery exchange mechanisms and procedures;
- Conduct prototype tests with technical and economical evaluation of all complete systems;
- Mobile PV-System increase the efficiency of this configuration;
- Develop mini grid to utilize maximum generation surplus capability; and
- Prepare a layout of a three phase 400 V grid connection to a cable feed system using the pivot type cable suspension system for high power electric tractors (Operating on the field and drawing power directly from the public grid).

Figure 137 – Adjustable ratio transmission belts

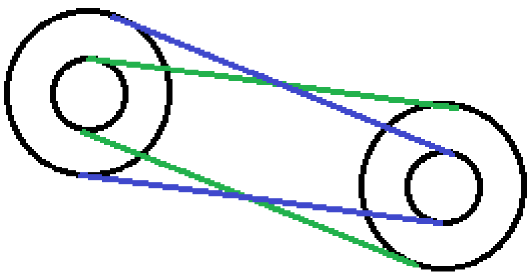

Source: Prepared by the Author.

REFERENCES

ABNT. **NBR IEC 61851-1 – Sistema de recarga condutiva para veículos elétricos. Parte 1: Requisitos gerais**. Rio de Janeiro, 2013.

ABNT. **NBR IEC 61851-21:2013. Sistema de recarga condutiva para veículos elétricos Parte 21: Requisitos de veículos elétricos para a conexão condutiva a uma alimentação em corrente alternada ou contínua**. Rio de Janeiro, 2013.

ABNT. **NBR IEC 61851-22:2013. Sistema de recarga condutiva para veículos elétricos Parte 22: Estação de recarga em corrente alternada para veículos elétricos**. Rio de Janeiro, 2013.

ABNT. **NBR IEC 62196-2:2013. Plugues, tomadas, tomadas móveis para veículo elétrico e plugues fixos de veículo elétrico — Recarga condutiva para veículo elétrico**. Rio de Janeiro, 2013.

ACKERMANN, T. **Wind Power in Power Systems**. Royal Institute of Technology, Stockholm: John Wiley & Sons, 2005.

AGARWAL, T. **DEC-DC converter operating**. Available at: <https://www.efxkits.co.uk/dc-dc-converter-operating-principle-functionality/2015> and <https://www.maximintegrated.com/en/app-notes/index.mvp/id/2031>. Access on: 22 Nov. 2016.

AGORA ENERGIEWENDE. **Understanding the Energiewende. FAQ on the ongoing transition of the German power system**. Publication: October 2015. Available at: <https://www.agora-energiewende.de/fileadmin/Projekte/2015/Understanding_the_EW/Agora_ Understanding_the_Energiewende.pdf>. Access on: 14 Jan. 2016.

AGRIWORLD. **Tratores elétricos, atualidade e análise de seu futuro**. v.9, n.31, p.30, 2018.

ALBIERO, D. **Desenvolvimento e avaliação de máquina multifuncional conservacionista para a agricultura familiar.** FEAGRI: Campinas, 2010.

ALBIERO, D.; CAJADO, D.; FERNANDES, I.; MONTEIRO, L.; ESMERALDO, G.. **Tecnologias agroecológicas para o Semiárido**. Fortaleza: Authors' edition, 2015. Available at: <http://www.ppgea.ufc.br/images/diversos/TecnologiasAgroecologicas. pdf>. Access on: 14 Jan. 2016.

AMERICAN SOCIETY OF AGRICULTURAL ENGINEERS (ASAE). **ASAE Standards 1997**. 1st Ed., St. Joseph: ASAE, 1997.

AMERICAN SOCIETY OF AGRICULTURAL ENGINEERS (ASAE). **ASAE D497.4. AGRICULTURAL MACHINERY MANAGEMENT DATA**. *In*: ASAE STANDARDS: Standards, Engineering Practices Data. St. Joseph: American Society of Agricultural Engineers, 2003, p.373-380.

AMERICAN SOCIETY OF AGRICULTURAL ENGINEERS (ASAE). **ASAE Standards**, Standards Engineering Practices Data. 2001.

ARAÚJO, K. L. B. **Avaliação do Desempenho Operacional e Energético de Um Conjunto Trator de Rabiça-Rotoencanteirador**. XLIV Congresso Brasileiro de Engenharia Agrícola - CONBEA 2015, Sep. 2015, São Pedro – SP, Brasil.

ASABE. **STANDARD SAE J1194 ROLLOVER PROTECTIVE STRUCTURE (ROPS) FOR WHEELED AGRICULTURAL TRACTORS**. Nov. 2016.

AUERHAMMER, H.; SEIFERT, A.; TEICHERT, A.; BERNHARDT, H.. **Digitalisierte Bilder und Schriften Agrartechnik in der AgTecCollection in mediaTUM®**. Referate der 33. GIL-Jahrestagung, Feb. 2013, Potsdam. Available at: <http://mediatum.ub.tum.de/node?id=1172013>. Access on: 14 Jan. 2016.

BARGER E.L.; LILJEDAHL, J.B.; CARLETON, W.M.; McKIBBEN, E.G.. **Tratores e seus motores**. USAID, Rio de Janeiro, 398 p., 1966.

BARICELO, L. G.; BACHA, C. J. C.. Oferta e demanda de máquinas agrícolas no Brasil. **Revista de Política Agrícola**, Brasília, ano 22, n.4, p.67-83, out./nov./dez., 2013.

BARNIM, Bus Company mbH. **TROLLEY Transnational Manual on Advanced Energy Storage Systems**. TROLLEY Project, External expert: Fraunhofer IVI. Sep. 2013.

BATTERIE SIEMS. **Antriebsbatterien – Motive Power**. Wartungsfreie dryfit traction Blockbatterien, Baureihe GF-V (dryfit traction Block). Bad Zwischenahn, Available at: <http://www.akkusys-shop.de/shop/Exide-Sonnenschein-GF-06-180-V-dryfit-Blei-Gel-Antriebsbatterie-6V-180Ah-5h-VRLA>. Access on: 10. Sep. 2017.

BAWDEN, O.; BALL, D.. **A Lightweight, Modular Robotic Vehicle for the Sustainable Intensification of Agriculture**. 2014.

BELTRÃO, N. E. M. Economia agrícola, ecofisiologia e relações solo-água-planta no semiárido nordestino: a opção algodão. **Revista Econômica do Nordeste**, v. 32, n. 2, p. 252-273, 2001.

BERGELT, H. **Photovoltaik – Solarzelle**. Available at: <www.schuelerlabor.tu-freiberg.de>. Access on: 21 Jun. 2012.

BLASQUES, L. C. M. **Estudo da Viabilidade Técnico-Econômica de Sistemas Híbridos para Geração de Eletricidade**. Dissertação de Mestrado, Programa de Pós-Graduação em Engenharia Elétrica da UFPA, 2005.

BRASIL. **Portal Brasil – Agronegócio**. Available at: <http://www.brasil.gov.br/sobre/economia/setores-da-economia/agronegocio/print>. Acess on: 07 Aug. 2014.

BRASIL, Ministério de Minas e Energia. **Balanço Energético Nacional**. Available at: <https://ben.epe.gov.br/downloads/Resultados_Pre_BEN_2012.pdf>. Acess on: 07 Aug. 2014.

BRASIL, Ministério de Minas e Energia. **Programa Luz para todos**. Available at: <http://luzparatodos.mme.gov.br/luzparatodos/Asp/dados_estaduais_principal.asp>. Access on: 01 Nov. 2015.

BRITO, P. A. **Degraus:** uma história de vida. Ceará, 2014.

BRIXIUS, W. W.; WISMER, R. D.. **The role of slip in traction**. ASAE Paper No. 781538. St. Joseph, Mich.: ASAE.

BRODELL, G.; JENNINGS, A.. **Work p.10**. Department of Agriculture. Agricultural Statistics, p. 432, 1962.

BURTON, T. **Wind energy handbook**. 2003.

CALLUM, R.; BRADLEY, F.. **Energy autonomy in sustainable communities—A review of key issues**. University of Strathclyde, 131 Rottenrow, Glasgow, G40NG, Scotland(UK), 2012.

CARVALHO, P. **Geração Eólica**. Fortaleza: Imprensa Universitária, 2003. 146f.

CARMO, M. S.; SALLES, J. T. A.. **Sistemas familiares de produção agrícola e o desenvolvimento sustentado**. *In*: ENCONTRO DA SOCIEDADE BRASILEIRA DE SISTEMAS DE PRODUCÃO, 1998.

CASA SOLAR. **Painel Solar 320W**. Canadian Solar - CS6U-320P. SKU 1419. Available at: <https://www.minhacasasolar.com.br/produto/painel-solar-de-320w-canadian-solar-cs6u-320p-79057?atributo=178:UNICA&atributo=25:U&atributo=26:ÚNICA>. Access on: 01 Nov. 2015.

COMIT, ZOPP. **An Introduction to the Method – COMIT**. Berlin, May 1998. Available at: <http://portals.wi.wur.nl/files/docs/ppme/ZOPP_introduction.pdf>. Access on: 19 Dec 2016.

CRAWFORD, P. BRYCE, P. (2003). Project monitoring and evaluation: a method for enhancing the efficiency and effectiveness of aid project implementation. **International Journal of Project Management**, v.21, n.5, p.363-373. Available at: <http://www.memoireonline.com/02/16/9442/m_Project-selection-and-management-in-international-development-organisations19.html>. Access on: 19 Dec. 2016.

CROLLA, A. D. (Ed.). **Automotive Engineering Powertrain, Chassis System and Vehicle Body**. 2009.

CRUZ, T. **Estudo da utilização de conversores de frequência em sistemas fotovoltaicos**. I Congresso Brasileiro de Energia Solar – ABENS, Fortaleza, 2007.

DAFF, Sub-Directorate. **Guide to machinery costs 2015 – 2016**. Available on: <http://www.daff.gov.za/Daffweb3/Portals/0/Statistics%20and%20Economic%20Analysis/Economic%20Analysis/2015%20-%202016%20%20%20GUIDE%20%20TO%20%20MACHINERY%20%20COSTS%20%20%20INDEX%20%20INTRODUCTION%20.pdf>. Access on: 19 Dec. 2016.

DAHLMANN, D. **Darum sind E-Autos so teuer**, March 2017, Available at: <http://ngin-mobility.com/artikel/warum-sind-e-autos-so-teuer/>. Access on: 19 Dec. 2016.

ELSMAR. **FMEA**. 2009. Available at: <http:// www.elsmar.com>. Access on: 24 Jun. 2016.

EMBRAPA – EMPRESA BRASILEIRA DE PESQUISA AGROPECUÁRIA. **Mudanças Climáticas Globais e a Agropecuária Brasileira**. Available at: <http://livraria.sct.embrapa. br/liv_resumos/pdf/00071250.pdf>. Access on: 01 Nov. 2015.

ENVIRONMENTAL POLLUTION. **Project Report on Noise Pollution, 2016**. Available at: <http://www.environmentalpollution.in/project-report/noise-pollution-project-report/project-report-on-noise-pollution/2160>. Access on: 25 Oct 2016.

FEDRIZZI, M. C. **Procedimentos para realização de ensaios com sistemas de bombeamento fotovoltaico em bancada de teste**. I Congresso Brasileiro de Energia Solar – ABENS, Fortaleza, 2007.

FEITOSA, E. O. **Energia Eólica Aplicada ao Bombeamento da Água para Irrigação por Gravidade na Agricultura Familiar**. 2014. Dissertation (Master's in Agricultural Engineering) – Center of Agricultural Sciences, Federal University of Ceará, Fortaleza, 2014. Available at: <http://www.repositorio.ufc.br/bitstream/riufc/17909/1/2014_dis_eofeitosa. pdf>. Acess on: 24 May 2016.

FERNANDES, J. M. R. **Proposição de abordagem integrada de métodos da qualidade baseada no FMEA**. Dissertação de Mestrado (Engenharia de Produção e Sistemas). Pontifícia Universidade Católica do Paraná, Curitiba. p.188, 2005.

FRAUENHOFER Institute for Solar Energy Systems. **Die Berechnung der Stromgestehungskosten LCOE**. Available at: <https://www.ise.fraunhofer.de/content/ dam/ise/en/documents/publications/studies/Fraunhofer-ISE_LCOE_Renewable_Energy_ technologies.pdf>. Access on: 12 Dec. 2016.

FUNCEME – CEARÁ INSTITUTE FOR METEOROLOGY AND WATER RESOURCES. **Chuvas por postos pluviométricos**. Available at: <http://www.funceme.br/produtos/ script/chuvas/Grafico_chuvas_postos_pluviometricos/entender/entender2.htm>. Access on: 02 Nov. 2015.

FUNCEME – CEARÁ INSTITUTE FOR METEOROLOGY AND WATER RESOURCES. **Rede Monitoramento Funceme.** Available at: <http://www.funceme.br/produtos/script/ rede_monitoramento/Pcd/ inmet/?regiao=B&sensor=22&intervalo=1>. Access on: 28th Feb. 2018.

GASCH, R.. **Windkraftanlagen**. Teubner, 2007.

GERTHSEN, C. E.; VOGEL H.. **Physik**. Springer Verlag, 1993.

GOVERNO DO ESTADO DO CEARÁ. **Atlas Solarimétrico do Ceará de 2008**, 2008.

GOVERNO DO ESTADO DO CEARÁ. **Balanço Energético do Ceará**. Fortaleza, 2006.

GRAEF, F.; HAIGIS, J. Spatial and temporal rainfall variability in the sahel and it's effects on for men management strategies. **Journal of Arid Environments**, v.48, p.221-231, 2001.
GREENPRO. **Energia Fotovoltaica**. 2004.

GREENPEACE. **Panorama global da energia eólica**. Cenários GWEC. Greenpeace, 2008.

GREENPEACE. **Sumário executivo, cenário energético global, perspectivas para uma energia global sustentável**. Xuan Canxiong, 2007.

GREINER, O. **Fakten-Check Mobilität 3.0**. 2017. Available at: <https://www.horvath-partners.com/de/media-center/studien/detail/fakten-check-mobilitaet-30-1/>. Access on: 28 Feb. 2018.

HALDIN, R. **Mean pass of Intertropical Convergence Zone, July vs. January**. Available at: <https://pt.wikipedia.org/wiki/Zona_de_convergência_intertropical>. Access on: 12 May 2015.

HELFAND, S.; PEREIRA, V. **Determinantes da pobreza rural e implicações para as políticas públicas no Brasil**. Brasília, 2012.

HEIER, S.. **Nutzung der Windenergy**. Solarpraxis AG, 2007a.

HERON, E. **Analysis of Variance – ANOVA**. Universität Regensburg, 2009.

HINDRICH, R.; KLEINBACH, M.. **Energia e o Meio Ambiente**. 3ed., Editora Thompson, São Paulo, 2004.

HONG, G. W. **Sustainability assessment of renewable energy projects for off-grid rural electrification: The Pangan-an Island case in the Philippines, George William Hong*, Naoya Abe**. International Development Engineering Department (IDE), Tokyo Institute of Technology, 2-12-1-I4-4, Ookayama, Meguro-ku, Tokyo 152-8550, Japan, 2013.

HUYNH, P-L; **Beitrag zur Bewertung des Gesundheitszustands von Traktionsbatterien in Elektrofahrzeugen**. **Wissenschaftliche Reihe Fahrzeugtechnik**. Universität Stuttgart, Springer, 2016.

INSTITUTO BRASILEIRO DE GEOGRAFIA E ESTATÍSTICA (IBGE). **Censo agropecuário**. Rio de Janeiro, 2006.

INSTITUTO DE PESQUISA E ESTRATÉGIA ECONÔMICA DO CEARÁ (IPECE). **A Caracterização da Extrema Pobreza no Estado do Ceará Baseado nos dados do Censo 2010**. Instituto de Pesquisa e Estratégia Econômica do Ceará, Fortaleza, 2010.

_____. **Ceará em Números – 2010**. Available at: <http://www2.ipece.ce.gov.br/publicacoes/ceara_em_numeros/2010/completa/Ceara%20em %20Numeros%202010.pdf>. Access on: 01 Jul. 2016.

_____. **Indicadores Sociais do Ceará 2011**. IPECE: Fortaleza, 2011.

INTERNATIONAL ENERGY AGENCY. **Global EV Outlook 2017**. OECD/IEA, 2017. Available at: <https://www.iea.org/publications/freepublications/publication/GlobalEVOutlook2017.pdf>. Access on: 28th Feb. 2018.

JANSCH, P.; BIRKHOFER, F.. **The Development of The Guideline VDI 2221**. Dubrovnik, 2006.

KELLOGG, W. D., NEHRIR, M. H., VENKATARAMANAN, G. e GEREZ, V.. **Generation Unit Sizing and Cost Analysis for Stand-alone Wind, Photovoltaic, and Hybrid Wind/PV Systems**. IEEE Trans. Energy Conversion, v.13, n.1, p.70-75, 1998.

KULK, J.; PEREZ, T.; RUSSEL, R.. **School of Electrical Engineering and Computer Science**. Queensland University of Technology Garden's Point, Queensland.

LACERDA, E. **Avaliação da Demanda Energética e Custos de Produção de um Trator de Rabiças em Função das Velocidades de Deslocamento no preparo de solo**. *In*: XLII Congresso Brasileiro de Engenharia Agrícola; CONBEA, 2014.

LEAL, F. **Análise do efeito interativo de falhas em processos de manufatura através de projeto de experimentos simulados**. Tese de Doutorado (Engenharia Mecânica). Universidade Estadual Paulista, Guaratinguetá, 2008.

LEAL, F.; PINHO, A. F.; ALMEIDA, D. A.. **Análise de falhas através da aplicação do FMEA e da teoria Grey**. Revista Gestão Industrial, v.2, n.1, p.79-88, jan.-mar. 2006.

LEITE, A. L. **Wind Energy ATLAS of Brazil**. Electric Energy Research Center - CEPEL, DEWI Magazin Nr. 19, Aug. 2001.

LILIEDAHL, J.; TURNQUIST, P.; Smith, D.; MACOTO, H.. T**ractors and their power units 1989**. AV1 Book, New York, 1989.

MALVEZZI, R. **Semiárido:** uma visão holística. Brasília: CONFEA, 2007.

MACMILLAN, R. H. **The mechanics of tractor-implement performance: theory and worked examples: a textbook**. Minerva Access is the Institutional Repository of The University of Melbourne, The mechanics. 2002. Available at: <http://hdl.handle.net/11343/33718>. Access on: 02 Nov. 2017.

MAKEHAM J. P., MALCOLM R. The Economics of Tropical Farm Management. Cambridge University Press, digital printing 1999, Available at: <https://books.google.de/books?id=MAvcS2jf2AIC&pg=PA129&lpg=PA129&dq=tractor+hours+hectar&source=bl&ots=81xHRsxuh8&sig=rAeeALlaedCfIw_Xi3xJ9JxL3EQ&hl=de&sa=X&ved=0ahUKEwjYlsOs3qHWAhUMaVAKHZB_A6cQ6AEIRTAF#v=onepage&q=tractor%20hours%20hectar&f=false>. Access on: 02 Nov. 2015.

MANN, G. **Propyläen Weltgeschichte**. Ullstein Buchverlage Berlin, Propyläen Verlag, Berlin, 1986.

MÁRQUEZ, L. **Solo tractor 90**. Madrid: Laboreo, 1990, Page 231.

MEHRDAD, E.; YIMINI, G.; EMADI, A.. **Modern Electrical Hybrid Electric and Fuel Cell Vehicles**. 3. ed., Boca Raton FL, CRC Press, 2010.

MELLO, F. **A história das barragens no Brasil, Séculos XIX, XX e XXI**. Rio de Janeiro 2011: CBDB, 2011. ISBN 978-85-62967-04-7.

MELO, R. P. **Desenvolvimento e avaliação do protótipo de uma Semeadora puncionadora para agricultura familiar**. UFC, Fortaleza, 2017.

MIALHE, L. G. **Máquinas motoras na agricultura**. Vol. II, EDUSP, 367 p., São Paulo, 2006.

MISHAN, E. J. **Cost-Benefit Analysis**. Preager Scientific, fifth edition, New York, 2007.

MIT – MASSACHUSETTS INSTITUTE OF TECHNOLOGY. **Interactive Community Planning. ZOPP: Goal Oriented Project Planning**. Available at: <http://web.mit.edu/urbanupgrading/ upgrading/issues-tools/tools/ZOPP.html>. Access on: 19 Dec. 2016.

MONTEIRO, L. A. **Desempenho Operacional e Energético, Segundo a Norma OECD - CODE 2 de Dois Tratores Agrícolas 4x2 TDA com Motores de 132 kW em Pista Concreto e Solo Agrícola**. Botucatu, 2011.

MONTGOMERY, D. C. **Design and analysis of experiments**. 3ed. New York: John Wiley and Sons, 1991.

MONTGOMERY, D. C. **Introdução ao controle estatístico da qualidade**. 4o Ed. Rio de Janeiro: LTC, 2004.

MOSTBÖCK, S. **Einführung in Statistik**. Universität Regensburg, 2011.

MOUSAZADEH, H. **Evaluation of alternative battery technologies for a solar assist plug-in, hybrid electric tractor**. Department of Agricultural Machinery Engineering, University of Tehran, Karaj, Iran. Transportation Research Part D 15 (2010) 507–512, Elsevier: 2010.

MUELLER, C. C. **Organização e ordenamento do espaço regional do Nordeste – Projeto Áridas**. Brasília: MI, 2012. Available at: <www.mi.gov.br>. Access: 10 Jul. 2012.

MUGARUKA, L. **Project selection and management in international development organizations**. University of Hertfordshire, Master's in Project Management, 2014.

NASA – NATIONAL AERONAUTICS AND SPACE ADMINISTRATION. **Technical Memorandum 89915 AIAA-87-9080**. 1987.

NASCIMENTO E. M. **Avaliação da eficiência energética e do nível de ruído de um microtrator de duas rodas**. Edições UFC: Fortaleza, 2012.

Noise insulation case, Basics of acoustics. Available at: <http://personal.inet.fi/koti /juhladude/acoustics.html>. Access on: 25 Oct. 2016.

OECD – ORGANISATION FOR ECONOMIC CO-OPERATION AND DEVELOPMENT. **Tractor performance test**. Available at: <http://www.oecd.org/tad/code/02%20-%20Code%202%20-%20Final(February%202016).pdf>. Access on: 25 Oct. 2016.

OECD. Standard. **Codes for the Official Testing of Agricultural and Forestry Tractors – 2016**. Available at: <http://www.oecd.org/tad/code/oecd-standard-codes-official-testing-agricultural-forestry-tractors.htm>. Access on: 25 Oct. 216.

OLMSTED, A. L.; RHODE, P. W**..** Reshaping the landscape: The impact and diffusion of tractor in american agriculture 1910 – 1960. **Journal of Economics History**, Cambridge, 2001.

OPENEI. **Brazil Global Horizontal Solar Radiation, 2005**. Available at: <http://prod-http-80-800498448.us-east-1.elb.amazonaws.com/w/images/7/71/NREL-brazil-glo.pdf>. Access on: 01 Jul. 2016.

ÖSTERREICHISCHER VEREIN FÜR KRAFTFAHRZEUGTECHNIK. **Batterie Elektrische Fahrzeuge in der Praxis**. Institut für Fahrzeugantriebe und Automobiltechnik, Technische Universität Wien, Okt. 2012.

PHYSICS STACK EXCHANGE. **Solar Radiation**. Available at: <http://physics.stackexchange.com/questions/116782/proportion-of-solar-radiation-that-reaches-the-earth-surface>. Access on: 17 Dec. 2016.

PILLAY, A.; WANG, J.. **Modified failure mode and effects analysis using approximate reasoning**. Reliability Engineering & System Safety, v.9, p. 69–85, 2003.

PINHO, J. T. **Soluções Energéticas para a Amazônia: Eletrificação de Comunidades Isoladas – Módulo: Sistemas Híbridos**. Apostila do Curso. Programa Luz Para Todos, PNUD, BID-FUMIN, MME, 2007.

PUENTE, J.; PINO, R.; PRIORE, P.; FOUENTE, D. L. A decision support system for applying failure mode and effects analysis. **International Journal of Quality & Reliability Management**, Bradford, v.19, n.2, p.137-151, 2002.

QUALITY ASSOCIATES INTERNATIONAL (QAI). **Failure mode and effect analysis**. Available at: <http://www.quality-one.com/services/fmeaEdition4.php>. Access on: 12 Dec. 2014.

RENEWABLE ENERGY AGRICULTURAL MULTIPURPOSE SYSTEM FOR FARMERS (RAMseS). **General Report on the Environmental and Agricultural Impact of the Installed Integrated Systems on Rural Community and Stakeholders**. 2006.

RENUCA, F. **Getting on With It: Monitoring and Evaluation in the Third Sector**. Risk and Regulation. London School of Economics, 2012.

RUSSINI, A. **Projeto, construção e teste de instrumentação eletrônica para avaliação de tratores agrícolas**. 2009.

SANTOS, E. **A Seca no nordeste no ano 2012**. Universidade Federal do Ceará, 2012.

SCHNEIDER, S. **Aspectos multidimensionais da agricultura brasileira: diferentes visões do Censo Agropecuário 2006**. ISBN 978-85-7811-191-5, Instituto de Pesquisa Econômica Aplicada. CDD: 338.10981.

SILVA, V. P. R.; PEREIRA, E. R. R.; AZEVEDO, P. V.; SOUSA, R. A. S.; SOUSA, I. F. **Análise da pluviometria e dias chuvosos na região Nordeste do Brasil**. Revista Brasileira de Engenharia Agrícola e Ambiental, v.15, n.2, p.131-138, 2011.

SONNENSCHEIN. **Lithium_Produkt_Datenblatt, Version 2.0**. Feb. 2014.

SPIEGEL. **KULAN mobil**. Available at: http://www.spiegel.de/auto/aktuell/kulan-e-mobil-mit-leichtbau-auf-der-iaa-nutzfahrzeuge-a-987951.html>. Access on: 02 Nov. 2015.

SPORN, P. **Changing Requirements and the Role of Energy in Expanding Economy**. Agricultural Engendering, 1957.

STÖLZER, M. **Hinweise zur Fehlerrechnung**. Universität Halle. Available at: <http://www.physik.uni-halle.de/Lehre/Grundpraktikum/gpfehler.htm>. Access on: 12 Apr. 2012.

SUDENE – SUPERINTENDÊNCIA DO DESENVOLVIMENTO DO NORDESTE. **Principal temporary crops in the semi-arid region**. SUDENE, 2012; IBGE, 2012. Available at: <http://www.ibge.gov.br/home/estatistica/economia/pam/2012/default_temp_xls.shtm>. Access on: 24 Sep. 2015.

SUDENE – SUPERINTENDÊNCIA DO DESENVOLVIMENTO DO NORDESTE. **Estatísticas do Nordeste - Nordeste em Números 2015**. Recife, 2016. Available at: <http://www.sudene.gov.br/system/resources/W1siZiIsIjIwMTYvMDgvMDMvMTZfNDlfNDZfOTI2X05FX0VNX05VTUVST1NfMjAxNS5wZGYiXV0/NE-EM-NUMEROS-2015.pdf>. Access on: 24 May 2016.

TALLIÁN, M. **When the Soviets built an electric tractor**. Available at: <http://jalopnik.com/5796595/when-the-soviets-built-an-electric-tractor>. Access on: 02 Nov. 2015.

TAN, C. M. **Customer-focused build-in reliability: a case study**. International Journal of Quality & Reliability Management, v.20, n.3, p.378-397, 2003.

TINGAY, J. **Frequency Weighting Curves – 'A', 'C' & 'Z'**. Available at: <http://www.cirrusresearch.co.uk/blog/2011/08/what-are-a-c-z-frequency-weightings>. Access on: 12 Nov. 2016.

TOLEDO, J. C.; AMARAL, D. C.. **FMEA – Análise do tipo e efeito de falha**. São Carlos: GEPEQ/UFSCar, 2008.

UNGER, R. M. **Desenvolvimento do Nordeste como Projeto Nacional**. Secretaria de Assuntos Estratégicos da Presidência da República. Brasília, 2009.

UNITED NATIONS. **Relatório Brundtland 1987**. Comissão Mundial sobre Meio Ambiente e Desenvolvimento. Washington, 1987.

UNITED STATES PATENT. **US1391794, Suspension Apparatus**. Massachusetts, 1921, Available on: <http://www.google.ch/patents/US1391794>. Access on: 23 Jun. 2016.

UNI HOHENHEIM. **Maschinenkosten Kalkulation (approximative Kalkulation)**. 2016. Available at: <https://www.uni-hohenheim.de/i410a/etloes.def/makost.htm>. Access on: 23 Jun. 2016.

UNIVERSITÄT DUISBURG-ESSEN. **Physikalisches Grundlagenpraktikum – Fehlerrechnung**. Available at: http://www.uni-due.de/agfarle/grundlagenpraktikum/ ANLEITUNGEN/F.pdf>. Access on: 10 Sep. 2016.

UNIVERSITÄT KASSEL. **Photovoltaic Systems Technology**. 2003.

UNIVERSITÄT KIEL. **The Li-Ion Battery**. Available at: <https://www.tf.uni-kiel.de/matwis/amat/ elmat_en/kap_2/advanced/t2_1_3.html>. Access on: 25 Oct. 2016.

UNIVERSITY OF NEBRASKA–LINCOLN. **NTTL:** Only U.S. OECD Tractor Test Lab. Available at: <http://tractortestlab.unl.edu/>. Access on: 25 Oct. 2016.

U.S. DEPARTMENT OF LABOR. **Walsh-Healthy Act. Official recommendation to the present suitable levels for noise exposure time per day**. US Department of Labor, Occupational Safety and Health Administration. Available at: <https://www.osha.gov/ dts/osta/otm/new_noise/>. Access on: 15 Jun. 2016.

VDI-Richtlinie 2222. **Konzipierentechnischer Produkte**. VDI-Verlag, Düsseldorf, 1973.

VDI-Richtlinie 2221. **Methodikzum Entwickeln und Konstruierentechnischer Systeme und Produkte**. VDI Verlag, Düsseldorf, 1993.

VILLA, M. A. **Vida e morte no sertão. História das secas no Nordeste nos séculos XIX e XX**. São Paulo: Editora Ática, 2001.

WALLENTOWITZ, H.; FREIALDENHOVE, A.. **Strategien zur Elektrifizierung des Antriebsstranges, Technologien, Märkte und Implikationen**. Vol. 2, überarbeitete Auflage, Vieweg+Teubner Verlag. Springer Fachmedien Wiesbaden, 2010.

WHITE, W. J. **Economic History of Tractors in the United States**. Research Triangle Institute. Available at: <http://eh.net/encyclopedia/economic-history-of-tractors-in-the-united-states>. Access on: 02 Nov. 2015.

WITNEY, B. **Choosing and using farm machines**. Longman Higher Education December, 1988.

YUGI, T.; TAGAMI, K.; YANAGI, S. Calculating top event probability of a fault tree with many repeated events. **Journal of Quality in Maintenance Engineering**, v.12 n.4, p.364-372, 2006.

ZOZ, F. M. **Predicting tractor field performance (updated)**. St. Joseph: ASAE, 1987 (ASAE Paper No. 871623).

APPENDIX A – PATENTS

Patent 1

"DISPOSITIVO DE TRANSMISSÃO DE ENERGIA ELÉTRICA PARA UM OBJETO MÓVEL OPERANDO NUMA ÁREA DENTRO DO ALCANCE DO EQUIPAMENTO"

Deposit 15.04.2015

Application for grant of a patent for a power cable suspension system.

This patent pertains to a device designed to increase the work endurance of any kind of battery powered electric vehicles by means of transferring electric energy from an external source to the vehicle while it is operating within the range of the system. One possible approach is to provide a central tower structure featuring a boom designed to keep a power cable suspended above the vehicle. With the tower acting as a pivot, for the boom to reach a circular area with a radius corresponding to the length of the boom, represents the working range of the device. A mechanical connection between boom and vehicle causes the cable suspension system to follow the movement of the vehicle, and ensures uninterrupted power supply, as long as the vehicle is within the area covered by the system.

Esta patente trata de um sistema de aumento da autonomia de objetos móveis, propulsionados por eletricidade proveniente de bateria ou de eletricidade de célula combustível, por meio da transmissão de energia elétrica através de conexão com um cabo (condutor) elétrico, transferindo energia elétrica, de uma fonte externa para o objeto em movimento, enquanto o mesmo estiver operando dentro da área de atuação do sistema. Uma estrutura mecânica possibilita a transmissão de energia elétrica, através de cabo, que é sustentado pela porção inferior de um braço rotativo. O braço, que opera acima do objeto móvel e gira 360º em volta de uma torre central (pivô), delimita uma área circular de atuação do sistema, de raio correspondente ao seu comprimento. Um sistema mecânico de fixação no braço sustenta o cabo (condutor) elétrico, e o objeto móvel reboca o braço através de uma conexão mecânica, enquanto o mesmo estiver se movimentando dentro da área do sistema.

< Uso exclusivo do INPI >

INPI Ceará INSTITUTO NACIONAL DA PROPRIEDADE INDUSTRIAL PROTOCOLO GERAL
27/04/2015 013150000092 12:47 DECE
BR 10 2015 009365 9

Espaço reservado para o protocolo | Espaço reservado para a etiqueta | Espaço reservado para o código QR

INSTITUTO NACIONAL DA PROPRIEDADE INDUSTRIAL
Sistema de Gestão da Qualidade
Diretoria de Patentes

DIRPA	Tipo de Documento: Formulário	DIRPA	Página: 1/3
Título do Documento: **Depósito de Pedido de Patente**		Código: FQ001	Versão: 2
		Procedimento: DIRPA-PQ006	

Ao Instituto Nacional da Propriedade Industrial:
O requerente solicita a concessão de um privilégio na natureza e nas condições abaixo indicadas:

1. **Depositante (71):**

1.1 Nome: UNIVERSIDADE FEDERAL DO CEARÁ
1.2 Qualificação: INSTITUIÇÃO DE ENSINO SUPERIOR
1.3 CNPJ/CPF: 07272636000131
1.4 Endereço Completo: AV. DA UNIVERSIDADE 2853, BENFICA
1.5 CEP: 60020180
1.6 Telefone: 85-33669434 1.7 Fax: 85-33669941
1.8 E-mail: selma@ufc.br

☐ continua em folha anexa

2. **Natureza:** ☒ Invenção ☐ Modelo de Utilidade ☐ Certificado de Adição

3. **Título da Invenção ou Modelo de Utilidade (54):**

"DISPOSITIVO DE TRANSMISSÃO DE ENERGIA ELÉTRICA PARA UM OBJETO MÓVEL OPERANDO NUMA ÁREA DENTRO DO ALCANCE DO EQUIPAMENTO"

☐ continua em folha anexa

4. **Pedido de Divisão: do pedido Nº** **Data de Depósito:**

5. **Prioridade:** ☐ Interna (66) ☐ Unionista (30)

O depositante reivindica a(s) seguinte(s):

País ou Organização do depósito	Número do depósito (se disponível)	Data de depósito

☐ continua em folha anexa

INSTITUTO NACIONAL DA PROPRIEDADE INDUSTRIAL
Sistema de Gestão da Qualidade
Diretoria de Patentes

DIRPA	Tipo de Documento: Formulário	DIRPA	Página: 3/3
Título do Documento: **Depósito de Pedido de Patente**		Código: FQ001	Versão: 2
		Procedimento: DIRPA-PQ006	

11. Documentos Anexados:

(Assinale e indique também o número de folhas):
(Deverá ser indicado o número total de somente uma das vias de cada documento).

		Documentos Anexados	folhas
☒	11.1	Guia de Recolhimento da União (GRU).	01
☐	11.2	Procuração.	
☐	11.3	Documentos de Prioridade.	
☐	11.4	Documento de contrato de trabalho.	
☒	11.5	Relatório descritivo.	13
☒	11.6	Reivindicações.	05
☐	11.7	Desenho(s) (se houver). Sugestão de figura a ser publicada com o resumo: nº, 07 por melhor representar a invenção (sujeito à avaliação do INPI).	09
☒	11.8	Resumo.	01
☐	11.9	Listagem de sequências em arquivo eletrônico: _____nº de CDs ou DVDs (original e cópia).	
☐	11.10	Código de controle alfanumérico no formato de código de barras referente às listagem de sequências.	
☐	11.11	Listagem de sequências em formato impresso.	
☐	11.12	Declaração relativa à Listagem de sequências.	
☒	11.13	Outros (especificar) CONTINUAÇÃO DE INVENTORES	01

12. Total de folhas anexadas: 30 **fls.**

13. Declaro, sob as penas da Lei que todas as informações acima prestadas são completas e verdadeiras.

Fortaleza 15 de abril de 2015
Local e Data

Assinatura e Carimbo
Prof. Dr. Henry de Holanda Campos
Vice-Reitor no exercício da Reitoria

Patent 2

“SISTEMA DE TRATOR ELÉTRICO PARA AGRICULTURA EM REGIÕES SEMIÁRIDAS MOVIDO A ENERGIAS RENOVÁVEIS”

Deposit 27.02.2018

Esta patente trata-se de um sistema de disponibilização de energia renovável, que tem a radiação solar como fonte primária, utilizado: (a) para acionar um trator agrícola e (b) para aproveitamento da energia excedente produzida, com finalidade de processamento e comercialização da mesma no uso doméstico. A inovação proposta é um sistema de transformação de radiação solar em energia elétrica, acoplado a um sistema de transmissão dessa energia para um trator elétrico através de um sistema de troca (permuta) de conjuntos de bateria ou pela transmissão por cabo. O sistema está projetado para maximizar a autonomia de tratores acionados por motores elétricos, através de um mecanismo de baixas perdas mecânicas entre o motor e as rodas do trator. O trator elétrico que faz parte da inovação, é equipado com motores indutivos, tendo os motores acionando cada roda motorizado em separado, através de transmissão e redução por correntes mecânicas. Os motores controlados por inversores de frequência, gerenciados por um sistema que supervisiona a coordenação entre os motores. Em razão das características da curva de torque deste tipo de motor, o acionamento é direto, por correntes entre o motor e as rodas traseiras, sem a necessidade de marchas ou de embreagem.

INPI INSTITUTO NACIONAL DA PROPRIEDADE INDUSTRIAL

27/02/2018 870180015745 14:48

29409161801325897

Pedido nacional de Invenção, Modelo de Utilidade, Certificado de Adição de Invenção e entrada na fase nacional do PCT

Número do Processo: BR 10 2018 003866 4

Dados do Depositante (71)

Depositante 1 de 1

Nome ou Razão Social: UNIVERSIDADE FEDERAL DO CEARÁ
Tipo de Pessoa: Pessoa Jurídica
CPF/CNPJ: 07272636000131
Nacionalidade: Brasileira
Qualificação Jurídica: Instituição de Ensino e Pesquisa
Endereço: Av da universidade, 2853 - Benfica
Cidade: Fortaleza
Estado: CE
CEP: 60710-780
País: Brasil
Telefone: (85) 3366-9434
Fax: (85) 3366-9941
Email: patentes@ufc.br

PETICIONAMENTO ELETRÔNICO Esta solicitação foi enviada pelo sistema Peticionamento Eletrônico em 27/02/2018 às 14:48, Petição 870180015745

Dados do Pedido

Natureza Patente: 10 - Patente de Invenção (PI)

Título da Invenção ou Modelo de Utilidade (54): SISTEMA DE TRATOR ELÉTRICO PARA AGRICULTURA EM REGIÕES SEMIÁRIDAS MOVIDO A ENERGIAS RENOVÁVEIS"

Resumo: Esta patente trata-se de um sistema de disponibilização de energia renovável,que tem a radiação solar como fonte primária, utilizado: (a) para acionar um trator agrícola e (b) para aproveitamento da energia excedente produzida, com finalidade de processamento e comercialização da mesma no uso doméstico. A inovação proposta é um sistema de transformação de radiação solar em energia elétrica, acoplado a um sistema de transmissão dessa energia para um trator elétrico através

de um sistema de troca (permuta) de conjuntos de bateria ou pela transmissão por cabo. O sistema está projetado para maximizar a autonomia de tratores acionados por motores elétricos, através de um mecanismo de baixas perdas mecânicas entre o motor e as rodas do trator. O trator elétrico que faz parte da inovação, é equipado com motores indutivos, tendo os motores acionando cada roda motorizado em separado, através de transmissão e redução por correntes mecânicas. Os motores

controlados por inversores de frequência, gerenciados por um sistema que supervisiona a coordenação entre os motores. Em razão das características da curva de torque deste tipo de motor, o acionamento é direto, por correntes entre o motor e as rodas traseiras, sem a necessidade de marchas ou de embreagem.

Figura a publicar: 3

Dados do Inventor (72)

Inventor 1 de 2

Nome: DANIEL ALBIERO
CPF: 18819883848
Nacionalidade: Brasileira
Qualificação Física: Pesquisador
Endereço: departamento de engenharia agricola
Cidade: fortaleza
Estado: CE
CEP:
País: BRASIL
Telefone: (85) 336 69863
Fax:
Email: daniel.albiero@gmail.com

Inventor 2 de 2

Nome: HANS HEINRICH VOGT
CPF: 42719100315
Nacionalidade: Brasileira
Qualificação Física: Estudante de Pós Graduação
Endereço: Fortaleza, Av. Dr. Silas Munguba 835 Apto 302 C
Cidade: fortaleza
Estado: CE
CEP:
País: BRASIL
Telefone: (85) 997 890222
Fax:
Email: fori@oi.com.br

APPENDIX B – PROTOTYPE ELECTRIC TRACTOR TEST REPORT

Prototype electric tractor test report
PAGE 1

Test information

Date and hour: 28.02.2018 from 7:30 to 10:30am

Type of Test

- Drawbar Pull
- Acoustic test

The test is to determine the following parameters:

- Tractor Speed
- Force at drawbar
- Power at drawbar
- Engine speed
- Electricity consumption
- Slip
- Sound level the driver is exposed during test

Tractor designation:

1. Prototype electric micro tractor for semiarid family farming (DENA, UFC)

a. Tractor specification:

Motor data:

- Type: Three phase induction motor
- Designation: Motor Especial 100L IP55
- Manufacturer: WEG
- Nos: 2 motors one for each traction wheel
- Rated Power: 9 kW (two motors with 4,5 kW each)
- Rated voltage: 48 V
- Rated engine speed: 1715 rpm
- Electronic control of motor: WEG Inverter CVW300, 400 A

Inverter data:

- Designation: CVW300, Conversor Veicular WEG,
- Manufacturer: WEG DRIVES & CONTROLS - AUTOMAÇÃO
- Model: CVW300A0400D0NB66
- Rated input voltage: 24-72 V CC
- Rated current at 45 °C: 200 A
- Maximum current for2 min: 400 A

Prototype electric tractor test report
PAGE 2

Battery data:
- Type: Lead acid
- Configuration of battery pack: 4 batteries each with 6 cells
- Rated voltage: 12 V per battery
- Rated capacity: 200 Ah per battery
- Arrangement: serial

Transmission type
- Two stage chain transmission
- Transmission ration
- (gear teeth 10 – 75) = 1:7,5
- (gear teeth 13 – 60) = 1:4,6
- Total transmission ration = 1:34,6

Brakes
- Regenerative braking by the electric motors
- Conventional mechanical drum brake

Steering:
- Mechanical steering gear acting on front axle

Chassis:
- Ladder type frame made of 100 mm steel channel

Dimensions:
- Wheelbase: 1.700 mm
- Overall width: 1.400 mm
- Overall length: 2.000 mm
- Overall height (driver excluded): 1.100 mm
- Ground clearance: 280 mm

Tire sizes
- Front 13 175/70 (with 45 cm outer diameter)
- Rear 295/75 R15 (with 75 cm outer diameter)

Weights and balances:
- Total weight 700 kg (with batteries)
- Front axle 300 kg (150 +150)
- Rear axle 400 kg (200 + 200)

Prototype electric tractor test report
PAGE 3

b. TEST CONDITIONS

Item	Description
Type of test	Traction and acoustic test
Test track geographical data (location / elevation)	03º43’02”S, 38º32’35”W; 19m
Test track type OECD-Code 2 (2008)	Concrete test track DENA - UFC
Track dimensions	2 X 75 m
Type of Tractor to be dragged	
Environmental conditions (Funceme) Air temperature Air pressure Wind speed Wind direction	 30^0 C 1010 hPa 4 km/h SE
Name of test coordinator	Heiner Vogt
Name of driver - electric tractor	Rodnei Regis
Name of driver - tractor being dragged	Delean Santiago
Test data monitoring	Rodnei Regis

Source: Prepared by the Author.

c. TRACTOR’S CONFIGURATION AND PHYSICAL PARAMETERS

Motor 1 temperature before test	“
Motor 2 temperature before test	“
Inverter temperature before test	“
Motor 1 temperature after test	**See matrix**
Motor 2 temperature after test	**with**
Inverter temperature after test	**test results**
Ballasted Mass	**in Appendix**
Centre of gravity, distance from rear axle	“
Dynamic center of gravity, distance from rear axle	“
Battery charge level before test	“
Battery charge level after test	“

Source: Prepared by the Author.

d. TEST DATA DOCUMENTATION

List of data to be recorded during the test by the monitoring system:

Force at draw bar [N]	
Battery tension [V]	
Battery current [A]	
Motor speed [RPM]	
Motor current [A]	
Inverter temperature [^{0}C]	

Source: Prepared by the Author.

Prototype electric tractor test report
PAGE 4

Record of testing equipment

Logger 1	HBM Quantum X MX804A
Logger 2	DaqPRO
Load cell	HBM, model RSCC, max force 10 kN
Inverter	CVW300, Conversor Veicular WEG
Sound exposure meter	VOLTCRAFT SL-200 Sound level meter
Thermometer	Infrared DT8380

Source: Prepared by the Author.

Configuration of monitoring system, list of sensors connected

Motor encoder	WEG Motor integrated encoder
Motor temperature	Motor integrated sensor
Inverter temperature	Inverter integrated sensor
Load cell	HBM, model RSCC, maximum force 10 kN
Inverter data output:	inverter temperature, motor speed, motor torque, amperage, voltage
Battery tension	Tension sensor
Battery Amperage	Current sensor

Source: Prepared by the Author.

List of data to be recorded with separate apparatus (chronometer, sound exposure meter)

Sound meter	VOLTCRAFT SL-200 Sound level meter
Chronometer	Samsung j5

Source: Prepared by the Author.

Miscellaneous documents: photos / video clips

Photo	yes
Video clips	no

Source: Prepared by the Author.

Prototype electric tractor test report
PAGE 5

e. TEST RUNS

During the test runs, all relevant data are documented in the test data sheet such as, inter alia, temperatures of the tractor components, battery charge together with manually recorded values. The data registered on the monitoring system are processed and a graphical presentation of the results is generated.

f. FINAL TEST REPORT (includes the following documents):

Data sheet filled in and certified.

g. TEST TRACK DIMENSION

Test track pattern dimensions

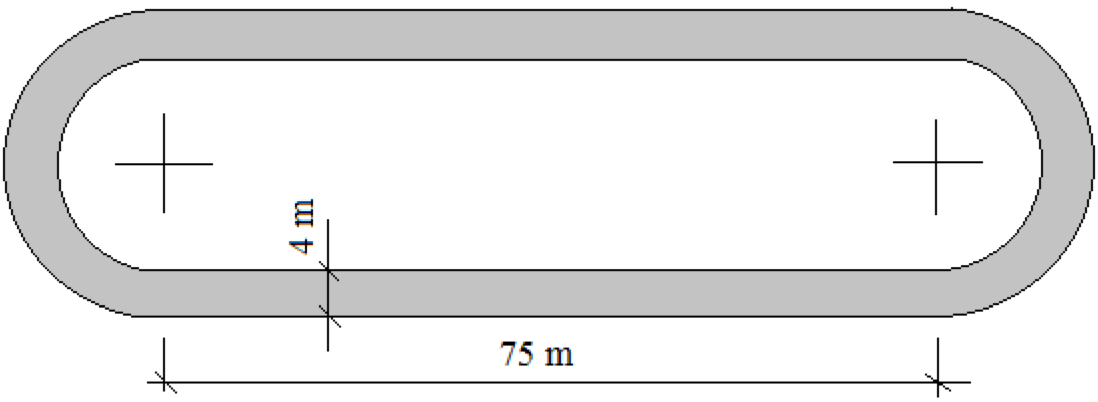

Source: Prepared by the Author.

h. APPENDIX

- Data sheets electric prototype tractor Test 0, 1, 2, 3, 4, 5, 6 and max; and
- Data sheets Tobata Test 1 and 2.

ELECTRIC TRACTOR PROTOTYPE TEST – 28.02.18

Test Results Summary

Table 1

	Electric tractor prototype							
Test number	0	1	2	3	4	5	6	max
Date	28.02.2018							
Test coordinator	Heiner Vogt							
Test data monitoring	Rodnei Regis							
Test driver test tractor	Rodnei Regis							
Test driver load tractor	Delean Santiago							
Pre-test motor temperature [C°]	31	35	36	36.5	39	40	40	40
Post-test motor temperature [C°]	33	36	36.5	37	40	40	40	40
Pre-test inverter temperature [C°]	30	31	32	33	34	35	35	35
Post-test inverter temperature [C°]	32	32	32	33	35	35	35	35
Driver over rear axle [kg]	91	91	91	91	91	91	91	91
Weight of passenger over rear axle [kg]	0	99	99	99	99	99	99	99
Ballast rear axle [kg]	8	8	8	8	8	8	8	8
Static empty weight forward axle [kg]	300							
Static empty weight rearward axle [kg]	400							
Dynamic reaction force forward axle [N]	1,355	2253	1871	2281	2293	2294	1910	1260
Dynamic reaction force rearward [N]	6,483	6557	6938	3585	6516	6516	6899	7549
Traction coefficient [Ψ, %]	69.39%	29.82	43.77	52.30	28.28	28.24	42.41	63.16
Dynamic center of gravity x [m]	0.40	0.39	0.34	0.40	0.40	0.35	0.24	0.24
Pre-test battery tension [V]	51.2	51	51	50.8	50.7	50.6	50.5	50.4
Post-test battery tension [V]	51	51	50.8	50.7	50.6	50.48	50.4	50.3

Source: Prepared by the Author.

Table 2

	Electric tractor prototype							Tobata	
Test number	1	2	3	4	5	6	max	Tobata 1	Tobata 2
Date	28.02.2018							28.02.2018	
Test coordinator	Heiner Vogt							Heiner Vogt	
Test data monitoring	Rodnei Regis							Rodnei Regis	
Test driver test tractor	Rodnei Regis							Sandoval J. Bezera	
Test driver load tractor	Delean Santiago							Delean Santiago	
Medium sound level [dB(A)]	77	78	76	78	76	79	79	82	84

	Electric tractor prototype							Tobata	
Maximum sound level [dB(A)]	80	82	81	81	80	83	83	85	86
Test run time (50m) [sec]	38	41	38	37.9	37.8	38.1	58.4	220	106
Speed [m/s]	1.3	1.2	1.3	1.3	1.3	1.3	0.9	0.2	0.5
Speed [km/h]	4.7	4.4	4.7	4.7	4.8	4.7	3.1	0.8	1.7
Theoretical speed [km/h]	5.4	5.1	5.4	5.5	5.5	5.5	4.8		
Slip [%]	12.28	13.92	12.28	13.65	13.42	14.10	35.79		
Power at draw bar [W]	2,573.2	3,704.2	2,467.02	2,429.4	2,433.9	3,839.9	4,082.2	538	646
Battery power [W]	3,998	5,900	3,880	3,795	3,685	5,915	7,145		
Efficiency Battery - Draw Bar [%]	64.36	62.78	63.58	64.02	66.05	64.92	57.13		
Mean force at draw bar [N]	1,956	3,037	1,875	1,841	1,840	2,926	4,768	2,365	1,370

Source: Prepared by the Author.

Summary tests of Drawbar force for EST.

Replication	0	1	2	3	4	5	6	Maximum
Samples	3801	1656	1856	1705	1956	1655	1856	2406
Mean value	4499,86	1955,60	1875,52	1841,48	2941,69	1766,12	2926,27	4767,99
Median	4510,60	1959,07	1874,93	1832,57	2939,24	1769,60	2914,84	4754,73
Minimum:	2278,31	1394,20	1276,72	1232,72	2268,18	1102,83	2101,31	2967,66
Maximum:	6862,54	2587,70	2605,04	2438,33	4281,86	2374,60	3750,54	6201,44
Range	4584,22	1193,50	1328,32	1205,60	2013,68	1271,77	1649,23	3233,77
Variance	101336,57	46100,40	46921,59	43415,21	60063,90	49349,94	51809,89	83130,46
Variance Coeficient	0,070	0,109	0,115	0,113	0,083	0,125	0,077	0,060
Mean deviation	318,37	214,77	216,67	208,42	245,14	222,21	227,67	288,38
Lower quartile:	4360,70	1817,65	1726,35	1698,89	2779,04	1616,19	2779,80	4599,70
Upper quartile:	4650,19	2097,53	2018,17	1978,02	3107,28	1916,80	3064,33	4924,36
Interquartile range:	289,49	279,88	291,82	279,13	328,23	300,60	284,52	324,66
Skew	-0,33	-0,03	0,05	0,074	0,19	-0,03	0,17	0,21
Kurtosis	-1,11	-0,11	-0,10	0,005	0,65	-0,17	0,60	-1,32

Source: Prepared by the Author.

Test 0

Traction [N]

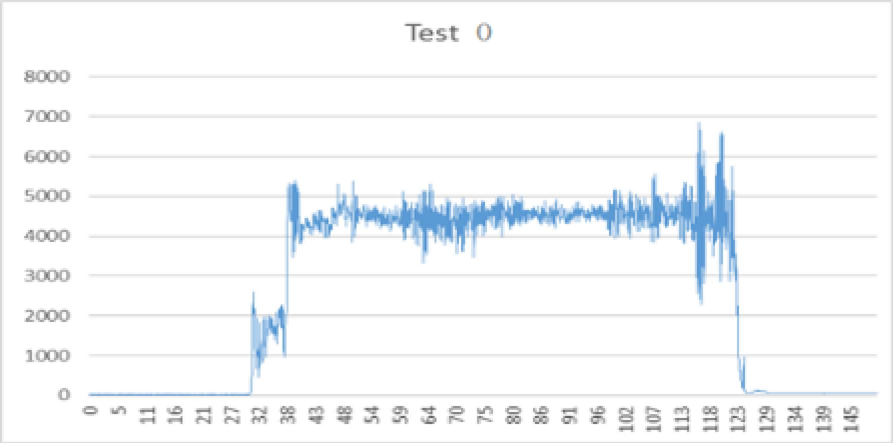

Source: Prepared by the Author.

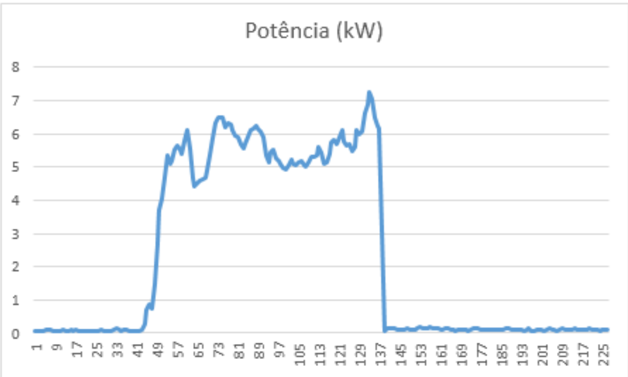

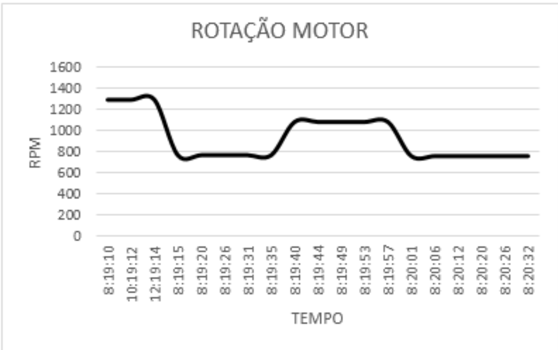

Source: Prepared by the Author.

Test 1

Traction [N], Time [sec]

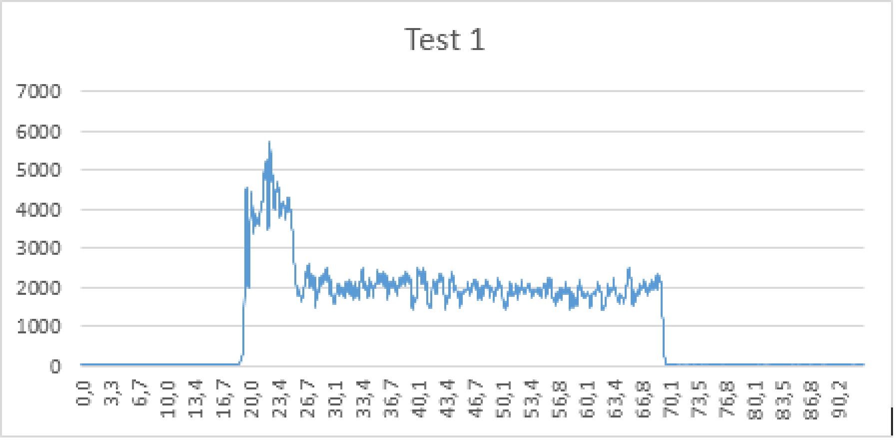

Source: Prepared by the Author.

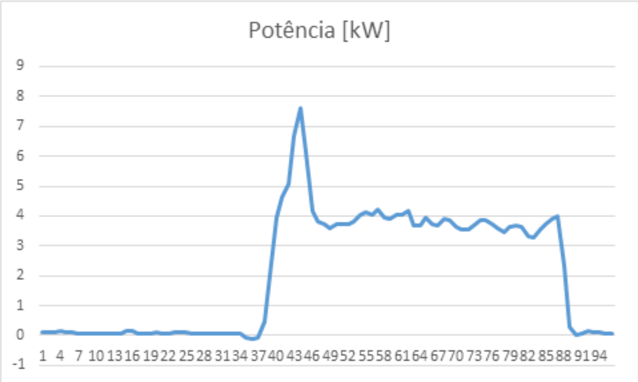

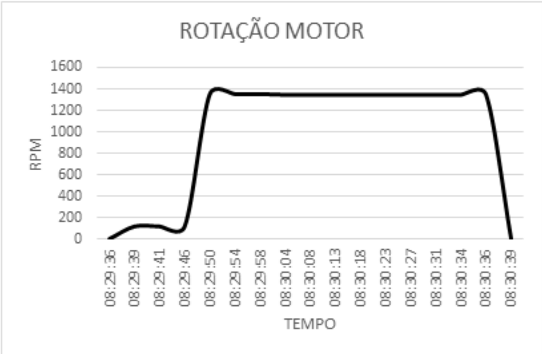

Source: Prepared by the Author.

Test 2

Traction [N], Time [sec]

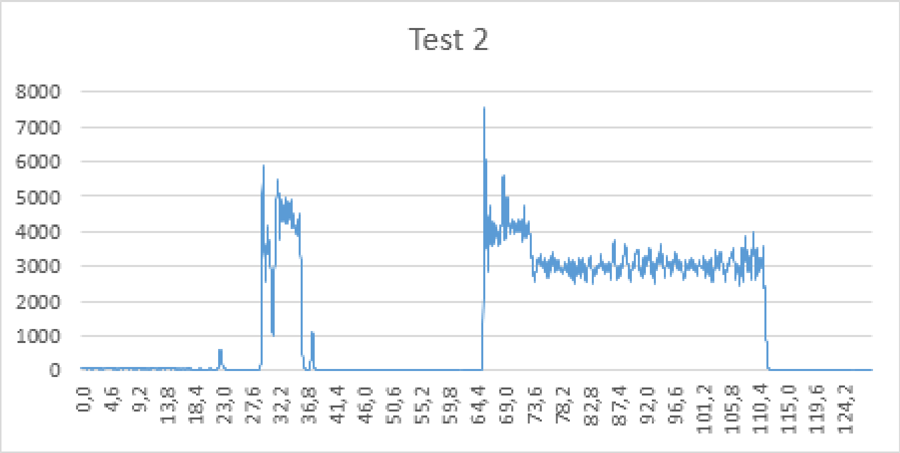

Source: Prepared by the Author.

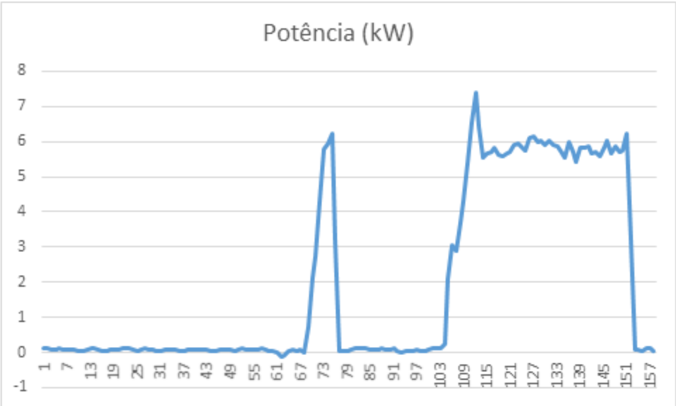

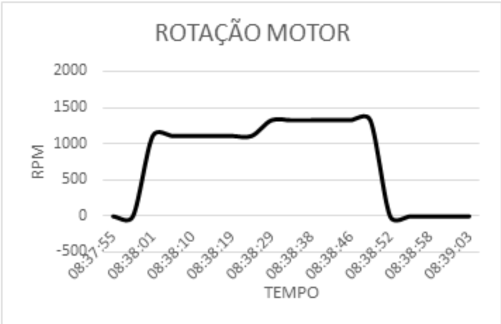

Source: Prepared by the Author.

Test 3

Traction [N], Time [sec]

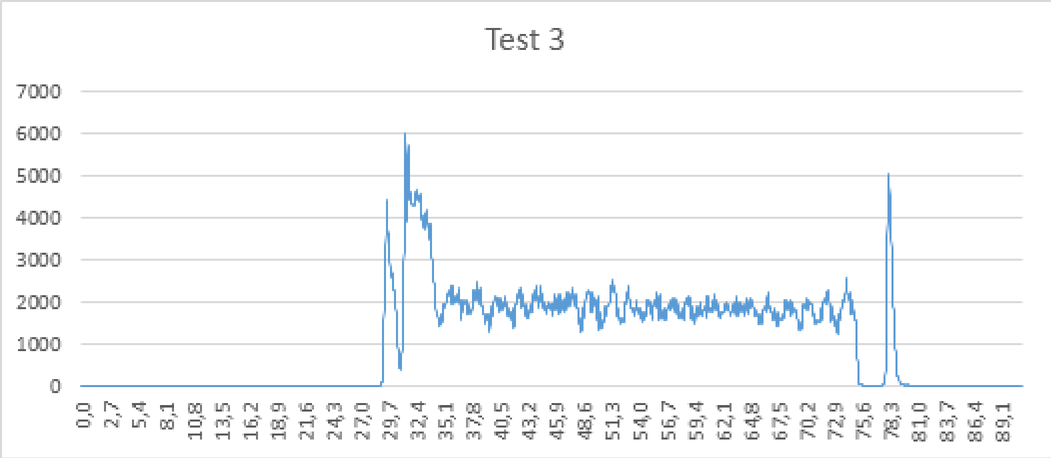

Source: Prepared by the Author.

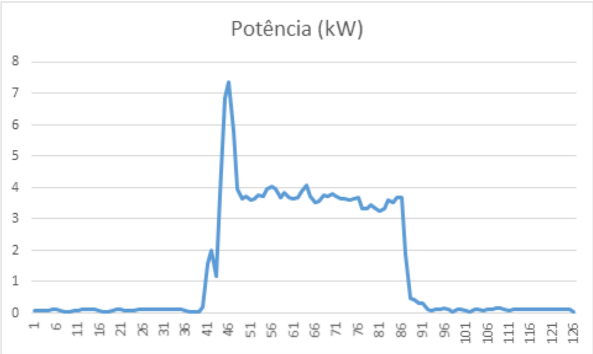

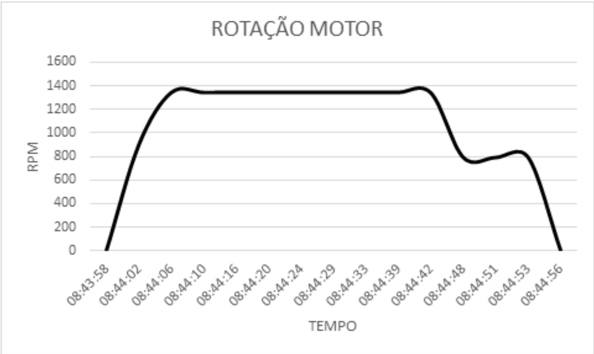

Source: Prepared by the Author.

Test 4

Traction [N], Time [sec]

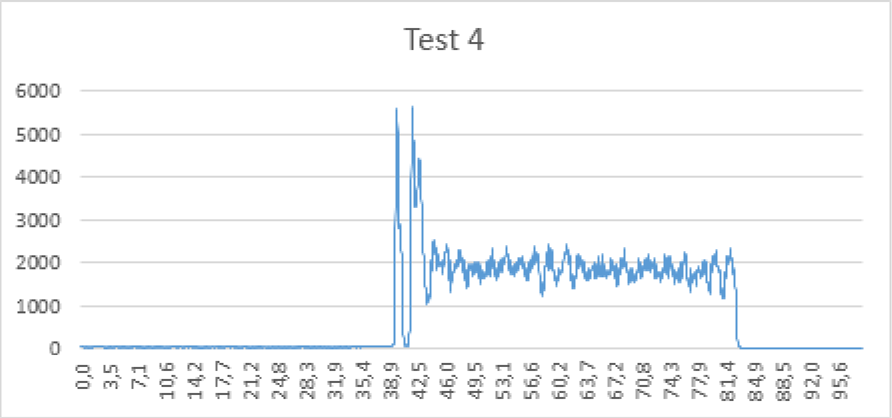

Source: Prepared by the Author.

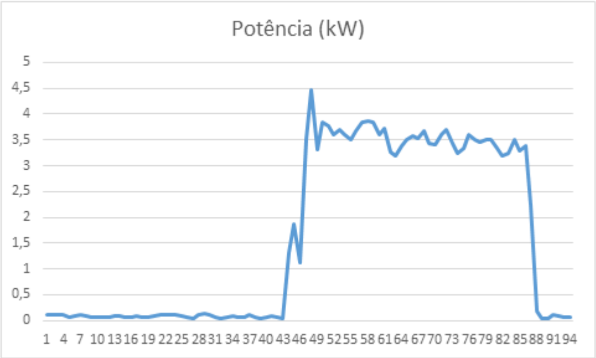

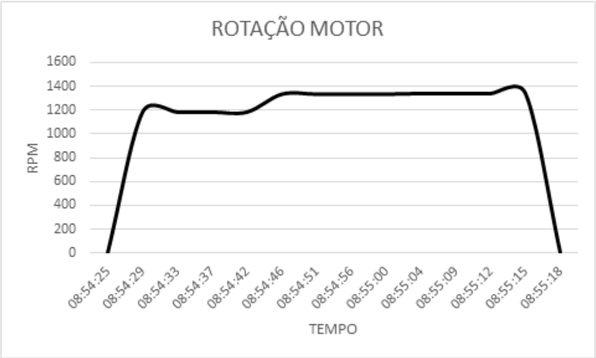

Source: Prepared by the Author.

Test 5

Traction [N], Time [sec]

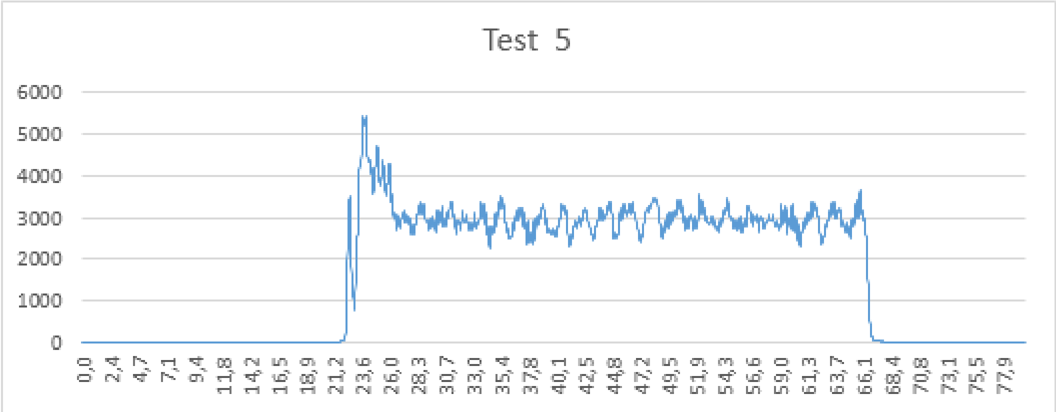

Source: Prepared by the Author.

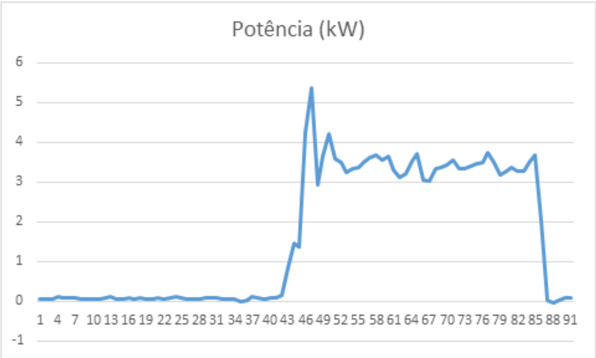

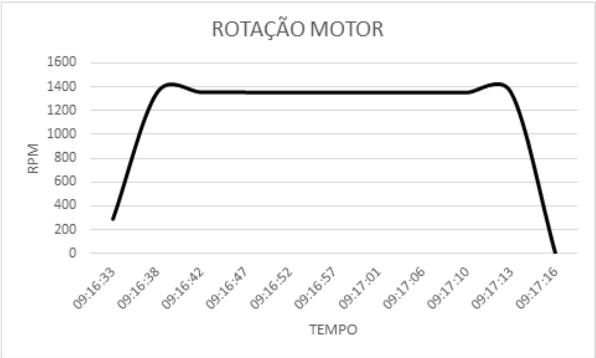

Source: Prepared by the Author.

Test 6

Traction [N], Time [sec]

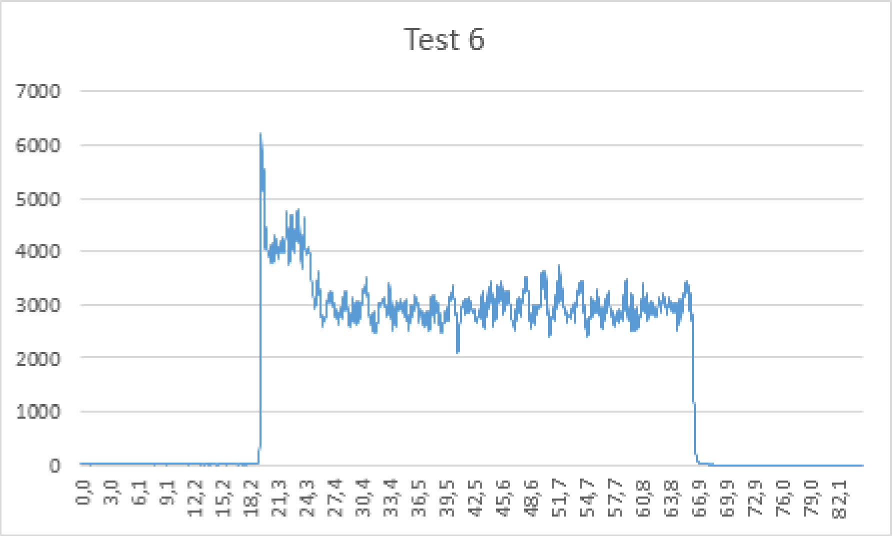

Source: Prepared by the Author.

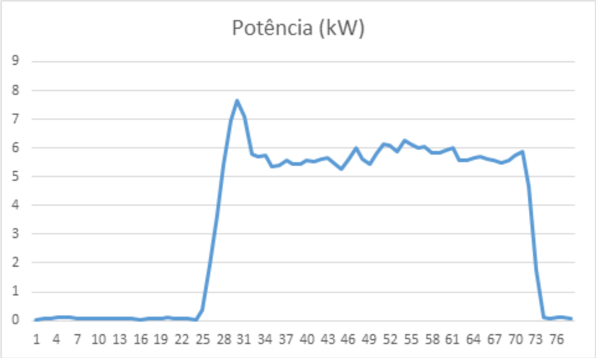

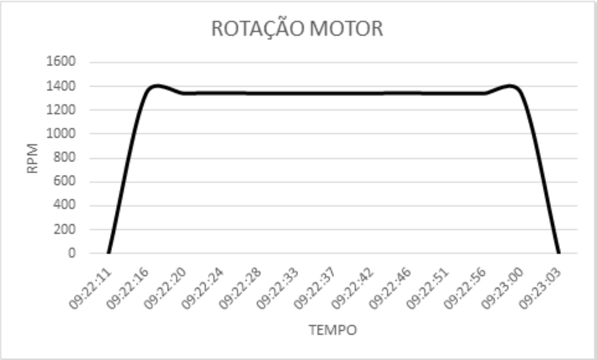

Source: Prepared by the Author.

Test Maximum

Traction [N], Time [sec]

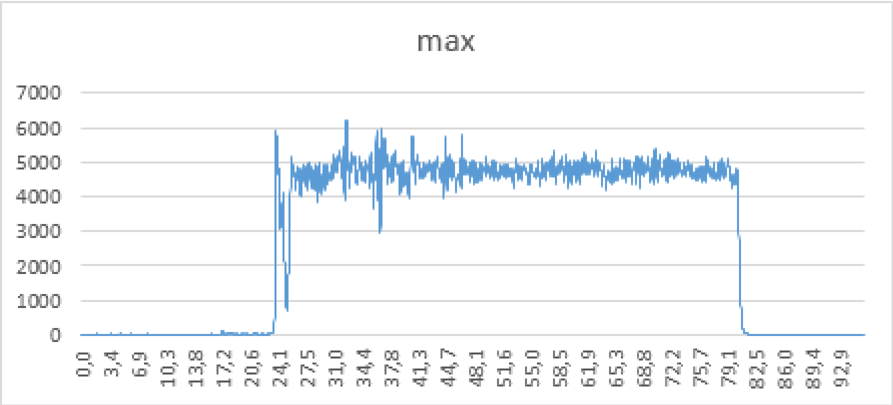

Source: Prepared by the Author.

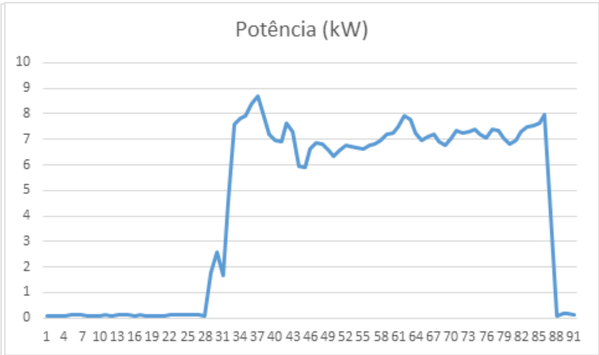

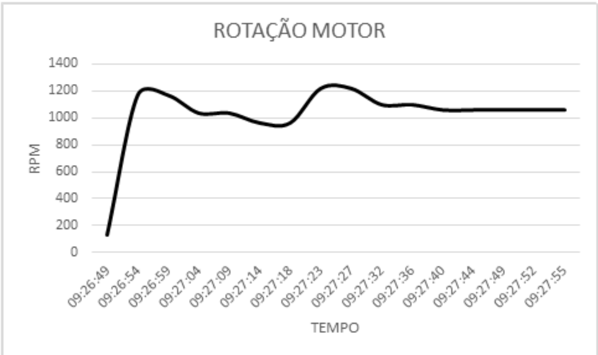

Source: Prepared by the Author.

Tobata 01

Traction [N], Time [sec]

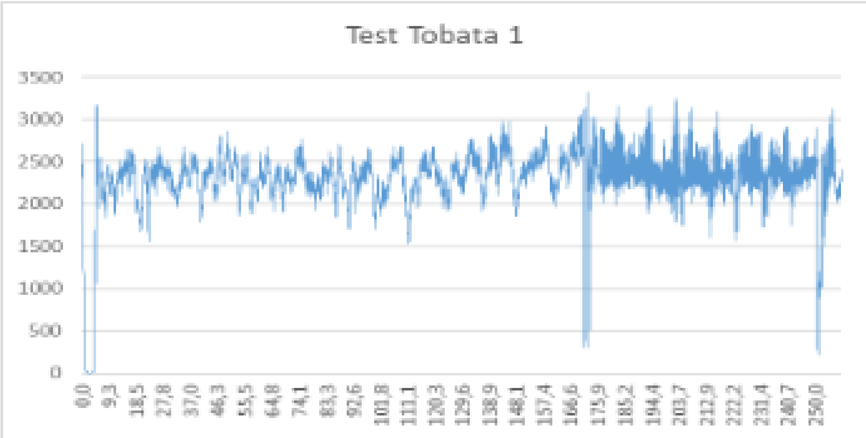

Source: Prepared by the Author.

Tobata 02

Traction [N], Time [sec]

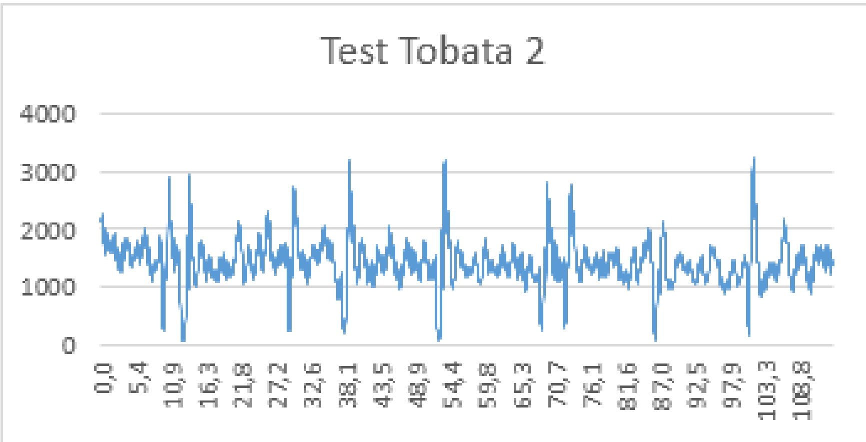

Source: Prepared by the Author.

APPENDIX C – COST CALCULATION DATA

(Price Levels as of Nov. 2017)

Electric tractor - Building costs

Item		Quantity	Unit Price	Total Item
Drive train				
	Motors	2	2500	5000
	Inverters	2	7200	14400
	Cable and electrical devices			750
	Accelerator (potentiometer)		3479	3479
	Main switch	1	198	198
	Inverter cables	6	78	468
	Chain 3/4 "	6	35	210
	Chain 1/2 "	5	62	310
	Chain wheels	8		620
	Rolling bearing 50mm kit with 2	2	140	280
	Rolling bearing 30mm kit with 2	3	54	112
	tires front 15"	2	130	260
	tires rear 16"	2	450	900
	Wheels front	2	165	330
	Wheels rear	2	270	540
Steering				1.460
Brakes		2	90	180
Chassis				
	Rectangular tube 40X20 U profile 100 mm	6	50	300
Tree Point				
	Hydraulics	1	244	244
	Mechanics	3	188	564
Roll bar		1	1350	
Emergency batteries charge				
	Solar panel 1,7m² 250W	1	550	550
	Charge control 10A	1	57	57
Assembly and debug				7200
		Real	**Total**	**39762**

Source: Prepared by the Author.

Transmission from stationary battery to pivot 570 m in three phase

Item	Quantity	Unit price (Euro)	Total price (Euro)	Specification or side
Cable 4 x 25 flat (100m)	5,7	1,575	8,978	NGFLGÖU 4X 25 SW
Inverter - Rectifier	6	805	4,830	STECA SOLARIX PLI 5000-48
Support structure			150	
			Total	**13,958 Euros** (**51,643 BRL**)

Source: Prepared by the Author. Note: Exchange Rate: 1 Euro = 3,7 BRL

Pivot Structure

Pivot structure			
Item	**Quantity**	**Unit price (BRL)**	**Total price (BRL)**
Terminal	1	109	109
Outer fix point	1	157	157
Standard	30	123	3,690
Cable (100 m)	0,7	5,670	3,969
Steel bar U (m)	50		1,000
Mast	1		2,000
Mast foundation	1		500
Interface mast - arm	1		500
		Total	**11,925**

Source: Prepared by the Author.

PV panels

Dimensions panel: 1960 x 990 x 50 (mm)	R$ 749.00
Fixture and cable 5 %	R$ 37.45
Total	**R$ 786.45** (equivalent to **405 Real/m²**)

Source: Prepared by the Author.

Trailer

Estimated trailer cost **7,000 BRL**

Battery cost

Cost per kWh Battery storage capacity Li-Ion			Cycle cost kWh			
US$	**BRL**	**Discharge in %**	**Cycles**	**BRL**	**US$**	**Euro**
220 (2017)	682	100	2,800	R$ 0.24	$0.08	0.07 €
120 (from 2020)	372	100	2,800	R$ 0.13	$0.04	0.04 €

Source: Prepared by the Author.

Costs variables

Variable	Unit	Value
Component efficiency values		
PV module		
PV panel	%	17
Battery		
Charge	%	90
Transmission efficiency values		
Inverter	%	93
Line	%	95
Charger	%	90
Tractor	%	93
Inverter	%	95.28
Motor	%	17
PV costs		
Solar radiation per day	kWh	5
PV generator per m^2	BRL/m^2	405
Electricity storage costs (without generation costs)		
Lead acid	BRL/kWh	0.87
Li-ion 2017	BRL/kWh	0.24
Li-ion 2020	BRL/kWh	0.13
Exchange rate (Sept. 4th, 2017)		
USD - BRL		3.1
Euro - BRL		3.7
Cost boundary conditions		
Tractor and trailer depreciation period	Years	15
PV depreciation period	Years	25
Others		
Insurance	Per year	1.5%
Maintenance	Per 100h	0.5%
Tobata Tractor		
Tobata M 160 HS	BRL	22,000
Fuel consumption per tractor hour	Litre	3
Fuel cost per litre of diesel	BRL	3.2
Energy compensation		
PV energy compensation per kWh	Euro	0.03

Source: Prepared by the Author.

ANNEX A

Sonnenschein Lithium HC (Hochleistungsmodule)

Die Produktreihe Sonnenschein Lithium bietet Lithium-Batteriemodule mit 12, 18 und 36 Volt. Im Vergleich zu Bleisäure-Batteriemodulen bieten diese Lithium-Module bei weniger Gewicht und Volumen eine deutlich verbesserte Zyklenlebensdauer und eine bessere Ladezeit.

Übersicht

Sonnenschein Lithium-Module sind die ideale Wahl für leistungsstarke Energiesysteme. Sie bieten eine hervorragende Zyklenlebensdauer und Ladeerhaltungsbetrieb, erfordern keine Wartung und ermöglichen den Endnutzern beträchtliche Betriebskosteneinsparungen und eine hohe Sicherheit, dank der chemischen Eigenschaften der Sonnenschein Lithium-Technologie.

Das Sonnenschein Lithium-Batteriemanagementsystem bietet in Zusammenarbeit mit den Sonnenschein Lithium-Modulen eine hervorragende Kontrollfunktionalität (einschließlich Fernüberwachung).

Weiterhin sind Überwachungs- und Diagnosefunktionen für die Sonnenschein Lithium-Module verfügbar, über die eine Erfassung von Systemdaten und detaillierten Leistungsparametern ermöglicht wird.

Merkmale

> 2.800 Zyklen mit 100 % Entladetiefe und 4.000+ Zyklen mit 80 % Entladetiefe*
> Außergewöhnliche Spannungsstabilität
> Kombinierbar bis 700 V und 1000 Ah
> Wartungsfrei
> Balancing innerhalb der Module
> Kompatibel mit GNB HP Ladegeräten
> Kommunikation der überwachten Daten per Batteriemanagementsystem (BMS)
> Robuste mechanische Ausführung
> Schwer entflammbarer Kunststoff
> LED Batteriestatusanzeige
> Tragegurte (SL12 110HC, SL12 138HC und SL18 69HC)
> In standardmäßigen BCI-Größen gefertigt

Source: SONNENSCHEIN (2014)[14].

[14] Reference: Lithium_Produkt_Datenblatt, Version 2.0. February, 2014. Available at: <http://www2.exide.com/au/en/product-solutions/network-power/product/sonnenschein-lithium-hc.aspx>. Access on: 10 Jan. 2018.

ANNEX B

Antriebsbatterien – Motive Power
Wartungsfreie dryfit traction Blockbatterien
Baureihe GF-V (dryfit traction Block)

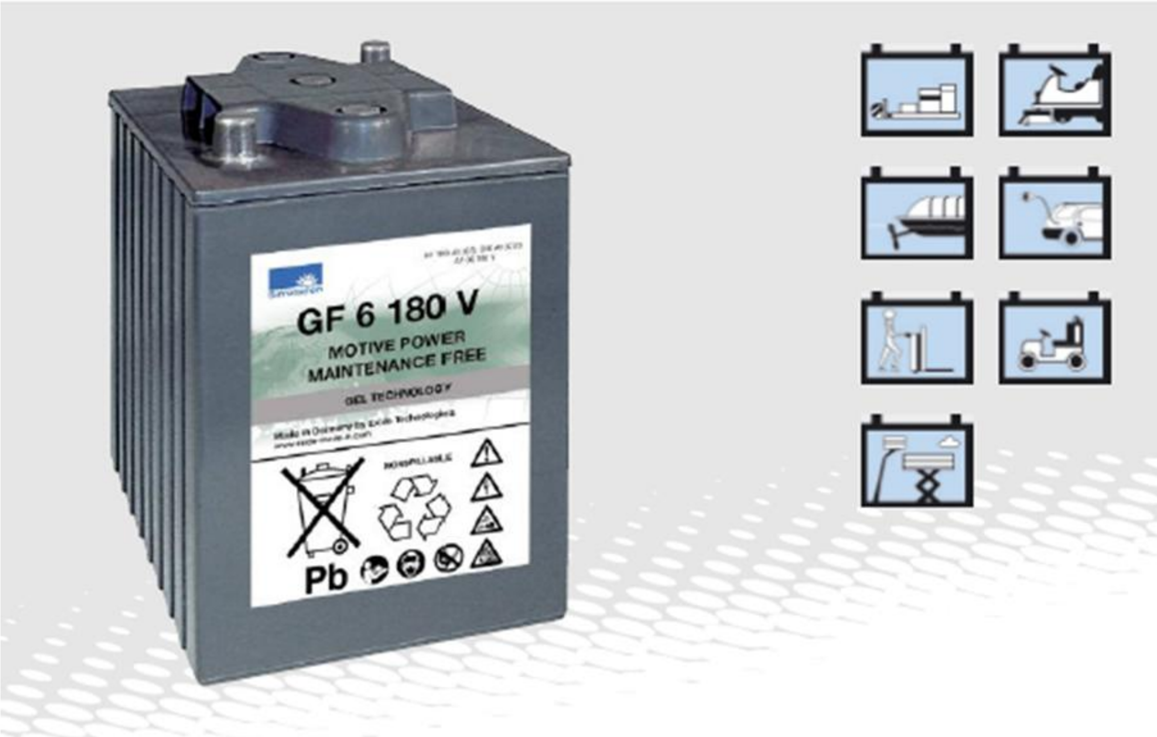

Wesentliche Produkteigenschaften und Vorteile

- Wartungsfreie Antriebsbatterien in Gel Technologie für den anspruchsvollen Einsatz
- Haltbar, sicher und zuverlässig
- Geringe Selbstentladung
- Produktpalette:
  6 V und 12 V Blockbatterien
  50 Ah bis 240 Ah (C_5)
  55 Ah bis 270 Ah (C_{20})
- 700 Zyklen nach
  DIN EN 60 254-1 / IEC 254-1
  mit 75 % Entladetiefe

Source: BATTERIE SIEMS